UNIVERSITY OF
KWAZULU-NATAL

INYUVESI
YAKWAZULU-NATALI

RESEARCH, DESIGN AND INVESTIGATION OF A MULTIPLE USER MIXED REALITY SYSTEM

Submitted by:

Mr. Dashlen Naidoo (BScEng, UKZN) – 215035381

Supervisor:

Prof. Glen Bright

Co-Supervisor:

Mr. James Edward Thomas Collins

April 2021

Submitted in the fulfilment of the academic requirements for the degree of Master of Science in Engineering at the School of Mechanical Engineering, University of KwaZulu-Natal.

DECLARATION 1: SUBMISSION

As the candidate's supervisor, I agree to the submission of this dissertation.

Supervisor: _____ Date: 12/04/2021

Prof. Glen Bright

As the candidate's co-supervisor, I agree to the submission of this dissertation.

Co-supervisor: _____ Date: 12/04/2021

Mr James Collins

DECLARATION 2: PLAGIARISM

I, Dashlen Naidoo, declare that,

i. The research reported in this dissertation, except where otherwise indicated, is my original research.

ii. This dissertation has not been submitted for any degree or examination at any other university.

iii. This dissertation does not contain other persons' data, pictures, graphs or other information, unless specifically acknowledged as being sourced from other persons.

iv. This dissertation does not contain other persons' writing, unless specifically acknowledged as being sourced from other researchers. Where other written sources have been quoted, then:

a. Their words have been re-written but the general information attributed to them has been referenced;

b. Where their exact words have been used, then their writing has been placed in italics and inside quotation marks, and referenced.

v. This dissertation does not contain text, graphics or tables copied and pasted from the Internet, unless specifically acknowledged, and the source being detailed in the dissertation and in the References sections.

Signed: _____ Date: 12/04/2021

DECLARATION 3: PUBLICATIONS

Details of contribution to peer-reviewed publications that include research presented in this dissertation. The undersigned agree that the following submissions were published and submitted as described and that the content therein is contained in this research.

PUBLICATION 1 (PUBLISHED): 17th International Conference on Informatics in Control, Automation and Robotics 2020 (ICINCO 2020)

Naidoo, D.; Bright, G. and Collins, J. (2020). Mid-air Imaging for a Collaborative Spatial Augmented Reality System.In Proceedings of the 17th International Conference on Informatics in Control, Automation and Robotics - Volume 1: ICINCO, ISBN 978-989-758-442-8, pages 385-393. DOI: 10.5220/0009779103850393

The paper was published and presented on 7 July 2020 in Durban, South Africa. Due to global Covid-19 restrictions the presentation of this paper was completed online via Zoom.

Dashlen Naidoo was the lead author of this paper and conducted all research and experimentation under the supervision of Professor Glen Bright and Mister James Collins.

Signed: _____ Date: 12/04/2021

ACKNOWLEDGEMENTS

I would like to acknowledge and thank my mother (Komaladevi Naidoo), my father (Kesarinandha Naidoo) and my brother (Vishendra Naidoo). Without the love and support I received from my family, I would not have made it this far in life, and for that, they deserve special thanks.

Special gratitude goes to my supervisors, Professor Glen Bright and Mr James Collins, for giving me the chance to pursue the topic of my dissertation, providing me guidance when I felt lost and positive encouragement when I struggled with my work. I would like to thank the Mechanical Engineering Workshop staff for their assistance with my System's fabrication. I want to give special thanks to Ms Wendy Janssens for the administrative support and assistance received.

I would like to thank Wesley Dharmalingum, Tyrone Bright and Ingrid Botha. Their advice, encouragement and support, lead to the completion of my dissertation.

I acknowledge the National Research Foundation (NRF) for the financial aid received. The NRF Postgraduate Scholarship, MND190718456990, covered expenses throughout the dissertation.

"Be completely engaged with what you are doing in the here and now, and instead of calling it work realize it is play"

~ Alan Watts

ABSTRACT

Current forms of virtual technology are limited by their single-user capability per device. Additionally, these technologies are listed at expensive price ranges due to the robust technology and processing power required for operations. These were identified as research challenges when a review of virtual technologies was undertaken. Research indicated the need for a system that allowed simultaneous user viewing and interaction without requiring robust hardware or system software.

This dissertation researched, designed and investigated a Mixed Reality (MR) System that allows multiple user viewing and interaction with mid-air images. Beam splitter theory was used to deliver the mid-air images on this system. Multiple user viewing was achieved through beam splitter selection of an ASKA3D Plate and the design of a novel system architecture that adjusted system components. A mechatronic actuation system was developed to automate the adjustment of system components that allowed seated and standing viewing within three height ranges. System operation and interaction were allowed through inputs on a laptop. Additionally, the implementation of gesture control was investigated using a web camera or a CaptoGlove™.

The testing performed on the manufactured MR System validated the design, actuation methods, viewing method and performance of the system. The laptop's Operating System (OS) was used to develop an MR game for entertainment testing, display images and videos for visual learning testing and operate SolidWorks™ for engineering design testing. The results of accuracy testing showed that the actuation methods had an accuracy range within the required 45-degree rotations with a highest possible error of 3° and the required vertical movements of 50 mm and 100 mm with a highest possible error of 0.5 mm. The results of repeatability testing showed the actuation methods had coefficients of variance with values less than 0.1, signifying a high repeatability. System performance was evaluated through user testing and proved the system as a tool to facilitate entertainment, education through visual learning and engineering design. Visual learning was found to be the most successful on the MR System with an average percentage rating of 100% and the overall system performance was given a rating of 80%. Actuation testing and user testing validated the hardware design, software design, electronic design and viewing method of the system.

The MR System operated as intended showing successful multiple user viewing without requiring robust hardware or software for system operation. The system was limited by the defined interaction method, the lack of multiple user testing and the limited programs used for testing the system's performance.

TABLE OF CONTENTS

LIST OF ACRONYMS AND ABBREVIATIONS

2D:	Two-Dimensional
3D:	Three-Dimensional
AHRS:	Attitude and Heading Reference System
AIP:	Aerial Imaging Plate
AR:	Augmented Reality
CAD:	Computer-Aided Drawing
CV:	Coefficient of Variation
DCRA:	Dihedral Corner Reflector Array
GPU:	Graphics Processing Unit
HD:	High Definition
HDMI:	Hight Definition Multimedia Interface
HMD:	Head-Mounted Display
HSM:	Half-Slivered Mirror
ICINCO:	International Conference on Informatics in Control, Automation and Robotics
IDE:	Integrated Development Environment
ISO:	International Organisation for Standardization
LCD:	Liquid-Crystal Display
LED:	Light-Emitting Diode
LLS:	Left Lead Screw
MARIO:	Mid-air Augmented Reality Interaction with Objects
MR:	Mixed Reality
MSc:	Master of Science
MVS:	Microsoft Visual Studio
NA:	Not Applicable
NEMA:	National Electrical Manufacturers Association
OS:	Operating System
PLA:	Polylactic Acid/Polylactide
PSU:	Power Supply Unit
QoE:	Quality-of-Service
QoS:	Quality-of-Experience
R:	Rand
RGB:	Red Green Blue
RLS:	Right Lead Screw
SAR:	Spatial Augmented Reality
SDK:	Software Development Kit
SF:	Safety Factor
TAF:	Total Axial Force
USB:	Universal Series Bus
VA:	Viewing Area

VD:	Viewing Distance
VGA:	Video Graphics Array
VR:	Virtual Reality

NOMENCLATURE

Latin Alphabet

A	Amperage
cm	Centimetre
d	Diameter
d_m	Mean diameter
d_o	Outer diameter
d_r	Root diameter
f	Friction coefficient between the lead screw and collar
g	Gram
I_{pos}	Observer position
kg	Kilogram
KN	Kilonewton
L	Lead
m	Meter
mA	Milliampere
MHz	Megahertz
mm	Millimetre
Nm	Newton-meter
P	Pitch
R	Reaction force
R_B	Reaction force at bearing support
R_{MS}	Reaction force at motor support
s	Second
T	Torque
T_L	Lowering torque
T_R	Raising torque
V	Voltage
VAC	Voltage amperage and frequency
W	Applied load
W_{BH}	Weight of bearing housing
W_d	Mid-air image width
W_{LS}	Weight of lead screw
$W_{M\&MH}$	Weight of motor and motor housing
W_p	Weight of mounting platform and collar

Greek Alphabet

α_n	Thread angle
θ_L	Depression angle
θ_w	Viewing angle
$^\circ$	Degrees
$\%$	Percentage

LIST OF FIGURES

LIST OF TABLES

1. INTRODUCTION

1.1 Project background and motivation

Virtual technology gives humans the ability to perceive, interact and control digital information through a physical medium. An article published by Marr [1] identified virtual technology as one of the next technology trends that will define the following decade. This trend digitally extends reality and creates immersive digital experiences using Virtual Reality (VR), Augmented Reality (AR) and Mixed Reality (MR) [1].

VR isolates its users from reality. A Head-Mounted Display (HMD) controls the user's vision, and earphones controls the users hearing. The user influences their environment using a controller or a glove that permits physical interactions. VR systems are robust devices and require high-performance computer systems for their operation. A VR device acts as a medium for the computer system so that users can experience the immersive environment created by the computer system.

AR overlays virtual information onto the world around us [2]. An AR environment can be produced using an HMD, which is light weight and does not encase the user's vision. The lightweight HMD allows the user to perceive the world around them. AR devices do not isolate their users hearing which enables them to be aware of their environment. Some AR devices limit user interaction and are used for display purposes only. Those that allow interaction, use a hand-held controller, glove, or the user's hands to interact with the AR environment.

MR combines digital and real-world environments and should not be confused with virtual information over-layering (AR). MR and AR are commonly mistaken as they both try to keep users aware of their surroundings while presenting a virtual environment. MR does not require a pre-existing physical marker to display its virtual information; this is how it differs from AR. MR devices deliver holograms/mid-air images without using wearable interfaces such as HMD's or controllers [3].

Digitally extending reality is not a new concept. VR, AR or MR technologies are currently employed to improve our daily lives and experiences [4]. They are ranging from education and entertainment to training and design.

Education at any level can be improved using VR and AR technology. In primary and secondary education, learning can be enhanced through the dynamic visual experience provided by these technologies. At a tertiary level of education, AR or VR technologies still find relevance which varied according to the field of study. Training was a specific type of education used at an adult level to increase employees' work proficiency. The training provided by VR and AR technologies was more practical and interactive than computer training which created a better learning environment. Companies have shown their interest in VR and AR for training, operations, command and control and decision support [5]. Walmart performed employee training in 2019 using the Oculus Go headset, AR device [6]. These technologies can be used in active working environments such as maintenance and repair. In maintenance and repair, AR was used to assist the user by increasing their situational awareness. Additionally, users were displayed information to increase their productivity [7]. The information provided to employees were suggested actions, cautionary information, visual hints, etc.

Entertainment is one of the largest areas where VR, AR and MR technology were used (Figure 1-1). VR headsets gave players an immersive experience that was highly stimulating. These VR headsets could range from cellphone docking stations to computer-controlled HMD's. AR has grown popular over the past three to four years due to

its implementation in games and applications. The most significant contributors to this were PokemonGO™ [8] and SnapChat™ [9] due to AR's social interaction. The success of VR, AR and MR technologies in entertainment is due to their ability to add another dimension to user experiences.

Graphical design such as artwork and advertising could implement these technologies that stimulated the viewing experience, hence, it provided information in a captivating way [10]. In civil and architectural design, AR and VR allowed designers to simulate all stages of a design project [11]. This enabled designers to identify design errors and possible improvements. In mechanical design, AR and VR were used to generate completed 3D designs to allow user investigation [12]. Through inspection, potential faults were identified, and corrective procedures were implemented before production.

Since its inception, virtual technology has grown in relevance. Due to the increased investment in the technology, new areas of interest were identified, as shown in Figure 1-1. Figure 1-1 displayed the worldwide investment focus on virtual technology in 2016, 2018 and 2019 [13]. Additionally, this showed how certain areas had received an increased investment over this period of three years.

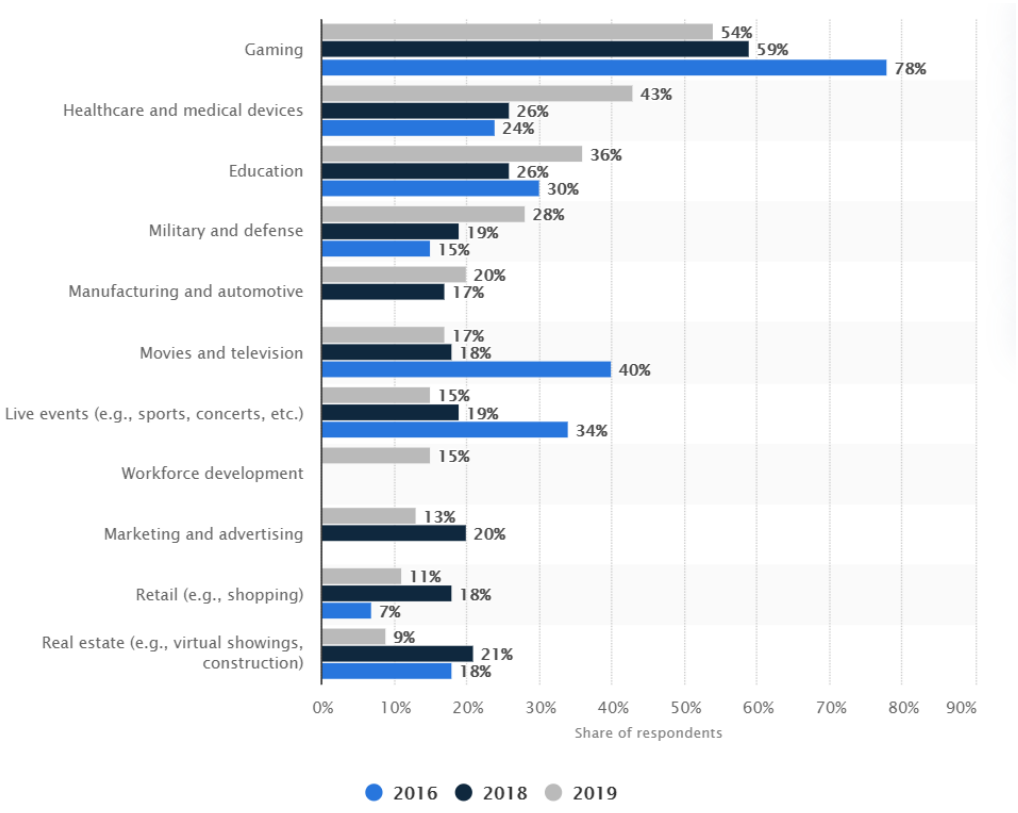

Figure 1-1: Statista diagram showing worldwide investment priority into virtual technologies [13]

It is expected that this market would increase in value in the near future. Data provided by Accenture [14] had proven this to be accurate. A prediction of the worldwide market spending by industries into virtual technologies could be seen in Figure 1-2. This displayed a gradual increase in virtual technology's market spending for every specified area where this technology could be used.

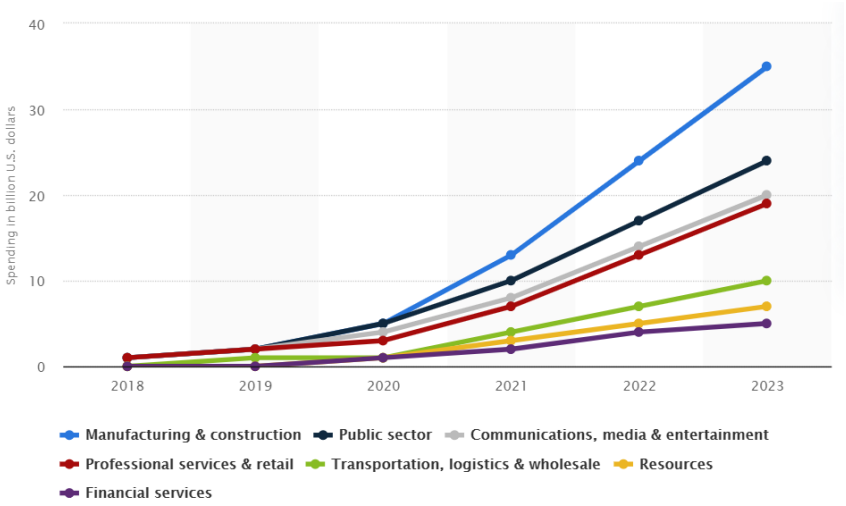

Figure 1-2: Statista diagram showing market spending into virtual technologies [15]

1.2 Research challenge

Currently, there are various VR and AR devices available, while MR devices have not seen any significant development. The confusion between MR and AR has led to this lack of development in MR; an example of this was the Microsoft HoloLens™. The Microsoft HoloLens™ was a virtual technology advertised as an "MR headset" [16], but MR should not require a headset. By requiring a headset to deliver an MR environment, it cannot be considered as an MR device. Therefore, there was a need to develop a system aligned to the definition of MR systems to investigate methods of implementation, methods of interaction and future uses of a completely MR system.

A completely MR system could allow multiple users on a single device, this is impossible with VR and AR technology. Each user is required to possess a device to interact and view in VR or AR. MR systems not requiring any wearables or hand-held devices creates situations where users are not restricted by hardware requirements to view and interact with the virtual scenes created. The benefit of creating such a system could alleviate user discomfort due to headsets and other wearables. It could deliver a virtual experience to more than one user on a single device. A completely MR system will create new virtual experiences while overcoming the current disadvantages of wearable devices seen with VR and AR technologies.

Delivering this completely MR System required the following research: comparative research on current MR systems, research into mid-air imaging techniques and research to provide an interactive experience for users.

The expected MR System will be a medium-scale system that will allow multiple user viewing and collaboration. The MR System will require a laptop for its operation; the computer system will not require high processing power like common AR and VR devices. This makes the system portable since it will not be attached to a dedicated desktop computer. The MR System will use the connected laptop (Operating System) OS to run programs that deliver MR operations and interaction. This system will not require any additional hardware when in use.

1.3 Research aim and objectives

Aim

To research and design a Mixed Reality system that allows multiple user viewing with the potential implementation for entertainment, education and engineering design.

Objectives

1. Investigate literature centred around digital extended realities with a focus on Mixed Reality.
2. Research and design a Mixed Reality desktop system that will allow multiple user viewing without utilizing robust technology.
3. Build and test the proposed Mixed Reality System, repeatability and accuracy testing for mechanical components and user testing at three levels (entertainment, education and engineering design) for measuring the MR System's success.
4. Discuss and conclude the designed MR System by addressing the research question of this dissertation.

1.4 Methodology

The research for this dissertation followed the steps presented as follows:

- Review literature to build on the content and understanding around MR.
- Research methods to implement the desired MR System.
- Perform conceptual designs of possible system implantations.
- Deliver a final MR System design including operation, hardware, software and electrical considerations.
- Manufacture and assemble the designed MR System.
- Research, develop and implement accuracy and repeatability testing of any mechatronic sub-systems.
- Research, develop and implement performance and user testing of the constructed MR System.
- Report on the findings of this research in an MSc dissertation.

1.5 Scientific contribution of the dissertation

This research had the following contributions:

I. Delivering multiple user viewing of mid-air images on an MR system.
II. Operation of a virtual system without requiring a robust computer system.
III. Developing an improved viewing method based on the system hardware design.
IV. Investigating the usage of MR technology for entertainment, education and engineering design.

Research Question: What contribution can a multiple user Mixed Reality System operated using a laptop deliver to current areas of virtual technology?

Hypothesis Statement: A Mixed Reality System that adjusts to user height will allow multiple user viewing and can be used to facilitate entertainment, education and engineering design.

1.6 Overview of dissertation

Chapter 1: Introduced the background of the research with a motivation for the study. This was followed by the identified research challenges leading to a statement of the aim and objectives. The chapter concluded with the methodology of the dissertation and the contribution of the study.

Chapter 2: Presented literature on MR systems, a review of beam splitter theory, a comparative analysis on mid-air imaging systems, interaction methods, and MR development software.

Chapter 3: Presented the concept generation of the MR System, showing three possible system implementations.

Chapter 4: Presented the physical design and operation of the MR System.

Chapter 5: Presented the software consideration and design of the MR System.

Chapter 6: Presented the testing and operation analysis of the MR System to validate its performance.

Chapter 7: This chapter discussed the design, implementation and performance of the MR System.

Chapter 8: Concluded the dissertation by addressing the aim, objectives and research question. Statements on limitations, recommendations and future work were given.

1.7 Chapter summary

This chapter introduced the reader to the concept of "digitally extended realities" and virtual technologies such as VR, AR and MR. This chapter presented the background on these technologies mentioned above, the current usage of virtual technologies and the research challenges. The aim and objectives were then presented, followed by the methodology of the dissertation. The contributions of the dissertation were presented with the research question of the study. Finally, an overview was given on the chapters presented in this dissertation.

The next chapter presented the literature review that discussed and compared material that influenced the MR System's design and operation.

2. LITERATURE REVIEW

2.1 Introduction

Virtual technology started with VR, which led to AR and now MR [17]. VR and AR technology are becoming more popular in public circles due to their availability; people can easily interact with a VR or AR environment using their phone. VR and AR have seen tremendous use on hand-held devices. Since most hand-held devices are equipped with a display, sensor technology and a camera, this made a perfect platform for these applications [18]. When an immersive virtual experience was needed, people could use an HMD system. MR is challenging to deliver to the public since it cannot rely on any hardware or wearables. This signified that MR systems would not be as portable as current VR and AR systems. It would be a fixed system that allowed multiple users to be a part of its virtual environment.

Research into MR led to the discovery of a particular type of AR system. These systems were called Spatial Augmented Reality (SAR) systems, and they possess qualities similar to MR systems. SAR splits the display from being physically on the user [19], allowing the user to be a part of an AR environment without the need for a headset or hand-held device. SAR systems enabled user interaction through glove technology or controller input. This information showed that MR and SAR are similar. Therefore, research in SAR systems could lead to more knowledge in developing an MR system. The primary benefit of creating an MR system improved the viewing and interaction of standard VR and AR systems.

Viewing is improved by removing the display system physically present on the user. This delivered a better system; it would allow multiple users to view the virtual scenes on a single device compared to current VR and AR systems that only allow one user per device. Furthermore, any physical discomfort that would be present due to an HMD would be non-existent on an MR system. HMD's have weaknesses such as incorrect focus cues, small field of view, tracking inaccuracies and inherent latency as presented by [20], which resulted in user discomfort. These weaknesses can be overcome with MR technology and will be a reference to test against once the MR system is developed.

Virtual interaction is improved by not requiring users to have glove or controller hardware. Anyone can approach the system and use it without requiring additional technology. This can be implemented through hand tracking techniques that can register hand motion and occlusions with virtual objects. Gesture control and voice control can be used to improve this interactive experience. Any one of these interaction techniques would deliver an MR system, but a combination of the three could create a more interactive MR system. Current VR and AR interaction occur through controllers that restricted hand positions and allow interaction through buttons and triggers. Gloves were also used to deliver VR and AR interaction, but these were expensive and uncomfortable when used. MR interaction removed restrictions on hand movement and possible discomfort while allowing users a natural method of interaction.

Research on creating an MR system was centered around three topics, mid-air imaging techniques, interaction techniques and software tools to deliver a virtual environment. This included a comparative study on existing MR or SAR systems for each topic.

2.2 Mid-air imaging

Determining a method to display virtual images was important, different display techniques come with their strengths and weaknesses. While there are many mid-air projection methods, the half-slivered mirror (HSM) technique was selected as the method to deliver the necessary viewing experience. This projection technique allowed the system display to be separate from the user while still providing a virtual environment. This technique has been used in SAR systems that deliver mid-air images for user viewing and, in some cases, user interaction.

The hardware needed to use this method was limited to an LCD screen to act as a light source and a half-slivered mirror to act as the beam splitter. The LCD screen displays a digital image, and the beam splitter projects the image from the LCD screen into the air. Users perceive this as a hologram or a floating object. To fully understand how this projection takes place, the characteristics of a beam splitter is illustrated in Figure 2-1, where "a" is the light source, "b" is the reflected light, and "c" is the transmitted light [21].

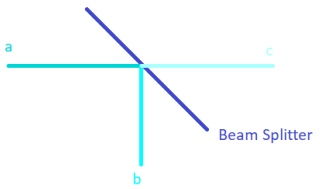

Figure 2-1: Diagram of beam splitter behaviour

Understanding existing MR/SAR systems can lead to insights on system development and identifying areas of improvement. Two systems were identified to have used the HSM technique to achieve mid-air image projection: the HoloDesk system [20] and the Mid-air Augmented Reality Interaction with Objects (MARIO) system [18]. While both systems use the HSM technique, their implementation was different.

2.2.1 HoloDesk imaging technique

The HoloDesk system was designed to be a tabletop virtual system. Hilliges et al. [20] sought to deliver a viewing experience where users were not restricted from directly interacting with the virtual scenes. In HSM designs, the beam splitter lies between the user and the virtual scene, restricting interaction and viewing. Users were required to look through the beam splitter to view the virtual scene. Hilliges et al. [20] overcome the HSM designs' weakness was by creating a system layout that allowed direct interaction behind the beam splitter with direct viewing through the beam splitter. This design layout can be seen in Figure 2-2.

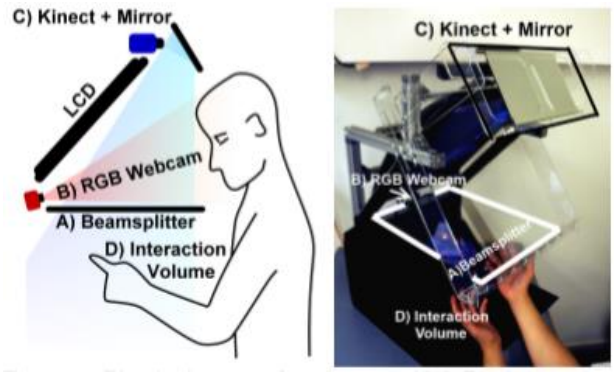

Figure 2-2: HoloDesk system setup [20]

The system delivered by [20] was a desktop system that allowed one user to view and interact with virtual scenes comfortably. The LCD screen was positioned so that light from the screen would hit the beam splitter, thus projecting the images underneath the beam splitter at a 90-degree angle to the LCD screen. The LCD screen and beam splitter are the only elements that effect viewing capability and the interaction region in this system.

Figure 2-2 indicates the scale and usability of the HoloDesk. A weakness of this layout lay in its visual appeal. It delivered an incomplete and cluttered feeling due to the visible structural components and fixtures. This did not affect the system's performance, but it did affect user impression. With multimedia devices, success is measured by the user experience and visual impression of these devices. A less cluttered system welcomed user interaction, focused user attention and grabbed user interest. This was taken into consideration during the system design.

The interaction volume delivered by this layout allowed users to move their hands without obstruction. Physical interaction was limited to virtual objects and scenes within the area of the beam splitter. While the interaction volume was open, it was small. This was due to the size of the LCD screen and beam splitter used. The major weakness of the interaction volume was its position. The interaction volume located in its current position restricted user viewing positions. Thus, users could only view and interact with the virtual scene so long as they looked through the beam splitter. A possible improvement lies in creating a method that allows the system to correct itself to the user's position and not the other way around. It was noted that the interaction volume required a darkened surface behind the virtual scenes to view the projections better. This was a possible design limitation and required further study.

The literature on the HoloDesk system presented little information on its mid-air imaging technique as Hilliges et al. [15] focused on the system's interaction technique. Regardless, [20] did overcome the restricted interaction and viewing experience in HSM designs through their system layout.

2.2.2 MARIO imaging technique

The MARIO system created a novel interaction experience by displaying images in three-dimensional space and creating a spatial link between these mid-air images and physical objects. Kim et al. [18] sought to deliver an improved viewing experience by performing comparative studies on different types of beam splitters and how they deliver mid-air image projection.

HSMs are a type of beam splitter, and the method of projecting images into mid-air (Figure 1-1) was commonly used with an HSM. This was due to the distortion-free imaging granted by the HSM, but there was a disadvantage of using this beam splitter. Virtual images can only be placed behind the HSM and not in front, resulting in design and interaction limitations. HSMs behave like regular mirrors. They form virtual images by reflecting incident light from an LCD screen [18]. This created a linear relationship between the virtual image position and the HSM and LCD screen distance. Additionally, this image position can be changed without distorting the virtual image projection [18].

Kim et al. [18] investigated beam splitters for their MARIO system to deliver distortion-free imaging while delivering virtual images in front of the beam splitter. Kim et al. [18] performed tests on five different beam splitters to determine their characteristics regarding distortion-free imaging and imaging in front of optics. The results of their tests can be seen in Table 2-1.

Table 2-1: Characteristics of different beam splitters identified by [18]

Beam splitter	Distortion-free	Mid-air imaging in front of optics
Half-slivered mirror	Yes	No
Convex mirror	No	Yes
Concave lens	No	Yes
Dihedral Corner Reflector Array (DCRA)	Yes	Yes
Aerial Imaging Plate (AIP)	Yes	Yes

An AIP was selected as the beam splitter that could deliver the characteristics desired by Kim et al. [18] for their MARIO system. Kim et al. [18] defined a geometric relationship between the AIP and the display. Two equations were used to represent this relationship. The first being the horizontal viewing angle equation, and the latter being the vertical viewing angle equation. Kim et al. [18] expected and proved that the closer the light source was to the AIP, the greater the viewing angle, both horizontally and vertically.

The system setup of MARIO can be seen in Figure 2-3. The overall system was comprised of three sub-systems: object detection, mid-air imaging display and shadow projection [18]. The mid-air imaging display had an LED-backlit display as the light source mounted on a linear actuator that changed the distance between the AIP and the light source. This affected the position of the mid-air image in front of the user. An AIP was located directly above the display at an angle of 45°. It was mounted in this position to reflect the light from the display in front of the beam splitter at a distance defined by the linear actuator's travel path. Figure 2-3 indicated that this was a robust system built on a permanent structure. It was assumed that it would not have ample mobility.

This system's interaction volume was defined by the display size and the linear actuator controlling the LCD and AIP distance. Additionally, the AIP was large enough to cover the display area to project the display images in mid-air. There were no obstructions around the interaction volume allowing free hand movement for users. It was noted that the MARIO system did not require a darkened surface to display its projections. Still, Kim et al. [18] operated the MARIO system in low light conditions so that the projections would be sharper. They found that in natural and artificial lighting conditions, the projections lose their sharpness and appear opaque.

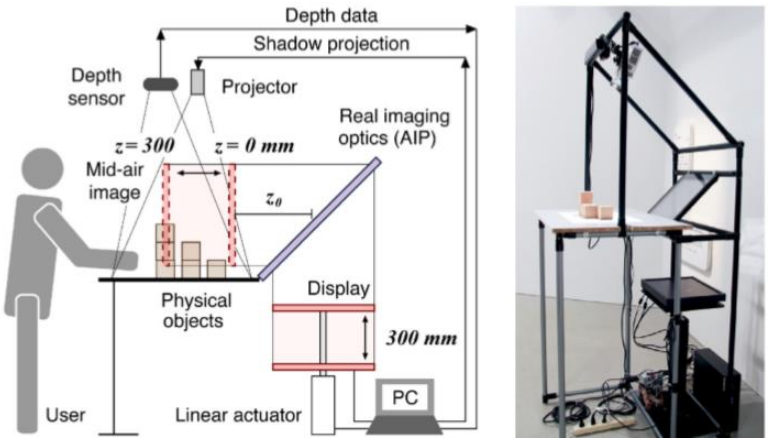

Figure 2-3: MARIO system setup [18]

The MARIO system presented a detailed analysis on mid-air projection techniques. They performed a comparative study on different types of beam splitters until they found one that met their system's needs. The research they provided gives a better understanding of beam splitter properties and methods of implementation.

When comparing the MARIO and HoloDesk systems mid-air imaging techniques, the MARIO system delivered a better mid-air imaging technique by performing an investigation on different types of beam splitters. The HoloDesk system used an HSM beam splitter with its disadvantage of having the optics behind the beam splitter but overcame this disadvantage through the system layout allowing direct user interaction with the virtual scene.

2.2.3 ASKA3D beam splitter

The research presented by Kim et al. [18] and further evidence published by Zhang et al. [22] emphasized the advantages of using an AIP as the beam splitter for a mid-air imaging system. Therefore, a supplier was required for either one of these beam splitters as Kim et al. [18] did not specify the supplier they used in their study. ASKA3D™ was found as a supplier of AIPs and could deliver their products to South Africa as the company was situated in Japan.

ASKA3D™ is a company that exclusively manufactures and sells AIPs, which they called ASKA3D Plates. ASKA3D Plates do not require any robust equipment to deliver mid-air images. This technology allowed the projection of videos and pictures in mid-air without losing 3D immersion [23]. ASKA3D™ suggested that their plate could deliver high-quality mid-air imaging in bright conditions, which was an area of concern identified in the MARIO and HoloDesk systems.

ASKA3D Plates are separated into two categories: plastic ASKA3D Plates and glass ASKA3D Plates. The plastic plates are produced at one size, 200 x 200 x 6 mm and have an image transmittance of 20% [23]. Glass plates are produced at four different sizes, from 244 x 244 x 5.3 mm to 975 x 975 x 8.8 mm and have a transmittance of 50% [23]. Plastic plates delivered mid-air images at a lower quality when compared to glass plates. Additionally, glass plates were more expensive due to their transmittance percentage and size. ASKA3D™ defined two layouts in which their plates could be used. These can be seen in Figure 2-4 and Figure 2-5.

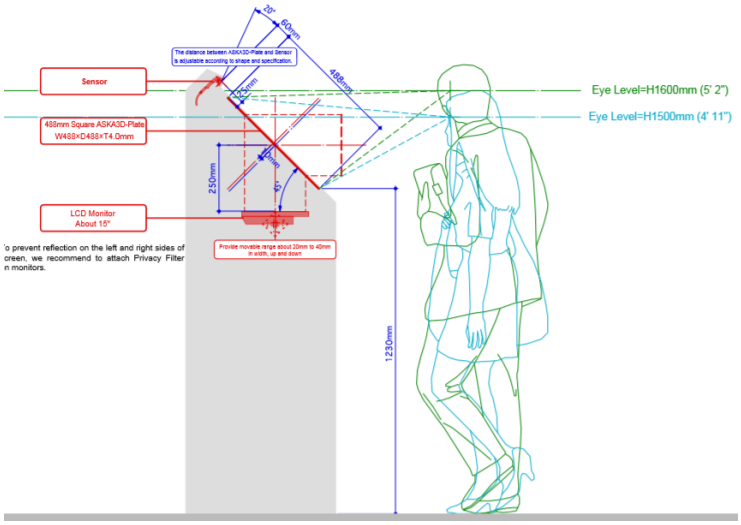

Figure 2-4: ASKA3D Plate layout 1 [23]

The layout seen in Figure 2-4 allowed users to view and interact with mid-air images by looking forward toward the ASKA3D Plate. This layout could be used either standing or sitting, depending on how the system was built. In this layout, the LCD screen was mounted parallel to the ground directly beneath the ASKA3D Plate. The ASKA3D Plate was mounted at an angle of 45° to the display.

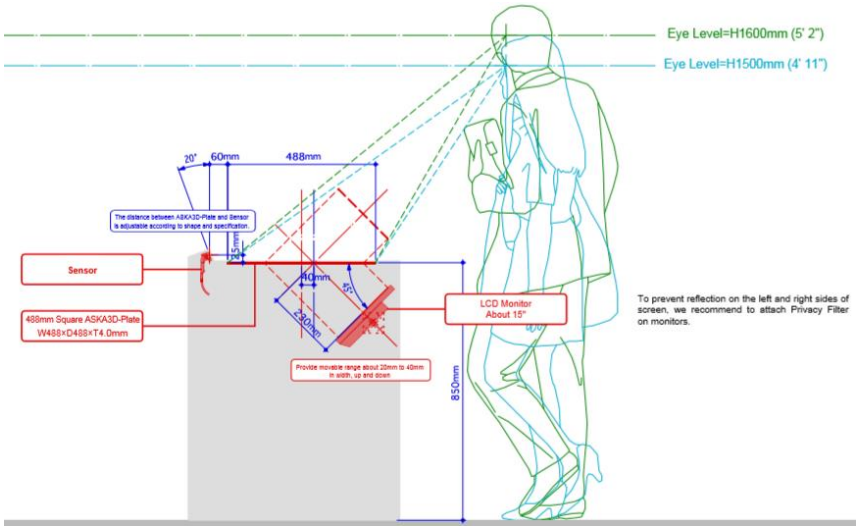

Figure 2-5: ASKA3D Plate layout 2 [23]

The layout seen in Figure 2-5 allowed users to view and interact with mid-air images by looking down, toward the ASKA3D Plate. In this layout, the ASKA3D Plate was mounted parallel to the ground with the LCD screen positioned below the plate at 45°.

All the dimensions (excluding screen and plate angles) present in Figure 2-4 and Figure 2-5 are subject to change as these values were dependent on how the system was built. ASKA3D™ supplies their customers with the formulas to calculate their unique viewing angles and viewing positions based on how they use the ASKA3D Plate. These datasheets can be found in Appendix B.1, B.2 and B.3.

2.2.4 Methods to improve viewing experience

It was possible to improve the user viewing experience without purchasing sophisticated hardware or creating complex system software. Methods of head-tracking, environmental light control and structural design can further enhance projected mid-air images.

Research presented by Radkowski and Oliver [24] discussed how standard virtual systems deliver virtual images that can only be viewed from a specific position. If viewed differently, the virtual image would appear distorted. These systems lacked natural visual perception, overcoming this required view-dependent rendering. This method changed the virtual information's position the viewing position of the user [24]. This was based on head tracking. Deering [25] supported the notion that systems without head-tracking would be fixed viewing systems. Head tracking as a possible method would allow corrective 360-degree viewing for any user height but would limit the number of users on the system. Systems can only track and display the corrected viewing of virtual objects one user at a time.

Roo et al. [26] presented research on essential factors considered when designing a SAR system. These were geometry, position and light conditions. Aligning the geometry and position of virtual and real objects delivered visually correct scenes that improve the quality of experience given by a system. Natural and artificial light could directly affect virtual projections, delivering mid-air images that look transparent or opaque [26]. Overcoming this required a system design that shields the mid-air projection from these lighting conditions or limits the system to be operated in a darkened environment. Controlling light conditions delivered sharp and more detailed mid-air projections [26].

The factors mentioned above were used in the HoloDesk and MARIO systems. The HoloDesk system used an RGB webcam to perform head tracking that delivered view-dependent rending. Users could view virtual objects with changing head positions. Additionally, HoloDesk controlled the system's light conditions by having the projection area located at the bottom of the design enclosed by black surfaces to better view mid-air projections. The MARIO system required users to operate the system in a darkened room without natural or artificial light, thus delivering a sharper image quality. The shadow projection sub-system gave the users of MARIO a sense of 3D. The MARIO system displayed 2D mid-air images, and shadows were placed underneath the mid-air images in real-time using a projector. In this way, the MARIO system makes use of position and geometry conditions, including light control.

2.3 Interaction methods

Virtual systems allow users to visualize objects or information in a three-dimensional space. To further this technology, designers sought to give users the ability to influence virtual objects. Hand-held controllers, glove control and hand interaction methods were developed to influence virtual objects [27]. An MR system requires direct hand interaction or gesture manipulation with mid-air images.

2.3.1 Glove interaction

Glove technology offers users the ability to interact with virtual scenes directly. There are a variety of glove technologies available to consumers, such as HaptX [28], Plexus [29], or CaptoGlove™ [30], to name a few. Virtual glove technology is a developing field of research. This was seen in the research presented by Shigapov et al. [31] and in research presented by Hilman et al. [32]. Each proposed unique designs and implementations in creating digital glove technology. In their research, glove technology was divided into two categories: complex glove systems and simple glove systems.

Complex glove systems do not follow a set template in their designs. These gloves deliver a unique real interaction experience to users. A common feature of these gloves was their ability to allow direct user interaction. They vary based on the device's size, the power needed to run the device and the quality of interaction granted. An example of a complex glove is the HaptX glove (Figure 2-6). This glove system allowed realistic touch, force feedback, high accuracy with 6 degrees of freedom per digit and occlusion free interaction [28]. This is a robust glove device and required a direct connection to a power source and a computer system.

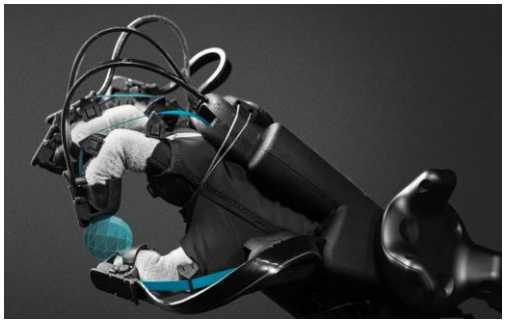

Figure 2-6: Example of HaptX™ glove [28]

Simple glove systems are similar and barely had any difference between each other. A common shared feature was the inability to provide direct interaction with virtual objects. These gloves provide users with gesture control of their systems, and they can be programmed to replace the mouse of a computer system. These gloves are lightweight, portable, programmable and are inexpensive glove systems. These gloves did not deliver the best type of interaction but can be programmed to suit the user's interaction needs. An example of a simple glove system is the CaptoGlove™ (Figure 2-7). The CaptoGlove™ is composed of a single pair of wireless gloves with five bending sensors, one or more pressure sensors and a CaptoSensor™. The bending sensors and pressure sensors in this system can be programmed to execute pre-defined instructions, creating a unique method of interaction with a computer system. The CaptoSensor™ is a high precision, high reliability, attitude and heading reference system (AHRS). The CaptoGlove™ can determine orientation relative to an absolute reference orientation in real-time using the AHRS [30].

Figure 2-7: Example of the CaptoGlove™ [30]

The glove devices mentioned above are only a few of the many devices available. The purpose of learning about glove interaction was to consider it as a solution if the quality of interaction delivered by hand interaction is inadequate.

2.3.2 Hand interaction

Hand interaction allowed users to directly influence virtual scenes using their hands without the need for any wearable device. This interaction ranged from precise finger and palm interaction with virtual objects to users controlling virtual objects' position without coming into direct contact with the virtual scene. Hand interaction requires hand tracking without the use of sensor technology located physically on a user. Many devices were available to perform object detection, which allowed hand interaction, to name a few devices, RGB cameras, laser scanning sensors, ultrasonic sensors, or infra-red depth sensors. A popular device used for virtual systems was the

Microsoft Kinect™ sensor, this is an infra-red depth sensor. This device has been used in the MARIO and HoloDesk systems to obtain their respective hand interaction. These sensors' limitation required a direct line of sight between the user's hands and the sensor. When comparing the interaction granted by the MARIO and HoloDesk systems, they both allowed direct hand interaction. The MARIO system allowed rudimentary interaction, while the HoloDesk system allowed precise hand interaction.

The interaction permitted on the MARIO system allowed its users to influence the mid-air image position by placing an object or the user's hand in the interaction volume. There was no precise finger tracking present in the system. Instead, the user's hands and any foreign objects were detected by the overhead Microsoft Kinect™ depth sensor. When new objects or hands entered the interaction volume, the depth sensor produces data for the physical object. The shapes and orientations of these objects can be estimated using this depth data [18]. This depth data was acquired using the Microsoft Kinect Software Development Kit (SDK). Utilizing this SDK and the depth data acquired, Kim et al. [18] determined the distance from the depth sensor to these objects within millimeters of precision. They were able to determine the highest point of any new object in the interaction volume.

The program run by the MARIO system had the mid-air image jump along a parabolic path towards the highest point of any new object within the interaction volume. This interaction method can be seen in Figure 2-8, showing the user influencing the scene by placing a new block in the interaction volume and having the mid-air image move parabolically toward the new object.

Figure 2-8: MARIO user interaction through block placement [18]

The HoloDesk system allowed precise interaction giving users the ability to push, scoop, pick up and rotate virtual objects. This interaction was made possible using a Microsoft Kinect™ sensor. Hilliges et al. [20] provided real-time tracking of the user's hands within the system's interaction volume. Hands and other objects can interact with the virtual scene through a physics-based representation of the virtual objects [20]. This interaction was enabled by a GPU based algorithm that processed the raw depth data from the depth sensor and represented objects or hands in a 3D physics simulation [20]. A depth aware optical flow algorithm was used to model friction forces imposed on objects. This allowed the natural grasping of virtual objects.

An example of the interaction granted on this system can be seen in Figure 2-9, where the user picked up a square cube and placed it on top of another cube. This interaction took place about the centroid of the virtual object and not along the object's surface. Hilliges et al. [20] modelled the system's physics interaction around the centroid objects.

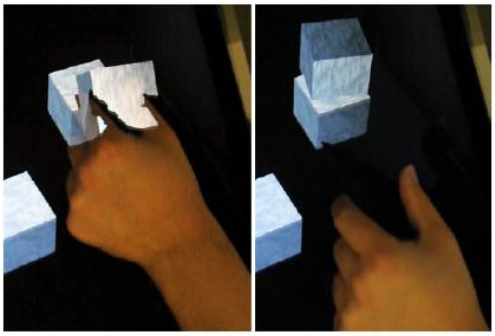

Figure 2-9: Interaction granted on the HoloDesk system [20]

When looking at alternative hand interaction methods that would not require sophisticated equipment, gesture control was identified as a possible method [33]. Research completed was limited to gesture detection using a laptop camera to investigate if it was possible to promote flexibility and simplicity when using gesture control.

Research presented by Yeo [34] explored different methods for gesture recognition using a laptop-web camera. While investigating three methods, he weighed the pros and cons of each method. Yeo's [34] motivation for his research was to create a more natural control technique for computer systems and programs. He elaborated that it was more natural to point and tap on icons with our fingers than using a mouse to move a cursor. He developed the system flow chart in Figure 2-10 for his gesture control method.

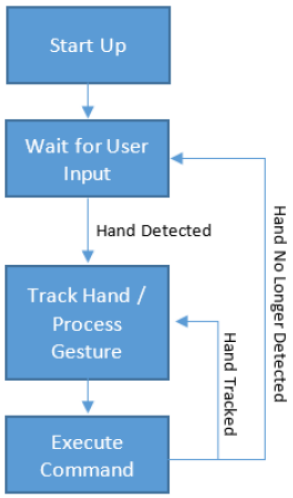

Figure 2-10: Yeo's flow chart for gesture control [34]

Upon startup, Yeo's [34] system constantly scanned and segmented what was seen through the laptop camera, trying to identify a hand's presence. Once a hand was detected, the system tracked the hand's position and movement to determine what command to execute. After the system executed the command, it goes back to scanning for a hand's presence and repeats the same processes indefinitely. Yeo's [34] focus was to identify the user's hand in a non-simple background since the program would be run on a laptop whose background environment was not kept constant. To perform this identification, he explored methods to segment a user's hand from the background of the camera. Through Yeo's [34] testing, background separation was found to be the most robust and most straightforward implementation. This method required the laptop to read multiple frames and

subtracting the aggregate values from future frames [34]. This method was not dependent on the exact colour of the user's hand like other methods, making it less susceptible to lighting changes in the environment.

Additionally, the system returned the segmentation as a binary image, which makes the process of gesture recognition simpler. The primary weakness of this method and other segmentation methods was that the system would not detect the user's hands in a dark environment efficiently. An example of the background separation achieved by Yeo [34] can be seen in Figure 2-11.

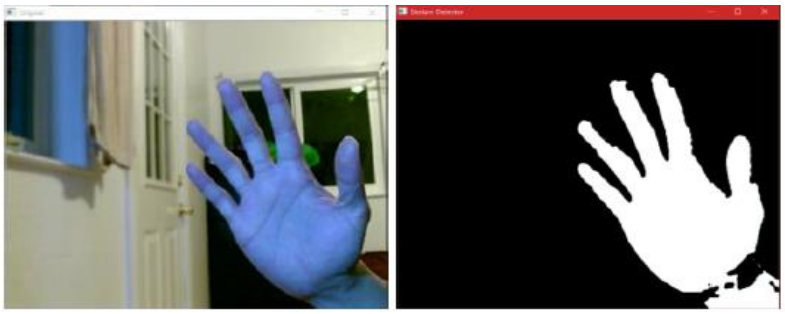

Figure 2-11: Yeo's [34] hand detection and binary image processing

Gesture recognition came after segmentation was completed. Yeo [34] implemented two basic gesture controls for his system, cursor movement and a mouse click. These controls were implemented using the Convex Hull method. This method took the outline of a shape and identified convex and concave points along the outline. Yeo [34] was able to calculate the centroid of the shape using this identification of convex and concave points. The program then tracked the centroid the moment the hand was identified and shifted the cursor based on the hand's movement. Since the program could identify concave and convex points, Yeo [34] could define a threshold of convex points to implement a cursor's click. For a single hand, there should be five convex points (these correlated to one for each finger) and four concave points (these were the number of gaps separating each finger). Therefore, users could control cursor motion with their hand movement and click with the number of fingers they held up to the camera. Yeo [34] discovered two possible weaknesses for this system. The first being the number of identified defects was higher than expected. This was due to the shape of the hand not being smooth when segmented. The second being the noise generated by the hand's contour which led to additional defects.

Yeo [34] developed his interaction program using functions found on OpenCV™ to perform background separation and gesture recognition of the binary images obtained from background separation.

2.4 Mixed Reality software

Microsoft Windows was the OS used to run or build software programs for the MR System due to the high number of users on this OS. Additionally, the desired MR System required a laptop to deliver an MR environment and not a dedicated computer system.

2.4.1 Virtual software design tools

VR systems require software to create a fully immersive 3D environment, thus completely isolating users from the real world. AR system software creates an experience like VR, except users, were still aware of the physical environment. The system software constantly scans the user's environment and overlays the virtual content on the physical environment. The system software must find a balance between allowing the user to perceive natural

sounds in the environment while playing artificial sounds to experience virtual content. VR and AR software focused on controlling the user's sight, touch and hearing. These systems require complex software as three variables need to be simultaneously controlled. VR and AR software were developed on similar programs with each program promising different design features, to name a few, Unity3D™, Unreal Engine™, 3DS Max & Maya™ and Blender™. These programs can be used with libraries and toolkits such as Apple ARKit™, ARToolKit™, OpenCV™ and OpenFace to improve the software being designed.

MR software development programs are scarce. A common tool for MR development was Windows Mixed Reality software. Windows Mixed Reality taught developers how to create unique 3D objects and holograms when using a headset. Interaction on this software was obtained using voice commands and hand gestures [35]. Thomas et al. [36] presented a paper on an inexpensive MR software tool for training medical students. The software developed by [36] integrated the ARToolkit™ and Visualization Toolkit™ to deliver a novel interaction environment. This demonstrated how existing VR or AR software tools could be used to create an MR program.

2.4.2 Investigation of system software

The beam splitter projection technique did not require any dedicated software for image projection. It required an OS to display pictures, videos and programs. Any MR programs for this system will be created using Unity3D™ as it was a common software used to create programs for AR and VR systems. The popularity of Unity3D™ for the design of VR, AR and possible MR programs came from the many features available on the software, which allowed realistic environments that were governed by real-world physics. Additionally, Windows Mixed Reality was explored as a possible development tool for creating an MR program. Windows Mixed Reality was a software tool that helped develop holographic or mixed reality experiences with HMD's. Therefore, it was found to be unsuitable for developing MR software as MR systems should not require the use of an HMD.

View-dependent rendering was previously discussed as a possible method to improve the viewing experience for the MR environment. View-dependent rendering requires a software program that can track a user's gaze and head positions. OpenFace is a software that could perform this function. OpenFace is a facial behaviour analysis toolkit. The code for this software was open source and prided itself in being state of the art, allowing facial landmark detection, head pose estimation, facial action recognition and eye/gaze estimation without specialist hardware [37]. This software required a camera to view the user's face and head position to perform head and gaze tracking.

Direct hand interaction requires both sophisticated hardware and software. From the information reviewed in the MARIO [18] and HoloDesk [20] research papers, it was discovered that using a Microsoft Kinect™ sensor was the best method to deliver a high-quality interaction experience. Additionally, this device came with an SDK which made it easier to process the information obtained by the depth sensor. The depth data alone would not deliver interaction on the system. An algorithm was required to interpret the depth data to provide physical interaction with the virtual scene. The robust hardware and software for this interaction method dismissed this method for the MR System's interaction.

Gesture control was researched as a possible method of interaction. The method used by Yeo [27] was the most favourable. His research delivered indirect user interaction using gestures on a laptop camera. The software for the interaction was developed using OpenCV™. OpenCV™ was a library of programming functions that dealt

with computer vision. The function used by Yeo [34] for segmentation of the images captured by the camera was "BackgroundSubtractMOG". This was a highly customizable function that enabled background subtraction of an image. This function was applied to every frame captured by the camera in real-time. The functions used for gesture recognition of the frames that underwent background subtraction were findContours(), convexHull() and convexityDefects() [34]. The use of these three functions identified the hand's centroid and the convex and concave points on the hand. Yeo [34] created a program that could link hand movement to cursor movement and fingers detected to the clicking of the cursor. This method created the ideal interaction for the desired MR System, but due to this method's inconsistency, glove interaction was explored as a possible solution.

2.5 Chapter summary

This chapter delivered a focused and comparative study on significant research that will help meet the aim, objectives, and research question set. A brief introduction was provided on MR and SAR technology, giving motivation to MR's advantages over VR and AR technologies. This led to the statement of the topics to be explored later in the chapter. The mid-air imaging topic was fundamentally explained, leading to a detailed comparison of the HoloDesk and MARIO systems method of mid-air projection. This led to thorough research on AIPs, and a supplier of AIPs called ASKA3D™. This was significant as this product can create the desired multiple user mid-air imaging. Next, interaction methods on virtual systems were discussed, thus identifying possible interaction techniques for the final MR System. Finally, a detailed investigation was performed on different software that could be operated on the desired system depending on the design choices to be made.

The next chapter was the start of the initial design phase, where the desired MR System prototyping took place. Concept designs were presented with motivations and analysis before a single concept was selected to be the final MR System design foundation.

3. CONCEPT GENERATION AND SELECTION

3.1 Introduction

The knowledge obtained from Chapter 2 is used to produce prototypes of the desired MR System. What follows are three concept designs of different MR Systems. These concepts are presented by a motivation statement on how the MR System operated, followed by design specifications, concept presentation and material selection. Finally, a decision matrix is developed for the generated concepts.

The motivation statement introduced the system's operation and how it will meet the required aim and objectives. The design specifications included specific characteristics, either numerical or physical, that the system would have to meet. Material selection for each concept considered the cost, manufacturability, and fatigue characteristics (among other things) of the system. These considerations delivered a better understanding to the construction of the physical system. The concept presentation displays an image of the design created using SolidWorks™. Finally, a decision matrix is presented where each concept was rated against specified criteria, and the concept that had the highest rating would deliver the better MR System. The better concept will be used as the foundation for the final MR System.

3.2 Robust system concept design

This design aimed to take the favourable characteristics from the systems and techniques explored in Chapter 2 and put them together into a single system. The focus was to deliver a collaborative MR experience for a variety of users. The system would be large to accommodate more than a single user. Additionally, the system would be in a fixed position due to its large work area. Users could operate this system as they would a normal computer system, except they would view their desktop screen as a mid-air image. When using MR programs on this system, users would interact with the virtual scene using a depth sensor for hand interaction, view the mid-air image using an ASKA3D Plate and observe the virtual scenes under gaze tracking to deliver view-dependant rendering. While this system will have a large size, it will allow for various uses and not strictly MR viewing and interaction.

3.2.1 Design specifications

What follows are specifications for the concept:

- Large scale viewing system.
- The system must not require any additional hardware for its operation.
- The system must host multiple users simultaneously.
- Users must be allowed to interact with their scene and can share their work with other users on the system.
- The system must be designed to be operated by users who are seated.
- The system must use an ASKA3D Plate in a fixed orientation for seated viewing (Figure 2-5).
- Provide direct hand interaction using a depth sensor that is in line with the mid-air image.
- An RGB web camera must be mounted in full view of each user's head to perform view-dependant rendering.

3.2.2 Robust concept

A sketch of the system was generated using the specifications and motivation mentioned above. This sketch can be found in Appendix C.1. This design created a system comprised of several MR workstations that were all connected and in constant communication.

The initial focus of this concept was on the shape of the work area. This would help identify locations to position the Mixed Reality workstations. It would also help determine how many workstations could comfortably fit in the system architecture. The shape of the overall system was made cylindrical as the design's soft curve would contribute to the aesthetics while delivering eight suitable locations to install the MR workstations. These workstations comprised an LCD screen, ASKA3D Plate, RGB web camera and a Microsoft Kinect™ sensor. It was possible to deliver a mid-air image that tracks the users viewing while enabling precise hand interaction with the MR scenes. A computer system controlled each workstation, and each computer system was connected to the other. This allowed users to share their work amongst other workstations, thus creating a collaborative user environment.

The overall system's height was defined so that users must be seated to use the system correctly, this created a more comfortable user experience. Due to the large scale of the system, it would require a unique frame that was strong and stable enough to house all the required components. Additionally, these components were fixed in specific positions to deliver the system's mid-air imaging. For example, the LCD screen was positioned 45° to the ASKA3D Plate.

When operating the system, the user selects a workstation and powers the workstation similar to a standard desktop computer. The workstation's LCD screen activates, which results in the ASKA3D Plate taking the image on the screen and projecting it in mid-air. The user is then prompted to log into the computer by typing their log-in details to the required fields seen in mid-air. Once logged in, the user can initialise a developed MR program. This program will ask the user if they are working with any other users currently on the system or working by themselves. If the user is working with other users on the system, they can share their screens to view each other's work or access other users' work on the system. If the user is working by themselves, the user starts their work. When the Microsoft Kinect™ sensor is on, it tracks the user's hands within the interaction volume, this allows hand interaction. This interaction is implemented using the algorithm for hand interaction that the HoloDesk system established. The RGB web camera activates and using OpenFace software the camera tracks the user's gaze to deliver view-dependant rendering. The use of the depth sensor and camera are dependant on the MR program developed and operated on the robust system.

This concept can be investigated to meet the aim, objectives and research question set in Chapter 1, but further improvement could be required for this concept to deliver the desired MR System. A design of this concept was developed using SolidWorks™ and can be seen in Figure 3-1. This gives an indication of the expected concept before any improvements can be made.

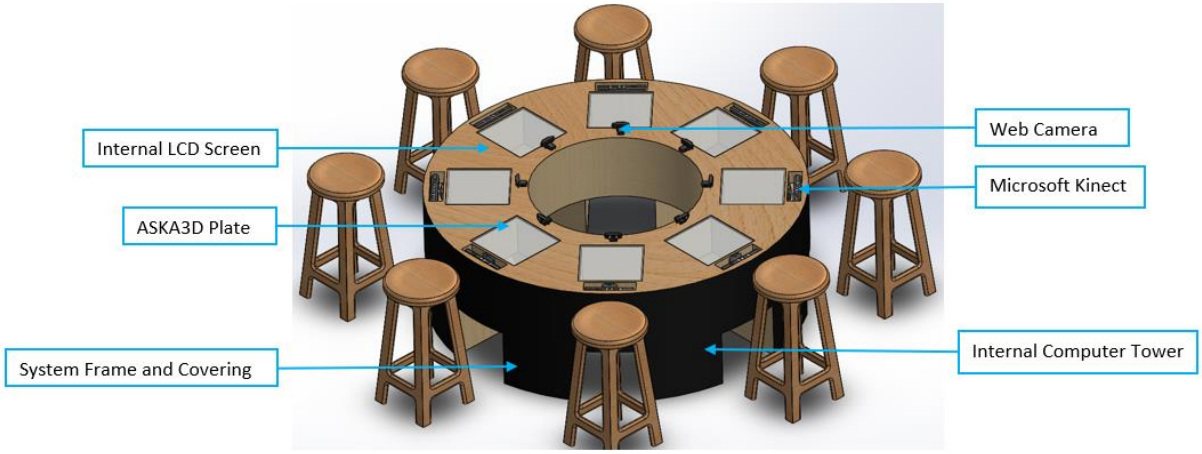

Figure 3-1: Robust system concept design

3.2.3 Material selection

Table 3-1 was produced to highlight the robust system design's key components with corresponding material selection, quantity specification, and reasoning on the selected material. Table 3-1 gives an early consideration for manufacturing this concept. If this concept was selected, it would become the base of the final MR System.

Table 3-1: Material selection for the robust concept design

No.	Component	Material	Quantity	Reasoning
1	System frame	Modular aluminium tubes	1	The frame needs to be rigid, strong, and sturdy. Additionally, this material can provide unique design choices at a lighter weight.
2	Frame covering	Wood & plastic	1	This will deliver an aesthetic design that was welcoming to the user. Wood will be used for larger sections of the system, while plastic will be used for smaller areas around the system when necessary.
3	Mounting brackets	Stainless steel	16	The brackets need to be sturdy to hold the weight of other components without deflecting or misaligning. Stainless steel will deliver this strength.
4	LCD screen	NA	8	NA
5	ASKA3D Plate	Glass	8	The glass ASKA3D Plate delivers a better viewing experience with an image transmittance of 50%.
6	Microsoft Kinect™	NA	8	NA
7	RGB web camera	NA	8	NA
8	Computer tower	NA	8	NA

3.3 Compact system concept design

This design aimed to deliver an MR system that would focus on providing the best possible MR experience at a reduced size and cost. Due to the previous design's large scale and capability, the build's purchasing and manufacturing cost was expected to be expensive. Therefore, this compact concept would remove any costly and unnecessary components while keeping a high-quality MR experience. This system would accommodate a single primary user with multiple user viewing. This system will be a secondary piece of technology that can be added to a computer system. This system will be designed to be fully operational using a laptop to promote the ease of operation.

Additionally, the concept will be a small-scale desktop system to boost portability and suit laptop function in any environment. When using MR programs with this system, the user will view the mid-air images through two possible layouts that the user can manually change to meet their needs. The interaction will take place using gesture recognition using the laptop's web camera, and view-dependant rendering will take place using an adjustable camera situated on the front of the system.

3.3.1 Design specifications

What follows are specifications for the concept:

- Small scale desktop system.
- The system must be portable.
- The system must be operated using a laptop.
- The system must house a single user at a time with multiple user viewing.
- The user can manually change the ASKA3D Plate and screen positions so that the system can use both layouts possible for the ASKA3D Plate (Figure 2-4 and Figure 2-5).
- Interaction must be obtained through gesture control using a web camera.
- An RGB web camera must be located on the system to deliver view-dependant rendering.

3.3.2 Compact concept

A sketch of the system was generated using the motivation and specifications mentioned above; this can be found in Appendix C.2. This concept was designed to be a single user interaction system with multiple user viewing that delivered an MR experience without sophisticated technology. This would reduce the overall cost to manufacture the system and reduce the processing power needed to operate the system.

The concept's initial focus was to create a small-scale portable system so that users could experience an MR environment in their chosen location. When delivering a mobile system, weight reduction is an essential factor to consider. Therefore, the entire system would be 3D printed with a low percentage infill. This includes all structural components and the mounting areas for the ASKA3D Plate and LCD screen. 3D printing the whole system aids in weight reduction and manufacturability. It allows unique designs that is not usually be possible. If components break, they can be easily replaced with almost no need for additional material processing. Additionally, the system is designed to be completely disassembled by its user so it can be easily transported. This is possible using multiple components that slide into one another to deliver a structurally sound system.

This system gives the user the ability to choose how they interact with the MR environment. The user can physically move the ASKA3D Plate and LCD screen to either one of the two available layouts seen in Figure 2-4 and Figure 2-5. This allows users the choice of using the system, either standing or seated. The aesthetics of this system is not prioritised. This is seen by the LCD screen protruding out of the system structure, which is not pleasing to the eye (Figure 3-2).

When operating the system, the primary user will have to ensure the adjustable web camera is powered and in line with their face. This delivers view-dependant rendering giving an improved user experience to suit the user's height. The user would then have to place their laptop next to the system within arm's reach. This is due to the system interaction requiring a direct line of sight of the user's hand to perform hand tracking and gesture control. The user will have to connect a USB cable from the compact system to a USB port on the laptop. Once connected, the system displays a mid-air image of the user's desktop screen from their laptop. The user can then start a developed MR program; the system would then display a mid-air image that the user could control using gestures. Secondary users will only be allowed viewing of the mid-air images. They will not experience view-dependant rendering and gesture interaction. They are limited to viewing the actions and perspective of the primary user on the system.

This concept can be investigated to meet the aim, objectives and research question set in Chapter 1, but further improvement could be required for this concept to deliver the desired MR System. A design of this concept was developed using SolidWorks™ and can be seen in Figure 3-2. This gives an indication of the expected concept before any improvements can be made.

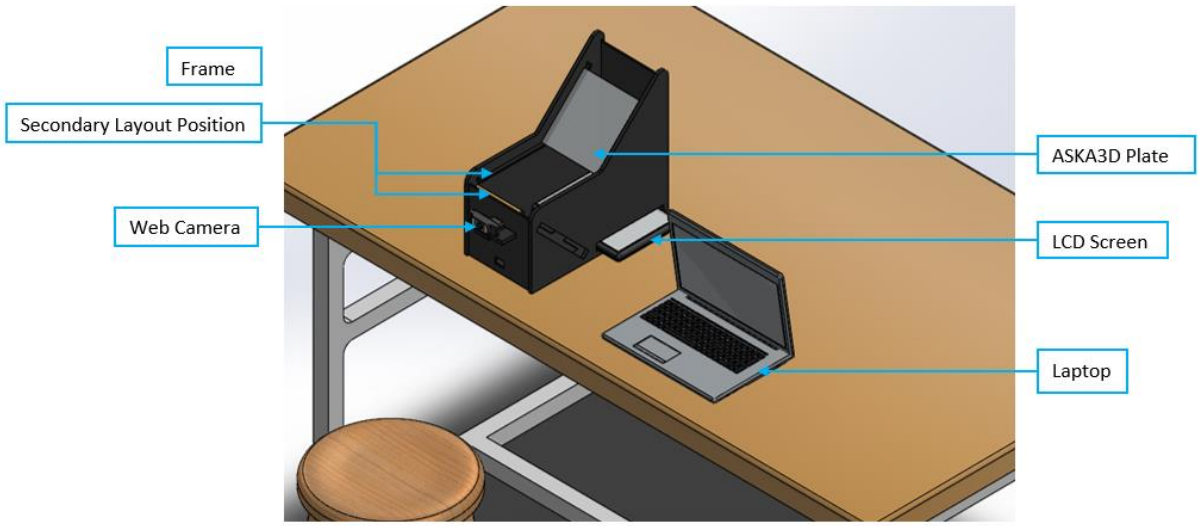

Figure 3-2: Compact system concept design

3.3.3 Material selection

Table 3-2 was produced to highlight the compact system design's key components with their corresponding material selection, quantity specification, and write-up on the selected material. Table 3-2 gives an early consideration for manufacturing this concept. If this concept was selected, it would become the base of the final MR System.

Table 3-2: Material selection for the compact concept design

No.	Component	Material	Quantity	Reasoning
1	Frame	PLA	1	The system frame and structure will be 3D printed in PLA. This would reduce the overall weight of the system and allow ease of manufacturing.
2	ASKA3D Plate	Glass	1	The glass ASKA3D Plate delivers a better viewing experience with an image transmittance of 50%.
3	LCD screen	NA	1	NA
4	RGB web camera	NA	1	NA
5	Laptop	NA	1	NA

3.4 Flexible system concept design

This design's goal was to give its users control over how they would view and interact with the MR environment. Users would not have to adjust themselves to the system, but the system would adjust itself to its users. Additionally, this system took the previous two concepts' strengths and weaknesses into consideration in its design.

The robust system's strengths were identified by its usability, interaction environment, aesthetics, user collaboration, and multi-user viewing. The compact system's strengths were identified by its portable design, low processing power required for operation, and its ability to alternate between the two layouts possible for the ASKA3D Plate. The robust system's weaknesses were identified by its large size, fixed viewing position, and high processing power required for operation. The compact system's weaknesses were identified by its lack of multi-user interaction, limited viewing space, and poor aesthetics.

The new system is designed with three essential functions. First, is the detection of the users' position. The system detects the users' position in an environment and then adjust itself so that the system automatically faces the users. Second, was layout selection. The system allows users to select which ASKA3D Plate layout they would like to use before automatically adjusting the components to the users liking. The third function enables the system to adjust its height automatically so that users of different heights could comfortably view the mid-air images. The system is transportable and operational using a laptop. The laptop initiates MR programs and delivers gesture interaction on this system. View-dependant rendering is not implemented as that would result in a single user viewing device, this goes against the collaborative environment the system must achieve.

3.4.1 Design specifications

What follows are specifications for the concept:

- The system should be moderately sized to make it portable.
- The system must be controlled using a laptop.
- The system must be able to rotate through 360° to position itself to users around the system.
- The user must be able to control the height of the LCD screen and ASKA3D Plate automatically.
- The user must be able to set the layout of the ASKA3D Plate and LCD screen automatically.

- Interaction must be obtained using the laptops web camera to achieve gesture control.
- The system must be able to host multiple users simultaneously.
- Components must be 3D printed where necessary to help with weight reduction and manufacturability.

3.4.2 Flexible concept

A sketch of the system was generated using the motivation and specifications mentioned above, this can be seen in Appendix C.3. This concept was designed to adjust itself to the users of the system. This was based on the users' position, height and viewing preferences.

The system was designed as a medium-scale, portable desktop system. This required design choices that minimized the system's weight and would be achieved using 3D printing for manufacturing specific system components. These components would range from mounting brackets to coverings that hide internal components. The system's base and base covering would be made from Masonite board to reduce the system weight and give the system a more natural aesthetic appeal. The system was designed to be controlled using a laptop to run programs that would deliver an MR environment.

The system has three autonomous sub-systems that creates the flexibility of the system. These sub-systems adjust the entire system according to the users' specifications. The first autonomous system is the face detection sub-system. This sub-system has a camera rotating along a 360-degree path looking for a user. Once a user is found, the entire system then rotates to face the camera's position. This is achieved by rotating the whole system, using a motor and gearbox, by the same number of degrees registered by the camera performing face detection. The second autonomous system controls the height position of the ASKA3D Plate and LCD screen. Depending on the users' heights, the system will move these two components to the best viewing position. This is achieved by users inputting their heights into the system. The system then uses a pair of motors, lead screws and collars that are directly coupled to move these two components up or down. The third autonomous system allows the user to switch between the two layouts when using an ASKA3D Plate. This is achieved using a motor directly coupled to the ASKA3D Plate and a second motor attached to the LCD screen. The system then controls these motors to rotate the plate and screen to their required positions. The users' control these autonomous systems through a microcontroller connected to the laptop. Interaction takes place using the laptop's web camera for gesture control. This would limit the processing power required by the system and would deliver a wearable-free interaction environment. After the users have programmed the system to their liking, they can run MR programs on the laptop that will allow them to view and interact with MR scenes on the system.

This concept can be investigated to meet the aim, objectives and research question set in Chapter 1, but further improvement could be required for this concept to deliver the desired MR System. A design of this concept was developed using SolidWorks™ and can be seen in Figure 3-3. This gives an indication of the expected concept before any improvements can be made.

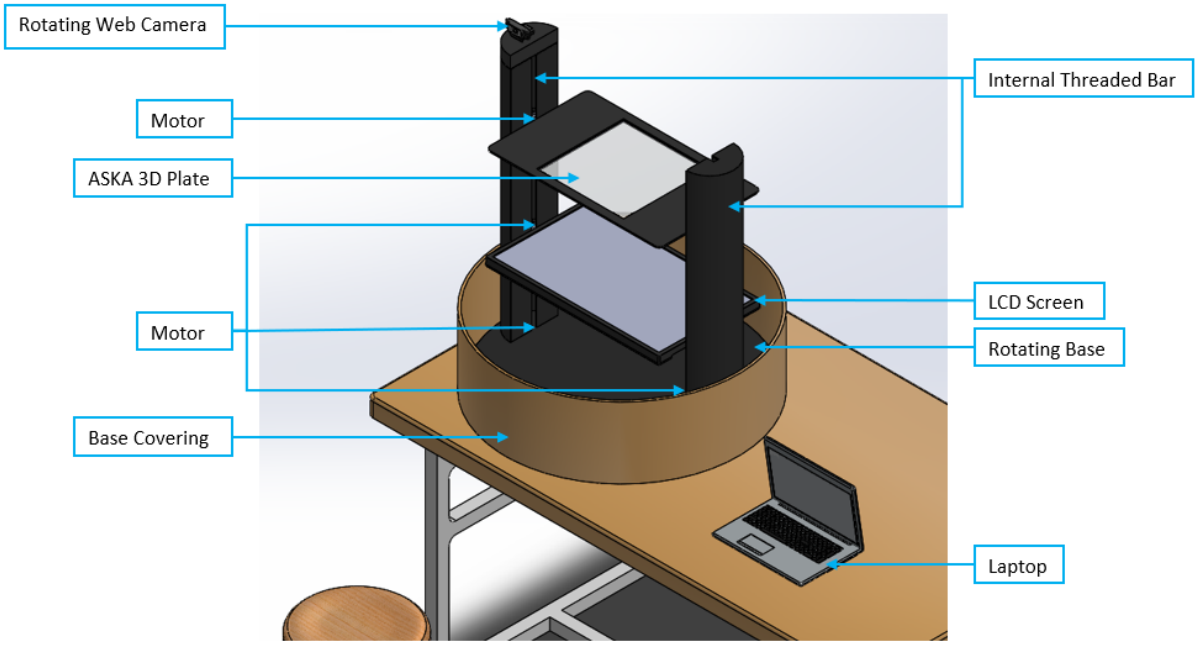

Figure 3-3: Flexible system concept design

3.4.3 Material selection

Table 3-3 was produced to highlight the flexible concept design's key components with its corresponding material selection, quantity specification, and write-up on the selected material. This was completed to deliver an early consideration to the manufacture of this concept. If this concept was selected, it would become the base of the final MR System.

Table 3-3: Material selection for the flexible concept design

No.	Component	Material	Quantity	Reasoning
1	Base covering	Masonite	1	This will deliver a lightweight covering for the system.
2	ASKA3D Plate	Glass	1	The glass ASKA3D Plates deliver a better viewing experience with an image transmittance of 50%.
3	LCD screen	NA	1	NA
4	Camera	NA	1	NA
5	Motor	NA	6	NA
6	Threaded bar	Stainless steel	2	Stainless steel was selected due to its strength and fatigue properties.
7	Collar for power screw	PLA	4	The collars will be 3D printed. PLA is the type of filament that will be used to make the components. This will help reduce the overall weight of the system.
8	Mounting components	PLA	4	The mounting components for the ASKA3D Plate and LCD screen will be 3D printed. PLA is the type of filament that will be used to make the components. This will help reduce the overall weight of the system.

3.5 Decision matrix

Deciding on a single concept to produce a final system design required each concept to undergo an evaluation to assess its strengths and weaknesses. A decision matrix was used to evaluate the generated concepts. The criteria for the decision matrix generated in Table 3-4 are explained with a corresponding scoring range.

- Aesthetics:
  The physical appearance of a system directly affects users as they are more likely to interact with a system that was pleasing to the eye. Especially with VR, AR and MR devices, as multimedia systems, their success is directly related to how visually pleasing they are to the user.

- Collaborative environment:
  This research aimed to create an MR system that could allow multiple users on a single device as this was a common trait that current virtual systems do not have. They require the same number of systems as the number of users. The desired MR system should create a collaborative environment between multiple users on the system.

- Cost:
  The overall cost of the system should be as low as possible while delivering a high-quality MR experience. This will make the system more accessible to consumers as current VR, AR, and MR systems are not readily available to consumers due to their high prices, resulting in limited stock due to production cost. Therefore, systems with a reduced cost should be favoured.

- Manufacturability:
  This was considered for ease of manufacture, assembly and to ensure parts can be easily replaced.

- MR entertainment, education, and design environment:
  This was one of the objectives that were set for the desired system. Therefore, each concept should be evaluated to identify which one delivered a better MR environment under these conditions.

- Portability:
  This considers how easy it would be to transport the system for usage in other locations.

- Workspace:
  The system's overall size could be a possible issue with regards to finding a suitable location to use the system. Therefore, it would be favourable for the system to be sized to fit many environments.

- System flexibility:
  This considers whether users can freely control how they can use the system and perform alterations to allow them a customized experience.

- User Interaction:
  This considers how well the system's interaction technique meets the interaction required for an MR environment.

- Viewing experience: This considers the quality of mid-air images obtained by looking at the techniques the system used to deliver its viewing experience.

Scoring: 5 = High 3 = Medium 1 = Low

Table 3-4: Decision matrix for concept selection

Criterion	Weight	Robust Concept	Compact Concept	Flexible Concept
Aesthetics	4	$4(\times 4) = 16$	$3(\times 4) = 12$	$3(\times 4) = 12$
Collaborative environment	5	$4(\times 5) = 20$	$3(\times 5) = 12$	$5(\times 5) = 25$
Cost	3	$1(\times 3) = 3$	$5(\times 3) = 15$	$4(\times 3) = 12$
Manufacturability	3	$2(\times 3) = 6$	$5(\times 3) = 15$	$4(\times 3) = 12$
MR environment	5	$5(\times 5) = 25$	$2(\times 5) = 10$	$4(\times 5) = 20$
Portability	3	$1(\times 3) = 3$	$5(\times 3) = 15$	$4(\times 3) = 12$
Workspace	2	$1(\times 2) = 2$	$5(\times 2) = 10$	$4(\times 2) = 8$
System flexibility	5	$1(\times 5) = 5$	$2(\times 5) = 10$	$5(\times 5) = 25$
User interaction	4	$5(\times 4) = 20$	$3(\times 4) = 12$	$3(\times 4) = 12$
Viewing experience	5	$4(\times 5) = 20$	$3(\times 5) = 15$	$4(\times 5) = 20$
Total		**120**	**126**	**158**

The decision matrix result (Table 3-4) showed the flexible concept design had a greater weighting than the other two concepts. This was due to the overall characterises that were required for the MR System. A final system will be designed using the flexible concept as a reference. Improvements and changes will be made to ensure that a working MR System is created.

3.6 Chapter summary

This chapter presented three rudimentary concepts of an MR System; these concepts were created using the knowledge obtained in Chapter 2. The three concepts presented were a robust system, a compact system and a flexible system. Each design was presented with a motivation describing the system's operation and goals. These concepts were not fully explored, and system operation was generally explained with an accompanying model created using SolidWorks™. After the three concepts were presented, a decision matrix (Table 3-4) was created to select one of the three concepts as the foundation for the final MR System design. This decision matrix was made using criteria specific to meeting the aim and objectives of the dissertation. The decision matrix showed that the flexible concept had the greatest weighting and would deliver a better MR System and user experience than the other concepts.

The next chapter will present the final MR System that was designed. This includes a system operation write-up leading to the system's classification into three sub-systems. Each sub-system had a full mechanical design write-up including decomposition diagrams, motivations, calculations, material selections, electrical designs, CAD models, manufacturing tables and assembly precedence diagrams. The final MR System was then presented with feedback on the manufacturing process that took place.

4. MIXED REALITY SYSTEM DESIGN

4.1 Introduction

The following system design is based on the flexible concept design explored in Section 3.3. This concept is the foundation of the final MR System. In this chapter, the system's operation is defined to identify what components were required. The system is then broken into sub-systems that each perform a specific function to deliver the desired system. The sub-systems are fully defined regarding their operation, physical design, electrical design, manufacture and assembly. Afterwards, the final MR System is manufactured, and the insights gained during the manufacturing processes are presented.

4.2 System operation

The final MR System is a portable desktop system that delivers an MR experience to multiple users. This system is connected to a laptop and allows multiple users to view and interact with mid-air images. The system's operation is dependent on how users view the virtual information on the system. Once operation is defined, the system is divided into sub-systems to perform the functions needed to enable multiple user viewing.

For VR and AR devices, visual appeal was the foundation of these systems as they enticed users based on what they viewed and how they viewed it. Therefore, this system defined how users would view MR scenes. Viewing was dependent on the heights of users and the layout of the ASKA3D Plate in the system.

4.2.1 The effect of user height

The height of the system is dictated by the heights of users that would interact with the system. The system is designed to adjust its components to suit a user's height, thus allowing accurate viewing of the mid-air images. A range of user heights with corresponding system heights was used to determine optimal viewing positions for the system's users.

ASKA3D™ supplies its customers with a datasheet showing the two layouts allowed using their AIP (Appendix B.3). Each layout was specified to allow viewing for users between the height of 1500 mm and 1600 mm. This height range accounted for many users, but it was more precise to account for user heights that considered men and women's mean height. Data obtained from Roser et al. [38] presented the global mean height of men and women born in 1996; this was found to be 1710 mm and 1590 mm, respectively. Therefore, the system was designed to operate between the following user height ranges; $1500\,mm \leq h \leq 1600\,mm$, $1600\,mm \leq h \leq 1700\,mm$ and $1700\,mm \leq h \leq 1800\,mm$. These three ranges were used to calculate the different screen and plate adjustments needed to deliver precise viewing for users depending on what height range they were classified to and what ASKA3D Plate layout they selected (Section 4.4.3).

4.2.2 Viewing method

An ASKA3D Plate can be used in two layouts that allow mid-air image projection. Delivering a flexible system that allowed users to control how they view the MR scene required the system to switch between the two available layouts. Due to this system flexibility, users would need to understand under what circumstances should each layout be used.

The ASKA3D Plate layout seen in Figure 2-4 placed the mid-air image directly in front of the user. This layout allowed users to view mid-air images while standing. It was noted that this layout created an unnatural interaction

environment. Users would have to interact with scenes directly in front of them at a height equivalent to the height of the user. A solution to this required the layout to be used at a lower height by seated users. Now, users could naturally view and interact with mid-air images. Additionally, using the system in this layout while seated can promote good posture since users would need to comfortably view the mid-air images with a straightened back. Therefore, this MR System was operated in the layout seen in Figure 4-1 when users wanted to experience an MR environment while seated. The seated system layout had the ASKA3D Plate at 45° to the LCD screen, parallel to the ground (0°). An example of this can be seen in Figure 4-1.

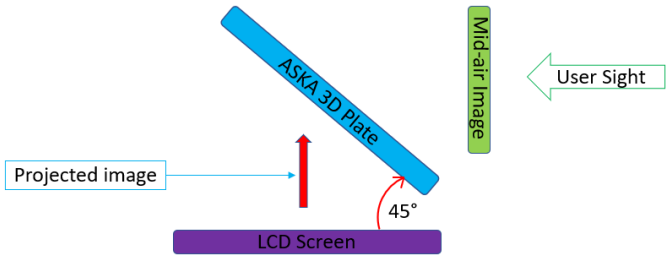

Figure 4-1: Seated system layout

The ASKA3D Plate layout seen in Figure 2-5 had the user viewing the mid-air images at a depression angle of 45°, which had them looking downward. This layout allowed users to view the mid-air images while standing and delivered a natural interaction environment. This was due to the height of the displayed mid-air image; it simulated an object at table height. It reminded users of real-life interactions with physical objects. Therefore, this MR System was operated in the layout seen in Figure 4-2 when users wanted to experience an MR environment while standing. The standing system layout had the LCD screen at 45° to the ASKA3D Plate, parallel to the ground (0°). An example of this can be seen in Figure 4-2.

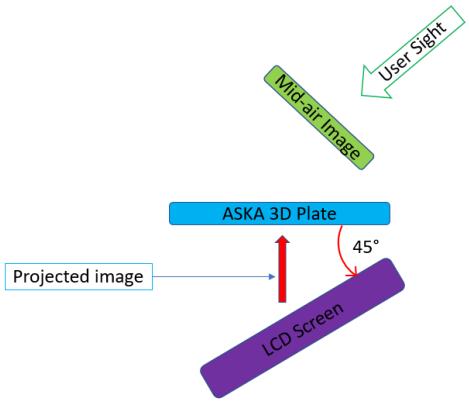

Figure 4-2: Standing system layout

The final MR System allowed seated and standing operation, giving users a choice to experience their mid-air images. User height had a direct effect on the implementation of the two layouts. Specifications for the system's operation at different user heights were calculated in Section 4.4.3. Additionally, the viewing angle, viewing position, viewing distance and observation range were calculated for the system in Section 4.4.3. According to ASKA3D™, these values were not affected by the layout used or the user's height.

4.2.3 Sub-system classification

The expected MR System was divided into three sub-systems using the information discussed in Sections 4.2.1 and 4.2.2. These sub-systems were classified to perform a specific function to deliver the desired MR environment.

The first sub-system would automatically control the layout of the ASKA3D Plate and LCD screen. This directly affected how the system was operated by its users (standing or seated layouts). This sub-system was called the Layout Control sub-system. The second sub-system would automatically control the height position of the ASKA3D Plate and LCD screen. This sub-system made height adjustments according to its users' height range when seated or standing. This sub-system was called the Hight Control sub-system. The third sub-system would be the base of the system used to mount the sub-systems mentioned above, thus providing a stable base on which the MR System can be assembled. Additionally, this sub-system acted as the control box for the MR System as it housed all the electrical control components. This sub-system was called the System Stand.

When operating the system, users would first position themselves in front of the device. Once the users were within the system's viewing angle, they will input information regarding the system operation. The Height Control sub-system and the Layout Control sub-system then takes this information describing the height and the layout they have selected (seated or standing). The system makes the required adjustments, thus allowing users to experience a personalised MR environment. A decomposition diagram showing the MR System and its respective sub-systems and be seen in Figure 4-3.

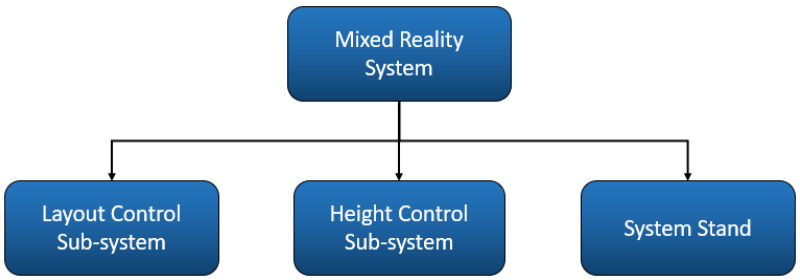

Figure 4-3: Mixed Reality System decomposition diagram

A detailed write-up on each sub-system is presented, explaining the sub-system operation, design considerations, electrical design, physical design, manufacture, and assembly. The software that was used for system operation and interaction was explored in Chapter 5 of the dissertation.

4.3 Layout Control sub-system

The purpose of this sub-system was to alternate the ASKA3D Plate and LCD screen layout of the MR System. The layout of these two components was dependant on the angle of the ASKA3D Plate and LCD screen. An example of the two layouts can be seen in Figure 4-1 (seated layout) and Figure 4-2 (standing layout). Therefore, the main function of this system was to alternate the angles of these two components. This was achieved by designing a system that allowed users to physically move these components or automatically change the angle of the components using an actuator.

Automatic layout control was selected for this sub-system so that these components can accurately rotate to their required positions. This was achieved using a motor and bearing mount directly coupled to the ASKA3D Plate and a second motor and bearing mount that was directly connected to the LCD screen. When the user selected the

system's layout, they chose between seated operation and standing operation using the laptop's keyboard. If the seated operation was selected, the motor attached to the ASKA3D Plate was instructed to rotate by 45° clockwise. The LCD screen was instructed to rotate to a position parallel to the ground (Figure 4-1). If the standing operation was selected, the motor attached to the ASKA3D Plate was instructed to rotate to a position parallel to the ground, and the LCD screen was rotated 45° clockwise (Figure 4-2). A decomposition diagram can be seen in Figure 4-4 showing the components of the sub-system.

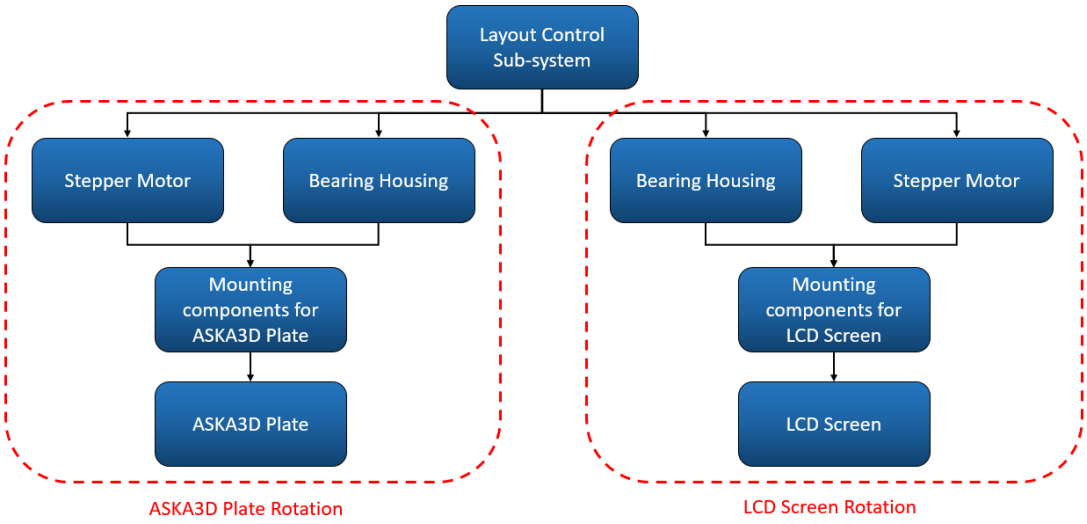

Figure 4-4: Layout Control sub-system decomposition diagram

4.3.1 Physical design

The physical design section presented and elaborated on the components used to enable plate and screen rotation. The decomposition diagram from Figure 4-4 was used to draw the physical components of this sub-system. These components were assembled to obtain an indication of how the sub-system will look once manufactured. Figure 4-5 displayed the fully assembled sub-system. The assembly drawing was presented in Appendix H, drawing number B1. The platforms on which the motors and bearing housings were mounted are not a part of this sub-system. They can be found in the Height Control sub-system design, Section 4.4.

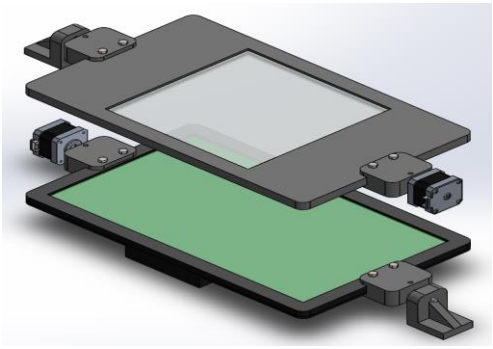

Figure 4-5: Fully assembled Layout Control sub-system.

The components of this sub-system were explained as follows, including design motivations, component specification and material selection. A drawing of each component was created using SolidWorks™ and can be found within Appendix H.

Ten components were designed to enable the rotation of the ASKA3D Plate and LCD screen. The components used to enable rotation of the ASKA3D Plate and LCD screen were the same. They only differed on the housing components for the screen and beam splitter. This was done to keep a uniform design and method of rotation. Rotation was enabled using a motor fixed to one side of the ASKA3D Plate or LCD screen; on the opposite side was a fixed shaft running through a bearing holder. This allowed a distribution of the forces acting on the motor shaft, thus allowing a stable rotation of the ASKA3D Plate and LCD screen. Figure 4-6 displays an assembly of the ASKA3D Plate with corresponding labels of each component. Figure 4-7 displays an assembly of the LCD screen with corresponding labels of each component. Stepper motor selection for this sub-system was explored in the electrical design write-up (Section 4.3.4).

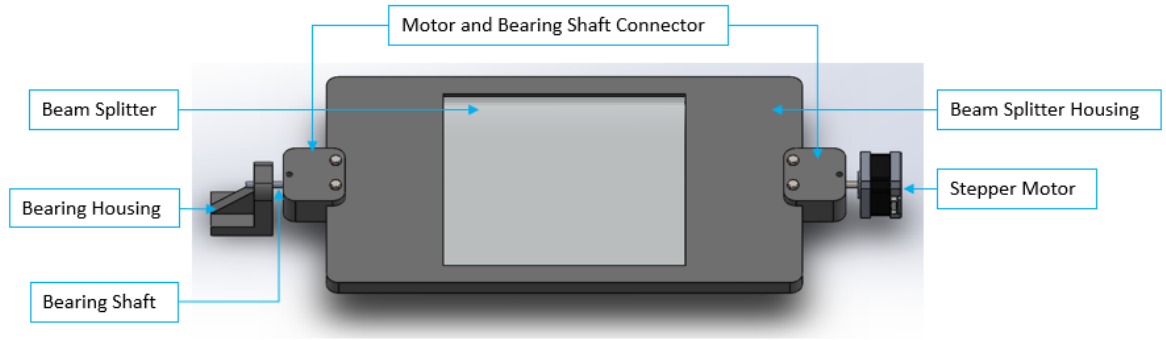

Figure 4-6: Labelled diagram of ASKA3D Plate assembly

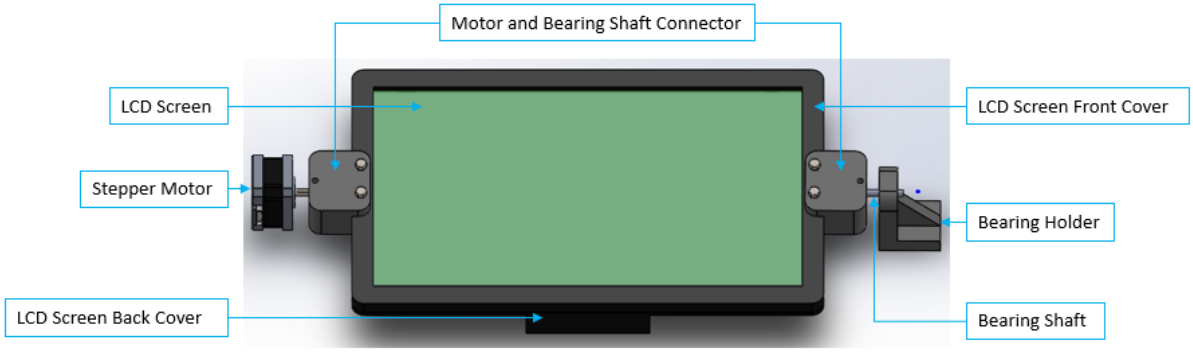

Figure 4-7: Labelled diagram of the LCD screen assembly

Beam Splitter

The beam splitter created an illusion that the user was viewing the image floating in mid-air when the image lies on the beam splitter's surface. The beam splitter that purchased for this system was the ASKA3D-200NT Plate. This was the most affordable plate available from ASKA3D™; it was made from plastic and was the smallest size plate available from ASKA3D™. Although this was the most inexpensive plate, it allowed mid-air image projection. A better-quality plate can be used in future work to improve the system's operation. The cheapest plate was selected due to the high cost of the other plates from ASKA3D™. The purchased beam splitter specifications can be found in Appendix B.1, B.2 & B.3. These include datasheets providing more information on the use of the ASKA3D-200NT Plate.

Beam Splitter Housing

The ASKA3D-200NT Plate was required to rotate in this sub-system. Therefore, a component was designed to securely hold the ASKA3D Plate and allow rotation of the plate. This component was called the beam splitter housing. It would act as a sleeve for the ASKA3D Plate with a square cut-out allowing mid-air image projection. Additionally, the housing had two mounting areas for the motor and bearing shaft connector components. These connectors were fixed to the housing using nuts and bolts, thus creating a compressing force to hold onto the housing. Figure 4-8 showed the isometric view of the component with labels for additional information. The drawing of this component with all its relevant dimensions can be found in Appendix H, drawing number B6.

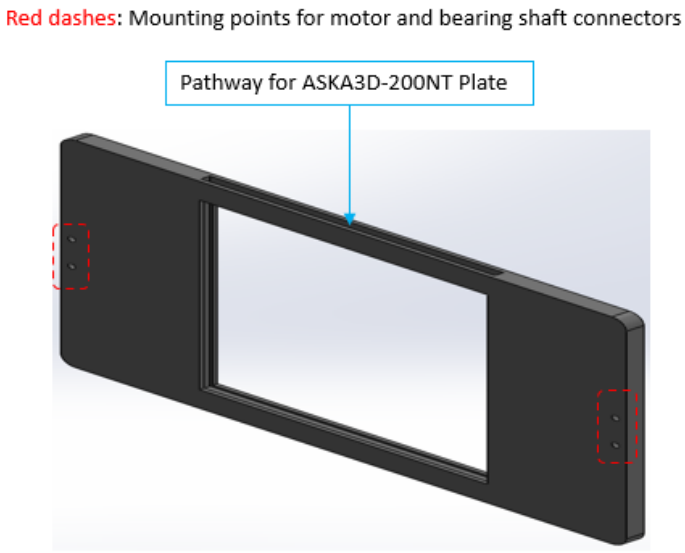

Figure 4-8: Beam splitter housing

LCD Screen

The LCD screen acted as the source of the image projected in mid-air. Therefore, an LCD screen was purchased for the sub-system's operation. The criteria for the screen's selection lay in the overall size and image quality. The purpose of basing the selection of the beam splitter and LCD screen on size was to create a portable and lightweight desktop system. Since the ASKA3D Plate selected was small in size, the LCD screen had to match or be close to the size of 200 mm by 200 mm (size of ASKA3D Plate).

The AOC E1659FWU 15.6" portable USB monitor was purchased for this sub-system due to its size and display specifications. Additionally, this monitor connected to computer systems via a USB port, unlike standard monitors requiring either an HDMI or a VGA port. This monitor was then stripped to its bare components leaving the LCD screen, motherboard and USB port. This was to reduce the overall weight and size of the monitor's existing cover. A new cover was designed to house these components compactly while keeping the cover's weight at a minimum. The specifications of the purchased monitor can be found in Appendix B.4. This included information on the image quality delivered by the AOC E1659FWU 15.6" Portable USB Monitor.

LCD Screen Front Cover

The first half of the cover was designed to mount the LCD screen of the purchased monitor. This component was called the “LCD Screen Front Cover”, and the main function of this component was to securely hold the LCD screen while being lightweight and covering a small area of the screen. Additionally, this half of the cover was designed to create mounting points for the “Motor and Bearing Shaft Connectors” (Figure 4-11) so that the motor and bearing shaft would be positioned in line with the centre of the LCD screen. Figure 4-9 shows the component's front and back view, including labels for additional information. The drawing of this component with all its relevant dimensions can be found in Appendix H, drawing number B4.

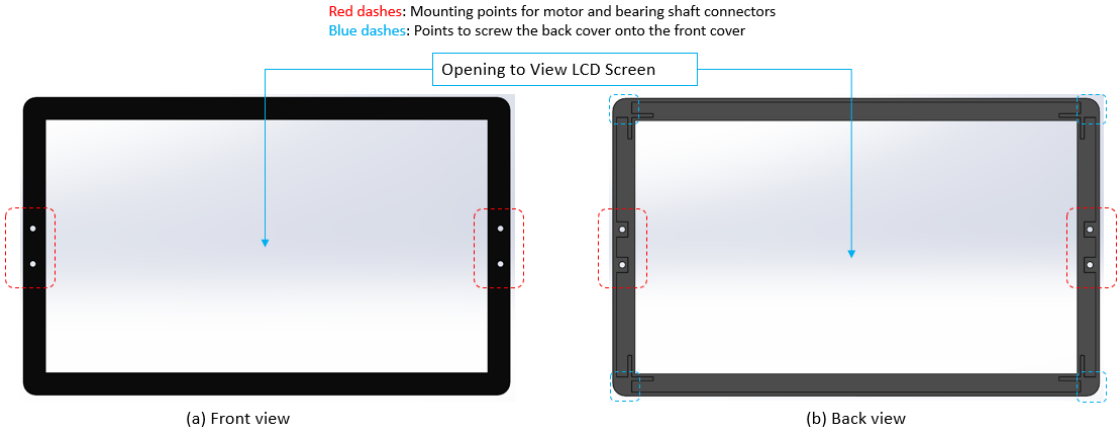

Figure 4-9: LCD screen front cover

LCD Screen Back Cover

The second half of the cover was designed to mount the motherboard and USB port of the monitor. Additionally, it would enclose the LCD screen keeping it protected. Figure 4-10 shows an isometric view of this component with labels for additional information. The drawing of this component with all its relevant dimensions can be found in Appendix H, drawing number B5.

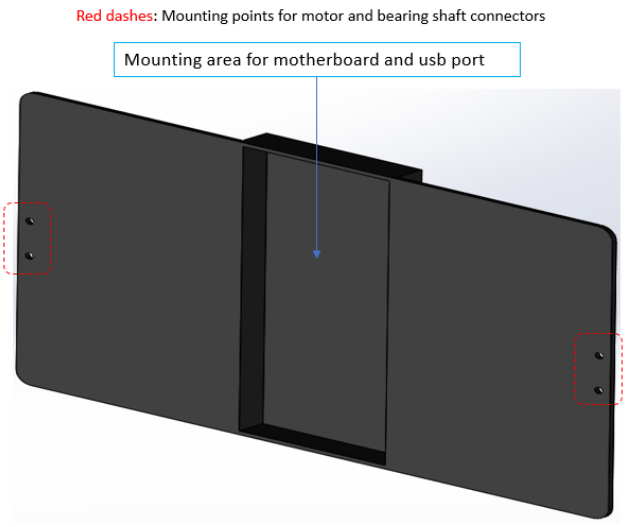

Figure 4-10: LCD screen back cover

Motor and Bearing Shaft Connectors

The following components were designed to securely hold the LCD screen cover and beam splitter housing while allowing a motor shaft or bearing shaft to be fixed to the component. The connector's primary function was to translate the motor shafts rotation to the attached component. This connector was attached to either side of the beam splitter housing and the LCD screen cover. It translated the rotation from the motor shaft to the bearing shaft, which helped with the beam splitter housing and LCD screen's weight distribution and stability. Nuts and bolts were used to connect this component to the housing and cover. A grub screw was used to fix the motor shaft and bearing shaft to the connectors. Figure 4-11 shows the isometric view of the component with labels for additional information. The drawing of this component with all its relevant dimensions can be found in Appendix H, drawing number B7.

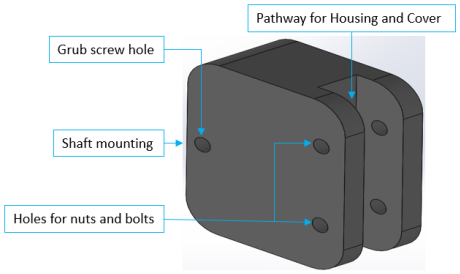

Figure 4-11: Motor and bearing shaft connector

Bearing Shaft

The bearing shaft's main function was to translate the rotary motion from the screen and cover to the ball bearing positioned within the bearing housing. The bearing shaft was attached to the screen cover and plate housing using the Bearing Shaft Connector. This component was designed to be a rigid object that could withstand sub-system components' weight with limited deflection not resulting failure. The drawing of this component with all its relevant dimensions can be found in Appendix H, drawing number B8.

Bearing Housing

The bearing housing's primary function was to securely hold a ball bearing that would withstand the bearing shaft's rotating motion. Additionally, the bearing housing would equally distribute the beam splitter and LCD screen's weights to allow stable rotation of these two components. The bearing housing design was based on the size of the motor used so that the components would be level. Figure 4-12 shows an isometric view of the bearing housing with labels for additional information. The drawing of this component with all its relevant dimensions can be found in Appendix H, drawing number B9.

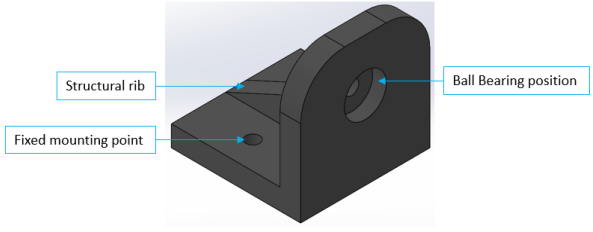

Figure 4-12: Bearing housing

Ball Bearing

The ball bearing for this sub-system was fixed within the bearing housing component and mounted onto the bearing shaft. This component allowed the bearing shaft to rotate without the rotation affecting the fixed bearing housing. This kept the plate housing and screen cover in a stable position. The ball bearing selected for this sub-system was based on the calculated force that the bearing would need to tolerate in this sub-system (Section 4.3.3). Table 4-1 displays the technical specification of the ball bearing used for this application.

Table 4-1: Ball bearing specifications

Bearing Type	**Radial Ball Bearing**
Inner Diameter	5 mm
Outer Diameter	16 mm
Thickness	5 mm
Dynamic Load Rating	1.73 KN

Stepper Motor

The stepper motor used for this sub-system was required to be lightweight while delivering enough torque to rotate the plate housing and screen cover components. The expected radial force on the motor shaft was calculated and was used as a guide for motor selection (Section 4.3.3). A motor whose allowable radial capacity was greater than the expected force on the shaft was selected for this sub-system. Therefore, a NEMA 17 stepper motor was selected to fit this application. This was further elaborated upon in the calculations performed for this sub-system (Section 4.3.3) and within this sub-system's electrical design (Section 4.3.4).

4.3.2 Material selection

The components for this sub-system have been described in full, explaining each design's purpose with corresponding diagrams. A detailed explanation was required for each component's material selection; this helped identify manufacturing methods. Additionally, material selection delivered more information on the choice of design regarding cost, weight reduction and ease of manufacture.

For the Layout Control sub-system, most of the physical components were designed to be 3D printed. This allowed unique design choices in creating the lightweight MR System. Therefore, the components in this sub-system were made of PLA plastic. This is a common 3D printing material. Components that were required to be more rigid with better strength characteristics were designed to be manufactured using stronger material. The material selection carried out for each component can be found in Table 4-2.

Table 4-2: Layout Control sub-system material selection

#	Component Name	Quantity	Material	Reasoning
1	LCD screen	1	NA	An AOC E1659FWU 15.6" Portable USB Monitor was purchased for this system. Therefore, there was no need to specify its material.
2	LCD Screen Front Cover	1	PLA Plastic	3D printing components using this material are more forgiving with minimal warpage issues.
3	LCD Screen Back Cover	1	PLA Plastic	3D printing components using this material are more forgiving with minimal warpage issues.
4	ASKA3D-200NT Plate	1	Plastic	The ASKA3D-200NT Plate was purchased from ASKA3D™. This type of plate was made from plastic as specified by the supplier.
5	Beam Splitter Housing	1	PLA Plastic	3D printing components using this material are more forgiving with minimal warpage issues.
6	Motor and Bearing Shaft Connector (LCD Screen)	2	PLA Plastic	3D printing components using this material are more forgiving with minimal warpage issues.
7	Motor and Bearing Shaft Connector (ASKA3D Plate)	2	PLA Plastic	3D printing components using this material are more forgiving with minimal warpage issues.
8	Bearing Shaft	2	Mild Steel	Mild steel was selected for its strength characteristics and its rigidity properties. The bearing shaft component would need to distribute forces along the shaft without deflection.
9	Bearing Housing	2	PLA Plastic	3D printing components using this material are more forgiving with minimal warpage issues.
10	M5 Ball Bearing	2	Stainless Steel	The ball bearings used in this sub-system would be purchased. Therefore, there was no need to elaborate on its material selection.
11	NEMA 17 Stepper Motor	2	NA	The stepper motors used in this sub-system were purchased. Therefore, there was no need to elaborate on its material selection.

4.3.3 Sub-system considerations and calculations

This sub-system considered the viewing specifications that applied to both system layouts. Viewing specifications were values that defined the viewing experience. They provided measurable restrictions and instructions on how the sub-system should be used. These specifications were defined as depression angle, observer position, viewing angle, viewing distance and the observation range/viewing area. The purpose of these specifications are explained with the calculated value for each specification.

A depression angle is formed when the user looks slightly downward to view the mid-air image. This was defined by the ASKA3D™ datasheet (Appendix B.2), the depression angle when using the system was 45°. Observer position defined the minimum distance the user must be positioned away from the system. If the user was positioned less than the minimum distance, they would not be able to view the mid-air image. The observer position for this system was calculated to be 430 mm. The system's viewing angle defined the horizontal angle created from the viewing focal point, located at the centre of the mid-air image. This value was calculated and found to be 13°. The ASKA3D™ datasheet further specified that the observation range becomes wider as the user moves away from the system. Therefore, a small viewing angle does not restrict the system so long as the users can position themselves adequately away from the system. The system's viewing distance was a user-defined measurement that specified the maximum user position from the observer position. The maximum user position was set to 2500 mm. This distance was selected to accommodate more users to view and interact with the mid-air images. The observation range was defined by the calculated viewing angle and the specified viewing distance. The observation range was calculated to be 1154 mm. The calculations for these values can be found in Appendix D.1. These values are tabulated to easily represent the sub-system's viewing specifications (Table 4-3).

Table 4-3: Layout Control sub-system viewing specifications

Viewing components	Value
Depression angle	45°
Observer position	495 mm
Viewing angle	13°
Viewing distance	2500 mm
Observation range	1154 mm

The motor and bearing selection were based on the weight these components would have to accommodate in the sub-system. SolidWorks™ was used to construct the components mounted on the motor shaft and bearing shaft for the plate and screen. It was possible to calculate the mounting components' mass using the Mass Property function on SolidWorks™ and Cura. These mass values with the plate and screen's corresponding mass gave the total weight that would be directly coupled to each motor shaft and bearing. A force balance diagram was drawn to calculate the forces present on each motor shaft and bearing. These calculated forces can be seen in Table 4-4. The calculations and force diagrams can be found in Appendix D.2.

Table 4-4: Forces on the motor shafts and bearings

	Force	Force (with SF)
Motor shaft and bearing for ASKA3D-200NT Plate	3.01 N	4.52 N
Motor Shaft and bearing for LCD Screen	4.44 N	6.66 N

4.3.4 Electrical design

This sub-system's electrical design enabled the ASKA3D Plate and LCD screen to alternate between the two possible layouts. Stepper motors were selected to perform accurate and precise angle control of these two components. The stepper motor selection for this sub-system was based on the weight of the plate and screen components.

Using the calculation found in Appendix D.2, the total force present on each motor shaft was calculated and tabulated in Table 4-4. The stepper motors selected for this application had an allowable radial force greater than the calculated forces at the motor shafts. A safety factor of "1.5" was applied to the calculated forces, and the motor selection was based on these new forces. These values can be seen in Table 4-4.

The Wantai NEMA 17 stepper motor was selected to use in this sub-system as the maximum radial force allowed on the motor shaft was 28 N. This value was above the calculated forces that were present on the motor shafts in this sub-system. Two TB6560 Stepper Motor Drivers were selected to control these stepper motors. The voltage supplied to the stepper drivers and stepper motors were controlled using a power supply that can account for the total amperage (0.8 A) and voltage (12 V) required for the NEMA 17 stepper motors. An LRS Compact 24 V 6.5 A 156 W PSU was selected for this electric design to control the motors' voltage in this sub-system. Table 4-5 displays the electrical components used in this sub-system with specifications for each component. Appendix B.8, B.9 and B.10 contain the datasheets for the components specified in Table 4-5.

Table 4-5: Layout Control sub-system specifications for electrical components

Component	Quantity	Specification
Wantai NEMA 17 Stepper Motor	2	Step angle: 1.8° Voltage: 12 V Current: 0.4 A Holding Torque: 0.28 Nm Weight: 0.2 kg Max Axial Force: 10 N Max Radial Force: 28 N Appendix: B8
TB6560 Stepper Motor Driver	2	Operating voltage: 10 V to 35 V Rated output: ±3 A Selectable excitation modes: 1/1, 1/2, 1/8, 1/16 step Appendix: B9
LRS Compact 24V 6.5A 156W PSU	1	Output Voltage: 24 V Output Current: 6.5 A Power: 156 W Input Voltage: 170 – 264 VAC Efficiency: 89% Appendix: B10

This electrical system operated using mains power from a wall socket. This ran to the power supply, which stepped down the socket voltage to 12 V. This power supply was directly connected to two stepper drivers connected to the NEMA 17 stepper motors. These drivers controlled the motors by limiting the amount of current supplied to the stepper motors to a value of 0.4 A. Furthermore, these stepper drivers received instructions from an Arduino microcontroller which was programmed using a computer system. When the Arduino required the stepper motors to rotate, they communicated with the stepper drivers. The stepper drivers then make the stepper motors rotate to the specified position. This rotated the ASKA3D Plate and LCD screen, respectively. The electrical connections for this sub-system are given by a flow diagram seen in Figure 4-13.

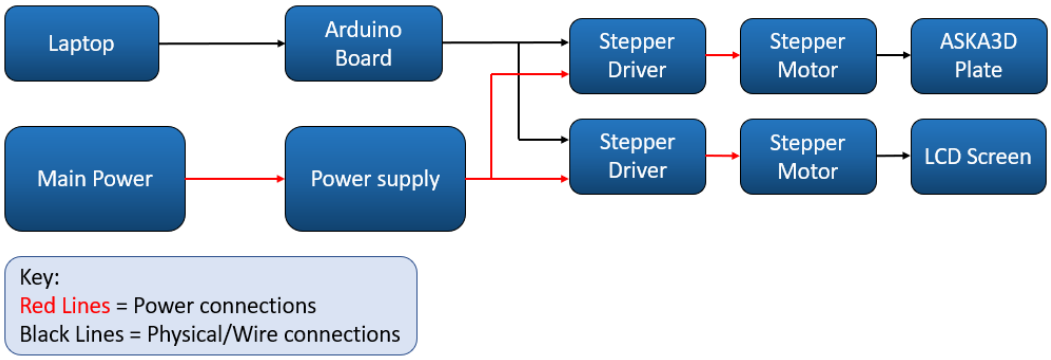

Figure 4-13: Flow diagram of electrical connections for the Layout Control sub-system

The electrical components of this sub-system required a control code to operate as intended. In Section 5.2 of the dissertation, this sub-system's operation is described, and the control code presented.

4.3.5 Manufacture and assembly of the sub-system

The manufacture of the Layout Control sub-system components is explained using Table 4-6. Afterwards, the assembly method for this sub-system is described with the aid of an assembly precedence diagram (Figure 4-14) and corresponding table (Table 4-7).

4.3.5.1 Sub-system manufacture

Table 4-6 presented the process used to manufacture each component, the post-processing performed, the manufacturing method's tolerances and the drawing number for the component in Appendix H. University equipment was used to manufacture 3D printed components. Components that were purchased and not manufactured were recorded as “NA” under the “Process” column of Table 4-6.

Table 4-6: Manufacturing table of the Layout Control sub-system

#	Component	Process	Post-processing	Tolerances	Drawing No.
1	LCD Screen	NA	Disassembly of AOC Portable USB Monitor.	NA	NA
2	LCD Screen Front Cover	3D Printing	Sanding of surface	± 0.25 mm	B4
3	LCD Screen Back Cover	3D Printing	Sanding of surface	± 0.25 mm	B5
4	ASKA3D-200NT Plate	NA	NA	NA	NA
5	Beam Splitter Housing	3D Printing	Sanding of surface	± 0.25 mm	B6
6	Motor and Bearing Shaft Connector (LCD Screen)	3D Printing	Sanding of surface	± 0.25 mm	B7
7	Motor and Bearing Shaft Connector (ASKA3D Plate)	3D Printing	Sanding of surface	± 0.25 mm	B7
8	Bearing Shaft	Metal extrusion	None	± 0.5 mm	B8
9	Bearing Housing	3D Printing	Sanding of surface	± 0.25 mm	B9
10	M5 Ball Bearing	NA	NA	NA	NA
11	NEMA 17 Stepper Motor	NA	NA	NA	NA

4.3.5.2 Sub-system assembly

The following steps were taken for the assembly of the Layout Control sub-system. Additionally, this assembly was shown using an exploded view of this sub-system in Appendix H, drawings B2 and B3.

1. The AOC E1659FWU 15.6" Portable USB Monitor was disassembled with the LCD screen, motherboard and USB port removed from the monitor.
2. The LCD screen was mounted within the LCD Screen Font Cover with the motherboard, and the USB port mounted on the LCD Screen Back Cover. The Front and Back Cover of the LCD Screen was fixed together using four screws, positioned at the cover's corners.
3. Two Motor and Bearing Shaft Connectors were mounted to the LCD Screen cover at the specified mounting points using four nuts and bolts.
4. The NEMA 17 stepper motor was then connected to the LCD Screen's left side using the attached Connector. The motor shaft was placed within the connector and held in place using a grub screw.
5. The Bearing Shaft component was connected on the right side of the LCD Screen using the attached Connector. The Bearing Shaft was placed within the connector and held in place using a grub screw.
6. A ball bearing was then fitted into the Bearing Housing component. This was then fitted onto the Bearing Shaft component attached to the LCD Screen via the Connector component.

At this stage, all the components used for LCD screen rotation were fully assembled. What followed was the assembly of the components used for the rotation of the ASKA3D Plate

7. The ASKA3D-200NT Plate was purchased from ASKA3D™ and inserted into the Beam Splitter Housing component.

8. Two Motor and Bearing Shaft Connectors were mounted to the Beam Splitter Housing component at the specified mounting points using four nuts and bolts.
9. The NEMA 17 stepper motor was then connected to the Beam Splitter Housing's right side using the attached Connector. The motor shaft was placed within the connector and held in place using a grub screw.
10. The Bearing Shaft component was connected on the Beam Splitter Housing's left side using the attached Connector. The Bearing Shaft was placed within the connector and held in place using a grub screw.
11. A ball bearing was then fitted into the Bearing Housing component. This was then fitted onto the Bearing Shaft component which was attached to the Beam Splitter Housing via the Connector component.

Figure 4-14 displayed an assembly precedence diagram for the Layout Control sub-system. Table 4-7 provided the descriptions and quantities of the components shown in Figure 4-14.

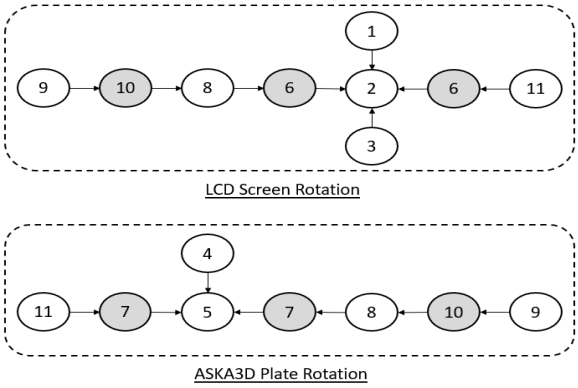

Figure 4-14: Assembly precedence diagram for the Layout Control sub-system

Table 4-7: Resources for the assembly precedence diagram (Layout Control sub-system)

Item	Component Name	Quantity
1	LCD Screen	1
2	LCD Screen Front Cover	1
3	LCD Screen Back Cover	1
4	ASKA3D-200NT Plate	1
5	Beam Splitter Housing	1
6	Motor and Bearing Shaft Connector (LCD Screen)	2
7	Motor and Bearing Shaft Connector (ASKA3D Plate)	2
8	Bearing Shaft	2
9	Bearing Housing	2
10	M5 Ball Bearing	2
11	NEMA 17 Stepper Motor	2

At this stage, the Layout Control sub-system was fully assembled and was ready to be mounted onto the Height Control sub-system at the designated mounting points.

4.4 Height Control sub-system

The purpose of this sub-system was to change the height position of the ASKA3D Plate and LCD screen to match the user height range for users operating the system. It should be noted that the ASKA3D Plate and LCD screen remain at a fixed distance of 100 mm apart. Specifications for the height of these two components were given from the ground to the centre of the ASKA3D Plate (Appendix B.2). The ASKA3D Plate is at the highest point in the system.

These two components required automatic height adjustment, as manually adjusting the height can result in inaccuracies due to human error. Therefore, the system was required to move the plate and screen together either upward or downward. To achieve this motion a pair of lead screws and collars were used to move the plate and the screen upward or downward. This lead screw system contained two threaded bars that were rotated by two motors. The two threaded bars each had a pair of collars; the first pair of collars moved the LCD screen component, and the second pair of collars moved the AKSA3D Plate component. When the motors rotate the threaded bars, they simultaneously moved the two pairs of collars either upward or downward depending on the rotation direction.

The user height ranges were calculated for two situations; when the system was used in its standing layout (Figure 4-2) and when the system was used in the seated layout (Figure 4-1). These user height values were measured from the ground to the users' eye level, either seated or standing. A decomposition diagram can be seen in Figure 4-15 showing the expected components of the sub-system.

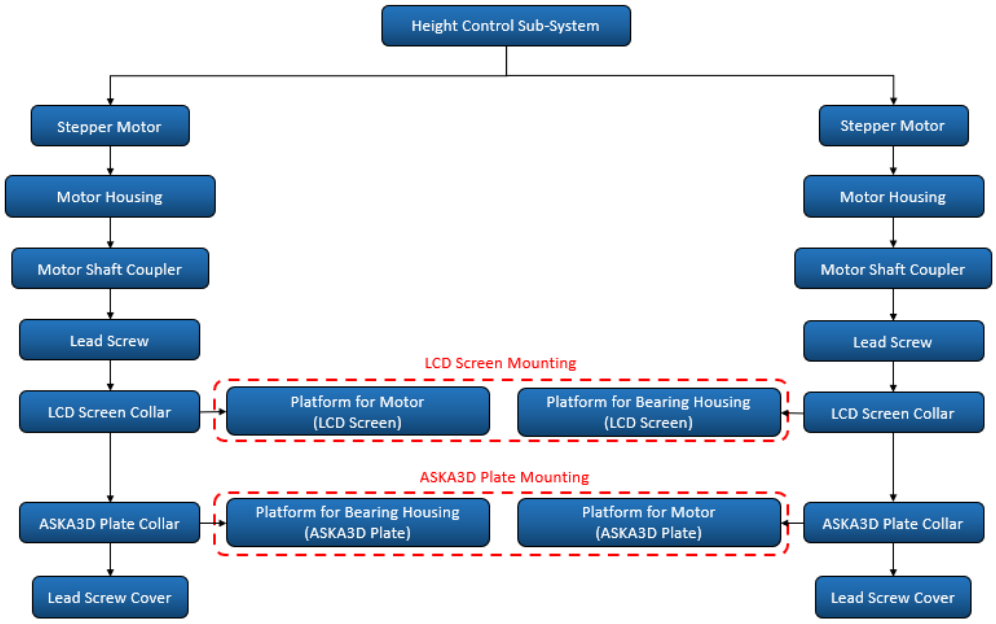

Figure 4-15: Height Control sub-system decomposition diagram

4.4.1 Physical design

The physical design section elaborates on the components used to enable this sub-system's primary function; the height control of the ASKA3D Plate and LCD screen. The decomposition diagram from Figure 4-13 was used to draw the physical components of this sub-system. These components were assembled (Section 4.4.5) to obtain

an indication of the manufactured sub-system. Figure 4-16 displays the fully assembled sub-system. The CAD model of this assembly was presented in Appendix H, drawing number C1.

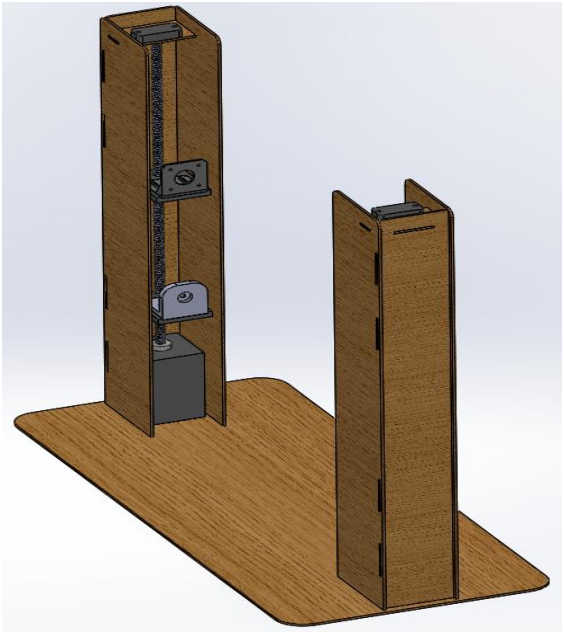

Figure 4-16: Fully assembled Height Control sub-system

The components of this sub-system were explained as follows, including design motivations, component specification and material selection.

4.4.1.1 Components for vertical actuation

The vertical motion was obtained using a lead screw and collar combination; as the lead screw was rotated, the collars on that lead screw move upward or downward depending on the rotation direction. Due to the LCD screen and ASKA3D Plate requiring mounting locations on either side of these components, the following design used two lead screws and four collars to move the LCD screen and ASKA3D Plate. Each lead screw had two collars, the collars located at the lowest point on the lead screws were used to move the LCD screen, and the collars located at the highest point were used to move the ASKA3D Plate. These collars were attached to platform components that were used to mount the Layout Control sub-system.

A directly coupled stepper motor rotated each lead screw. The motor will not experience the weight of the components directly on its motor shaft as spacers were used to withstand the forces from the lead screws. This was done as a precaution as there was a possibility that the axial forces along each lead screw would exceed the allowed axial force for the selected stepper motor. A calculation was performed to determine the possible axial forces on the motor shafts to determine if a spacer was required (Section 4.4.3). Finally, all these components were assembled on a base platform. A labelled diagram can be seen in Figure 4-17 showing the actuation components of this sub-system.

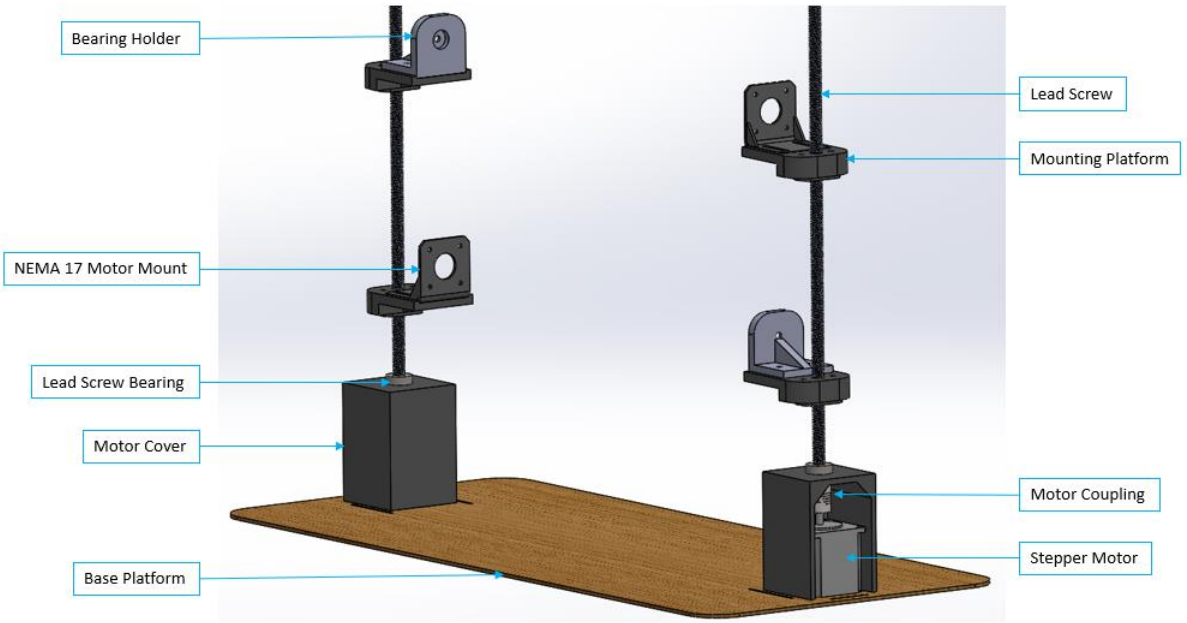

Figure 4-17: Labelled diagram of the Height Control sub-system

System Base

The purpose of the system base was to hold the weight of the mounted components without deflection. A major concern for strength lay in the material selection for this component and its thickness. The System Base had six areas that were used to mount six components of this sub-system. The four holes on either side of the system base were used to mount the sub-system's two stepper motors. This would firmly hold the motors in place, so there was no movement of the motors, that could result in misalignment of the lead screws. The three slots on either side of the system base were used to mount the Lead Screw Cover that was used to hide components and stabilise the lead screws. Finally, the two 'U' shaped grooves on either side of the system base were used as a guide to place the Motor Cover component. There was no need to bolt this component to the base as the grooves will prevent the component from moving along the surface. Additionally, the downward weight of the lead screw and the axial forces of the sub-system will hold this component in place on the System Base. A labelled diagram of this component can be seen in Figure 4-18. The drawing of this component with all its relevant dimensions can be found in Appendix H, drawing number C4.

Figure 4-18: System base

Motor Cover

This component achieved two goals, to enclose the stepper motors mounted to the System Base thus protecting the motors from damage, and withstanding the axial forces present on the lead screw. Two of these components were used in the sub-system, mounted on either side of the System Base. A labelled diagram of this component can be seen in Figure 4-19. The drawing of this component with all its relevant dimensions can be found in Appendix H, drawing number C5.

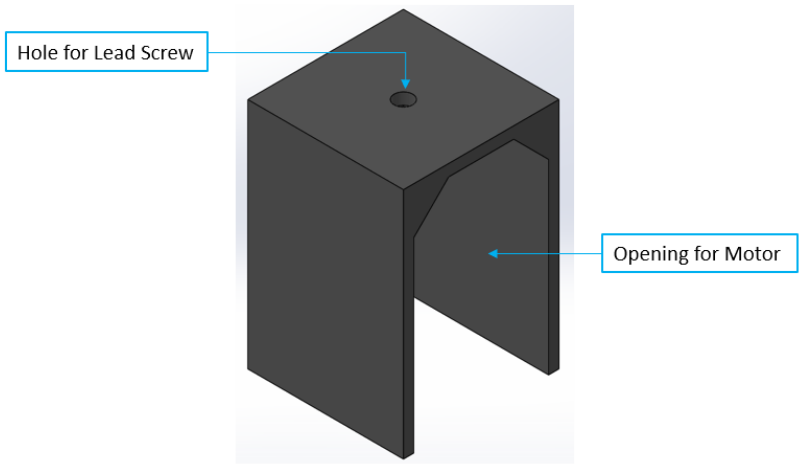

Figure 4-19: Motor cover and lead screw spacer

Stepper Motor and Coupling

Two stepper motors were required to rotate the lead screws in this sub-system. These motors were directly attached to the lead screws using a motor coupling. The stepper motors used in this sub-system were NEMA 23 stepper motors. This selection was made due to the findings from the calculations completed in Section 4.4.3. This motor selection was further elaborated in this sub-system's electrical design section (Section 4.4.4). The two motor couplings that were used in this system were Flexible Aluminium Motor Couplings. The relevant datasheets for these two components can be found in Appendix B.7 and B.12, respectively. The flexible coupling was a safety measure in case failure occurred due to misalignment of the lead screws and motor shafts.

Lead Screw and Collar

The lead screw and collar in this sub-system were the main components contributing to the LCD screen and ASKA3D Plate's vertical movement. Two lead screws were used in this sub-system. Each lead screw had a machined shoulder on each end so that the motor shaft was directly coupled to one end while a bearing was attached to the other end to align the lead screw. The sub-system required four collars, with two collars on each lead screw. The collars on the lower end of the lead screws were level to move the LCD screen, and the collars on the upper end of the lead screws were level so that they could move the ASKA3D Plate. The selected lead screw and collar specifications can be found in Table 4-8 with a labelled diagram seen in Figure 4-20 displaying the lead screw designed for this sub-system. The drawing of the lead screws can be found in Appendix H, drawing number C6. The relevant datasheets for these two components can be found in Appendix B.5 and B.6

Table 4-8: Lead screw and collar specifications

Lead Screw	
Outer Diameter	10 mm
Pitch	2 mm
No. of starts	1
Thread Type	Trapezoidal (30°)
Length	500 mm
Quantity	2
Collar	
Outer Diameter	22 mm
Inner Diameter	10 mm
Length	20 mm
Pitch	2 mm
No. of starts	1
Thread Type	Trapezoidal (30°)
Quantity	4

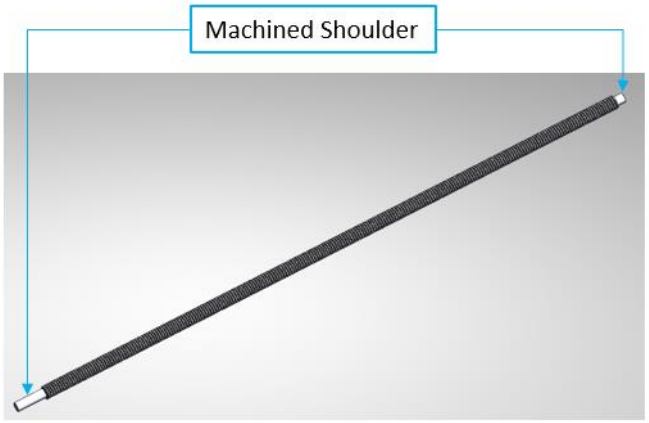

Figure 4-20: Lead screw

Mounting Platform

The Mounting Platform was an essential component of this sub-system. It was responsible for attaching the Layout Control sub-system onto the Height Control sub-system. This component had a main body enclosed around the collars on the lead screw. When the collar moved upward or downward, the main body of this component moved with the collar. The Mounting Platform was designed to attach the NEMA 17 Mounting Bracket and Bearing Housing to this component. This was done to have a single component responsible for mounting the Layout Control sub-system. A labelled diagram of this component can be seen in Figure 4-21. This component's drawings with all their relevant dimensions can be found in Appendix H, drawings C7, C8, C9 and C10.

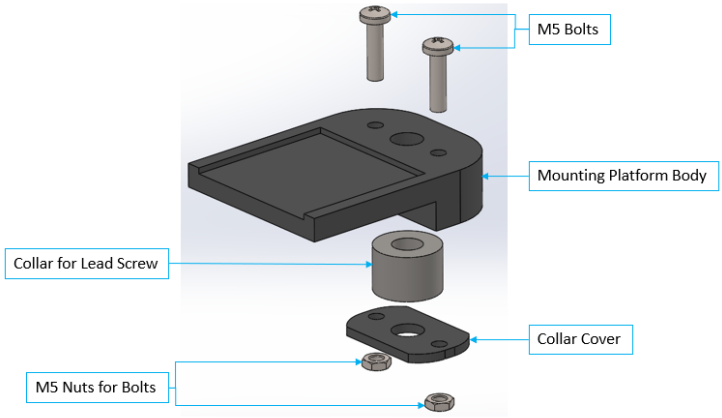

Figure 4-21: Mounting platform

NEMA 17 Mounting Bracket

The NEMA 17 Mounting Bracket was used to securely hold the NEMA 17 stepper motors from the Layout Control sub-system onto the Mounting Platform mentioned above. This component had four holes on which a NEMA 17 motor was mounted, and two guides used to bolt the Mounting Bracket to the Mounting Platform. A labelled diagram of this component can be seen in Figure 4-22. The relevant datasheet for this component can be found in Appendix B.11.

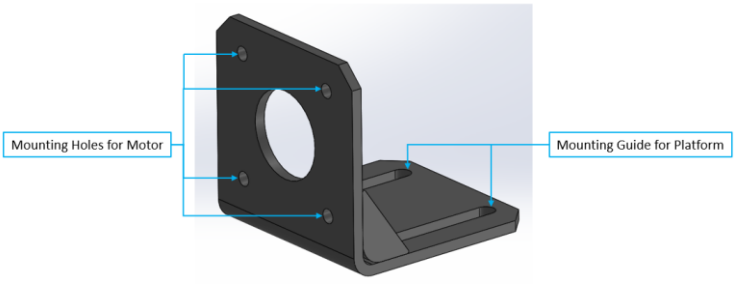

Figure 4-22: NEMA 17 mounting bracket

M8 Ball Bearing

The ball bearing used in this sub-system allowed the rotation of the lead screws when they were mounted on the Motor Covers. When assembled, the ball bearing acted as a spacer between the Motor Covers and lead screws. Each lead screw fitted through a bearing sitting on the Motor Cover and was directly coupled to the motor shaft. Table 4-9 displays the technical specification of the ball bearing used for this application.

Table 4-9: M8 ball bearing specification

Bearing Type	Radial Ball Bearing
Inner Diameter	8 mm
Outer Diameter	22 mm
Thickness	7 mm
Dynamic Load Rating	3.293 KN

4.4.1.2 Components for Lead Screw Cover

The lead screw cover was used to align and securely hold the lead screws in this sub-system. Additionally, these covers concealed the components used for vertical movement of the LCD screen and ASKA3D Plate. This was implemented to conceal any features that might draw the users' attention while viewing the system's mid-air images. If user attention were drawn away from the virtual scenes, the system would have failed to deliver an immersive user experience. The cover was designed as thin sections of Masonite board slotted into each other. Therefore, the weight of each section would hold the cover together. A labelled diagram can be seen in Figure 4-23 showing the Lead Screw Cover and its components. An exploded view of this cover was presented in Appendix H, drawing number C3.

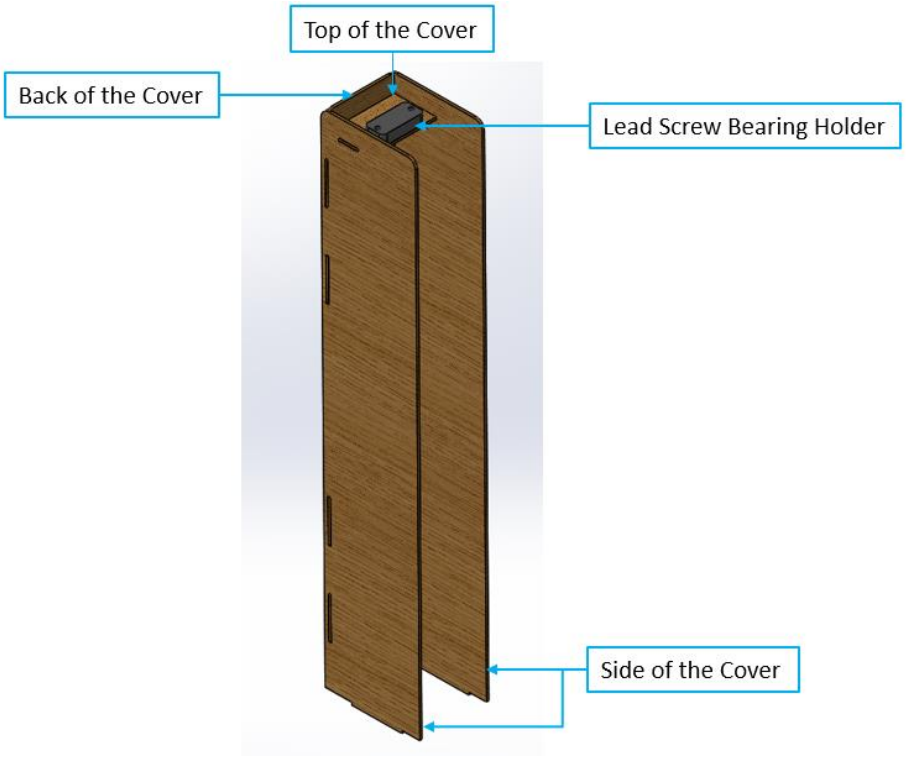

Figure 4-23: Lead screw cover

Side Cover

The Side Cover comprised of four slots to attach the Back Cover, a single slot to attach the Top Cover and a single tab to attach the component to the System Base. The Lead Screw Cover consisted of two Side Cover components. A labelled diagram of this component can be seen in Figure 4-24. The drawing of this component with its relevant dimensions can be found in Appendix H, drawing number C11.

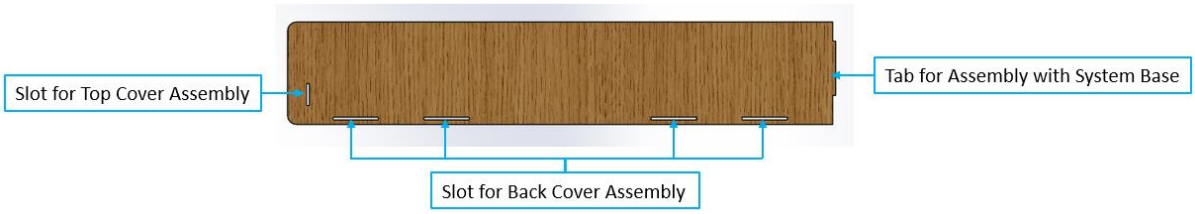

Figure 4-24: Side cover

Back Cover

The Back Cover comprised of eight tabs to attach the two Side Covers, a single slot to attach the Top Cover and a single tab to attach the component to the System Base. A labelled diagram of this component can be seen in Figure 4-25. The drawing of this component with all its relevant dimensions can be found in Appendix H, drawing number C12.

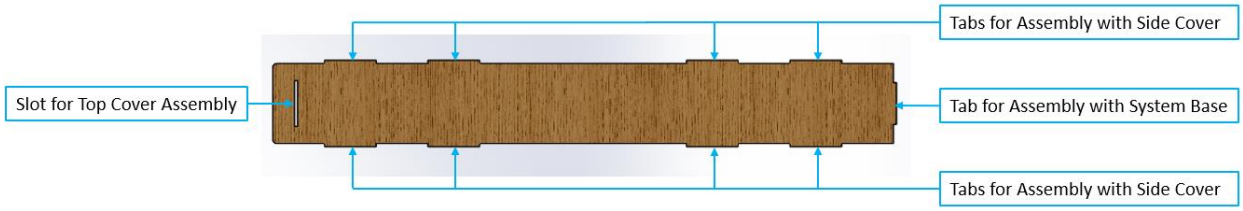

Figure 4-25: Back cover

Top Cover

The Top Cover consisted of three tabs, two of which were attached to the Side Covers and one attached to the Back Cover. Additionally, there were three holes on this component. The hole in the centre was made to fit around the machined end of the lead screw. The other two holes were used to mount the Bearing Holder to align the system's lead screws. A labelled diagram of this component can be seen in Figure 4-26. The drawing of this component with all its relevant dimensions can be found in Appendix H, drawing number C13.

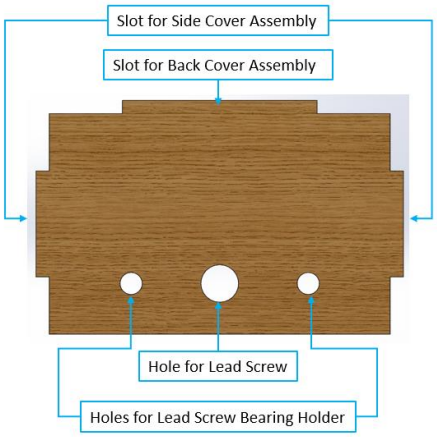

Figure 4-26: Top cover

Bearing Holder

The Bearing Holder was used to mount a bearing on the top end of the lead screw component. This end of the lead screw was machined to securely fit into an M8 ball bearing (Table 4-9). Additionally, this component helped align and securely hold the lead screws in this sub-system. This component was attached to the Top Cover component using a pair of nuts and bolts. A labelled diagram of this component can be seen in Figure 4-27. The drawing of this component with all its relevant dimensions can be found in Appendix H, drawing number C14.

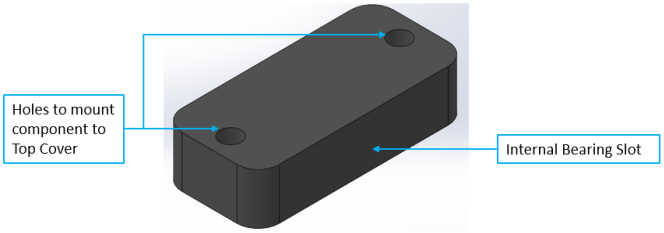

Figure 4-27: Bearing holder

4.4.2 Material selection

This sub-system's components have been described in full, explaining each design's purpose with corresponding diagrams. A detailed explanation was required for each component's material selection; this helped identify methods of manufacture. Additionally, material selection delivered more information on design choices regarding cost, weight reduction and ease of manufacture.

The Height Control sub-system required material selection to follow a lightweight design, thus promoting system portability. The material selected for these components differed based on the necessary function of the component. The material selection carried out for each component can be found in Table 4-10.

Table 4-10: Height Control sub-system material selection

#	Component Name	Quantity	Material	Reasoning
12	System Base	1	Masonite Board	Masonite was a solid hardboard wood selected to withstand the weight of the components of this sub-system.
13	Motor Cover	2	PLA Plastic	3D printing components using this material are more forgiving with minimal warpage issues.
14	NEMA 23 Stepper Motor	2	NA	The stepper motors used in this sub-system would be purchased. Therefore, there was no need to specify its material selection.
15	Flexible Aluminium Motor Coupler	2	Aluminium	This was the standard material for this purchased component.
16	Lead Screw	2	Carbon Steel	This was a purchased component. It was made from this material due to its rigidity and strength.
17	Collar	4	Carbon Steel	This was a purchased component. Its material selection was based on increasing the friction force between the lead screw and collar to promote self-locking.
18	Mounting Platform	4	PLA Plastic	3D printing components using this material are more forgiving with minimal warpage issues.
19	NEMA 17 Mounting Bracket	2	Mild Steel	This was a purchased component. It was made from this material due to its rigidity and strength.
20	M8 Ball Bearings	4	Mild Steel	This was a purchased component. It was made from this material due to its rigidity and strength.
21	Side Cover	4	Masonite Board	This material was selected due to its lightweight and natural visual appeal.
22	Back Cover	2	Masonite Board	This material was selected due to its lightweight and natural visual appeal.
23	Top Cover	2	Masonite Board	This material was selected due to its lightweight and natural visual appeal.
24	Lead Screw Bearing Holder	2	PLA Plastic	3D printing components using this material are more forgiving with minimal warpage issues.

4.4.3 Sub-system considerations and calculations

This sub-system controlled how the viewing method changed with user height. Calculations were performed to obtain values that defined how the sub-system should be used. Additionally, the amount of torque required to rotate the lead screws directly coupled to the NEMA 23 motor shafts were investigated in this sub-system. Finally, a calculation was performed to prove the collar selected for this application was a self-locking collar.

Identifying the effect of user height was investigated under two situations: seated viewing for different user heights and standing viewing for different user heights. A direct relationship between the user height and the ASKA3D Plate height was identified in systems that used the ASKA3D Plate. Therefore, it was theorized that any change in user height would require the ASKA3D Plate and LCD screen to change their height position according to the user height change that would take place. This would hold true for both the standing layout and seated layout of the system. Using the three user height ranges that were specified in Section 4.2.1, it was possible to calculate height changes for the ASKA3D Plate and LCD screen in the sub-system. A base measurement of user height and corresponding system height was needed to calculate the height of the ASKA3D Plate for the different user height ranges.

- Viewing while standing

The datasheet displaying system layouts for the ASKA3D Plate (Appendix B.3) was used to obtain a base measurement of a user height range and corresponding ASKA3D Plate height. A user height between $1500\ mm \leq h \leq 1600\ mm$ required the ASKA3D Plate to be at a height of 850 mm from the ground. It was possible to calculate the height of the ASKA3D Plate for the remaining two ranges using this base measurement (Appendix D.3.1). Table 4-11 displays the height of the ASKA3D Plate for the three user height ranges when users were standing and operating the MR System.

Table 4-11: Standing user height ranges and corresponding height values for the ASKA3D Plate

User Hight Ranges when Standing	Height of ASAK3D Plate
1500 mm $\leq$ h $\leq$ 1600 mm	850 mm
1600 mm $\leq$ h $\leq$ 1700 mm	950 mm
1700 mm $\leq$ h $\leq$ 1800 mm	1050 mm

- Viewing while seated

The datasheet in Appendix B.3 was used to calculate the height of the ASKA3D Plate for different seated height ranges. An initial study was completed to find a factor or a method that would take a user's height while standing and use that value to calculate the height of the ASKA3D Plate when users of these height ranges were seated. This was not possible as two variables have a direct effect on a user's height while seated. These variables were the height of the table used and the height of the chair used. Since all chairs and tables were not made the same, it was impossible to give a standard specification for the height of the ASKA3D Plate when users of the three height ranges were seated. Therefore, new height ranges were calculated for users who were seated. These height ranges would be measured from the ground to the user's eye level when seated at their table. To calculate these new height ranges for seated users, the height of the ASKA3D Plate was predefined. It was possible to calculate the minimum and maximum seated user height ranges working with these defined height values. The predefined

ASAK3D Plate height values were obtained from Table 4-11 as these were height positions that the ASKA3D Plate would already be travelling through. Three user height ranges while seated were calculated in Appendix D.3.2, and the results of these calculations can be seen in Table 4-12.

Table 4-12: Seated user height ranges and corresponding height values for the ASKA3D Plate

User Height Ranges when Seated	Height of ASAK3D Plate
947 mm $\leq$ h $\leq$ 1047 mm	850 mm
1047 mm $\leq$ h $\leq$ 1147 mm	950 mm
1147 mm $\leq$ h $\leq$ 1247 mm	1050 mm

The second consideration in respect of this sub-system was the stepper motor selection. Two key points were considered: whether the stepper motor was able to withstand the axial forces present on the motor shaft when directly coupled to the lead screw and whether the stepper motor had enough torque to rotate the lead screws in the sub-system.

First, the total axial force present on each lead screw was calculated. This calculation can be found in Appendix D.3.3, and the calculated axial force can be seen in Table 4-13. It was found that the motor shaft would need to withstand exactly 14.29 N of axial force, but since this was an approximately calculated value, it was safer to design with a safety factor of "1.5". Therefore, the motor selection considering an axial force of 21.44 N. An initial motor selection was completed and found that motors with an allowable axial force greater than the axial force calculated were too robust and costly for this sub-system. Therefore, the Motor Cover component was designed so that the axial forces on the lead screw would not be directly on the motor shaft but on the Motor Cover. This way, the stepper motor would not experience the axial forces calculated. Therefore, the motor selection was based on the torque required to rotate each lead screw.

Table 4-13: Axial force values along the lead screws

	Axial Force	**Axial Force (**with SF**)**
Right Lead Screw	14.29 N	21.44 N
Left Lead Screw	14.29 N	21.44 N

The torque required to rotate each lead screw was calculated using the axial forces present on the lead screw, the type of lead screw used, and the type of collar used. This torque calculation consisted of two parts: the torque required to raise the collar on the lead screw and the torque required to lower the collar on the lead screw. Since the axial forces were the same on both lead screws, the calculated torque values will apply to both lead screws. These values can be found in Table 4-14, and the full calculation of these values can be found in Appendix D.3.3. Therefore, when selecting a stepper motor for this sub-system, the stepper motor needs to deliver a torque of 0.030 Nm or more.

Table 4-14: Torque values for motor selection

	Required Torque	**Required Torque (**with SF**)**
Raising the Collar	0.020 Nm	0.030 Nm
Lowering the Collar	0.011 Nm	0.017 Nm

Finally, a calculation was done to investigate if the selected collar would be a self-locking collar or an over-hauling collar. An over-hauled collar was a collar that lowers itself when placed under a load. This was due to the low friction between the collar and lead screw. A self-locking collar was desired; it would not lower itself due to a load. This calculation was completed in Appendix D.3.3, and it was found that the collar used in this sub-system was a self-locking collar.

4.4.4 Electrical design

The electrical design of this sub-system enabled the vertical movement of the Layout Control sub-system. This was achieved by rotating the lead screws in this sub-system, which moved the collars on the lead screws upward or downward. This rotation was delivered by stepper motors directly coupled to the lead screws. A stepper motor was selected as the type of motor used for this sub-system to perform accurate and precise height control of the collars.

The Wantai NEMA 23 stepper motor was selected for this sub-system as this motor had a torque rating of 1 Nm. This was above the calculated torque required to both raise or lower the collars on the lead screws. Two TB6560 Stepper Motor Drivers were selected to control the two stepper motors. The voltage supplied to the stepper drivers and stepper motors were controlled using a power supply that can account for the total amperage (4 A) and the voltage (3 V) required for the NEMA 23 stepper motors. An LRS Compact 24 V 6.5 A 156 W PSU was selected for this electrical design to control the voltage to the motors in this sub-system. Table 4-15 displayed the electrical components used in this sub-system with specifications for each component. Appendix B.7, B.9 and B.10 contained the datasheets for the components specified in Table 4-15.

Table 4-15: Electrical components for the Height Control sub-system

Component	Quantity	Specification
Wantai NEMA 23 Stepper Motor	2	Step angle: 1.8° Voltage: 3 V Current: 2 A Holding Torque: 1 Nm Weight: 0.68 kg Max Axial Force: 15 N Max Radial Force: 75 N Appendix: B.7
TB6560 Stepper Motor Drivers	2	Operating voltage: 10 V to 35 V Rated output: ±3 A Selectable excitation modes: 1/1, 1/2, 1/8, 1/16 step Appendix: B9
LRS Compact 24V 6.5A 156W PSU	1	Output Voltage: 24 V Output Current: 6.5 A Power: 156 W Input Voltage: 170 – 264 VAC Efficiency: 89% Appendix: B.10

This electrical system operated using the main power from a wall socket. This ran to the power supply, which stepped down the socket voltage to 3 V. This power supply was connected to two stepper drivers who were connected to the NEMA 23 stepper motors. These drivers controlled the motors by limiting the amount of current supplied to the stepper motors to a value of 2 A. Furthermore, these stepper drivers received instructions from an Arduino microcontroller which was programmed using a computer system. When the Arduino required the stepper motors to rotate, they communicate with the stepper drivers. The stepper drivers then instructed the stepper motors to rotate to the specified position. This rotated the collars on the lead screw, thus moving the platforms on which the Layout Control sub-system was mounted. The electrical connections for this sub-system were given by a flow diagram seen in Figure 4-28.

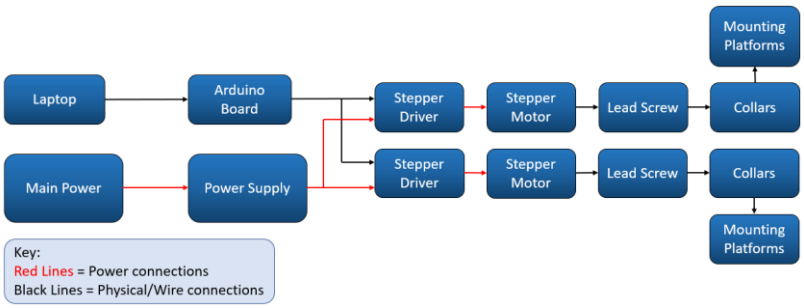

Figure 4-28: Flow diagram of electrical connections for the Height Control sub-system

The electrical components of this sub-system required a control code to operate as intended. In Section 5.2 of the dissertation, this sub-system's operation is described, and a control code presented.

4.4.5 Manufacture and assembly of the sub-system

The methods used to manufacture the designed components for the Height Control sub-system is tabulated. Afterwards, the method of assembly for this sub-system is described with the aid of an assembly precedence diagram.

4.4.5.1 Sub-system manufacture

Table 4-16 presented the process used to manufacture each component, post-processing performed, the manufacturing method's tolerances and the drawing number for the component in Appendix H. University equipment was used to manufacture 3D printed components. Components that were purchased and not manufactured were recorded as “NA” under the “Process” column of Table 4-16.

Table 4-16: Manufacturing table of the Height Control sub-system

#	Component	Process	Post-processing	Tolerances	Drawing No.
12	System Base	Laser Cutting	Painting of surface	± 0.13 mm	C4
13	Motor Cover	3D Printing	Sanding of surface	± 0.25 mm	C5
14	NEMA 23 Stepper Motor	NA	None	NA	NA
15	Flexible Aluminium Motor Coupler	NA	None	NA	NA
16	Lead Screw	NA	Machining of ends	± 0.5 mm	C6
17	Collar	NA	None	NA	NA
18	Mounting Platform	3D Printing	Sanding of surface	± 0.25 mm	C7
19	NEMA 17 Mounting Bracket	NA	None	NA	NA
20	M8 Ball Bearings	NA	Press fitting on machined lead screws	NA	NA
21	Side Cover	Laser Cutting	Painting of surface	± 0.13 mm	C11
22	Back Cover	Laser Cutting	Painting of surface	± 0.13 mm	C12
23	Top Cover	Laser Cutting	Painting of surface	± 0.13 mm	C13
24	Lead Screw Bearing Holder	3D Printing	Sanding of surface	± 0.25 mm	C14

4.4.5.2 Sub-system assembly

The following steps were taken to assemble the Height Control sub-system. This assembly was shown using the exploded views of this sub-system which can be found in Appendix H, drawings C2 and C3.

1. The System Base was placed on a level surface.
2. The two NEMA 23 stepper motors were then attached to the System Base using M5 nuts and bolts.
3. Two Flexible Aluminium Motor Couplers were then attached to the NEMA 23 motor shafts.
4. The Motor Covers were placed over the NEMA 23 motors into the grooves on the System Base.

At this stage, the lead screws were prepared to mount onto the Motor Cover. Afterwards, they were directly coupled to the motor shafts.

5. The four Collars were placed within the Mounting Platform components and then sealed.
6. Two Mounting Platforms were mounted on each lead screw. When comparing the two lead screws, the Mounting Platforms on each lead screw were level with a 100 mm height difference between each pair of Mounting Platforms.
7. An 8 mm diameter radial ball bearing was then fitted on the longer machined end of each lead screw.
8. The two lead screws were mounted onto the Motor Covers, and the Flexible Couplers were tightened around the machined lead screw ends.
9. Each pair of Moving Platforms had a Bearing Housing, and NEMA 17 Motor Mount fixed to the component using nuts and bolts.

At this stage, the Height Control sub-system was ready to mount the Layout Control sub-system. Before this was completed, the Lead Screw Covers were assembled and attached to the System Base.

10. Two lead screw covers were assembled by slotting in the tabs for the Back, Side and Top Covers together.
11. Two M8 ball bearings were then slotted into the Bearing Holder components before each one was mounted onto the Top Cover of the lead screw covers.
12. Once assembled, the two covers were then slotted into the System Base at the specified slots ensuring the top end of the lead screw slides into the bearing at the top of the cover.

Figure 4-29 displays an assembly precedence diagram for the Height Control sub-system. Table 4-17 provided the descriptions and quantities of the components shown in Figure 4-29.

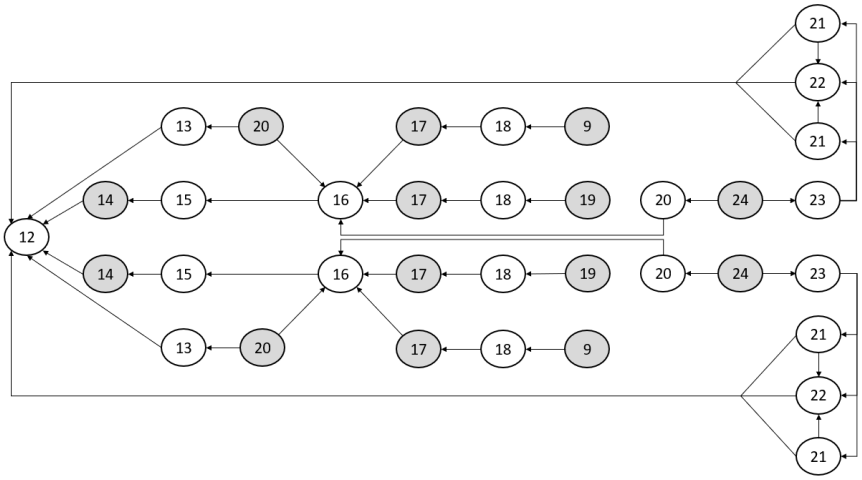

Figure 4-29: Assembly precedence diagram for the Height Control sub-system

Table 4-17: Resources for the assembly precedence diagram (Height Control sub-system)

Item	Component Name	Quantity
12	System Base	1
13	Motor Cover	2
14	NEMA 23 Stepper Motor	2
15	Flexible Aluminium Motor Coupler	2
16	Lead Screw	2
17	Collar	4
18	Mounting Platform	4
19	NEMA 17 Mounting Bracket	2
20	M8 Ball Bearings	4
21	Side Cover	4
22	Back Cover	2
23	Top Cover	2
24	Lead Screw Bearing Holder	2

At this stage, the Height Control sub-system was fully assembled and ready to be mounted onto the System Stand at the designated mounting points.

4.5 System Stand

The purpose of this sub-system was to house the electrical components used to actuate the stepper motors in the Layout Control and Height Control sub-systems. While an electrical control box can be bought to accomplish the same outcome, it would not create a cohesive system as a purchased electrical box would not fit the current system architecture. Therefore, the System Stand was designed to serve two goals, safely housing all the electrical components and securely holding the weight of the Layout Control and Height Control sub-systems. This acted as the MR System base; this was a large and rigid design made to remain level. This control box required space to house all the electrical components with the corresponding wires. This sub-system's main consideration lay in its ability to keep the electrical components from overheating by providing regular airflow. A decomposition diagram can be seen in Figure 4-30 showing the expected components of the sub-system.

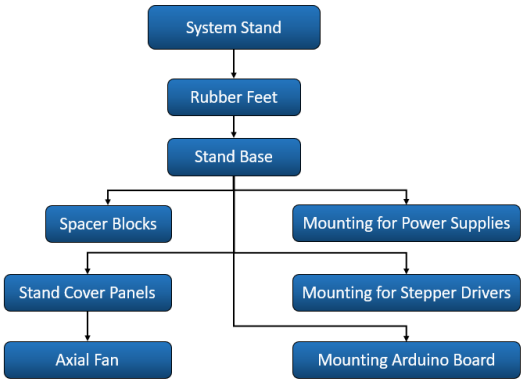

Figure 4-30: Decomposition diagram of the System Stand

4.5.1 Physical design

The physical design section elaborated on the components designed to safely store the previous two sub-systems' electrical components and provide a base onto which the Height Control sub-system can be mounted. The decomposition diagram from Figure 4-30 was used to draw the physical components of this sub-system. These components were assembled to obtain an indication of how the sub-system would look once manufactured. Figure 4-31 displayed the fully assembled sub-system, and the CAD model for this assembly was presented in Appendix H, drawing number D1.

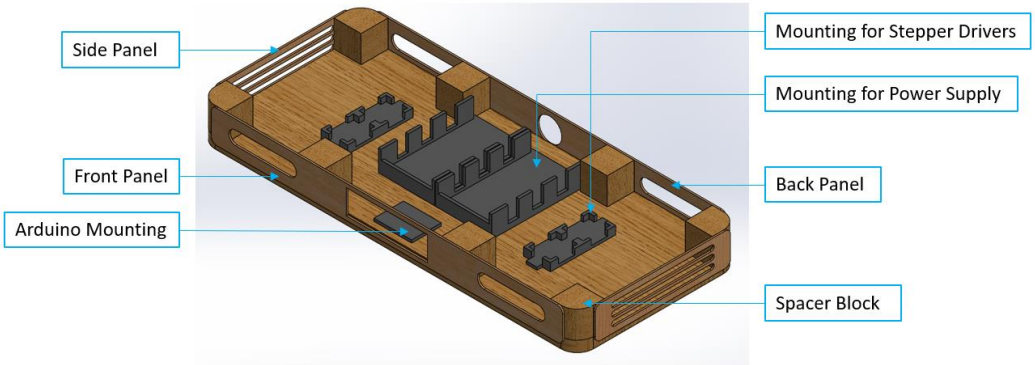

Figure 4-31: Fully assembled System Stand

The components of this sub-system are explained, including design motivations, component specification and material selection.

Stand Feet

The purpose of this component was to elevate the entire system from sitting flush with the ground. This assisted with the transportation of the MR System. Additionally, rubber feet were used to prevent any slippage and resist any instantaneous force acting to slide the sub-system. This was a purchased component.

Stand Base

This component was used to provide a solid and rigid surface that was the System Stand's base. This component was designed to be large and thick enough to hold the previous two sub-systems' weight without deflection. Additionally, this created a large enough area to house all the electrical components of this system without overcrowding the components and wires. The drawing of this component with all its relevant dimensions can be found in Appendix H, drawing number D3.

Spacer Blocks

This component provided an adequate gap between the Stand Base and the System Base component. This delivered ample height to house the components and wires that were placed within this sub-system. There were two types of Spacer Blocks used for this sub-system; one was a standard cube, while the other was a cube that had a single chamfered curve on one corner. This second type of Space Block was used at the corners of the System Stand to correspond to the systems architecture of having soft curves in its design. There was a total of four curved Spacer Blocks and four cube Spacer Blocks, this can be seen in Figure 4-31. The drawing of this component with all its relevant dimensions can be found in Appendix H, drawing number D7.

Stand Panels

These components completed the System Stand structure by covering the open areas around the stand and protecting the electrical components within. While performing this task, these components prioritised cooling the electrical components within. These panels contained numerous slots creating open areas for airflow to take place. When the MR System is in operation, electrical components would generate heat and required natural airflow to help cool down the environment around these components. Without this consideration the sub-system ran the risk of becoming a fire hazard. A labelled diagram of these components can be seen in Figure 4-32. The drawings of these components with all their relevant dimensions can be found in Appendix H, drawings D4, D5 and D6.

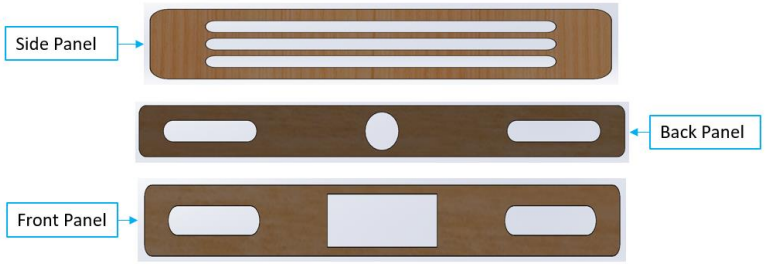

Figure 4-32: System Stand panels

Power Supply Holder

Two power supplies were required to operate the stepper motors in this system. These were housed within the System Stand. Power supplies cannot be placed in an environment without considering the possible hazards involved. Therefore, two issues were identified; these components needed to be fixed to the Stand Base, and they required cool air temperature to prevent overheating. Keeping the components fixed prevented them from moving within the control box and colliding with other components. Keeping them at a cool temperature prevented possible fire hazards. This was done using a heat conducting material that separated the power supplies from direct contact with the Stand Base and allowing airflow over the power supplies. This removed any stagnant hot air in the System Stand. The Power Supply Holder component securely held the power supplies used in this sub-system while providing an open design allowing natural heat dissipation. A diagram of this component can be seen in Figure 4-33. The drawing of this component with all its relevant dimensions can be found in Appendix H, drawing number D8.

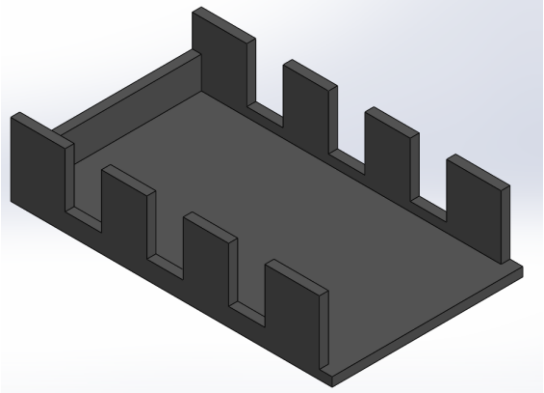

Figure 4-33: Power supply holder

Stepper Driver Holder

This component was used to prevent the Stepper Drivers in this sub-system from overheating while securing the drivers to the Stand Base. Each Stepper Driver Holder housed two stepper drivers. Since this system used four stepper drivers, two of these components were required for this sub-system. This was an open housing design that allowed natural heat dissipation to the surrounding environment. A diagram of this component can be seen in Figure 4-34. The drawing of this component with all its relevant dimensions can be found in Appendix H, drawing number D9.

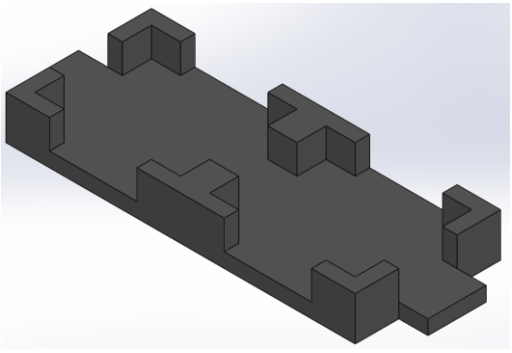

Figure 4-34: Stepper driver holder

Arduino Spacer Block

The Arduino Spacer Block component securely fixed the Arduino board used to control the motors in this sub-system to the System Stand Base. The drawing of this component with all its relevant dimensions can be found in Appendix H, drawing number D10.

4.5.2 Material selection

The components for this sub-system have been described in full, explaining each design's purpose with corresponding diagrams. A detailed explanation was required for each component's material selection; this helped identify methods of manufacture. Additionally, material selection delivered more information on the choice of design regarding cost, weight reduction and ease of manufacture.

The System Stand required stringent material selection due to this sub-system acting as the MR System's control box. These materials were selected to create a low-risk environment with no direct contact between electrical components and flammable materials. The material selection carried out for each component can be found in Table 4-18.

Table 4-18: Material selection for the System Stand

#	Component Name	Quantity	Material	Reasoning
25	Stand Feet	4	Rubber	Rubber feet was selected due to their high friction properties with surfaces. This will prevent the system from sliding on surfaces uncontrollably.
26	Stand Base	1	Plywood Board	Plywood was selected due to its rigidity and strength properties that it grants at large sizes.
27	Stand Side Panel	2	Masonite Board	This material was selected due to its lightweight and natural visual appeal.
28	Stand Back Panel	1	Masonite Board	This material was selected due to its lightweight and natural visual appeal.
29	Stand Front Panel	1	Masonite Board	This material was selected due to its lightweight and natural visual appeal.
30	Spacer Block	8	Plywood	Plywood was selected due to its density and would perfectly perform as a spacer block without adding excessive weight to the system.
31	Power Supply Holder	2	PLA Plastic	3D printing components using this material are more forgiving with minimal warpage issues.
32	Stepper Driver Holder	2	PLA Plastic	3D printing components using this material are more forgiving with minimal warpage issues.
33	Arduino Base Platform	1	PLA Plastic	3D printing components using this material are more forgiving with minimal warpage issues.

4.5.3 Sub-system considerations and calculations

The major focus of this system was to reduce the overall heat generated by the electrical components during system actuation.

The air temperature within the System Stand was regulated in two ways. An axial fan was positioned on the Back Panel to remove the hot air generated by the Power Supplies. These were a major source of heat generation compared to the other electrical components in the sub-system. The panels around the System Stand (Figure 4-32) allowed airflow over the components, thus negating any issue by keeping this volume partially open. The specifications of the axial fan used can be found in Table 4-19. The datasheet for this component can be found in Appendix B.15.

Table 4-19: Axial fan specifications

Name	SUNON 12 V 4010 Silent Axial Fan
Operating Current	12 V
Operating Voltage	0.31 mA
Power Connector	2 Pins
Dimensions	40 x 40 x 10 mm

4.5.4 Electrical design

There was no specific electrical design required for the System Stand as there was no actuation present in this sub-system. The only component in this sub-system that required an electrical design was the axial fan used for air circulation. This was a simple electrical design where the axil fan was powered by a 9 V battery pack that ran through a switch connected to the fan (Figure 4-35). Users could control when to use the fan to conserve battery life.

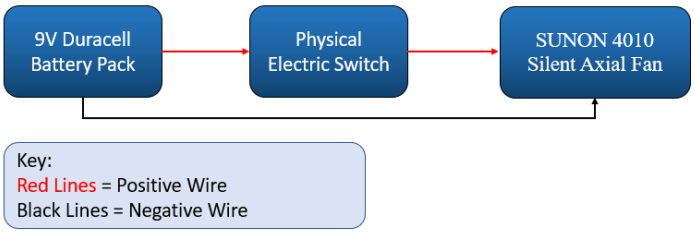

Figure 4-35: Flow diagram of electrical connections for the axial fan

4.5.5 Manufacture and assembly of the sub-system

The methods used to manufacture the designed components for the System Stand are tabulated. Afterwards, the assembly method for this sub-system is described with the aid of an assembly precedence diagram.

4.5.5.1 Sub-system manufacture

Table 4-20 presented the process used to manufacture each component, post-processing performed, the manufacturing method's tolerances and the drawing number for the component in Appendix H. University equipment was used to manufacture 3D printed components. Components that were purchased and not manufactured were recorded as “NA” under the “Process” column of Table 4-20.

Table 4-20: Manufacturing table of the System Stand

#	Component	Process	Post-processing	Tolerances	Drawing No.
25	Stand Feet	NA	NA	NA	NA
26	Stand Base	Rough Lumber Sorting	Filleting corners of the base.	± 1 mm	D3
27	Side Panel	Laser Cutting	Painting of surface.	± 0.13 mm	D4
28	Back Panel	Laser Cutting	Painting of surface.	± 0.13 mm	D5
29	Front Panel	Laser Cutting	Painting of surface.	± 0.13 mm	D6
30	Spacer Blocks	Rough Lumber Sorting	Filleting a single corner of four blocks out of eight.	± 0.5 mm	D7
31	Power Supply Holder	3D Printing	None.	± 0.25 mm	D8
32	Stepper Driver Holder	3D Printing	None.	± 0.25 mm	D9
33	Arduino Base Platform	3D Printing	None.	± 0.25 mm	D10
34	Axial Fan	NA	NA	NA	NA

4.5.5.2 Sub-system assembly

The following steps were taken for the assembly of the System Stand. This assembly was illustrated using an exploded view of this sub-system in Appendix H, drawing D2.

1. The four Stand Feet were fixed to the bottom corners of the Stand Base using four screws.
2. The spacer blocks were then fixed onto the Stand base at the specified locations seen in Figure 4-31.
3. The holders for the power supplies, drivers and Arduino were then fixed onto the Stand Base using a set of screws.
4. Afterwards, the power supplies, drivers and Arduino board were placed into the holders.
5. The System Stand panels were attached to the spacers blocks in the system using a set of screws that held the panels in place.
6. Finally, the axial fan, battery pack and switch were mounted to the Back Panel.

Figure 4-36 displays the assembly precedence diagram for the System Stand, while Table 4-21 provided the descriptions and quantities of the components shown in the assembly precedence diagram.

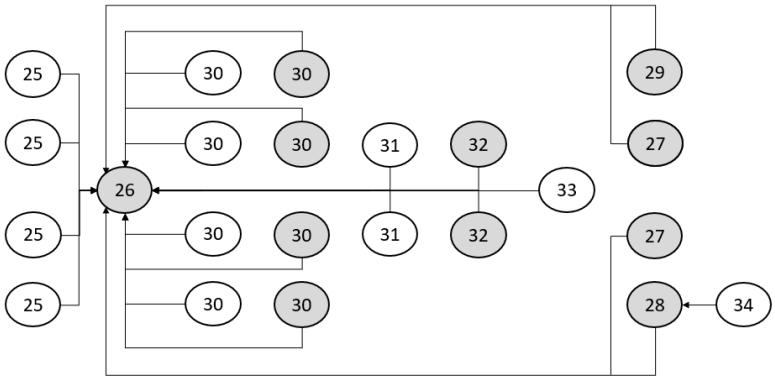

Figure 4-36: Assembly precedence diagram of the System Stand

Table 4-21: Resources for the assembly precedence diagram (System Stand)

Item	Component Name	Quantity
25	Stand Feet	4
26	Stand Base	1
27	Side Panel	2
28	Back Panel	1
29	Front Panel	1
30	Spacer Block	8
31	Power Supply Holder	2
32	Stepper Driver Holder	2
33	Arduino Base Platform	1
34	Axial Fan System	1

At this stage, the System Base from the Height Control Sub-system could be mounted on top of the assembled System Stand. The System Base was held in place using screws fixed into the spacer blocks of the System Stand.

4.6 Mixed Reality System

The sub-systems that were initially identified were fully designed to meet their required functions. Finally, these sub-systems were combined to deliver the completed MR System. An example of the fully assembled MR System can be seen in Figure 4-37 with the CAD models of this assembly presented in Appendix H, drawings A1, A2 and A3.

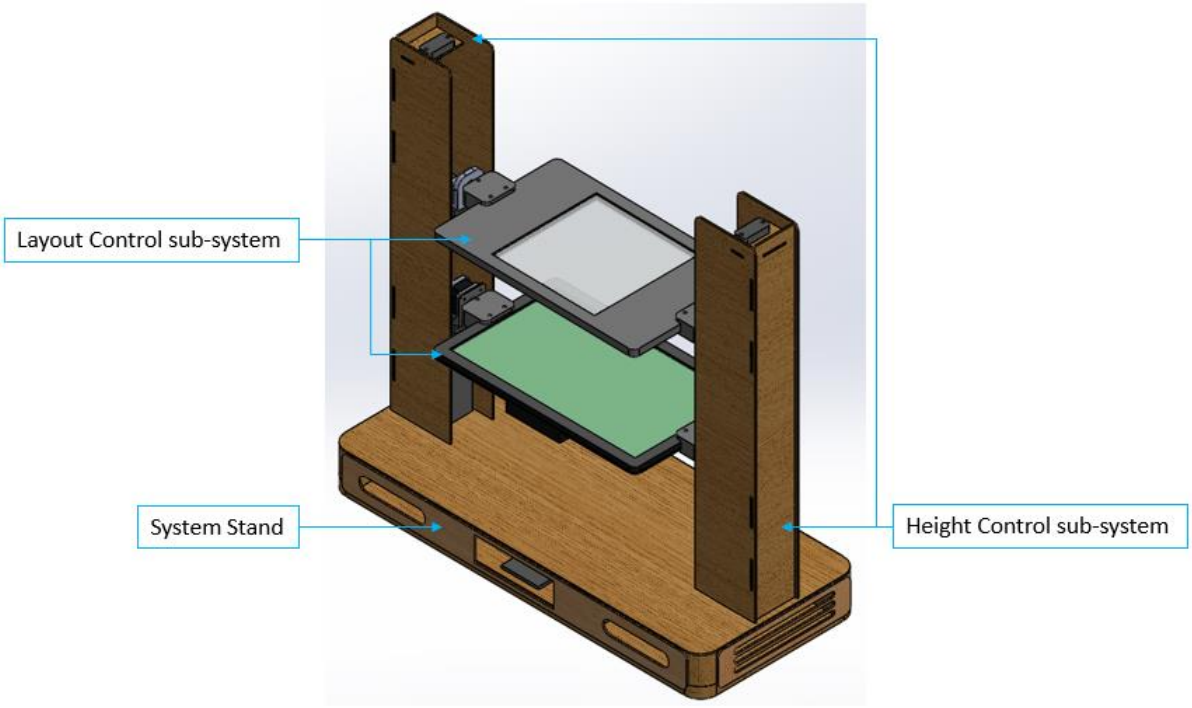

Figure 4-37: Concept of the fully assembled Mixed Reality System

Each sub-system was designed to be assembled with ease by following the exploded views found in Appendix H. Now that the MR System was fully designed, it was manufactured so that testing can be performed to obtain a measurable result of the systems success in meeting the aim and objectives. The system construction is elaborated, including insights obtained, improvements made and accompanying pictures of system construction.

4.6.1 Mixed Reality System construction

Each sub-system was manufactured and assembled as specified in their design chapters. What follows are the insights obtained during the manufacturing and assembly of the MR System.

4.6.1.1 System Stand

Assembly of the MR System started at the System Stand as this was the base of the system. Manufacturing each component was successful with no issues identified. The components used to hold power supplies, motor drivers and Arduino board were not manufactured. Instead, sections of sheet metal were cut to lie between these components and the system base's wooden surface. This was done to save on time and manufacturing cost as the original ‘holder’ components had long printing times. Using sheet metal to separate the electrical components from the base's surface was safer as it reduced the system’s risk as a fire hazard. The components risk of sliding within the System Stand was found to be non-existent. The weight of the power supplies held them in place; they could also be screwed down by a tab provided on the component. The motor drivers were found to keep their

positions due to the tension created from the wires running to the motors and power supplies. The Arduino board was also held in place due to the tension created by the connected wires to the system's stepper drivers.

The wiring of the components started with the power supplies. A three-pin cable was salvaged from a monitor power cable. This was then stripped at the opposite end, exposing the ground, neutral and live wires. These wires were then fed into a terminal that took these three wires as inputs and delivered six wires as the output. The purpose of the terminal was to create a pair of ground, neutral and live wires. These wires were then connected to two power supplies, with each pair going to a single power supply. The four motor drivers were then connected to the power supplies at the voltage ports. Two drivers were set to allow 4 A of current, these drivers were used to control the NEMA 23 stepper motors. The last two drivers were set to allow 0.4 A of current, these drivers were used to control the NEMA 17 stepper motors. The current was set using the stepper driver's datasheet in Appendix B.9. The stepper motors were then connected to their respective drivers using the coil diagrams found in Appendix B.7 (NEMA 23) and Appendix B.8 (NEMA 17). These diagrams dictated the stepper driver pins that the stepper motor wires were connected to. Finally, the drivers were connected to the Arduino board for control. This was done by taking the positive CLK and CW pins from each driver to an input on the Arduino board and taking the negative CLK and CW pins from each driver to a common negative (using breadboards), then connecting it to the negative pin on the Arduino board. Once the wiring was completed, the electronics were tested to ensure current was running to the motors before placing them within the System Stand. Figure 4-38 displayed the manufactured and wired System Stand.

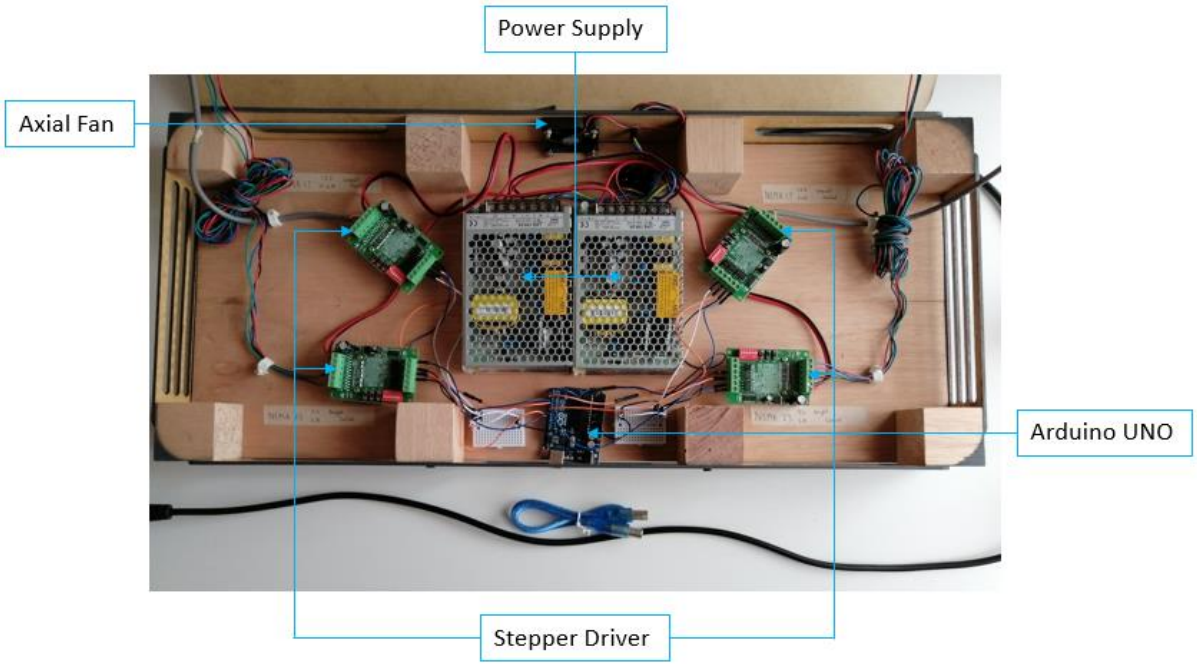

Figure 4-38: Manufacture System Stand

There was a minor change to the position of the switch used to control the axial fan. Due to limited space on the back panel where the axial fan was installed, the switch was attached to the System Base component of the Height Control sub-system (Figure 4-39).

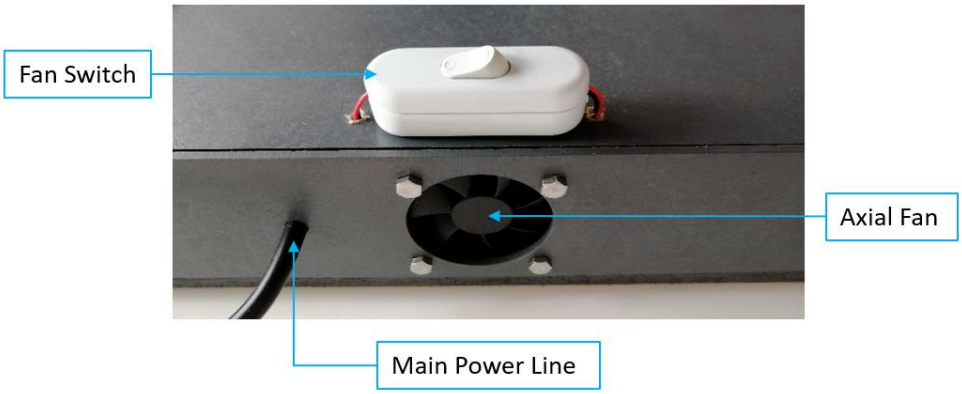

Figure 4-39: Axial fan switch position

4.6.1.2 Height Control sub-system

Upon constructing and wiring the System Stand, the Hight Control sub-system was manufactured, assembled and attached to the System Stand. Manufacturing of the components in this sub-system was successful, with no issues identified. A single addition was made to the sub-system. This was the placement of support blocks under the NEMA 23 motors. Due to the length of the System Base component, the weight of the motors on either side produced a slight deflection of the component. Figure 4-40 displayed the current MR System with the NEMA 23 motors mounted to the System Base without deflection and the wired NEMA 17 motors ready for installation.

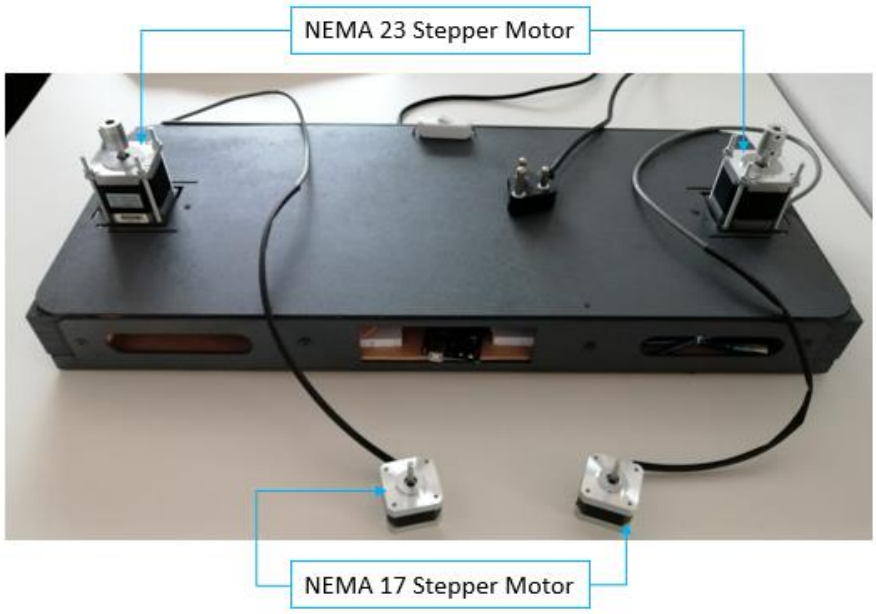

Figure 4-40: Enclosed System Stand with mounted NEMA 23 motors

The completion of the sub-system assembly progressed as described in Section 4.4.5. An example of a single lead screw attached to a motor shaft can be seen in Figure 4-41.

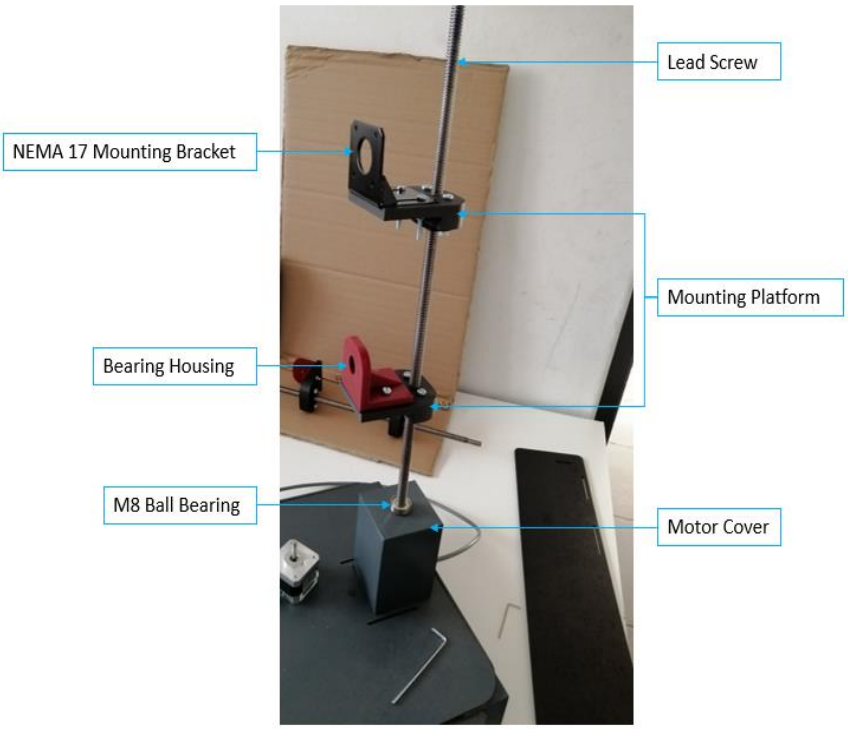

Figure 4-41: Example of a single lead screw during assembly

Due to the flexible motor coupling, the attached lead screw was deflecting and did not remain stable. An improvement to this would lay in using a rigid coupling on the motor shaft. This deflection was expected and corrected using the lead screw covers. When the lead screw covers were attached to the System Base, they held the lead screws in a stable position. It was discovered that the Back Cover component created a small volume for the NEMA 17 motor wires which resulted in the wires obstructing the motion of the Mounting Platforms. Therefore, this component was removed from the lead screw covers. At this stage, the System Stand and the Height Control sub-system have been manufactured and assembled. An example of this structure can be seen in Figure 4-42.

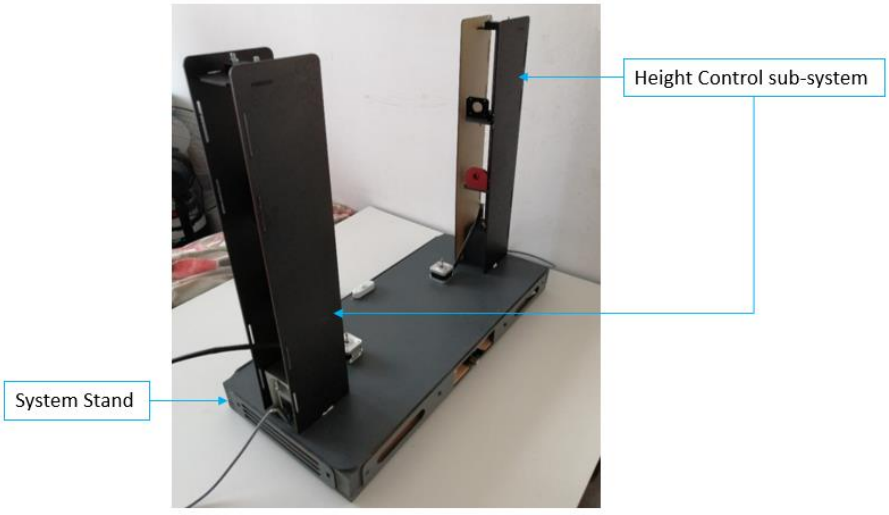

Figure 4-42: Mixed Reality System with the assembled System Stand and Height Control sub-systems

4.6.1.3 Layout Control sub-system

The final step to complete the MR System was assembling the Layout Control sub-system and attaching this sub-system to the current system architecture. Manufacturing the components for the Layout Control sub-system was successful. The assembly of the Layout Control sub-system progressed as expected in Section 4.3.5. A single change was made in the sub-system assembly. The Bearing Holder component was attached to the Mounting Platform and not to the Layout Control sub-system. This improved the method used to mount the components of this sub-system onto the current system architecture. The Layout Control sub-system's assembled components can be seen in Figure 4-43, ready to be attached to the current system (Figure 4-42).

Figure 4-43: Assembled components of the Layout Control sub-system

The Layout Control sub-system was then attached to the current system architecture using the assembly method described in Section 4.3.5. The lead screw covers made it difficult to perform this attachment. Therefore, they were removed when this sub-system was attached and installed afterwards. The designed Mixed Reality System was constructed, and its mechatronic components were operational. The manufactured MR System can be seen in Figure 4-44.

Figure 4-44: Fully manufactured Mixed Reality System

This concluded the hardware design and manufacture of the MR System. This physical system's control code and operation programs are described in Chapter 5, thus completing the MR System design.

4.7 Chapter summary

This chapter presented an MR System design that allowed multi-user viewing by giving users the ability to adjust the systems viewing capability to match their heights and viewing preference. This system focused on accommodating a wide variety of users through the flexibility of its operation. The components that were designed and bought for the system were described with accompanying diagrams, specifications and datasheets. Furthermore, the electrical design of the components used to actuate the system's height and layout were presented and elaborated upon. The chapter concluded with the manufacture and assembly of the hardware and electrical components of the MR System.

The next chapter completed the MR System designed in Chapter 4. The software used for electronic control was discussed and presented along with MR programs developed and explored for MR operations.

5. SOFTWARE DESIGN

5.1 Introduction

The completion of the MR System's physical design left the final half of the design process. This was the software design of the system. The operation of the system is dependent on the system software and not entirely on the physical components.

Currently, the system could deliver mid-air imaging without requiring dedicated software. Connecting a USB cable from the LCD screen to the laptop displayed its desktop screen in mid-air. The system successfully delivered a mid-air image, but this did not provide an advantage over normal computer viewing. Therefore, unique software was required to make full use of the MR System's physical capabilities. The software created would define the system's usage. The MR System creates a platform on which a variety of MR applications can be developed and researched.

There were three main components to the MR System's software: the software required to control the system's automated components, the software required to generate specific MR environments, and the software that allowed interaction with the mid-air images.

5.2 Software for electronic control

This system required a microcontroller to control the electronic components from the Layout and Height Control sub-systems. This was a component that delivered specific instructions to the motors in the system. Users could accurately control the motors in the system using a microcontroller and its corresponding interface to generate code that carried out the specific instructions. An Arduino UNO microcontroller was used to perform precise control of the electronics in the system. Therefore, the software used to control the system's electronics was the Arduino IDE software. The specifications of the Arduino UNO microcontroller were presented in Table 5-1.

Table 5-1: Arduino UNO specifications

Input Voltage	7 to 12 V
Input Voltage Limits	6 to 20 V
Digital I/O Pins	14
PWM Channels	6
Analog Input Channels	6
DC Current per I/O Pin	40 mA
DC Current for 3.3 V Pin	50 mA
Clock Speed	16 MHz

There are two areas in this system that required automated control. The Layout Control sub-system required separate control of two stepper motors, and the Height Control sub-system required simultaneous control of two stepper motors.

5.2.1 Electronic control

The two motors' main objective in the Layout Control sub-system was to perform a 45-degree rotation of the ASKA3D Plate and LCD screen. This was dependant on the layout selected when using the system. Control codes were generated and tested on the Arduino IDE to perform this specific actuation presented in Section 4.2.2. Finally, a single working script was generated and successfully tested on the NEMA 17 motors used in this sub-system. This code enabled the rotation of two NEMA 17 motors to a specified angular position, at the same speed, one motor at a time. This code can be found in Appendix E.1.

The two motors' main objective in the Height Control sub-system was to move the ASKA3D Plate and LCD screen either upward or downward using a lead screw mechanism. This movement aimed to adjust these components to fit the height range of the users on the system. In a lead screw system, the rotation of the motor shaft results in direct linear movement. Therefore, a measure was required relating vertical movement to the motor shafts' rotation in this sub-system. It was possible to determine the vertical movement given from one rotation of the motor shaft using the specifications from Table 4-8. A single start lead screw was used in this system with a 2 mm pitch. This translated into 2 mm of vertical movement for every rotation of the lead screw. It was possible to identify the number of rotations that related to specified vertical movements. This was used to develop different codes to control the rotation of the NEMA 23 motors until a final working code was developed; this code can be found in Appendix E.2. This code simultaneously rotated the two NEMA 23 motors at the same speed and delivered the same number of rotations.

The two scripts mentioned above functioned similarly. They controlled each motor's rotation by specifying the number of steps and its direction by using positive(clockwise) and negative(anti-clockwise) signs in front of the step value. These stepper motors were specified to perform one rotation every 200 steps. This relationship was used to specify precise angle control for the Layout Control sub-system and specify the number of revolutions required in steps to control the Height Control sub-system. Additional specifications were made for the motors' speed to control how fast the shafts rotated. This was physically tested before a final value was obtained.

For the Layout Control sub-system, the control rule followed was 360 degrees, and 200 steps have a directly proportional relationship. Working with this ratio of 360°: 200 steps, it was possible to obtain the number of steps required to perform a 45-degree rotation. Dividing 360 by a value of 4 gives 45. Therefore, by dividing both sides of the ratio by four, the following was obtained; 45°: 25 steps. This meant that a motor instructed to rotate by 25 steps would rotate to a 45-degree angle from its rest position. In this sub-system, the ASKA3D Plate and LCD screen were rotated by 45°. This required 25 steps from the motors to obtain a 45-degree angle displacement on the motor shafts.

The Height Control sub-system's control rule lay in the relationship between the vertical movement required and the number of revolutions needed to obtain that vertical movement. Once the number of revolutions needed was obtained, it was possible to calculate the number of steps required. When users were required to move the ASKA3D Plate and LCD screen by a specific height, the users took this height value and divided it by a value of 2. The value obtained was the number of revolutions required from the stepper motors. Finally, the number of revolutions was multiplied by the number of steps required for a single revolution. This gave the steps required

from the motor shaft to perform the vertical movement on the system. This step value was used to control the motors in this sub-system.

Finally, a single script was generated to control all the electronic components in the MR System. This single script was used to control all four motors in this system. This included key comments in the script that reminded users of general rules to follow when programming the motors in this system. This final script was a combination of the scripts mentioned above and can be found in Appendix E.3.

5.3 Software for Mixed Reality operations

In Section 1.1, virtual technology was identified as a tool for entertainment, education and design. Therefore, these areas were investigated, and software was presented to test each category on the designed MR System.

5.3.1 Entertainment

Virtual technology showed early success as a tool for entertainment (Figure 1-1). This was due to the visual appeal given by this technology. VR and AR devices are used to play a multitude of games made readily available by developers. MR is an emerging technology, and games for these devices are scarce, with the majority being usable on dedicated MR Systems.

Due to the popularity of entertainment features on virtual devices (Figure 1-1), the MR System was tested as a tool for entertainment to determine its success in this field of technology. Game software was developed to test the system as a tool for entertainment. It would be easier to use existing game software, but this was not possible due to the scarcity of MR games. Additionally, it was better to develop a game software that took advantage of the designed MR System's viewing capability.

5.3.2 Entertainment software development

Section 2.4.2 highlighted the current platforms that enabled MR software development. Unity3D™ was selected to create this software due to its design flexibility and its previous history in developing VR, AR and MR programs.

5.3.2.1 Software development

This software design aimed to create an application that would entertain users on the MR System. This was achieved by creating a game that users could play on the system. This game was immersive, using colours and unique structures to draw users in and had a goal that the users needed to achieve. This creates a success and failure model; this is the foundation of most games. Success is the goal, but failure grants the motivation to succeed, thus making it entertaining for users.

The game developed was a 3rd person perspective game where the player was represented as a ball within this game scene. The goal of the game was to make it through all the obstacles in front of the player while the player was under a constant velocity that propelled them forward. The player had no control over their forward velocity; they could only control movement to the left and to the right within the game scene. This game added greater realism to the mid-air image technique of the system. An example of the game scene can be seen in Figure 5-1.

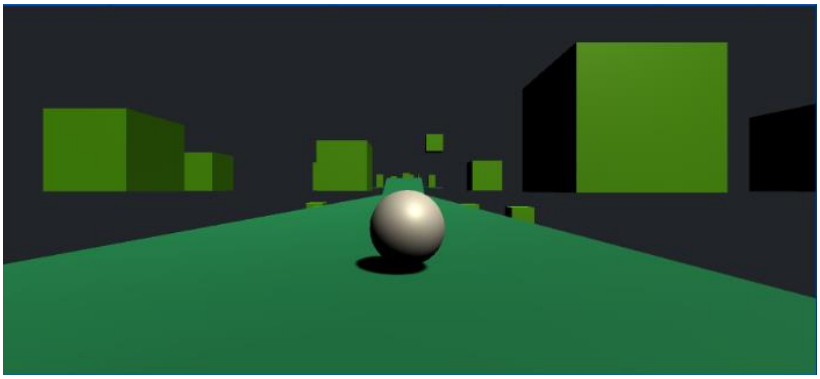

Figure 5-1: Example of the game scene

This game created an illusion of depth by forcing the player to progress further into the mid-air image. Furthermore, it was possible to add a second player to the game, thus creating a collaborative user environment allowing many users on this single device. This game creation took place within the Unity3D™ program. An image of this can be seen in Figure 5-2, displaying the general interface of Unity3D™ while showing the final game within the editor.

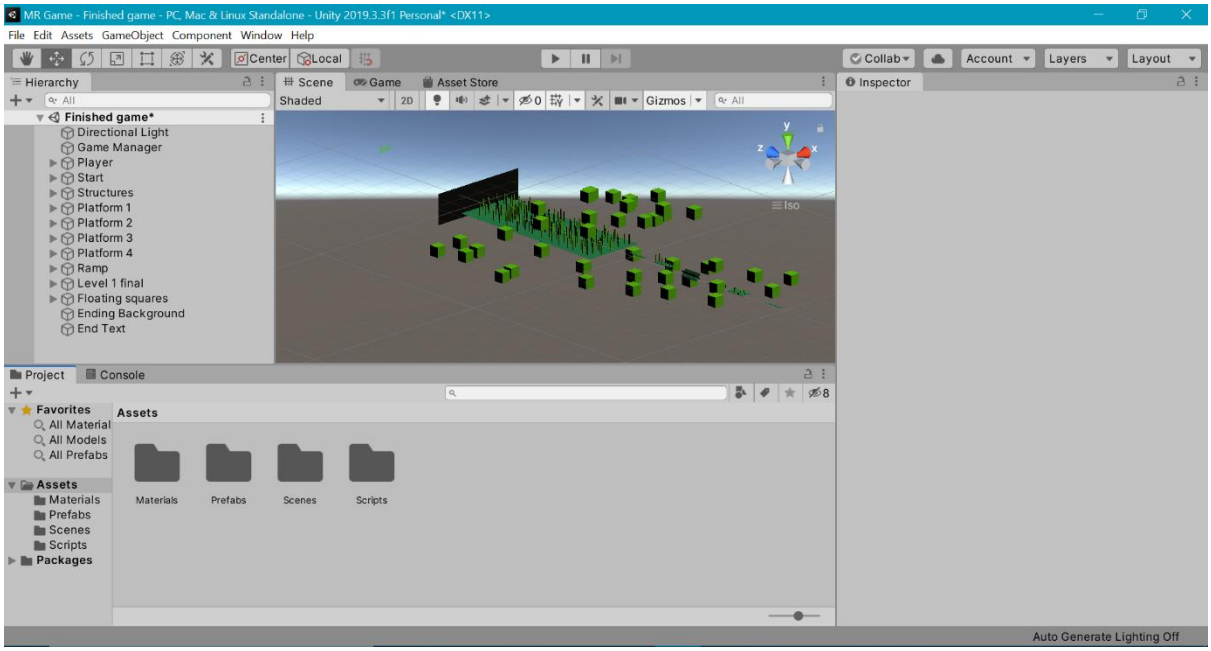

Figure 5-2: Unity3D™ interface example

The 3D objects in this game were created using the base functions on Unity3D™. The physics properties of this game were developed using scripts that imparted these physics properties to the game objects. These physics properties enabled the user to play the game as described above. The first physics property was the rigidbody model that could be attached to objects in Unity3D™. This was a base script on Unity3D™, and it imparted basic physics properties onto 3D objects. Once attached to an object, it was possible to alter that object's physics properties. An image of the rigidbody model when attached to an object can be seen in Figure 5-3. This shows the properties that are controlled when using the rigidbody model.

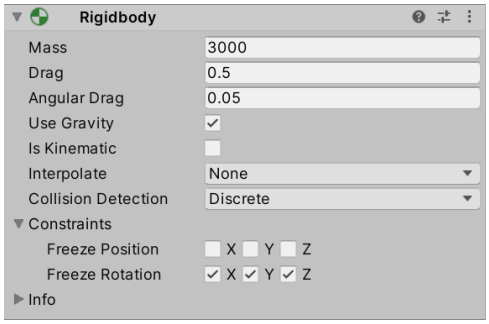

Figure 5-3: Properties of the rigidbody model

The next physics property was a constant velocity attached to the player of the game. This script was created and did not come as a base script with Unity3D™. Therefore, using Microsoft Visual Studio (MVS) it was possible to write out the code for this physics property and implement it within Unity3D™. This script can be found in Appendix F.1. Once this script was attached to an object, it was possible to program a constant velocity along the x, y or z-axis in the game scene. This was in the form of a specified magnitude, with the sign of the value defining the direction the object would travel along the specified axis. An example of the tab generated when this script was attached to an object can be seen in Figure 5-4.

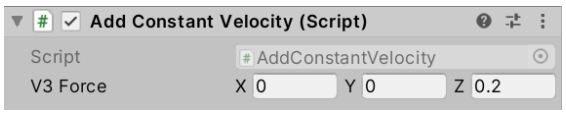

Figure 5-4: Constant velocity script seen within Unity3D™

The final physics property used was a player-controlled velocity. MVS was used to generate the required script (Appendix F.2); this script would allow the designer to specify the magnitude of a velocity applied to an object when the player provided a specific input. There were two inputs the user could provide; one would impart a positive value of the specified velocity, and the other would impart a negative value of the specified velocity. An example of this script, when added to an object, can be seen in Figure 5-5. The user controlled their movement to the left and right within the game scene. This script could be added multiple times to an object to control velocities attached to the object along different axes.

Figure 5-5: Player controlled velocity script seen within Unity3D™

A third script was generated for this game. This script was created to give users the ability to reset the game and start the game from the beginning. This allowed users to replay the game when they failed. The script to achieve this was created in MVS and can be found in Appendix F.3. This script can be added to any object in the game. Once it is added, the designer must select an input that would result in the game resetting. For this game software, the restart key was the letter “R” on the keyboard. An example of this script, when added into Unity3D™, can be seen in Figure 5-6.

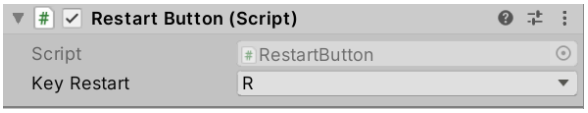

Figure 5-6: Restart button script seen within Unity3D™

Additional programming took place when creating the structures and viewing features in this game. Structures were created using basic functions available on Unity3D™. Third-person perspective viewing was made possible by attaching the camera in the game to the player. Preventing the camera from rotating with the player's rotation was an issue corrected during the game's design. Additionally, the game's physics properties required constant editing to ensure users could complete the game with realistic physics properties.

This software was created and used to test the MR System as a tool for user entertainment. Interaction on this software lay in the specified inputs programmed into the software. This can be changed in the editor to suit the interaction allowed on the system at any time.

5.3.3 Education

Initial research on the use of virtual systems helped discover the educational potential of this technology (Figure 1-1 and Figure 2-2). Companies were already implementing VR technology to educate their employees; thus, it can be identified that a consumer could use VR, AR and MR technology as tools for education. Education is a broad term describing many different teachings, one of which was identified to be effective on an MR System. Delivering educational content in the form of visual learning.

Visual learning is an education method that uses visual aids to deliver educational content. This method's benefit was its ability to reinforce the material taught due to the interactive nature of the teaching method. This method has seen success due to its ability to make the learning process more enjoyable and entertaining, thus holding student intertest over a longer period. A journal presented by Raiyn [39] reported that 75% of all information processed by the brain was derived from visual formats. Therefore, students can better understand and retain concepts, ideas and words with visual images.

An MR system's greatest advantage is the ability to draw the users' attention. This is due to its ability to present digital information in the real world. Therefore, visual learning methods would perfectly suit MR systems. MR systems focused on presenting an image that would hold users' interest and created an association they would not forget due to the unique visual experience.

There was no need to create software for education that focuses on visual learning. Instead, it was beneficial if the MR System could measure its capability of enabling visual learning. This did not require a specific program or software; the system would need to meet specific criteria when displaying its mid-air images. If it could meet these specified criteria, the system could be used as a tool for education, primarily focused on visual learning.

5.3.4 Visual learning potential

By investigating research completed on visual learning, it was possible to create a criterion that the MR System would need to meet to be considered a tool for education for visual learning. This list was created by studying the research presented by Clarke et al. [40] and Yen et al. [41]. These criteria are listed:

- Mid-air images must deliver diagrams, maps, videos and imagery that can support text or oral explanations.
- Mid-air images must deliver a strong sense of realism in the information displayed.
- Mid-air image must deliver a strong sense of colour and be colour orientated.
- Text displayed in mid-air must be readable.
- It must be possible to notice minute similarities and differences between different imagery displayed.

These points created the foundation of how the MR System was tested as a tool for education in Section 6.3.

5.3.5 Engineering design

The public generally understands virtual technology as a futuristic technology due to the influence of the movie industry. A common theme seen in movies was virtual technology used to design other technology. This was portrayed as users standing in an empty room but surrounded by virtual imagery that they could influence. Furthermore, published literature motivates MR in design prototyping. Kent et al. [42] presented "a classification of the benefits of Mixed Reality technology afforded to prototyping, the design process, and designers" [42]. Therefore, the MR System was investigated on its ability to perform engineering design.

Creating an engineering design software would be a monumental task and require a lot of time and coding proficiency. It was not something that could be achieved easily. Furthermore, there already existed engineering design software that has taken years of development and improvement to produce. Therefore, it was better to test an existing design software on this MR System and not create a new one. This way, the MR System could be tested as a design tool and could show its ability to use current design software.

5.3.6 Engineering design software selection

Several examples of engineering design software exist, each having unique features. Still, they all shared the same skeleton, as each program gives a sense of nostalgia when comparing interfaces and design tools. To name a few: SolidWorks™, Inventor™, Fusion 360™, AutoCAD™, etc. The four mentioned examples of software stood out due to their development and improvement over the years. Picking between these programs posed a difficult choice. Usage of design software was based on the user's preference and not due to a program's lack of ability. The MR System considered which software would best fit the viewing experience of the system. SolidWorks™ was found to best suit the MR System for engineering design. There was a possibility of biases in respect of this program selection. Therefore, it would be more appropriate to test each CAD program and investigate which one best fitted the system in future work. These programs' interaction lies in using a mouse for drawing and a keyboard for typing in numerical values.

5.4 Software for Mixed Reality interaction

An initial study on interaction techniques was explored in Section 2.3. The methods discussed in this section presented the possible interaction options available. Based on the information presented, a choice was made for the best possible method of interaction for the designed MR System.

Gesture control through a web camera was the better interaction technique for the current MR System. Due to the defects and inaccuracies with this method, it was determined that interaction using this technique in its current stage of development would reduce the quality of system operation. Therefore, until this method was improved,

the current MR System was operated using inputs on the connected laptop. This method of interaction conformed to the MR definition of not requiring wearable technology for system operation.

The CaptoGlove™ was used to simulate the desired gesture control on the MR System. This was implemented to investigate the desired interaction technique to determine if future work would solve the inaccuracy of gesture control using a web camera.

5.4.1 Programming of the CaptoGlove™

The CaptoGlove™ allowed seven operation modes. These modes allowed users to program how the glove would operate on the connected computer. A dedicated application called CaptoSuite™ was installed on the laptop to program the CaptoGlove™. When operating CaptoSuite™, the user was directed to an interface that allowed them to program the CaptoGlove™. This interface can be seen in Figure 5-7, which showed the customizability allowed on the CaptoGlove™.

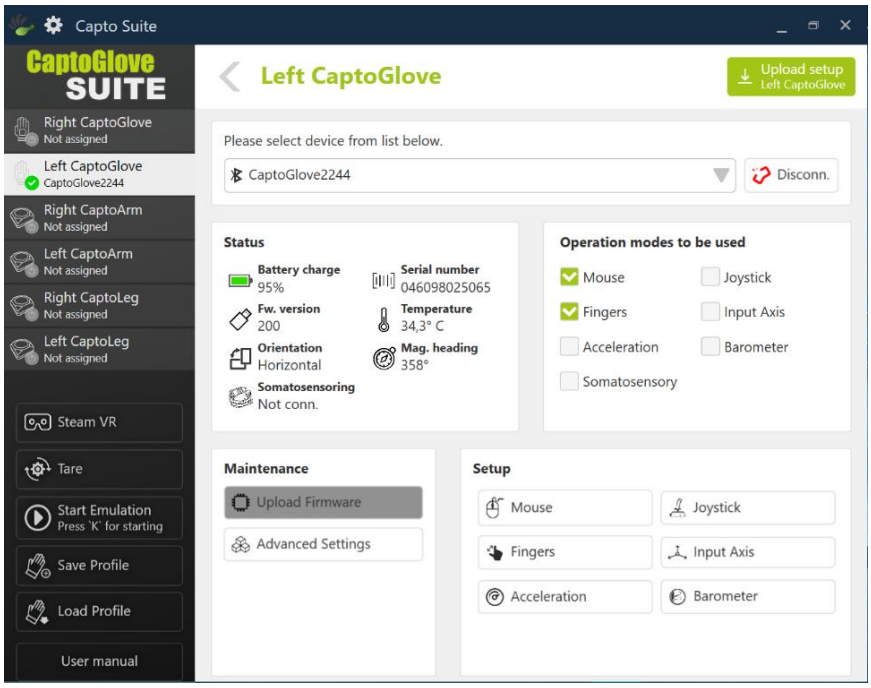

Figure 5-7: CaptoSuite™ interface

On this interface, the top left side showed the CaptoSensor™ that was selected to be programmed. The right side of this interface was used to program the selected sensor. The top right bar displayed the Bluetooth connection to the left CaptoSensor™ that was turned on. Below this lay the status and operation modes tabs; the status tab provided general information on the health of the connected CaptoSensor™. The operation modes tab allowed the user to select how the CaptoGlove™ was operated. Mouse and Fingers were selected for glove operation in Figure 5-7. The glove was programmed to mimic the laptop's cursor, and the fingers of the glove were used to deliver defined inputs on the laptop. When the user moved their hands, the cursor on the laptop would mimic their movements. When the user activated one of the finger sensors, this was registered as an input on the laptop.

The MR System required specific interaction based on the software operated. The CaptoGlove™ was programmed as a Mouse and allowed input actions due to finger bending. This selection was due to the entertainment software

created, which required input actions to control the player in the game as well as SolidWorks™, which required mouse control to perform engineering design.

Selecting the operation modes did not program the CaptoGlove™. This took place in the setup tab. The programmer could specify how the CaptoGlove™ would simulate a mouse on the laptop in the setup tab. When mouse setup was selected, a new window was opened on CaptoSuite™. An example of this window can be seen in Figure 5-8. In this window, the programmer could specify how horizontal or vertical movement of the CaptoGlove™ would result in the corresponding movement of the cursor on the laptop. The properties that were controlled for this translation of hand motion to cursor movement can be seen in Figure 5-8. This also showed the glove programming used for both the right and left glove when using SolidWorks™ on this MR System.

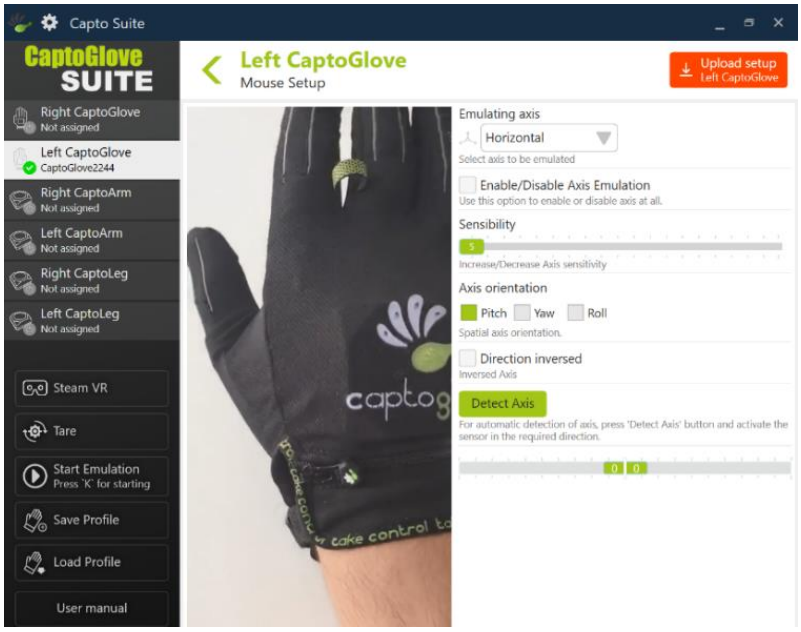

Figure 5-8: CaptoGlove™ mouse setup

When the "Fingers Setup" was selected, it opened a new window in CaptoSuite™. An example of this can be seen in Figure 5-9. The sensors in the CaptoGlove™ were programmed to perform a specific action in this setup window. The CaptoGlove™ product includes two gloves each having five bending sensors; one within each finger and a pressure sensor at the tip of the thumb. Programming was implemented one sensor at a time; "Sensor Selection" stated what sensor was currently being programmed. Once selected, this sensor was calibrated by pressing the relevant button. Afterwards, the sensor's trigger range was specified. Finally, the "Emulation Device" defined the sensor output when the sensor registered a force that lay within the trigger range. This output could be the mouse's clicking action or the action of pressing a specific button on the keyboard. Once the output was defined, the sensor was successfully programmed. Now it was possible to select the next sensor in the "Sensor Selection" tab and program the output that it would deliver. This could be done for all the sensors. Upon completion, the glove sensors would relate to specific actions defined by the programmer. The CaptoGlove™ "Finger Setup" was programmed in the following way for interaction with the developed entertainment software and SolidWorks™:

- The pressure sensor in each thumb controlled the left click on the mouse.
- The bending sensor in the index finger (right glove) correlated to pressing the right arrow key on the keyboard when triggered.
- The bending sensor in the index finger (left glove) correlated to pressing the left arrow key on the keyboard when triggered.

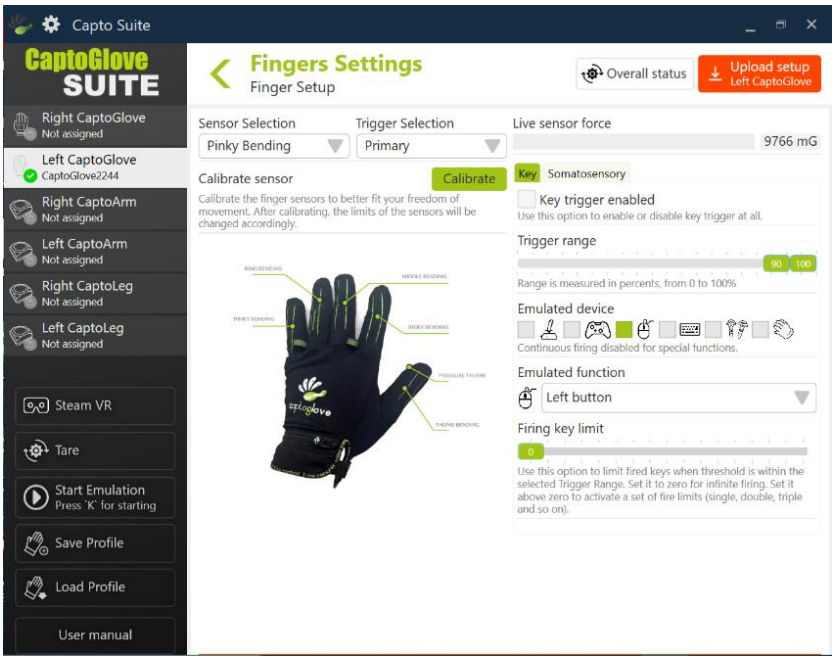

Figure 5-9: CaptoGlove™ finger setup

Once the operation mode setup is completed, the final step is to upload this control setup to the CaptoGlove™. This was done by clicking the red button at the top right of CaptoSuite™. When the upload was completed, the CaptoGlove™ was fully programmed and ready to use. Activating the CaptoGlove™ on the laptop was done by clicking the "Start Emulation" button on CaptoSuite™ or pressing the "K" key on the keyboard. Ending the emulation was performed by pressing the "K" key.

5.5 Chapter summary

This chapter presented software designed to control the electronics in this system and test the manufactured MR System's operation. The control script used for the MR System's automated motion was presented and explained. This included key control theory to obtain the required system actuation. A game was developed to test the system as a tool for entertainment. Criteria were identified to investigate the system's potential for visual learning, and SolidWorks™ was identified to test the system as a tool for engineering design. The motivations for these software choices were explained within the chapter, including an in-depth explanation of codes created for the developed game. System interaction was defined using inputs on the connected laptop or using a programmed CaptoGlove™.

The next chapter presented the methods of testing used to analyse the manufactured MR System. This testing evaluated the actuation and the MR experience provided by the system.

6. SYSTEM TESTING AND PERFORMANCE

6.1 Introduction

This chapter records the physical testing that was implemented for the manufactured MR System. It was possible to develop and implement testing procedures using the software designed or selected for system operation. The MR System and related equipment for operation can be seen in Figure 6-1.

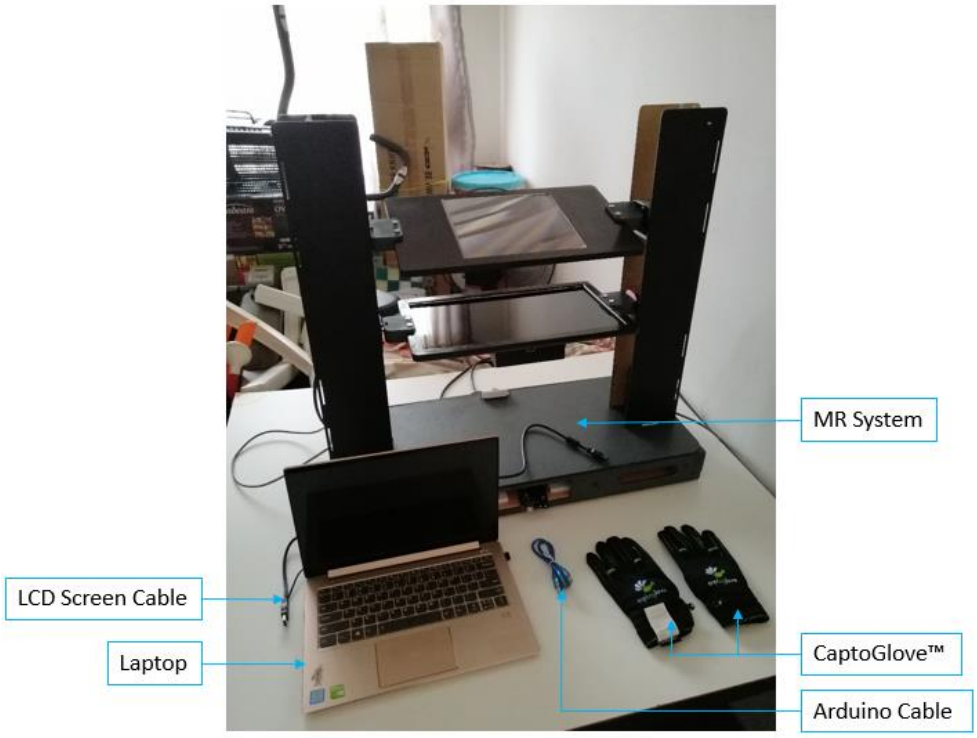

Figure 6-1: Setup for Mixed Reality System testing

Research by Zhang et al. [43] proposed that holographic multimedia devices could be analysed using traditional quality-of-service (QoS) parameters. They also recommended that a quality-of-experience (QoE) model could better evaluate these systems from user's perspective. This was due to virtual systems being human-centred. They were required to deliver the best possible experience to users on the system. This was further corroborated by Alexandrovsky et al. [44], they evaluated user experiences within MR as it delivered a better performance measure that standard QoE evaluations. Therefore, it was favourable to user test these types of systems to better evaluate the virtual experience granted. This MR System was evaluated under QoS and QoE parameters to determine the system's performance.

According to Zhang et al. [43], a QoS evaluation presented an introduction of fundamental hardware components, following series of technical evaluations on these components and their operation. For the MR System, a QoS evaluation was carried out on the two mechatronic sub-systems in this design (Layout Control sub-system and Height Control sub-system). These sub-systems were evaluated by the accuracy and repeatability of their automated functions. The Layout Control sub-system was tested by its ability to rotate the ASKA3D Plate and LCD screen. The Height Control sub-system was tested by its ability to move the ASKA3D Plate and LCD screen vertically. Measurable data was obtained from physically testing these automated functions. Calculations were performed on this data, and the results evaluated to determine these functions' accuracy and repeatability.

According to Zhang et al. [43], a QoE evaluation was centred around human involvement with technology. For the MR System, the QoE evaluation evaluated user satisfaction when viewing and interacting with mid-air images. Zhang et al. [43] stated that there were no well-known models of QoE evaluation for holographic systems. Therefore, they presented a method of user evaluation by creating a QoE framework. Their findings proved that their proposed QoE framework for holographic multimedia device evaluation could represent users' actual experiences and help evaluate other holographic multimedia devices [43]. By using this framework as a guide, the MR System will undergo a QoE evaluation.

The accuracy, repeatability, and user evaluation testing performed for the MR System are presented in Sections 6.2 and 6.3. This includes the method of evaluation, data presentation, and analysis of results.

6.2 Accuracy and repeatability testing

Accuracy testing was identified using the ISO 5725-2:2019 standard. This is a standard that defines accuracy as "the closeness of agreement between a test result and the accepted reference value" [45]. By performing a measurable action and comparing that measurement to a calculated reference value, the closeness between the two values would define the action's accuracy. This measure of closeness was obtained through statistical analysis.

Implementing the method presented by Beck [46], the accuracy of measurements was evaluated by determining their true value deviation. This method to evaluate the accuracy of measured results is presented as follows:

1. Collect as many measurements as possible for what was tested and call the total number of measurements "N".
2. Find the mean value of the measurements.
3. Find the deviation of each measurement by calculating the absolute value of the difference between each individual measurement from the mean value.
4. Calculate the average of all the deviations by adding them up and dividing them by "N".
5. This result will offer an indirect measure of the accuracy. The smaller the fraction, the higher likelihood the measurement was accurate.
6. Finally, compare the calculated mean value with its average standard deviation to the true value to determine this measurement's accuracy.

Repeatability testing was identified using the ISO 5725-2:2019 standard. This is a standard that defines repeatability as "the closeness of agreement between test results" [45]. This described an evaluation of replicated tests to identify if each test result agreed with the other. By performing the same experiment multiple times, the results can be compared to measure their closeness to define the experiment's repeatability. This measure of repeatability was obtained through statistical analysis.

Implementing the methods presented by Deziel [47] and Kaufmann [48], the repeatability of measurements was evaluated by determining the standard deviation and coefficient of variance for a series of experimental results. This method to evaluate the repeatability of measured results is presented as follows:

1. Perform the same testing experiment multiple times to obtain a large sample of data.
2. Find the mean of the data by summing the measured values and dividing by the number of results.
3. Calculate the sum of squares by subtracting each result by the mean, square this value and add the results.

4. Find the standard deviation by dividing the sum of squares value by the difference between the number of trials and a value of one, then take the square root of this fraction.
5. A standard deviation result of zero is ideal, meaning that there were no variations between the results. Therefore, high repeatability was signified by a standard deviation close to zero.
6. Finally, calculate the coefficient of variation (CV) by taking the standard deviation and dividing it by the mean. A CV greater than or equal to 1 represented a high variation, a CV lower than 1 represented a low variation.

These two methods were used to analyse the data obtained from testing the Layout Control sub-system and Height Control sub-system.

6.2.1 Layout Control sub-system

In this sub-system, two NEMA 17 motors were used to rotate an ASKA3D Plate and an LCD screen by 45-degree angles. Therefore, a test was required to investigate if the Layout Control sub-system can accurately and repeatedly rotate the desired components to their required positions. The rotation of these components must be accurate. If not, the MR System's mid-air images will not be displayed correctly.

The testing for this sub-system was completed in two parts: the ASKA3D Plate rotation and the LCD screen rotation. The components were programmed to rotate to a 45-degree angle starting from rest (0°) and then rotated back to their original rest position (0°). The purpose of working between these two angle rotations was due to the layouts granted for mid-air image projection (Figure 4-1 and 4-2). Therefore, these angle rotations held more relevance than other possible angle rotations when testing accuracy and repeatability.

The apparatus required for this test, the test's methodology, the results obtained, an analysis of these results, and a conclusion to the test followed.

6.2.1.1 Apparatus

- A blank cardboard backing to mark off the angle change of the two components
- A ruler
- A protractor
- A pencil
- An eraser

6.2.1.2 Methodology

1. The test constants were identified as the programable steps required for the two NEMA 17 motors to perform their rotation of 45° from rest and 45° to return to their rest positions.
2. The MR System was plugged in, and the power turned on, thus delivering power to the system's electronic components.
3. The cardboard backing was placed perpendicular to the system base, and points were marked to represent the ASKA3D Plate and LCD screen's current rest positions.
4. From rest (both components parallel to the ground), the ASKA3D Plate rotation accuracy was tested first.

5. The motor attached to the ASKA3D Plate was instructed to rotate by 25 steps which correlated to a rotation of 45° clockwise when facing the motor shaft directly. This was performed using the Arduino microcontroller.
6. The cardboard backing was then placed perpendicular to the system base, and two points were marked along the edge of the rotated component. A straight line was drawn connecting these two points while intersecting the line representing the rest position of the component.
7. The angle between these two lines was measured using a protractor and recorded.
8. Then, using the Arduino microcontroller, the ASKA3D Plate was instructed to rotate by -25 steps which correlated to a rotation of 45° anti-clockwise when facing the motor shaft directly.
9. The cardboard backing was then placed perpendicular to the system base, and two points were marked along the edge of the rotated component. The angle created by the new line's intersection with the old line was measured using a protractor and recorded.
10. Steps 5 to 9 were repeated four more times, thus obtaining five measured results for 45° clockwise rotation from rest and five measured results for 45° anti-clockwise rotation back to rest for the ASKA3D Plate.
11. Finally, steps 5 through 10 were repeated, except the component programmed to rotate (by the same number of steps) was the LCD screen and not the ASKA3D Plate.

6.2.1.3 Results

Following the methodology presented above, data was obtained, representing the rotation granted by the Layout Control sub-system. This data captured the real angle rotations performed by the ASKA3D Plate and LCD screen when rotating by 45° clockwise and anti-clockwise. The raw data captured can be found in Appendix G.1, Table G-1. The raw data was then evaluated using the methods presented in Section 6.2 to determine the measured values' accuracy and repeatability. The evaluation of the data was completed using an Excel document to perform the required calculations for these methods. This Excel document was printed and attached in Appendix D.4.

The calculated results for the accuracy evaluation can be found in Table 6-1. This table presents the mean values, deviation of the mean values, and the accuracy range of the ASKA3D Plate and LCD Screen when rotating clockwise and anti-clockwise. These values were compared to the reference value of 45° to determine the Layout Control sub-system's rotational accuracy. If the mean value with its allowable deviation placed the result close to 45°, the result was considered accurate.

Table 6-1: Accuracy test results (Layout Control sub-system)

ASKA3D Plate			
Criterion	**Mean Value (°)**	**Deviation (°)**	**Accuracy Range (°)**
Clockwise rotation	44.6	1.08	43.52 – 45.68
Anti-Clockwise rotation	43.8	0.96	42.84 – 44.76
LCD Screen			
Criterion	**Mean Value (°)**	**Deviation (°)**	**Accuracy Range (°)**
Clockwise rotation	42.3	2.3	40 – 44.6
Anti-Clockwise rotation	42.4	2.2	40.2 – 44.6

Figure 6-2 and Figure 6-3 display the measured results for rotational accuracy. Each measured result was shown with a corresponding error bar that signified the accuracy range of that measurement. This better indicated the accuracy of the measured results when compared to the reference value.

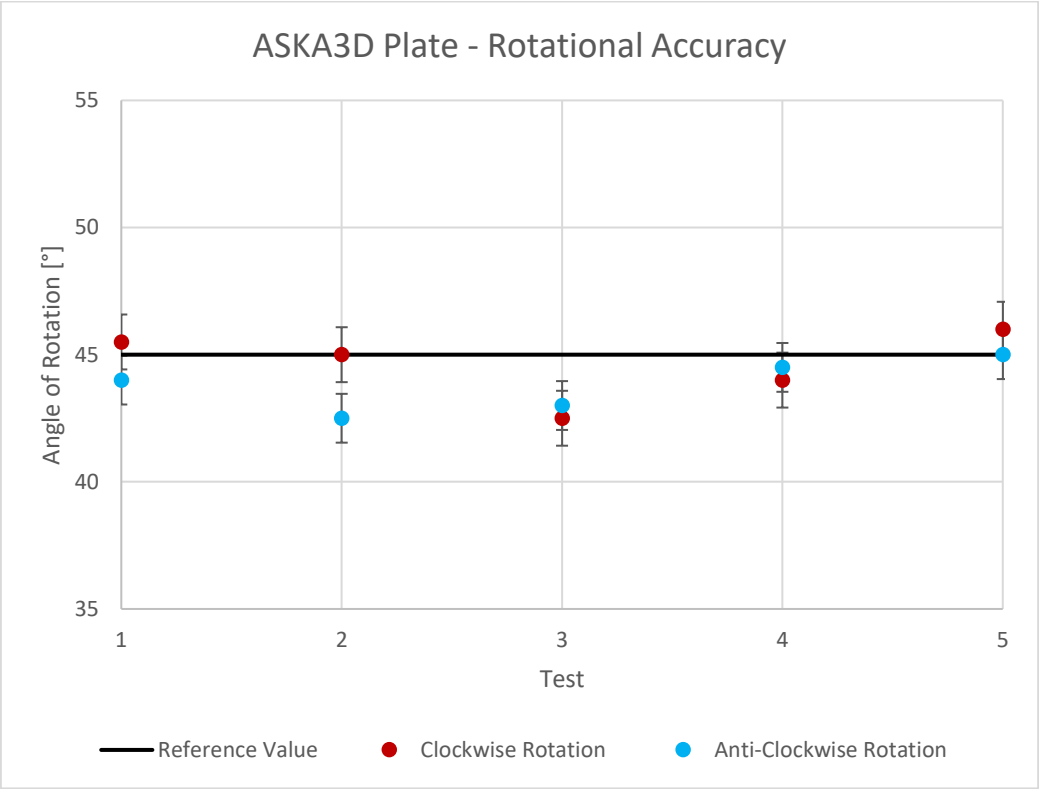

Figure 6-2: Rotational accuracy diagram (ASKA3D Plate)

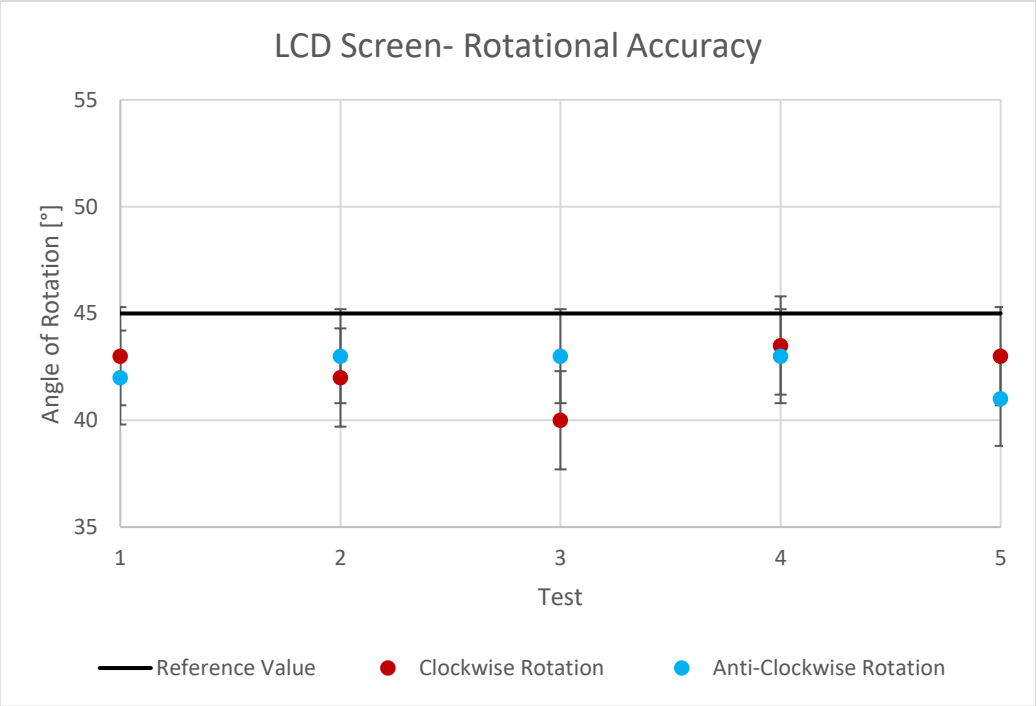

Figure 6-3: Rotational accuracy diagram (LCD screen)

The calculated results for the repeatability evaluation can be found in Table 6-2. This table presents the mean values, the standard deviation of the mean and the coefficient of variation of the ASKA3D Plate and LCD screen when rotating clockwise and anti-clockwise. The standard deviation was evaluated to determine the spread of the data and indicate possible outliers. Afterwards, the coefficient of variation was inspected to determine the variation of the results; this directly correlated to the sub-system's repeatability. Low variance indicated high repeatability, and the converse indicated low repeatability.

Table 6-2: Repeatability test results (Layout Control sub-system)

ASKA3D Plate			
Criterion	**Mean Value (°)**	**Standard Deviation (°)**	**Coefficient of Variation**
Clockwise rotation	44.6	1.39	0.03
Anti-Clockwise rotation	43.8	1.04	0.02
LCD Screen			
Criterion	**Mean Value (°)**	**Standard Deviation (°)**	**Coefficient of Variation**
Clockwise rotation	42.3	1.40	0.03
Anti-Clockwise rotation	42.4	0.90	0.02

6.2.1.4 Analysis

The rotational accuracy of the ASKA3D Plate was found to be accurate for clockwise rotation while slightly inaccurate for anti-clockwise rotation. The clockwise rotation results of the ASKA3D Plate were found to include the reference value of 45° within its calculated accuracy range of 43.52° – 45.68° (Table 6-1). Additionally, the mean value of the measurements had an error of 0.4° when compared to the reference value. This signified that rotating the ASKA3D Plate clockwise by 45° was accurate with a low chance of error. The anti-clockwise rotation of the ASKA3D Plate did not have the reference value within the accuracy range of 42.84° – 44.76°, and the mean value of the measurements had an error of 1.2° when compared to the reference value (Table 6-1). This inaccuracy was the result of human error when recording the anti-clockwise angle changes. The fourth and fifth test in Figure 6-2 showed two events where the measured result included the reference value within its accuracy range. Therefore, this showed the capability of accurate anti-clockwise rotation for the ASKA3D Plate. Additionally, this result's deviation was 0.96, which signified the rotation to be accurate due to its low magnitude.

The rotational accuracy of the LCD screen was found to be inaccurate for both clockwise and anti-clockwise rotation. The clockwise rotation had an accuracy range of 40° – 44.6° with a possible error of 2.7° when comparing the mean (42.3°) to the reference value (Table 6-2). The anti-clockwise rotation had an accuracy range of 40.2° – 44.6° with a possible error of 2.6° when comparing the mean (42.4°) to the reference value (Table 6-2). In both cases, the possible errors were almost identical, indicating that these rotations were performed with some degree of accuracy. The LCD screen component was found to be imbalanced, which resulted in this reoccurring rotational error. This was seen by the spread of data in Figure 6-3. The values obtained from each test tended towards a particular value below the reference value. The result obtained for the third test of clockwise rotation was an outlier of the data and indicated a hysteresis error occurred when measuring this angle change. The LCD screen rotation did have some accuracy since the results were almost identical when comparing the mean values for these

rotations (Table 6-2). Therefore, balancing the LCD screen would deliver an accurate rotation to the required reference value with a lower probability of error.

The rotational repeatability of the ASKA3D Plate was found to have a standard deviation of 1.39° for clockwise rotation and 1.04° for anti-clockwise rotation. These values were close to the ideal value of zero, signifying that the data obtained was centred around the mean with no significant outliers. The coefficient of variance calculated for these rotations was 0.03 for clockwise and 0.02 for anti-clockwise rotations. These coefficients were less than the value of 1, signifying a low variance between results. This represented high repeatability when rotating the ASKA3D Plate.

The LCD screen's rotational repeatability was found to have a standard deviation of 1.40° for clockwise and 0.90° for anti-clockwise rotations. These values were close to the ideal value of zero, signifying that the data obtained was centred around the mean with no significant outliers. The coefficient of variance calculated for these rotations was found to be 0.03 for clockwise and 0.02 for anti-clockwise rotations. These coefficients were less than the value of 1, signifying a low variance between results. This represented high repeatability when rotating the LCD screen.

6.2.1.5 Conclusion

In conclusion, the Layout Control sub-system was found to have an accurate rotation of the ASKA3D Plate. Due to the imbalance of the LCD screen, this component had a rotational error of approximately 3°. This issue could be rectified with the correct weight balancing of the component, thus giving accurate rotation. Additionally, the sub-system was found to have high repeatability when rotating the ASKA3D Plate and LCD screen.

6.2.2 Height Control sub-system

This sub-system used a pair of NEMA 23 motors and lead screws to perform the ASKA3D Plate and LCD screen's vertical movement. The movement of the two components was limited to a maximum height of 500 mm. It should be noted that these two components move vertically simultaneously. Therefore, the distance between the two components was expected to remain constant. A test was required to investigate how accurately the lead screws move the ASKA3D Plate and LCD screen upward or downward on the MR System.

Testing for this sub-system was done in two parts: by performing upward and downward vertical movements of the ASKA3D Plate and LCD screen. The magnitude of these movements was kept to 50 mm and 100 mm. The purpose of working with these magnitudes was to obtain an accurate measurement of small (50 mm) and large (100 mm) vertical movements for these components.

What follows is the apparatus required for this test, the test's methodology, the results obtained, an analysis of these results and a conclusion regarding the test carried out.

6.2.2.1 Apparatus

- A blank cardboard backing to mark off the height change of the two components
- A ruler
- A pencil
- An eraser

6.2.2.2 Methodology

1. The test constants were identified as the vertical movements of 50 mm and 100 mm for the ASKA3D Plate and LCD screen.
2. The MR System was plugged in, and the power turned on, thus delivering power to the system's electronic components.
3. The cardboard backing was placed perpendicular to the system base, and the height from the system base to the LCD Screen and ASKA3D Plate were marked off and measured to identify the initial position of these components.
4. The NEMA 23 motors were instructed to rotate by 5000 steps. This translated into 50 mm of downward vertical movement.
5. The cardboard backing was then placed perpendicular to the system base, and the new heights of the ASKA3D plate and LCD screen were marked off. These height values were measured using a ruler and recorded.
6. The NEMA 23 motors were instructed to rotate by -5000 steps which resulted in the two components moving upward by an expected value of 50 mm.
7. Step 5 was repeated, thus obtaining a measured result for a change in height when moving the components upward.
8. Steps 4 to 7 were repeated four more times, obtaining five measured results for 50 mm upward movements and five measured results for 50 mm downward movements.
9. Then steps 3 to 8 were repeated, except the magnitude of the steps specified was 10000, which correlated to a vertical movement of 100 mm.

6.2.2.3 Results

Following the methodology presented above, data was obtained, representing the vertical height change provided by the Height Control sub-system. The purpose of moving by two different increments was to evaluate the sub-system’s ability to perform small and large height changes. The raw data captured can be found in Appendix G.2, Table G-2 and Table G-3. The raw data was then evaluated using the methods presented in Section 6.2 to determine the measured data's accuracy and repeatability. This evaluation of the data was completed using an Excel document to perform the required calculations for these methods. This Excel document was printed and attached in Appendix D.4.

The calculated results for the accuracy evaluation can be found in Table 6-3. This table presents the mean values, deviation of the mean values, and the ASKA3D Plate and LCD screen accuracy range when moving upward and downward by 50 mm and 100 mm. These values were compared to the reference value of the vertical motion performed (either 50 mm or 100 mm). If the mean value and its corresponding deviation placed the result close to the reference values, the result would be considered accurate. Furthermore, a large deviation would indicate a possible error occurred.

Table 6-3: Accuracy test results (Height Control sub-system)

ASKA3D Plate			
Criterion	**Mean Value (mm)**	**Deviation (mm)**	**Accuracy Range (mm)**
Vertical motion (downward 50 mm)	39.9	9.72	30.18 – 49.62
Vertical motion (upward 50 mm)	42.2	7.96	34.24 – 50.16
Vertical motion (downward 100 mm)	100	0.2	99.8 – 100.2
Vertical motion (upward 100 mm)	100	0.6	99.4 – 100.6
LCD Screen			
Criterion	**Mean Value (mm)**	**Deviation (mm)**	**Accuracy Range (mm)**
Vertical motion (downward 50 mm)	41.2	9.56	31.64 – 50.76
Vertical motion (upward 50 mm)	43.1	7.68	35.42 – 50.78
Vertical motion (downward 100 mm)	100.5	0.2	100.3 – 100.7
Vertical motion (upward 100 mm)	100.3	0.56	99.74 – 100.86

The calculated results for the repeatability evaluation can be found in Table 6-4. This table presented the mean values, the standard deviation of the mean and the ASKA3D Plate and LCD screen's the coefficient of variation when moving upward and downward by 50 mm and 100 mm. The standard deviation was evaluated to determine the spread of the data and indicated possible outliers. The coefficient of variation was inspected to determine the variation of the results. This directly correlated to the repeatability of the measured values. Low variance indicated high repeatability, and the converse indicated low repeatability.

Table 6-4: Repeatability test results (Height Control sub-system)

ASKA3D Plate			
Criterion	**Mean Value (mm)**	**Standard Deviation (mm)**	**Coefficient of Variation**
Vertical motion (downward 50 mm)	39.9	11.41	0.29
Vertical motion (upward 50 mm)	42.2	9.36	0.22
Vertical motion (downward 100 mm)	100	0.35	0.0035
Vertical motion (upward 100 mm)	100	0.79	0.0079
LCD Screen			
Criterion	**Mean Value (mm)**	**Standard Deviation (mm)**	**Coefficient of Variation**
Vertical motion (downward 50 mm)	41.2	11.33	0.27
Vertical motion (upward 50 mm)	43.1	8.91	0.21
Vertical motion (downward 100 mm)	100.5	0.35	0.0035
Vertical motion (upward 100 mm)	100.3	0.76	0.0076

Once testing was concluded, the data obtained showed a possible error during the initial 50 mm height change test. The initial test values were all classified as outliers. The last two measured results for this test indicated that the height change was becoming more accurate as the tests were being performed. Therefore, to further evaluate the Height Control sub-system, five additional tests were carried out for the 50 mm height change movements. The data from these tests are presented in Appendix G.3, Table G-4. The results for the accuracy evaluation of these tests can be found in Table 6-5. The results for the repeatability evaluation can be found in Table 6-6.

Table 6-5: Additional accuracy test results (Height Control sub-system)

ASKA3D Plate			
Criterion	**Mean Value (mm)**	**Deviation (mm)**	**Accuracy Range (mm)**
Vertical motion (downward 50 mm)	50.4	0.72	49.68 – 51.12
Vertical motion (upward 50 mm)	50.2	0.52	49.68 – 50.72
LCD Screen			
Criterion	**Mean Value (mm)**	**Deviation (mm)**	**Accuracy Range (mm)**
Vertical motion (downward 50 mm)	50.4	0.72	49.68 – 51.12
Vertical motion (upward 50 mm)	50.6	1.12	49.48 – 51.72

Table 6-6: Additional repeatability test results (Height Control sub-system)

ASKA3D Plate			
Criterion	**Mean Value (mm)**	**Standard Deviation (mm)**	**Coefficient of Variation**
Vertical motion (downward 50 mm)	50.4	0.92	0.019
Vertical motion (upward 50 mm)	50.2	0.87	0.017
LCD Screen			
Criterion	**Mean Value (mm)**	**Standard Deviation (mm)**	**Coefficient of Variation**
Vertical motion (downward 50 mm)	50.4	1.00	0.020
Vertical motion (upward 50 mm)	50.6	1.51	0.030

The two sets of test data were used to create the diagrams seen in Figure 6-4 and Figure 6-5. Figure 6-4 displayed the height change data obtained by the ASKA3D Plate, and Figure 6-5 displayed the height change data obtained by the LCD Screen. These diagrams displayed the test results captured for the initial five tests and the secondary set of five tests due to the initial outliers identified. This indicated the difference between the two sets of results and displayed the actual trend of the data.

These two figures differed from previous diagrams displaying the accuracy of the results. This was due to the lack of error bars present on these diagrams. The error bars were removed from these diagrams as they would clutter the data. The data presented can be used in conjunction with Table 6-5 to read the accuracy range calculated for these values. The purpose of these figures was to show the accuracy of 50 mm movements and the data's improved trend.

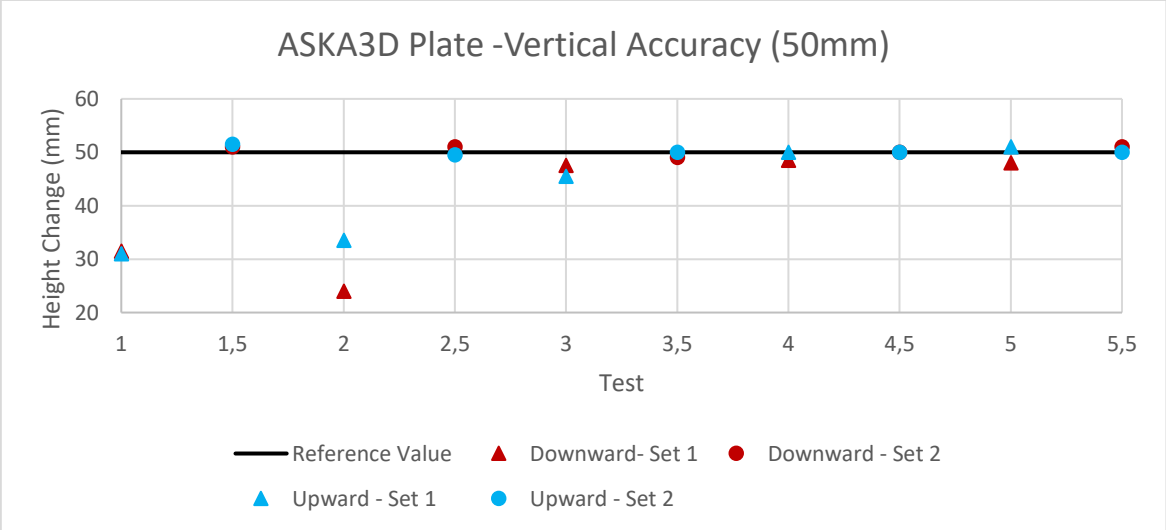

Figure 6-4: ASKA3D Plate vertical accuracy diagram (50 mm)

Set 1 referred to the first set of results captured, and they were number test 1 through test 5. Set 2 referred to the second set of results captured, and they were numbered test 1.5 to test 5.5.

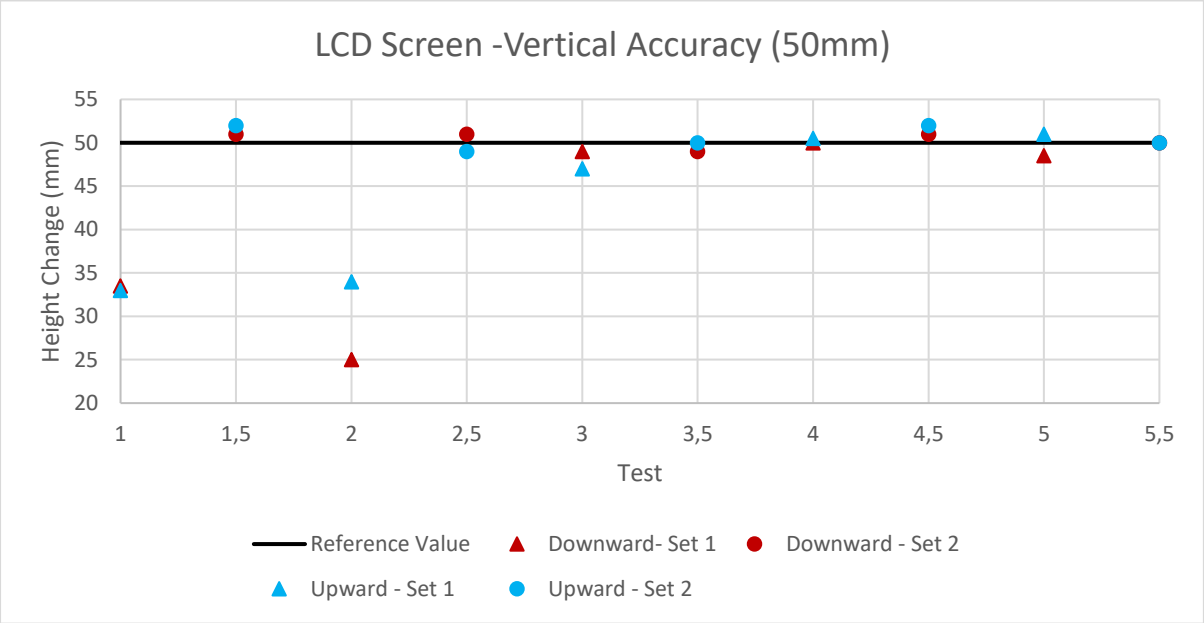

Figure 6-5: LCD screen vertical accuracy diagram (50 mm)

Figure 6-6 and Figure 6-7 were used to display the measured results for vertical accuracy at 100 mm height changes. Figure 6-6 displayed the height change data obtained by the ASKA3D Plate, and Figure 6-7 displayed the height change data obtained by the LCD screen. Each measured result was shown with a corresponding error bar that signified the accuracy range of that measurement. This better indicated the accuracy of the measured results when compared to the reference value of 100 mm.

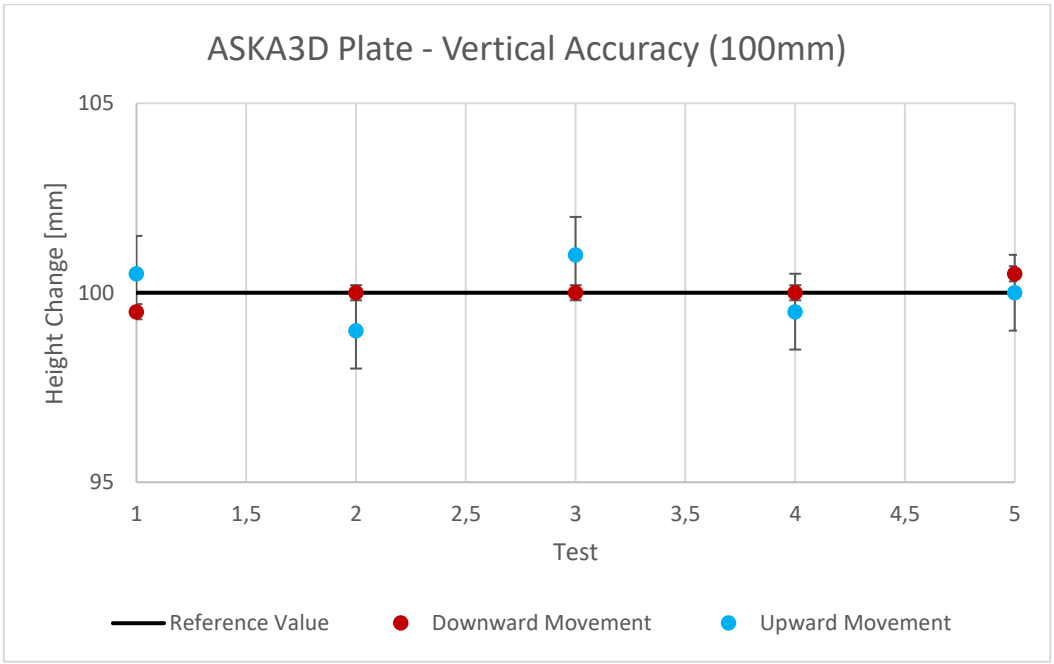

Figure 6-6: ASKA3D Plate vertical accuracy diagram (100 mm)

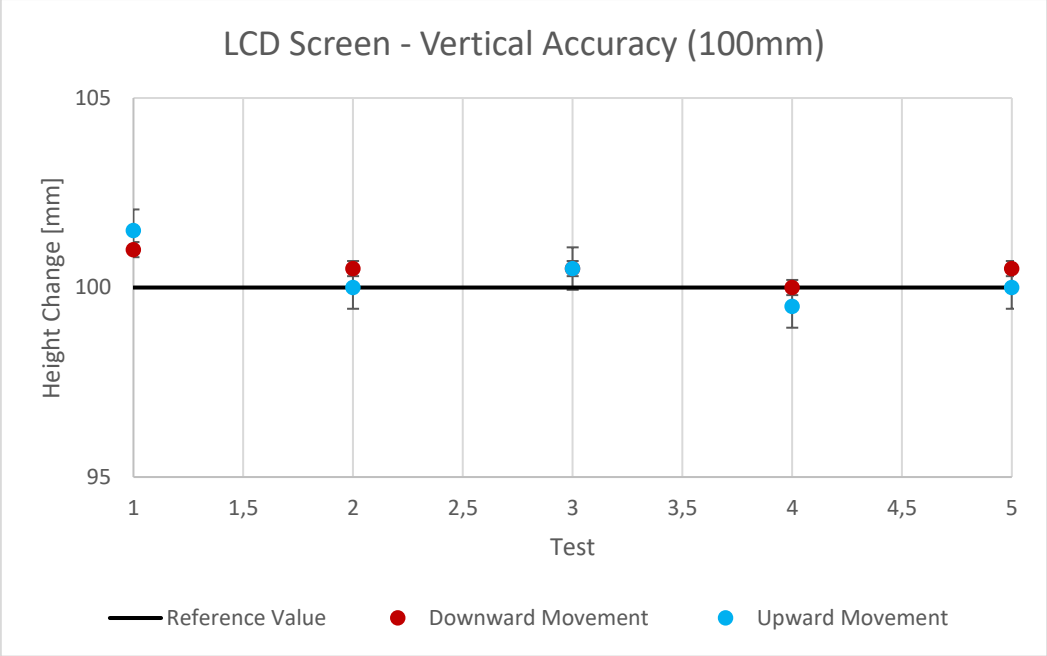

Figure 6-7: LCD screen vertical accuracy diagram (100 mm)

6.2.2.4 Analysis

The ASAK3D Plate and LCD screen were designed to move simultaneously when performing height changes on the MR System. For this analysis, each component was evaluated separately to investigate the accuracy and repeatability when performing upward and downward height changes of 50 mm and 100 mm.

The vertical accuracy of the ASKA3D Plate for the 50 mm height change was found to be poor for both movements. The mean values calculated for the upward movement is 39.9 mm, with those for the downward being 42.2 mm (Table 6-3). When comparing these mean values to the reference value of 50 mm, the values were identified as highly inaccurate. The large deviation obtained for these mean values indicated possible outliers in the data that was recorded. Therefore, an additional five tests were performed to obtain a second set of data to evaluate and determine the movement's true accuracy. The results showed an increase in the calculated mean values, with an upward movement of 50.4 mm and a downward movement of 50.2 mm (Table 6-5). Additionally, the mean value's deviation was much lower, which indicated a high accuracy when moving the ASAK3D Plate upward or downward by 50 mm. A comparison of the two data sets can be seen in Figure 6-4. This showed the initial outliers of the data that affected the initial mean values calculated. The secondary results showed the data's true trend, with all the results tending towards the reference value. Furthermore, the reference value of 50 mm was within the calculated accuracy range for the second set of data (Table 6-5). This indicated a good level of accuracy when moving the ASKA3D Plate by 50 mm either downward or upward.

The vertical accuracy of the ASKA3D Plate for the 100 mm height change was found to be good for both movements. The mean values calculated for both the downward and upward movement was 100 mm with a deviation of 0.2 mm and 0.6 mm, respectively (Table 6-3). Comparing the mean values with their deviations to the reference value of 100 mm highlighted the height change accuracy. Figure 6-6 displayed each measurement obtained from the tests with the corresponding accuracy range, showing how close each value was to the reference

value. This showed the high accuracy obtained when the ASKA3D Plate performed a height change of 100 mm either upward or downward.

The vertical repeatability of the ASAK3D Plate for the 50 mm height change had an initial standard deviation of 11.41 mm downward and 9.36 mm upward (Table 6-4). These deviations indicated a large variance resulting in low repeatability. Therefore, the second set of tests were evaluated for its repeatability (Table 6-6). The new standard deviation was found to be 0.92 mm downward and 0.87 mm upward. This result was favourable as it indicated the data was centre around the mean value with little variance. The second set of data delivered coefficient of variations equal to 0.019 for the downward and 0.017 for the upward motions. These coefficients were less than the value of "1", which signified a low variance between results. This represented high repeatability when moving the ASKA3D Plate by 50 mm either upward or downward.

The vertical repeatability of the ASKA3D Plate for the 100 mm height change had a standard deviation of 0.35 mm downward and 0.79 mm upward (Table 6-4). These values were close to the ideal value of zero, signifying that the data obtained is centred around the mean with no significant outliers. The coefficient of variance calculated for these vertical movements was 0.0035 downward and 0.0079 upward. These coefficients were less than the value of "1", which signified a low variance between results. This represented high repeatability when moving the ASKA3D Plate by 100 mm either upward or downward.

The vertical accuracy of the LCD screen movement for the 50 mm height change was found to be poor. The reason for this level of inaccuracy was the same as the ASKA3D Plate for its initial 50 mm movements. This can be seen in Table 6-3 by the mean and deviation values that were calculated. This was expected as these components move simultaneously. Therefore, like the ASKA3D Plate, this component was evaluated with the second set of data for 50 mm height changes. The results obtained using the second set of data showed an increase in the mean values, now 50.4 mm downward and 50.6 mm upward. The deviation for these mean values was 0.71 mm and 1.12 mm, respectively. When considering the mean and deviation values of the two motions, the results showed that the reference value of 50 mm lay within the accuracy range of these results (Table 6-5). A comparison of the two data sets can be seen in Figure 6-5. This showed the initial outliers of the data that affected the initial mean values calculated. The secondary data set showed the data's true trend, with the results tending towards the reference value. This suggests a good degree of accuracy when moving the LCD screen by 50 mm either downward or upward.

The LCD screen's vertical accuracy for the 100 mm height change was found to be accurate for both movements. The mean values calculated for the downward and upward movements,100.5 mm and 100.3 mm were within a deviation of 0.2 and 0.56, respectively (Table 6-3). Comparing these values with their deviations to the reference value of 100 mm highlighted the height change accuracy. Figure 6-7 displayed each measurement obtained with the corresponding accuracy range as error bars showing how close each value was to the reference value. This indicated that a good degree of accuracy was obtained when the LCD screen performed a height change of 100 mm either upward or downward.

The LCD screen's vertical repeatability for 50 mm height change was found to have a large standard deviation for its two motions. This was expected as the initial 50 mm height change data were outliers (Table 6-4). Therefore, the repeatability was evaluated using the second set of data measured and can be found in Table 6-6. The new

standard deviation was found to be 1.00 mm downward and 1.15 mm upward. This result was favourable as it indicated the data was centre around the mean value with a minimum variance of 1 mm. The second set of data delivered coefficient of variations equal to 0.020 downward and 0.030 upward. These coefficients were less than the value of "1", which signified a low variance between results. This represented high repeatability when moving the LCD Screen by 50 mm, either upward or downward.

The LCD Screen's vertical repeatability for the 100 mm height change had an initial standard deviation of 0.35 mm downward and 0.76 mm upward (Table 6-4). These values were close to the ideal value of zero, signifying that the data obtained was centred around the mean with no significant outliers. The coefficient of variance calculated for these vertical movements was found to be 0.0035 downward and 0.0076 upward. These coefficients were less than the value of "1", which signified a low variance between results. This represented high repeatability when moving the ASKA3D Plate by 100 mm, either upward or downward.

The ASKA3D Plate and LCD screen evaluated separately gave an in-depth review of each component's capabilities. The results obtained indicated if these components moved simultaneously, as they were designed to move. The 50 mm heigh change downward resulted in a mean value of 50.4 mm for both the ASKA3D Plate and LCD Screen, thus showing simultaneous movement. The 50 mm heigh change upward resulted in a mean value of 50.2 mm for the ASKA3D Plate and 50.6 mm for the LCD Screen, thus showing an deviation of 0.2 mm between the two components. The 100 mm height change downward resulted in a mean value of 100 mm for the ASKA3D Plate and 100.5 mm for the LCD Screen showing a deviation of 0.5 mm between the two components. The 100 mm height change upward resulted in a mean value of 100 mm for the ASKA3D Plate and 100,3 mm for the LCD Screen, thus showing an error of 0,3 mm between the two components. Of the four motions, three showed possible errors suggesting non-simultaneous movement of these components. These discrepancies could be due to a possible delay between the ASKA3D Plate and LCD screen's rotating collars. Additionally, the margin for error between the two components was low, with the highest being 0.5 mm. Therefore, these deviations would not severely impact the Height Control sub-system's ability to simultaneously move the ASKA3D Plate and LCD screen.

6.2.2.5 Conclusion

In conclusion, the Height Control sub-system was found to have high accuracy and repeatability when moving the ASKA3D Plate and LCD screen downward or upward either by a small or large height change. There was an initial error in the measurements obtained, creating outliers in the data, but additional testing rectified this issue. A possible reason for the initial outliers was the slippage of the collars on the lead screws, as this was the first time the system was operated. Additionally, the results obtained showed the simultaneous movement of the ASKA3D Plate and LCD screen, with the highest possible deviation being 0.5 mm.

6.3 Performance and user testing

User testing for the MR System was based on previous literature showing that common virtual technologies were used either for entertainment, education or design. Therefore, a method was required to experimentally measure the MR System's performance at these three levels.

This led to the discovery of research by Zhang et al. [43] who created a possible user testing method for multimedia AR devices based on a QoE framework model that they developed. Zhang et al. [43] proposed four major

parameters by which to evaluate an AR multimedia device: content quality, hardware quality, environment understanding, and user interaction. These major parameters were subdivided to illustrate the considerations when evaluating these devices. A diagram of this can be seen in Figure 6-8. They went on to test the accuracy of their framework as a possible method for user testing. Their findings proved their proposed QoE framework for holographic multimedia device evaluation could represent users' actual experiences and could evaluate other holographic multimedia devices [43].

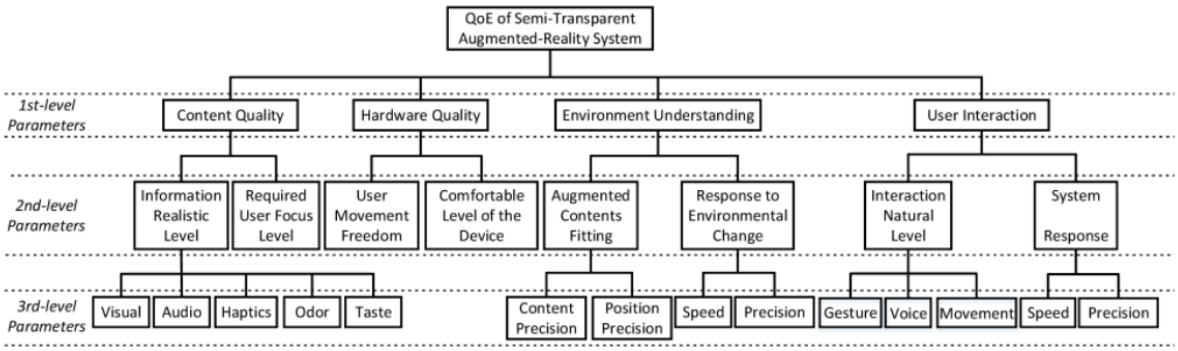

Figure 6-8: QoE framework model [43]

The test method used by Zhang et al. [43] had users operating a single holographic multimedia device. Afterwards, users answered a questionnaire to evaluate the experience on the device. The usage of a questionnaire to analyse a MR system or experience is further validated by Toet et al. [49] who proposed their own questionnaire to measure the visual presence of a MR experience. Therefore, questionnaire in this dissertation was created using the QoE framework proposed by Zhang et al. [43]. The users were questioned on four topics: content quality, hardware quality, environment understanding and user interaction. Additionally, Zhang et al. [43] created a game the users had to play on the Microsoft HoloLens™. The user's answers were based on the experience granted by playing this game on the Microsoft HoloLens™. Based on the positive results from this research, the MR System's user testing used the QoE framework by Zhang et al. [43] as a method of evaluation.

6.3.1 QoE framework for system evaluation

A QoE framework was developed based on the framework presented by Zhang et al. [43]. This differed from the original framework by evaluating the MR System for entertainment, education, and engineering design purposes. The seven main parameters of the framework (four original and three additional), with descriptions identifying the evaluated properties are presented.

6.3.1.1 Content quality

- The system must be evaluated to meet the user's basic requirements of realism. When generating a certain shape, the user should be able to see the shape exactly as intended and not otherwise. (i.e., a ball should look like a ball and not a book)
- The system must be evaluated to determine the user focus required when viewing mid-air images.
- The system must be evaluated to determine the transparency/opacity of the mid-air images delivered.
- The system must be evaluated to determine the sharpness of the mid-air images delivered.
- The system must be evaluated to determine the depth perception delivered when viewing mid-air images.

6.3.1.2 Hardware quality

- The system must be evaluated to determine the freedom of movement granted when viewing and interacting with the mid-air images. This took into consideration viewing angles and viewing distances.
- The system must be evaluated to determine the physical and visual comfort when viewing and interacting with the mid-air images.

6.3.1.3 Environment understanding

- The system must be evaluated to determine how changes in user position affected the mid-air image displayed.
- The system must be evaluated to determine the result of introducing a physical object in the MR environment and how that affected the users viewing experience.

6.3.1.4 User interaction

- The system must be evaluated to investigate the system's precision and speed response to user interaction.

6.3.1.5 Entertainment capability

- The system must be evaluated to investigate the experience when playing the MR game that was created. This evaluation focused on game immersion, user excitement, user interaction and users experience when playing the game on the system.

6.3.1.6 Visual learning capability

- The education potential of the system was evaluated on the criteria developed in Section 5.3.4.
- Users would investigate the system's ability to deliver diagrams, maps, videos and images that could support text or oral explanations.
- Users must evaluate the realism and depth of colour delivered by the mid-air images.
- Users must evaluate the system's ability to display readable text in mid-air.
- Users must evaluate their ability to notice minute similarities and differences between different the mid-air imagery displayed on the system.

6.3.1.7 Engineering design capability

- The ability to perform engineering design on the MR System must be evaluated. This focused on the user viewing experience, user interaction experience and the design experience.

The framework presented above was used to develop a questionnaire to accurately evaluate the MR System as a holographic multimedia device for entertainment, education and engineering design. The questionnaire that was created and completed for user testing can be found in Appendix G.4.

6.3.2 Apparatus

- The fully manufactured MR System presented in Chapter 4.
- One CaptoGlove™.
- A Laptop.
- USB cable for the LCD screen

6.3.3 Methodology

Due to the Covid-19 pandemic, multi-user testing was not performed for this MR System. The method of evaluation was not dependant on obtaining feedback from multiple users, but additional users would deliver results free from possible bias. The author previously proved multiple user viewing using similar components in a previous paper published in the ICINCO 2020 conference proceedings [50]. The author of the dissertation carried out the following method to user test the system:

1. The MR System was plugged into the main power supply.
2. The laptop was then connected to the Arduino board of the MR System.
3. The MR System was adjusted to the user's requested layout and height using the control script given in Appendix E.3.
4. The Arduino board was then disconnected, and the LCD screen was plugged into the laptop via a USB cable.
5. The user played the MR game created for the system.
6. Afterwards, the user was shown a collection of images, diagrams, videos and text to view on the MR System.
7. They were then asked to perform a simple design of their choice on SolidWorks™ using the MR System.
8. Finally, the user was then asked to complete a questionnaire to evaluate the MR System’s performance.

6.3.4 Results and analysis

The MR System was user-tested to obtain an indication of system performance; the success of the virtual system was measured by its ability to keep users captivated in the virtual experience. The MR System was user tested by the author of the dissertation using the methodology presented above. The author’s findings from this test were captured on the questionnaire presented in Appendix G.4. The system was set up according to the seating viewing heights presented in Section 4.4.3. These calculated values were found to be correct as they allowed viewing for the author, whose height was 1710 mm.

Below the author described their experience on the MR System, delivering their evaluation using the created QoE framework parameters and their answers from the questionnaire. The first four parameters evaluated the MR System's overall experience, with the last three parameters evaluating the systems capability as a tool for entertainment, education, and design. In the questionnaire, the author was asked to give an overall rating of each parameter. These ratings were used to create the diagram seen in Figure 6-9. This displayed the percentage rating given for each parameter of the framework.

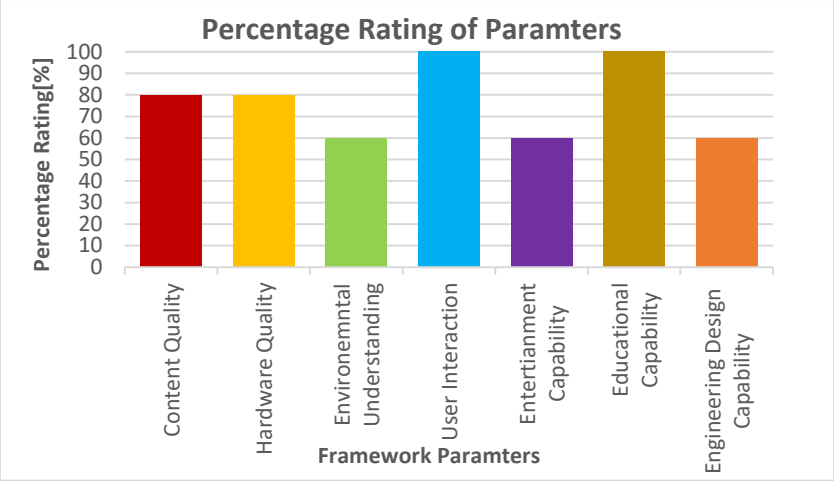

Figure 6-9: Percentage ratings of framework parameters

The first parameter evaluated was the Content Quality of the MR System. The displayed mid-air images were realistic and accurate in their representation, with a significant effect on the user's depth perception. Additionally, the images were solid with low transparency. The only exception to this occurred with low-quality source images that delivered blurry edges to the mid-air image. The source material used for mid-air projection was high-quality images, resulting in mid-air images with high sharpness and depth of colour. To initially view the mid-air images required extreme focus from the user. Once the user perceived the image in mid-air, their level of focus would drop while still viewing the mid-air images. The overall percentage rating for this parameter can be seen in Figure 6-9. A rating of 80% signified that the system's users would perceive high-quality mid-air image projection given that the source image was a high-quality image.

The second parameter evaluated was the Hardware Quality of the MR System. The system's hardware was located separate from the user and functioned independent of the user's movement. This gave the user freedom of movement due to the lack of wearable technology when viewing and interacting with the MR System. This freedom of movement was restricted by the viewing angle calculated for the device, including the minimal distance for viewing (Table 4-3). User eye strain on the device was dependant on the source image used for mid-air projection. If the source image was of low quality or included complex imagery, the user encountered significant eye strain when viewing the mid-air images. Source images that contained a single feature delivered almost no eye strain when viewing. The overall percentage rating for this parameter can be seen in Figure 6-9. A rating of 80% signified that users on the system would not be inhibited in their movements and were unlikely to encounter any physical or visual discomfort when using the MR System.

The third parameter evaluated was Environment Understanding of the MR System. Mid-air images were found to be temperamental when blending with their surrounding environment. This was due to the type of image displayed. If the image selected did not suit the environment, it delivered a foreign presence to the user. When foreign objects such as the user's hands encountered the mid-air images, there was no direct interaction present, showing that the mid-air images cannot perceive and interact with foreign objects. User position change in the environment directly affected the viewing of mid-air images. When the user shifted their position while staying within the allowed viewing angle, they would perceive the mid-air image following their viewing position. The

shifted mid-air image contained the same quality level so long as the user did not step outside of the viewing angle. Once they did, the image would distort, and mid-air image projection was lost.

Furthermore, the mid-air images displayed were restricted in size due to the size of the ASKA3D Plate. This resulted in the system allowing small to medium-sized image projection, but mid-air image projection was not perceived by the user when large images were used. Large images would lie outside the area of the ASKA3D Plate, and the user could not perceive any defining edges, which helped identify the mid-air image. Therefore, any image, video or program on the system must ensure they are restricted to fit within the area of the ASKA3D Plate. The overall percentage rating for this parameter can be seen in Figure 6-9. A rating of 60% signified that the mid-air image projection did have some degree of environmental understanding but could be further improved as it was currently limited.

The fourth parameter evaluated was User Interaction on the MR System. The interaction granted on the system was through physical inputs on the laptop or gesture control using the CaptoGlove™. The MR System was fully capable of hand interaction through gesture control. This was not implemented due to the inaccurate interaction it delivered on the device. Interaction using inputs on the laptop created an MR viewing and interaction experience. When used with the CaptoGlove™, the users were viewing in MR, but using gloves for interaction created a SAR experience. The user-tested both interactions on the MR System. In both cases, the interaction was precise with a fast response time. Therefore, it was a matter of preference to decide between interaction through inputs via the laptop or glove interaction.

Additionally, the MR system was fully capable of simultaneously allowing both types of interaction. User interaction could be further increased by having multiple keyboards or glove devices connected to the laptop. The overall percentage rating for this parameter can be seen in Figure 6-9. A rating of 100% signified that the MR System could deliver MR interaction to multiple users simultaneously. This rating was skewed as the interaction provided could be improved, but a score of 100% highlighted user satisfaction from the current interaction experience. Additional users testing the system would deliver an accurate representation.

The fifth parameter evaluated was the Entertainment Capability of the MR System. The evaluation of this parameter was based on the user playing the game created for this system. When playing the MR game, the user found the experience not enjoyable. This was due to the system's inability to deliver the game as a mid-air image. The game's screen size was larger than the area of the ASKA3D Plate, which led to the failure of mid-air image perception (Figure 6-10). This issue resulted in a lack of immersion for the user. The user found the core mechanics of the game enjoyable and challenging. Therefore, the MR game was re-programmed to encompass a smaller area, resulting in the user perceiving the game as a mid-air image. This resulted in an enjoyable game experience, although the game's finer details were lost with its size reduction. The user described the mid-air image as "squashed" and lacking in detail. These findings showed that the MR game was the limiting factor for this evaluation. The MR System had the potential to deliver an entertaining user experience but was restricted by the programmed game. The overall percentage rating for this parameter can be seen in Figure 6-9. A rating of 60% signified that the MR System had the potential to deliver an entertaining user experience, but this was dependent on the game created for the system. Games created for this system must take into consideration the small game-window size allowed by the ASKA3D Plate.

Figure 6-10: Failed image projection of the Mixed Reality game

The sixth parameter evaluated was the visual learning capability of the MR System. The user was shown a variety of images and videos on the MR System. Mid-air images were accurately displayed on the system with defined edges and depth of colour (Figure 6-11). These were properties desired to convey information to users visually. Diagrams and maps displayed on the system were accurately projected in mid-air, but the small font present on these resources was blurry and hard to distinguish. It would improve the user experience and understanding if the diagrams and maps delivered more information visually without using written text. The user was shown videos and animations to evaluate the effect a moving source image would have on the mid-air projection. This resulted in greater realism of the mid-air images being displayed. The motion of the images increased the immersion on the system. The MR System was then evaluated on its ability to deliver readable text in mid-air. This was successful as large text resulted in improved viewing of the mid-air image (Figure 6-12). It was possible to distinguish similarities and differences between the mid-air images displayed. This was reliant on high-quality source images as the source image's quality was directly proportional to the mid-air image quality. The overall percentage rating for this parameter can be seen in Figure 6-9. A rating of 100% signified that the MR System was fully capable of supporting visual learning.

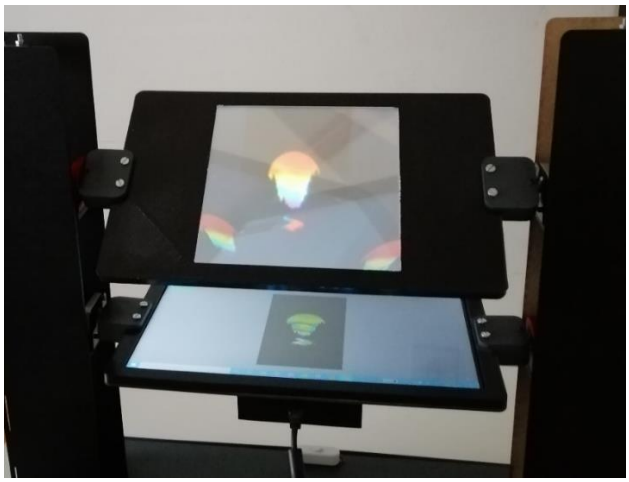

Figure 6-11: Image projection of sunset

Figure 6-12: Text projection

The seventh parameter evaluated was the engineering design capability of the MR System. This evaluation was performed using the SolidWorks™ CAD software on the MR System. When opening existing models on SolidWorks™, the system displayed these objects in mid-air with a high level of surface and edge detail. This was due to the application's neutral background, which made the model the focus of attention when projected in mid-air (Figure 6-13). The size of the models did not affect the system's mid-air projection ability. This was due to the ability to resize models on the SolidWorks™ application. Resizing the models allowed the projection of larger models, but this reduced the surface and edge quality. Creating new models on the system allowed dynamic viewing when drawing and extruding models but had one significant issue. This was the inability to view the user interface of the SolidWorks™ application as a mid-air image. Only the sketching area was displayed in mid-air. Using the laptop screen in conjunction with the mid-air image displayed created an acceptable design environment for this system. The interaction was subject to the user's preference, using mouse and keyboard or glove interaction. There was no limitation on the features available on the SolidWorks™ application. The user was able to perform extrusions, cuts, assemblies, etc. The overall percentage rating for this parameter can be seen in Figure 6-9. A rating of 80% signified that the system could facilitate engineering design using the SolidWorks™ CAD application. The MR System increased the visual appeal of the design process and improved model inspection. Additionally, there was no significant improvement to current design practices when using this MR System.

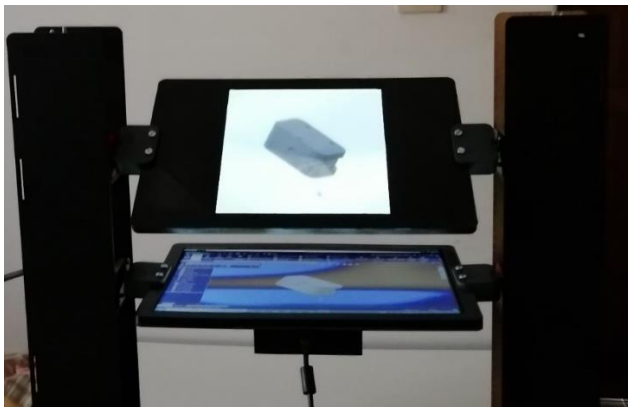

Figure 6-13: SolidWorks™ model projection

Please note that Figures 6-10, 6-11, 6-12 and 6-13 did not accurately represent the mid-air image perceived by the user. The camera was not able to accurately capture the mid-air projection experience provided by the system.

6.3.5 Conclusion

In conclusion, the MR System was found to be capable of facilitating entertainment, visual learning and engineering design. Each parameter was graded using a generated questionnaire. It was found that the system excelled as a tool for visual learning, followed by engineering design and then entertainment. Four other parameters were evaluated in conjunction with the previous three to determine the system's general performance. The results from the answered questionnaire graded the overall quality of the MR System as 80/100. This was a favourable result and indicated improvements could be made to improve the system's MR experience.

6.4 Chapter summary

A QoS and QoE evaluation was performed on the MR System through accuracy and repeatability testing of the Layout Control and Height Control sub-systems and user testing of the complete MR System. Each test recorded the test methodology, findings and conclusions drawn from the data obtained. The key findings of these tests are as follows:

- The Layout Control sub-system was found to accurately rotate the ASKA3D Plate to the required 45° angles. The rotation of the LCD screen was found to be less accurate, with an error of 3°. The component was not balanced correctly, resulting in this error. These findings applied to both clockwise and anti-clockwise rotations.
- The Layout Control sub-system was highly repeatable in the rotation of the ASKA3D Plate and LCD screen. This was given by the calculated coefficient of variances having values significantly less than a value of 1.
- The Height Control sub-system was found to have high accuracy and repeatability when moving the ASKA3D Plate and LCD screen downward or upward by a small (50 mm) or large (100 mm) change in height.
- User testing proved the system's capability to be used for entertainment, education and design. The limiting factors lay in the quality of the source images and the size of the ASKA3D Plate.

The next chapter presented the discussion for the conducted research. The main themes discussed included the literature reviewed, justification of the research, concept creation, insights, observations, system performance, and the MR System's research implications.

7. DISCUSSION

7.1 Introduction

The purpose of this dissertation was to answer the following research question: What contribution can a multiple user Mixed Reality System operated using a laptop deliver to current areas of virtual technology?

To answer this question, the dissertation sought to achieve four objectives. These objectives are as follows:

1. Investigate literature centred around digital extended realities with a focus on Mixed Reality.
2. Research and design a Mixed Reality desktop system that will allow multiple user viewing without utilizing robust technology.
3. Build and test the proposed Mixed Reality System, repeatability and accuracy testing for mechanical components and user testing at three levels (entertainment, education and engineering design) for measuring the MR System's performance.
4. Discuss and conclude the designed MR System by addressing the research question of this dissertation.

This chapter summarises the literature reviewed, the justification of the research, concept creation, insights, observations, system performance and research implications detailed in the dissertation. These were used to address the objectives set and provide an answer to the dissertation's research question.

7.2 Literature and justification

Virtual technology and its usage have been portrayed as a technology of the future. This has been represented in movies and has given viewers a sense of wonder as this visually stimulating technology has seemed out of reach in our current time. Virtual systems have the potential to change the world. Using VR and AR devices, users can experience a digital world outside their own reality. This world is used to play games, design technology or visually experience locations around the world from home. An important characteristic of this technology is its ability to revolutionise how humans perceive information, moving away from physical features and introducing an environment of mid-air images to display information.

Researchers have achieved these futuristic systems through the development of VR and AR technologies. VR and AR have seen substantial development over the past decade (Figure 1-1). The average consumer can own or use these technologies in their daily life. MR is the next stage in the development of virtual technology where multi-user collaboration is emphasized. VR and AR devices allowed user collaboration but required each user to possess a device. MR could allow multiple user collaboration on a single device showing a significant improvement on existing virtual technology. MR technology is under development and requires further research before it can be made available to the public. Once completed, this technology is expected to improve aspects of social living. This is the dissertation's foundation, providing substantial research into this field of virtual technology by developing an MR System that allows multiple users on a single device. This foundation led to the discovery of additional areas of improvement in the design of virtual technologies.

The current state of virtual technology is not consumer-friendly. This is due to the scarcity of devices, high price ranges and additional requirements for system operation. VR devices, unlike AR and MR, are readily available to consumers via online websites. These devices come at a high price and require a computer system with high

processing power to deliver the VR environment. Additionally, these devices used HMD's which required a physical connection to a computer system. This limited mobility and created user discomfort. AR devices offered consumers an improved viewing experience when compared to VR devices. AR devices were scarce due to companies manufacturing a limited number of devices. An example of this was Microsoft with their HoloLens™ and HoloLens™ 2. The limited availability was expected due to the manufacturing cost required to create these devices. This was seen in the high purchase price of these systems. Additionally, AR devices require a headset to create their virtual environment. These headsets have the computer system built into the device. Users required the headset and a controller for system operation. An advanced computer system stored within the headset increased the overall cost for these devices. MR devices are currently not available to consumers and are only seen in research papers. These research papers explore unique approaches to develop an MR system.

Reviewing current VR and AR systems identified two areas that required improvement; the high cost of manufacturing these systems and the high processing power required to operate these systems. These two areas were investigated when the MR System was designed to improve the current limitations of virtual technologies. Literature was reviewed in Chapter 2 that investigated the expected system operation, mid-air imaging techniques, interaction methods, and the programs used to develop virtual software.

System operation defined how the MR System was used. This was necessary to measure the system's performance once manufactured. Allowing multiple users on the system did meet the overall goal, but these users would need to view mid-air information for a specific purpose. It was identified that virtual technologies were primarily used as tools to facilitate entertainment, education and design (Figure 1-1 and Figure 1-2). These three areas were used to develop software that was implemented on the MR System to gauge its performance.

Creating an MR System required a method to deliver virtual information on a physical device separate from the user. This led to the discovery of beam splitter theory and half-slivered mirrors to deliver the required system viewing. The diagram illustrating beam splitter theory can be seen in Figure 2-1. This displayed how mid-air images were projected using this method. Literature was reviewed on systems that implemented this method of image projection. This led to the discovery of the HoloDesk and MARIO systems, which revealed the limitations of this method. Half-silvered mirrors in beam splitter theory created closed systems where images were projected behind the beam splitter. A solution to this was the use of an AIP as the beam splitter, not a half-slivered mirror. This delivered distortion-free imaging with imaging in front of the beam splitter. The use of an AIP created an open system that had the potential to allow multiple user viewing. An additional limitation was the restricted viewing positions required from users. This could be improved by having the system correct itself to the users viewing position, giving users more mobility. Finally, it was noted that the interaction volume for systems using this method of projection required a darkened surface and environment to better view the projections. This was identified as a possible design limitation.

Techniques were explored to improve the viewing experience when using an AIP. Head tracking and gaze recognition could be used to deliver view-dependant rendering on the system. This would create a viewing system that adjusted itself to the user's position. The use of this viewing technique with the system's projection method would not track more than a single user, thus going against the aim of the system. Additionally, these systems required the use of an RGB web camera and software to process the data. This would increase the manufacturing

cost of the system and the processing power required for operation. Environmental light control was the second technique identified to improve user viewing. A darkened environment delivers sharp and more detailed mid-air projections. In natural or artificial light, the mid-air images lose their detail and tend to become transparent. Light conditions were controlled with the system's design architecture and selecting the operation environment.

MR promotes the removal of wearable technology to experience virtual images. This applied to the viewing method and interaction allowed on the system. Therefore, research was conducted into interaction techniques on virtual systems without the use of wearable technology. A common technique identified was the use of a Microsoft Kinect™ sensor for hand tracking. Both the HoloDesk and MARIO systems used this technique for their hand interaction but differed on the level of interaction granted. The precise interaction of virtual images required the development of algorithms and physics models to process the data obtained from the Kinect™ sensor. This method of interaction was desired to deliver an experience that simulated real-life interaction. This method would increase the manufacturing cost of the system due to the cost of the sensor and would require high processing power from a computer system to deliver the interaction. Gesture control was investigated as a method of interaction. Research showed the possibility of gesture recognition using a web camera on a computer or laptop. Gesture control through a laptop's web camera would reduce manufacturing cost and would not require a robust computer system for interaction. Additionally, gesture control was identified by Yeo [34] as a natural control technique. The use of glove technology was explored. This was considered a solution if the quality of interaction delivered by gesture control was inadequate. A comparative investigation was completed on existing glove technology, and the CaptoGlove™ was identified as the best possible device for system interaction. This was due to its low cost and its ability to simulate gesture control. A programmable glove would allow for flexibility in the interaction techniques developed for system operation.

The software explored for the system operation focused on creating viewing programs and interaction programs. An investigation was completed on existing software used to create virtual programs. The following programs have previously been used to develop virtual programs: Unity3D™, Unreal Engine™, 3DS Max & Maya™, Blender™, Apple ARKit™, ARToolKit™ and Visualization Toolkit™. The use of these programs was dependent on the type of virtual program required. OpenCV™ was explored to develop an interactive program that delivered gesture control. This was based on the work presented by Yeo [34], who used OpenCV™ with a developed algorithm and a laptop web camera to achieve gesture control. This technique delivered cursor movement based on hand motion and clicking actions based on the number of fingers detected by the web camera. Additionally, finger detection could be programmed to deliver system outputs such as pressing specific buttons on the keyboard. Programming the CaptoGlove™ for interaction on the system required the personal SDK for this product called CaptoSuite™. This software application was used to program the CaptoGlove™ to deliver gesture control on a virtual system.

This research contributed to solving the current 'single user' disadvantage on virtual systems and making this technology readily available to the public by reducing manufacturing costs and the processing power required for system operation. The literature explored in Chapter 2 was used to develop the initial prototypes of the MR System.

7.3 Concept overview

The literature review assisted in identifying mandatory components that would be necessary to create the MR System. Additionally, this review identified current system architectures and their limitations. Due to this system's beam splitter projection method, there were two mandatory components: the beam splitter and LCD screen.

The beam splitter selected for system operation was an AIP due to the favourable characteristics identified by Kim et al. [18]which can be seen in Table 2-1. ASKA3D™ was found as a supplier that manufactured and sold AIPs, referred to as ASKA3D Plates. ASKA3D Plates allowed the projection of videos and pictures in mid-air without distortion. These plates were classified by material and size. Plastic plates were manufactured at a single size and allowed an image transmittance of 20%. Glass plates were manufactured at five different sizes and allowed an image transmittance of 50%. ASKA3D™ suggested their plate technology could deliver high-quality mid-air imaging under natural or artificial light. Initially, lighting was identified as a limiting factor in literature, and the use of this plate removed lighting conditions as a limiting factor on system operation. The ASKA3D Plate allowed image projection using two layouts, shown in Figure 2-4 and Figure 2-5. This was taken into consideration when designing the concepts for the MR System. The ASKA3D-200NT Plate was selected for system operation and used to develop possible concepts. This was the cheapest plate sold by ASKA3D to reduce the overall system cost.

An LCD screen was selected based on the size of the chosen ASKA3D plate. The size of the ASKA3D-200NT Plate was 200 x 200 x 6 mm. Therefore, a monitor was required to match the square area of the plate. The LCD screen could be larger than the ASKA3D Plate, but this would compromise the system architecture and ruin the aesthetics. The LCD screen selection was based on finding a monitor that had a square area slightly larger than the ASKA3D Plate. The monitor's image quality was a priority as the LCD screen was the source of the image projected in mid-air. The AOC E1659FWU 15.6" portable USB monitor (Appendix B.4) was selected for system operation and used to develop the MR System concepts. This monitor had the smallest size while delivering HD image quality. The LCD screen of this monitor was stripped from its original housing and used within a custom cover. This was done to reduce system weight and created a uniform system architecture.

The purpose of selecting the beam splitter and LCD screen was to obtain a constant measurement for the concept designs. This assisted with developing the scale of the concepts generated. Three concepts were generated in Chapter 3 that favoured a specific system quality. Each concept contained a motivation for the design, a description of system operation, system specifications, a material selection to identify manufacturing costs and a CAD model of the expected system.

The first prototype generated was a robust concept design that took the favourable features from the systems explored in literature and combined them into a single device (Figure 3-1). This did not consider mitigating cost or processing power but focused on delivering the best possible multi-user MR experience. This resulted in a large-scale system that achieved multiple user viewing with an ideal collaborative environment. Viewing was allowed using a single ASKA3D Plate layout. The layout used can be seen in Figure 2-5. This delivered the best possible MR experience but contained the same limitations affecting current virtual technology. Due to its large scale and a wide variety of components, the system would have a large manufacturing cost and would require

robust processing power. Additionally, this was a niche system design that would not see diverse consumer usage. It would be used by institutions that could afford the cost of the device.

The second prototype generated was the compact concept design (Figure 3-2). This design focused on creating a highly portable MR System with the lowest manufacturing cost and could be operated using a laptop. This resulted in a small-scale desktop system where users could swap between the two possible layouts allowed when using an ASKA3D Plate. The system architecture was comprised of components that could be disassembled to make transporting the system easier. These components were designed to be 3D printed. A web camera was used to deliver view-dependent rendering. This system allowed a single user to interact with the MR environment but allowed multiple user viewing. This viewing was from the perspective of the user interacting with the MR environment due to the view-dependent rendering tracking their head and gaze position. This design circumvented the disadvantage of view-dependent rendering which acted against multiple user viewing.

The third prototype generated was the flexible concept design (Figure 3-3). This design focused on delivering a system that would automatically adjust its physical components to suit the system's users. These adjustments were focused on delivering comfortable viewing to users at different heights, system rotation to suit a user's position and allowing users to select the layout of the ASKA3D Plate. These adjustments were designed to be automated and controllable by users. Additionally, the system was designed to be manufactured at a reduced cost and weight by 3D printing components where possible. System operation took place using a laptop connected to the LCD screen and allowed gesture control through the laptops web camera. This system flexibility replaced the need for view-dependent rendering as the physical system could adjust itself to the user's viewing position and viewing preference. This would allow multiple users to view the mid-air images projected by the system.

A comparative analysis was performed on the concepts generated using the decision matrix found in Table 3-4. The flexible concept design concept was selected to deliver the desired MR System. This was due to its ability to change its position to suite users on the system. Compared to the remaining concepts, this design delivered multiple user viewing and interaction without sophisticated technology. Additionally, the architecture of the concept was novel when compared to existing research systems. Therefore, this provided further insight into the usage of automated system components to deliver multiple user viewing for an MR System.

7.4 Hardware design insights

When designing the MR System's hardware, system operation was investigated to identify requirements from the hardware to meet the dissertation's objectives. The flexible concept design operation method was used to develop an improved system operation, described in Section 4.2. This gave a detailed account of the MR System's operation, including the automated layout and height control of the ASKA3D Plate and LCD screen. The viewing method of the ASKA3D Plate with its two layouts was discussed in Section 4.2.2, with an overview of user height and its effects discussed in Section 4.2.1.

The MR System required three physical functions: the ASKA3D Plate and LCD screen rotation, the vertical movement of the ASKA3D Plate and LCD screen, and a system stand that would act as the base and control box of the system. The MR System's functions were then classified into three sub-systems presented in Section 4.2.3.

7.4.1 Layout Control insights

The hardware designed for the ASKA3D Plate and LCD screen rotation considered sub-system stability, weight reduction, component size, and rotational accuracy. The method of rotational actuation had a single stepper motor rotating each component. This required a fixed mounting position located opposite the two motors and allowed rotation in the motor shafts' directions. This was successfully achieved with the design of the Bearing Housing component (Section 4.3.1). This delivered stability to the rotational components in this sub-system. The accuracy of the two component's rotation was dependant on the method used to transfer motor shaft rotation. This was achieved with the designed housings for the ASKA3D Plate and LCD screen and the Connector component attaching the housings to the motor shafts and bearing shafts. The design of these components was presented in Section 4.3.1.

These components were designed to be manufactured through additive manufacturing to promote weight reduction and compact system design. Weight reduction was required for motor selection. Calculations were performed in Appendix D.2.1 and D.2.2 to identify the total weight experienced by both motor shafts. These values were presented in Table 4-4. Based on these values, a NEMA 17 stepper motor was selected for the component rotations. The datasheet for the selected motor was presented in Appendix B.8. This motor size was the smallest of its range, which confirmed 3D printing the sub-system components aided with weight reduction and was still functional.

Viewing specifications of the system were defined in Section 4.3.3. Calculations were performed in Appendix D.1 to obtain measurable values that defined the MR System's viewing experience. These values were presented in Table 4-3. The viewing specifications were dependent on the size of the ASKA3D Plate and LCD screen, the distance between the two components and predefined measures given with the ASKA3D Plate. These calculated measures were found to be valid during the user testing of the system. They require further validation using specified testing to confirm the accuracy of these values further.

7.4.2 Height Control insights

The hardware designed for the ASKA3D Plate and LCD screen's vertical movement took into consideration sub-system stability, weight reduction, and the translation of rotational movement to vertical movement. An actuation method was required to move the ASKA3D Plate and LCD screen to different heights to accommodate multiple users within a specified height range.

Lead screw actuation was selected to keep the actuation components in the MR System uniform. This implemented two lead screws operating simultaneously to move the Layout Control sub-system vertically. Collars were used to transfer lead screw rotations to vertical movement. The datasheet for the selected lead screw and collar was presented in Appendix B.5 and B.6. The Mounting Platform component was designed in Section 4.4.1 to enclose the collars on the lead screws and transfer their movement to the component. This implementation was not common since there was no physical medium fixing the collars to the Mounting Platforms. This had the potential to reduce the sub-system's accuracy. This method was implemented to reduce the cost of manufacturing the sub-system as higher priced collars were required to attach the Mounting Platforms to the collars. The collar used for this operation was selected based on the self-locking calculation check performed in Appendix D.3.3.2. The result

of this calculation was discussed in Section 4.4.3. When testing this sub-system's operation in Section 6.2.2, the platforms were found to deliver the required actuation with high accuracy and repeatability.

Due to the vertical layout of the lead screws, the connected motor shafts were expected to experience a large axial force when connected to the lead screw. This was calculated in Appendix D.3.3.1, and a value of 14.29N was obtained. This required a robust motor to accommodate this axial force. Therefore, the Motor Cover component was designed in Section 4.4.1 to act as a shoulder for the lead screws and would experience the axial force in place of the motor shaft. The motor selection was then based on the required torque for lead screw rotation, calculated in Appendix D.3.3.2. The two lead screws had to generate 0.020 Nm of torque to raise the applied load and 0.011 Nm to lower the applied load. Based on these values, a NEMA 23 stepper motor was selected for this actuation method. The specifications of this motor were presented in Appendix B.7.

Placing lead screws in a vertical position where they were fixed on one end created a cantilever, compromising system stability. Additionally, a flexible coupling contributed to this instability as the coupling allowed deflection of the lead screw. The Lead Screw Cover was designed in Section 4.4.1 to stabilise the lead screws in the Height Control sub-system and hide the lead screws and the mounting components. This was done to mitigate any system features that would draw the user's attention away from the projected mid-air images. The Lead Screw Covers were designed to be lightweight and contained two side panels, one top panel and one back panel. Each panel was designed to slot into the other and was held together by their interference fit. The top cover housed a Bearing Holder component that was designed to securely hold the top of the lead screw, thus stabilising the component.

Viewing the mid-air images on this system required users to fall within specified height ranges. This understanding was obtained from the ASKA3D Plate layout datasheet (Appendix B.3). Therefore, to allow a diverse group of users, the height control sub-system adjusted the ASKA3D Plate and LCD screen height. This height adjustment of components allowed multiple users to view the mid-air images so long as they adjusted the components to the required height for their height range. The user height ranges calculated for the system were presented in Table 4-11 and Table 4-12. The calculations were split into two categories; Appendix D.3.1 presented the ASKA3D Plate height calculations using the defined height ranges for standing viewing. Appendix D.3.2 presented the user height calculations using the defined ASKA3D Plate heights from Appendix D.3.1 for seated viewing. These calculated values and methods were further discussed in Section 4.4.3.

7.4.3 System Stand insights

The hardware designed for the System Stand took into consideration the expected weight of the Layout and Height Control sub-systems, storage of all electrical components and heat removal for the electrical components.

The System Stand was designed using hardwood material to deliver rigidity at a low weight. This was designed as a rectangular prism to suit the ASKA3D Plate and LCD screen architecture in this system. Spacer blocks were used to stabilise the Height Control sub-system's base platform and provide adequate height within the System Stand to install the electrical components and corresponding wires. Housing electrical components within a wooden structure presented a possible fire hazard due to the heat generated from the electrical components. Three measures were developed to mitigate the potential of this hazard.

The first measure used an axial fan to remove hot, stagnant air within the System Stand (Section 4.5.4). The second measure was implemented to the designed side panels for the System Stand (Section 4.5.1). These panels were designed with slots to allow natural airflow allowing a secondary area for heat removal. The final measure was designing components that acted as insulation layers preventing direct contact between the wooden surfaces and the electrical components (Section 4.5.1).

7.5 Software design insights

Once manufactured, the MR System could deliver mid-air images. These images were of the desktop screen on the connected laptop. From this result, the system could provide multiple user viewing of virtual information on a separate device from the user. The manufactured system had the prerequisite hardware to allow MR viewing but required software to experience MR operations, interaction and automated control.

7.5.1 Operation software

Based on previous research, virtual systems were used in three areas: entertainment, education and design. System software was developed so that the MR System could be operated in these three areas.

Utilizing the MR System for entertainment required a developed game software or existing game programs to view gameplay mid-air. A possible issue with using existing game programs was the projection window's size removing details from the full view. Developing a game on the MR System would accurately evaluate the system's capability for entertainment as virtual systems were commonly used to play games. An initial review of programs that could be used to develop system software can be seen in Section 2.4. This led to the selection of Unity3D™ to develop the game software for the MR System. Unity3D™ was used to create an interactive game that took advantage of the system's mid-air viewing capability (Section 5.3.2). The game was designed to give users the illusion that they were moving further into the mid-air image. The game added the third dimension to the mid-air image by giving the users an illusion of depth, thus creating a 3D viewing experience. Due to the plate's small size, there was a concern that the game image on the LCD screen would be cropped to a smaller size when projected by the ASKA3D Plate. If the MR game was cropped due to its large window size on the LCD screen, the game program was resized in the Unity3D™ editor. This was achieved by adjusting the game camera. The full game design was explained in Section 5.3.2.1 with the accompanying codes developed to create the MR game.

Operating the MR System for education required the projection of images, diagrams, charts and videos. This was based on the education method of visual learning, which was shown to better educate students than standard teaching practices. This did not require the development of a software program as the laptop could display the required content. This required criteria to measure the successfulness of this MR System as a tool for education. These criteria were developed in Section 5.3.4 and were based on literature covering the topic of visual learning. Not requiring dedicated system software for this operation improved the system's functionality as common virtual systems require dedicated system software for operations. Users could view the required visual content so long as they had the resources stored on the connected laptop.

Developing a design software for the MR System was not feasible. Design software requires years of development and extensive knowledge of programming. Additionally, there existed a wide variety of design software that was held with high regard in industry. Therefore, a design software was selected and used on the MR System to investigate its engineering design ability. The benefit of using an existing software promoted the system’s usability

as it would not restrict users on their choice of design software. SolidWorks™ was selected to test the performance of the MR System during the user testing. This choice was made based on the author's personal preference. Other design software could be used and could potentially deliver a better design environment on the MR System than SolidWorks™. Key areas of concern initially identified were the user interface and the drawing capability on SolidWorks™.

7.5.2 Interaction software

The manufactured MR System after Chapter 4 was labelled a viewing system due to the lack of interaction technique specified. In some situations, such as visual learning, viewing the mid-air images was the main requirement for this operation area. The same could not be said for entertainment and design. These operation areas required user interaction to complete the MR experience granted by the system. Additionally, this interaction experience would have to conform to the interaction required for MR systems.

This required interaction without using wearable technology. This was possible by implementing gesture control using the laptop's web camera. This interaction method was based on Yeo's work [34], which was investigated in Section 2.3.2. While this interaction method would deliver MR interaction, this method's current disadvantages would reduce the overall system performance. It could not efficiently detect user hands in darkened environments. According to previous literature, the mid-air image quality was improved in darkened environments. Therefore, this interaction method and viewing method would compromise each other's functions. Additionally, Yeo [34] detected a higher number of defects during his tests due to the hand's shape not being smooth and the contours on the hand generating noise when performing hand detection. This method delivered the required hand interaction, but it would compromise the system performance.

Therefore, MR interaction on the system was performed using inputs on the laptop. Hand interaction using a laptop meets the interaction requirement, but it would not give users the desired experience of controlling MR operations through gestures. The CaptoGlove™ device was purchased to simulate gesture control on the MR System. This was used to substitute gesture control through the laptop's web camera to investigate how the MR System was operated when used as intended. This was done, expecting that future work on gesture control using web cameras delivered accurate interaction. If so, it could then be implemented on the manufactured system. When testing the MR System, the CaptoGlove™ was programmed using CaptoSuite™ to simulate the gesture control interaction by linking hand movement to cursor movement and finger bending to defined system outputs (Section 5.4.1).

7.5.3 Control software

The final software required to complete the MR System was the Layout and Height Control sub-systems control software. An Arduino Uno microcontroller with the Arduino IDE was used to deliver precise instructions to the MR System's stepper motors. These instructions required the development of a control script for the MR System. Two areas in the MR System required instructions: the two NEMA 17 stepper motors in the Layout Control sub-system and the two NEMA 23 stepper motors in the Height Control sub-system.

The Layout Control sub-system required the two NEMA 17 motors to rotate through a clockwise and anti-clockwise rotation of 45°. Writing this control script required the number of steps to perform 45-degree rotations, the rotation speed, and the order of rotation. The two motors were required to rotate separately to distribute the

system's vibrations over a period of time and not acing instantaneously. The control script developed for this actuation was presented in Appendix E.1, and the method used to develop this code was presented in Section 5.2.1.

The height control sub-system required the two NEMA 23 motors to rotate simultaneously at the same speed and deliver the same torque. This was required to simultaneously move the collars on both lead screws, thus keeping the ASKA3D Plate and LCD screen level. Additionally, a method was developed that related the motor rotation to the collars' vertical movement on the lead screw. This method was presented in Section 5.2.1. This method was used to develop a control script that instructed the motors to complete a specific number of rotations related to the vertical movement required from the collars mounted on the two lead screws. The script developed for this actuation was presented in Appendix E.2.

A single control script was generated using the scripts from Appendix E.1 and E.2. This was presented in Appendix E.3. This was completed to create a single control script that could control all the automated components in the MR System. A single script created homogenous system control. The MR control script was developed by combining the previous two control scripts with a hierarchy that made the components actuate as required. The script included instructions in the form of comments to aid users in programming component movements.

7.6 System performance

The MR System's performance was investigated using the testing procedures developed in Chapter 6. These tests evaluated the system hardware responsible for automated movements (QoS testing) and the MR experience granted by system operation (QoE testing). QoS testing evaluated the accuracy and repeatability of the actuation found in the Layout and Height Control sub-systems. QoE testing focused on user viewing and interaction to evaluate the MR System as a tool to facilitate entertainment, education and engineering design. The results of these tests were used to discuss the MR System's performance.

7.6.1 QoS testing

The accuracy and repeatability testing were performed to analyse the Layout Control sub-system's rotation and the vertical movement of the Height Control sub-system. These actuation methods were significant in the MR System's operation as they adjusted the system to the user's height and viewing needs.

Each sub-system was tested to obtain raw data regarding their actuation method. The Layout Control sub-system's testing method was presented in Section 6.2.1, and the testing method for the Height Control sub-system was presented in Section 6.2.2. The raw data for these tests were captured in Appendix G.1 and G.2, respectively. These raw data sets were then evaluated using Beck's [46] method for accuracy and a combination of Deziel's [47] and Kaufmann's [48] methods for repeatability. Beck's [46] method employed statistical analysis of the raw data to calculate the mean value of the data set and the average deviation. These two values were then compared to the true value. If the true value lay within the calculated mean value's allowable deviation, the actuation method was accurate. Additionally, the deviation indicated possible outliers that could have skewed the results. Deziel's [47] and Kaufmann's [48] methods were used to evaluate the actuation methods' repeatability. Deziel's [47] method used statistical analysis to determine the raw test data standard deviation. This standard deviation was then compared to a value of "0" as this signified an ideal scenario with no variations. The closer the standard deviation was to zero signified low variance, which correlated to high repeatability. Kaufmann [48] took this a

step further and used the calculated standard deviation to calculate the coefficient of variance. This coefficient gave a better classification of the variance of the raw data sets. If the coefficient was less than the value of "1", it represented a low variation which signified high repeatability of the actuation method.

7.6.1.1 Layout Control sub-system

The Layout Control sub-system was used to adjust the MR System to the two viewing layouts allowed for the ASKA3D Plate. The two layouts were investigated in Section 4.2.2, analysing the usage and implementation of the different layouts. Recommendations were given when the system should be used, either seated or standing. Initial system testing justified these viewing recommendations as the mid-air images were viewable in the seated (Figure 4-1) and standing (Figure 4-2) layouts as predicted. It was noted that the seated layout seen in Figure 4-1 was able to deliver comfortable viewing when users were standing. This showed layout flexibility, thus allowing users to define how they would experience their MR environment on the system. Obtaining these layouts required precise angle control of the ASKA3D Plate and LCD screen. If the components were not rotated to their required angle, the mid-air image was projected incorrectly. This compromised the illusion of mid-air image projection and could distort the image. Therefore, the accuracy of the ASKA3D Plate and LCD screen rotations were investigated. Data was obtained following the testing procedures in Section 6.2.1.

The ASKA3D Plate was instructed to perform five clockwise rotations and five anti-clockwise rotations. After each rotation, the angles were marked off and measured using a ruler and protractor. This data was then analysed using the evaluation method by Beck [46] presented in Section 6.2. The calculated mean values and average standard deviations were compared to the true value of 45° to indicate rotational accuracy. The calculated mean value for clockwise rotation was 44.6° with an average deviation of 1.01°. The calculated mean value for anti-clockwise rotation was 43.8° with an average deviation of 0.96°. Therefore, the ASKA3D Plate was found to deliver accurate clockwise rotation since the true value lay within this rotation's accuracy range with a possible error of 0.4° from the true value. Anti-clockwise rotation was found to be slightly inaccurate as the true value did not lie within the accuracy range of this rotation. When considering the highest possible deviation allowed (Table 6-1), this rotation was inaccurate by 0.24°. This margin of error was inconsequential; this did not have a substantial effect on mid-air image projection due to its small magnitude. Additionally, this error was identified as a hysteresis error. Therefore, the rotation of the ASKA3D Plate was considered accurate.

The LCD screen was tested, and its rotational data was evaluated using the same methods described above, which can be found in Section 6.2.1. The calculated mean value for clockwise rotation was 42.3° with an average deviation of 2.3°. The calculated mean value for anti-clockwise rotation was 42.4° with an average deviation of 2.2°. These two rotations were found to be inaccurate when compared to the true value of 45°. This inaccuracy was due to an imbalance of the LCD screen. The first indicator of this imbalance was from the mean and deviations obtained from the calculations. The values were almost identical with a 0.1° of error, showing that the rotation was tending towards the same value in both rotation directions. This relationship was displayed in Figure 6-3. The second indicator was from the screens tendency to rotate when at rest and not remain stationary. Therefore, in its current form, the LCD screen delivered inaccurate rotation. The results showed a degree of accuracy as the mean values tended towards the same value, showing the method of rotation used was accurate. Due to the imbalance, the rotation delivered was compromised but still accurate. Correcting the imbalance would deliver a result closer to the true value of 45°.

This actuation was further investigated for reliability on repeated rotations. Therefore, the rotational test data obtained (Appendix G.1) was evaluated using the methods of Deziel [47] and Kaufmann [48] to investigate the Layout Control sub-system's repeatability. The results from the repeatability calculations were presented in Table 6-2. The coefficient of variance for the clockwise rotation of the ASKA3D Plate and LCD screen was found to be 0.03, and the anti-clockwise rotation for these two components was found to be 0.02. Therefore, rotation of the Layout Control sub-system components was found to be repeatable due to the low variance between measured results.

Therefore, the actuation method used in the Layout Control sub-system was accurate and repeatable. However, the LCD screen's rotation will be inaccurate, pending the weight balancing required for the component.

7.6.1.2 Height Control sub-system

The Height Control sub-system was used to adjust the ASKA3D Plate and LCD screen's vertical positions to allow multiple user viewing on the MR System. Three height ranges were specified in Section 4.2.1 when it was identified that user height would significantly impact the MR System's viewing capability. These height ranges were specified on average adult height for both male and female users. These height ranges were used to calculate the corresponding component height positions in Section 4.4.3. Table 4-11 contained the user height and corresponding ASKA3D Plate height when the layout of the ASKA3D Plate was in the standing position. Table 4-12 contained the user height and corresponding plate height when the layout of the ASKA3D Plate was in the seated position. These tables gave users a guide to adjust the MR System to suit their height and improved viewing of the mid-air images. Due to the automated height movement allowed on the MR System, this method of actuation was analysed to determine its accuracy and repeatability. Accurate and repeatable height changes were necessary to achieve user comfort when viewing mid-air images on the system. Inaccurate height changes would result in users physically adjusting their height positions. This acted against the flexible nature of the system.

The height changes were tested on direction and magnitude. The components were instructed to move upward and downward by a small magnitude five times. Once completed, they performed the same motions but at a larger magnitude. The small magnitude selected was 50 mm, and the large was 100 mm. Each height change performed by the system was measured using a ruler and recorded in Appendix G.2. The raw data was then evaluated using Beck's [46] method for accuracy and a combination of Deziel's [47] and Kaufmann's [48] methods for repeatability.

The height change was recorded for both the ASKA3D Plate and LCD screen. This was done to evaluate if the components moved simultaneously, thus keeping the same distance apart. The accuracy of the 50 mm height change for the ASKA3D Plate and the LCD screen was evaluated, and the calculated results were presented in Table 6-3. The downward and upward motions of the ASKA3D Plate had mean values of 39.9 mm and 42,2 mm with a deviation of 9.72 mm and 7.96 mm, respectively. The downward and upward motions of the LCD screen had a mean value of 41.2 mm and 43.1 mm with a deviation of 9.56 mm and 7.68 mm, respectively. These values exhibited that 50 mm height changes to the ASKA3D Plate and LCD screen were inaccurate and would not move the components simultaneously. This was due to possible outliers in the data set and was confirmed when looking at the initial values obtained from the raw data in Appendix G.2. Therefore, this test was repeated. Additional test data was obtained and captured in Appendix G.3. The data was evaluated and presented in Table 6-5. The new

downward and upward motions of the ASKA3D Plate had mean values of 50.4 mm and 50.2 mm with deviations of 0.72 mm and 0.52 mm, respectively. The downward and upward motions of the LCD screen had mean values of 50.4 mm and 50.6 mm with deviations of 0.72 mm and 1.12 mm, respectively. This showed accurate height change when moving the components by 50 mm and simultaneous movement of the two components. The two sets of results were captured on a single diagram to illustrate the improved accuracy of the 50 mm height changes. Figure 6-4 displayed the height changes recorded for the ASKA3D Plate, and Figure 6-5 displayed the height changes recorded for the LCD screen.

The initial results were inaccurate as this was the first time the Height Control sub-system was actuated. This inaccuracy was the result of collar slippage during the initial lead screw rotations. The additional tests proved that further rotations of the lead screw deliver precise collar movement. This was further corroborated when actuating by 100 mm.

The repeatability for the 50 mm height changes were evaluated using the original and additional test data. The results using the original test data were captured in Table 6-4 and the results using the additional test data were captured in Table 6-6. Given that the original test data was inaccurate, the additional test data was a true reflection of the sub-system's capability. The 50 mm height change of the ASKA3D Plate was found to be repeatable with coefficients of variance of 0.019 and 0.017 for downward and upward movements. The 50 mm height change of the LCD screen was found to be repeatable with coefficients of variance of 0.020 and 0.030 for downward and upward movements.

The data obtained from the 100 mm height changes were accurate, and no additional testing was required. The results from the accuracy calculations for this test data were presented in Table 6-3. The downward and upward motions of the ASKA3D Plate had a mean value of 100 mm with allowable deviations of 0.2 mm and 0.6 mm, respectively. The downward and upward motions of the LCD screen had mean values of 100.5 mm and 100.3 mm with allowable deviations of 0.2 mm and 0.56 mm, respectively. This showed accurate height change of the ASKA3D Plate and LCD screen when moving by 100 mm.

Additionally, these results confirmed the simultaneous movement of the two components. To further illustrate this vertical movement's accuracy, Figure 6-6 and Figure 6-7 displayed each measured result with their corresponding error bars (accuracy range) to identify where they lay with respect to the true value of 100 mm. The results from the repeatability calculations were presented in Table 6-4. The 100 mm height change of the ASKA3D Plate was found to be repeatable with coefficients of variance of 0.0035 and 0.0079 for downward and upward movements. The 100 mm height change of the LCD screen was found to be repeatable with coefficients of variance of 0.0035 and 0.0076 for downward and upward movements.

Therefore, the actuation method used in the Height Control sub-system was found to be both accurate and repeatable. Additionally, these movements kept the ASKA3D Plate and LCD screen at a fixed distance apart as intended.

7.6.2 QoE testing

User testing determined if the designed and manufactured system could deliver an MR experience to its users. This was done by analysing the system operation in three main areas, identified in Section 5.3. The first operation used the system as an entertainment tool by playing the MR game developed in Section 5.3.1 and Section 5.3.2. The second operation used the system as a tool for visual learning by viewing images, videos, diagrams and charts on the MR System. Finally, the MR System was used for engineering design with the SolidWorks™ application. These three operations were primarily seen implemented on virtual platforms.

These operations were evaluated using a QoE framework that was developed in Section 6.3.1. This framework was based on a QoE framework created by Zhang et al. [43]. The framework was then used to create a questionnaire that would accurately evaluate the MR System's operations. The successfulness of using a questionnaire for the system's evaluation was proven by Zhang et al. [43]. The MR System was user tested following the methodology in Section 6.3.3, and the answered questionnaire was analysed in Section 6.3.4. The questionnaire initially focused on general system usage before its questions focused on analysing the three different operations. The parameters analysed on the questionnaire were given an average percentage rating. This was displayed on a bar chart in Figure 6-9.

The results from investigating general system usage supported the creation of an MR System. The system delivered mid-air images to multiple users without any technology physically present on the users. This applied to the system's interaction as users could influence the scene through inputs on a laptop. The following four parameters were used to evaluate the general system usage of the MR System. The last three parameters were used to evaluate the three specified system operations.

Content quality was a parameter evaluating the quality of the mid-air images displayed. This was given a rating of 80% in favour of projecting high quality and precise mid-air images on the current system. When evaluating this parameter, it was determined that the mid-air image quality was directly related to the quality of the source image. Therefore, to further improve the mid-air image quality, a high-resolution source image or an LCD screen with improved screen resolution would be required.

Hardware quality was a parameter evaluating the physical and visual effect the system hardware had on users. This was given a rating of 80% in favour of delivering a wearable free system. This parameter was significant as most virtual systems required physical hardware to view and interact with virtual information. This delivered physical and visual discomfort to users and was an area of improvement for virtual technology. The MR System's hardware delivered no physical discomfort due to the MR system's fundamental property of separate operation from its users. Visual discomfort was present when viewing the mid-air images at incorrect height ranges. Users had to ensure the system was set up to match their height to comfortable view the mid-air images. This parameter could be improved by further analysing the system height and user height relations. In some instances, users within their user height range had an issue with perceiving the mid-air images comfortably. This would require a testing procedure focused on user testing a sample group of people with different heights.

Environmental understanding was a parameter evaluating the system's ability to interact with physical objects and user position change when viewing the mid-air images. This was given a rating of 60% in favour of the system being aware of its surrounding environment. The MR System was not able to distinguish or interact with physical

objects. Therefore, it was impossible for the mid-air images on the system to adjust themselves due to the environment. This would require a camera tracking the interaction space to relate the position of any physical objects to the MR System. The system would then have to process this data and have the mid-air image react to this physical object's presence in its interaction volume. This technique was similar to the interaction technique used by the MARIO system [18]. So long as users were within the system's viewing angle, they could change their positions and still view the mid-air images. The MR System was not able to react to user position change outside the viewing angle. View-dependant rendering would adjust the source image to the user position change outside of the viewing angle. This solution would not be possible to implement as it would create a single user system. A possible solution was developed in the flexible concept design (Section 3.4). The system was designed to rotate through 360° to search for users in its surroundings. If the user stepped outside the viewing angle, the system could adjust its physical position to match the user's position change.

User interaction was a parameter that evaluated the interacting granted on the MR System. This was given a rating of 100% in favour of achieving MR interaction on the system. Interaction was required without the use of any wearable technology. This was made possible on the MR System by allowing interaction through the connected laptop. Users could control mid-air images using the keyboard and mouse. This interaction was not the ideal technique desired. Gesture control was the desired interaction technique, but current gesture recognition using a laptop's web camera was found to deliver inaccuracy's that would affect system performance. Therefore, the CaptoGlove™ device was used to simulate gesture control when using the system. This was done to evaluate gesture control over laptop interaction. Gesture control was found to deliver a more natural interaction experience than laptop interaction. Therefore, an improvement to the current system would be to overcome the inaccuracies found with web camera gesture recognition. In conclusion, MR interaction was achieved, but the interaction technique could be improved.

Entertainment capability was a parameter that evaluated the MR System as a tool for entertainment. This was given a rating of 60% in favour of using the system for entertainment purposes. Testing the MR System with the MR game developed proved the system had the capability for entertainment. Initially, the system could not project the MR game in mid-air due to the size of the game window on the LCD screen (Figure 6-10). Having a source image larger than the beam splitter cuts the mid-air image's outer edges. This was an essential feature for users to perceive the projections in mid-air. The operation was successful when the game window's size was reduced, but this resulted in a loss of detail. Entertainment operations were possible on the MR System but were limited by the entertainment software and size of the beam splitter (ASKA3D Plate). Improvements in this operation would lie in creating a new MR game that did not require a large screen size or using a larger ASKA3D Plate.

Educational capability was a parameter that evaluated the MR System as a tool for visual learning. This was given a rating of 100% in favour of using the system for visual learning purposes. The MR System was found to meet the criteria discussed in Section 5.3.4 to consider its mid-air images as a tool for visual learning. The projection of videos and imagery were visible, showing deep colours and defined edges (Figure 6-11). The projection of text was possible so long as the font size was large and contained within the beam splitter area (Figure 6-12). Charts and diagrams were also visible, although the text on the image sources was hard to distinguish due to their small font. It required the user to strain their eyes during testing to read the information displayed. This was not seen as an issue as visual learning focused on perceiving information through images in conjunction with text and oral

explanations. Additionally, the use of mid-air image projection was found to generate an immersive experience due to the innovative nature of displaying the image “floating” in mid-air.

Engineering design was a parameter that evaluated the MR System as a tool for engineering design. This was given a rating of 60% in favour of using the SolidWorks™ application on the MR System. It was possible to achieve engineering design using the MR System. The models created on SolidWorks™ were projected in mid-air, given that the window of the application was bigger than the ASKA3D Plate. This was due to the neutral background of the SolidWorks™ application as it highlighted the edges of the created model that was within the area of the ASKA3D Plate (Figure 6-13). Due to the ability to resize models on SolidWorks™, it was possible to project large scale models in mid-air at a reduced size. This reduction of size reduced the surface detail of models. The disadvantage of this projection was the missing user interface. The user interface surrounding the application was not viewable by the user as the model was the focus of the mid-air projection. The laptop screen or LCD screen had to be used in conjunction with the mid-air image to view the SolidWorks™ interface and perform model design on the MR System.

The percentage ratings given for each parameter require further review as these ratings were based on feedback from a single user test. Further user testing would be required to improve the accuracy of these results. The current ratings gave a general indication of system operation. A full description of these ratings was presented in Section 6.3.4.

7.7 System observations

The manufactured MR System was presented in Figure 4-44. When compared to the CAD model of the MR System seen in Figure 4-37, the two images were identical. This proved the system designed in Chapter 4 was fully manufacturable and could be assembled as intended. The following observations were identified from the manufactured MR System after system testing to discuss expected system properties and additional properties that were not expected.

7.7.1 Expected system properties

Multiple user viewing was proven in a research paper published by the author to investigate the viewing capability of the ASKA3D Plate. This paper was published in the ICINCO 2020 conference proceedings [50] and investigated the viewing capability of the ASKA3D Plate when used on a test rig designed to fit the layout seen in Figure 2-4. User testing was performed in this paper to evaluate the ASKA3D Plates ability to present mid-air images and its ability to allow multiple user viewing. The method of user testing was based on the work presented by Zhang et al. [43]. This paper's results proved successful mid-air image projection and allowed five users to view the mid-air image simultaneously. This multiple user viewing was only based on the ASKA3D Plate’s capability. Additionally, it only allowed multiple users to view the images at a fixed user height. Therefore, this dissertation's MR System had the same capability as it used the same ASKA3D Plate from the paper published by Naidoo et al. [50].

The user height adjustment of the MR System was found to be successful in its actuation and purpose. The actuation was found to be accurate and repeatable in Section 6.2. The purpose of the height adjustment was to allow multiple user viewing at different user heights. When the user was testing the system in Section 6.3, the calculated system height adjustments from Section 4.4.3 were found to be correct. The ASKA3D Plate was

actuated to a height of 1050 mm from the ground to accommodate the user's height when seated and testing the MR System. At this height, the user was able to view the mid-air images displayed. Thus, the additional two plate heights calculated were expected to allow viewing for their respective user height ranges. This proved the system's ability to be adjusted to different users thus adding to its ability to allow multiple user viewing in conjunction with an ASKA3D Plate.

The layouts implemented by the MR System was found to be successful in delivering their required viewing for seated or standing users. When the system was tested to confirm the accuracy and repeatability of the ASKA3D Plate and LCD screen rotations, the standing layout (Figure 4-2) did not provide the expected improved viewing experience. The seated layout (Figure 4-1) was found to deliver better viewing for users standing or seated. This was an observation from the user testing and required further testing by multiple users to confirm this observation.

7.7.2 Additional system properties

Tight tolerances were observed when attaching the Layout Control sub-system to the Height Control sub-system. This was seen between the Connector component from the Layout Control sub-system and the bearing holders and NEMA17 motor brackets attached to the Height Control sub-system. There was a concern that this would impede the ASKA3D Plate and LCD screen rotation due to the small distance between these components. This was found to be false as the component's rotation was not affected. Additionally, these tight tolerances were found to benefit the system. Due to the tight tolerance, there was a reduced moment acting on the bearing shafts holding the ASKA3D Plate and LCD screen components, thus mitigating possible shaft failure.

There were two key observations found from the LCD screen in the MR System. When mounted to the Height Control sub-system, the LCD screen tended to rotate anti-clockwise at rest. This resulted from an imbalance caused by the motherboard and USB port in the LCD screen cover. The motherboard was mounted in the cover away from the component's centroid, thus creating a rotational moment of the LCD screen in an anti-clockwise direction. This issue can be corrected by disassembling the LCD screen and mounting the motherboard at the LCD screen's centroid. The second observation was the USB cable connected to the LCD screen acting against screen rotation. This was due to the tension in the cable when connected to the laptop. This was corrected by removing the USB cable when the Layout and Height Control sub-systems were making their adjustments. The USB cable was connected when the components were in their specified positions.

The lead screw covers presented two properties that worked against the MR System. When the lead screw covers enclosed the Height Control sub-system components, it was observed that the enclosed space created by the covers would inhibit cable movement of the NEMA 17 motors. These motors were used in the Layout Control sub-system. The Height Control sub-system moving the NEMA 17 motors upward or downward would shift these cables. This cable movement was expected and designed for as the NEMA 17 motors were wired with extra length giving the cable slack. It was observed that within the lead screw covers, there was no space for the cable to comfortably move, which resulted in the cable tending towards the lead screw. This posed an issue as this could impede the collars' motion on the lead screw and result in inaccurate height movements. Therefore, the back cover was removed to allow the NEMA 17 motor cables to sit outside the system away from the lead screw.

The second property identified was a cantilever created by the lead screw covers. This created a structural instability in the covers and the lead screws that they enclosed. This instability was due to the components' height

and the method used to fix the covers to the System Stand. Additionally, the thin sections of the Masonite board used for the covers worked against the stability due to its light-weight. If the covers had greater weight, they would work with gravity to increase stability. However, this would be to a small degree. The tabs and slots manufactured created a small area of interaction that caused this instability. This type of attachment was practical as it prioritised disassembly. To improve this issue, L-brackets could create a fixed connection between the lead screw covers and the base platform of the System Stand.

When manufacturing the System Stand, manufacturing the holder components that provided insulation was not the ideal method of fire prevention. Due to the large wooden surface area within the System Stand, this created a potential flammable area. Therefore, sheet metal was used to insulate the base on which the components would be placed. This could be used in conjunction with the holder components to add further fire prevention. The use of sheet metal would increase the weight of the system to a small degree, but this was considered inconsequential to prevent any potential fires.

7.8 Implications of research

The design and investigation of an MR System were proposed to validate multiple user viewing on a single device, reduce the processing power required for mid-air projection, evaluate entertainment capability, evaluate education capability and evaluate design capability. The mid-air image projection was achieved using beam splitter theory in conjunction with AIP technology. This method was useful in delivering a mid-air image that could be view by multiple users. Additionally, it did not require complex software to achieve this projection and relied solely on the system hardware.

Studies showed that the creation of a low-cost multiple user MR System was required [51]. Current virtual systems came at a high cost, were in limited stock and could only be used one user at a time. Most consumers did not welcome these characteristics. This research validates the creation of an MR System that can give users a virtual experience without robust technology and high processing power. The system's architecture was designed to use additive manufacturing to reduce cost, reduce system weight and create unique components for its operation. Additionally, this system was designed to adjust to a user's height range and viewing preference. This contributed to the multiple user viewing experience.

The automated component adjustments for user height and viewing preferences were found to be accurate and repeatable. This validated the methods of actuation created for the system. From these results (Chapter 6), the MR System's layout control was unnecessary as the layout seen in Figure 4-1 delivered better viewing for seated and standing users. Therefore, the use of the layout seen in Figure 4-2 was unnecessary. User testing of the system confirmed system operation and performance. It was possible to view mid-air images on the system and use the MR System for entertainment, education and design applications. This was done to identify areas where this system could be used. From the three applications explored, education was found to be more successful on the MR System.

The current MR System was found to have unnecessary features that could be removed to improve the system's operation. Therefore, an improved MR System should not require the use of interchangeable layouts, should implement height adjustments, should allow gesture control and should be used for visual learning operations.

Resources can be allocated to improve these specific system operations instead of implementing system functions that delivered no significant improvement when operating the system.

7.9 Chapter summary

This chapter presented the research question, justifications, concept creations, insights, system performance, system observations, and research implications. The justification for this research was discussed with the reviewed literature to deliver the key findings. The knowledge obtained from the literature was used to create system prototypes to investigate different renditions of the MR System. This was discussed in the concept overview. The MR System's hardware and software design insights were discussed, focusing on key features that influenced system operation. Findings and observations concerning system performance were discussed using the results obtained from testing the MR System's QoS and QoE parameters. Observations discussed the expected system properties to confirm system goals and identified additional properties that were not expected from the MR System. The chapter concluded with the MR System's implications, stating the final thoughts on the MR System developed.

The next chapter concludes the research by discussing the fulfilment of the aim, objectives, research question, insights and system limitations of the dissertation. Recommendations were given based on the experience gained from developing the MR System. Future work on this dissertation was suggested to conclude this chapter.

8. CONCLUSION

8.1 Introduction

This chapter concluded the dissertation's findings against the aim and objectives presented in Section 1.4 and Section 1.5, respectively. Additionally, the research question of this dissertation is addressed when the research contribution is concluded. Limitations, recommendations and future work were presented to conclude the research findings discussed in Chapter 7.

This dissertation's aim was met when the developed MR System used an ASKA3D Plate in conjunction with the designed system architecture to allow multiple user viewing of mid-air images. Additionally, the system was tested and analysed in Section 6.3 to indicate its potential for entertainment, education and engineering design applications.

8.2 Research contribution

This dissertation's contribution was identified using the aim and objectives in Section 1.3 and Section 1.5. The developed MR System delivered multiple user viewing without a robust computer system to experience virtual scenes. Additionally, this system was designed to have an automated architecture that could adjust to its users' preferences. This was implemented to investigate the implications of allowing system adjustment to improve user viewing and allow multiple user viewing. This method was proposed as an alternative to view-dependant rendering. Finally, the system was investigated to determine the real-world implications of MR technology.

Current virtual systems available to consumers had the common trait of allowing a single user to view and interact with virtual scenes. This limited the usage of these virtual systems, and coupled with their price ranges, consumers were unlikely to purchase these devices. The MR System developed in this dissertation contributed to the development of multiple user viewing on virtual technology. Allowing multiple users to view virtual information was a new area of virtual technology currently being researched. Investigating its usage and effect could lead to its implementation to improve the current methods of viewing virtual images.

The MR System development in this dissertation sought to improve on the required processing power for viewing virtual scenes. Standard VR and AR systems required robust computational power to deliver their virtual scenes. This added a requirement for users to have a robust computer system to use VR devices and increased AR devices' prices due to the built-in computers. The MR System was designed to operate without a robust computer system and was proven to run operations using a connected laptop. In Section 6.3, the MR System was user tested using a laptop to run MR programs. This contributed to research on virtual systems that could deliver virtual information without requiring robust technology or complex system software.

View-dependant rendering was identified as a method to improve a user's viewing experience on virtual systems. This method adjusted virtual images using the system software to suit the user's viewing position. This was unsuitable for multiple user viewing when using beam splitter theory to project the MR System's mid-air images. Therefore, the MR System implemented a corrective viewing method that allowed multiple user viewing. This was implemented using automated position changes of the ASKA3D Plate and LCD screen. The MR System adjusted these components to the user's height range and viewing preference. This alternative to view-dependant

rendering was discussed in Section 7.4 and Section 7.7.1. The findings supported physical height adjustment. This contributed to research on improving multiple user viewing without the use of view-dependant rendering.

The MR System required software to investigate successful areas of system operation. Due to the scarcity of MR Systems, there were no defined operations for MR technology. Therefore, the MR System was evaluated based on operation areas commonly used on virtual systems. The system was evaluated as a tool for entertainment, education and engineering design in Section 6.3. These tests showed that the MR System supported visual learning with no significant improvement to the entertainment and design areas. Due to the viewing technique, there was no dedicated system software for the MR System. Users required an image displayed on the LCD screen to obtain mid-air projection. This was an improvement to current virtual systems as they required dedicated system software to view virtual information. These findings contributed to the future usage of MR technology by identifying current areas where the technology excels. Additionally, the lack of dedicated software contributed to creating a flexible system that supported MR program development on the connected laptop OS.

8.3 Insights of the Mixed Reality System

Mid-air image projection was based on beam splitter theory which created the illusion of users perceiving mid-air images. In reality, users were viewing the source image along the surface of the beam splitter. This method was used with an AIP to deliver distortion-free imaging and imaging in front of the beam splitter. Allowing mid-air projection in front of the beam splitter created an open viewing environment and promoted multiple user viewing.

The MR system allowed multiple users to view the mid-air images using an ASKA3D Plate as the beam splitter. These mid-air images were displayed in 2D using the system hardware. When used in conjunction with software programs, depth was added to the source images delivering 3D mid-air images. This increased the realism of the mid-air images projected.

The system architecture was designed to conceal system components that would draw away user attention. Additionally, dark colours were used on the surface of visible components to achieve the same effect. These methods were implemented to focus the user's view and improve their efficiency in perceiving the mid-air images. This was found to be true. The system architecture presented an open design unlike similar systems (HoloDesk). The findings from this implementation showed clear projection in both light and dark environments. The major drawback of this architecture was the instability of the lead screw covers.

The automated layout control of the AKSA3D Plate and the LCD screen was accurate and repeatable in its actuation, but unnecessary as a single layout could be used for both standing and seated users. The layout presented in Figure 4-1 was found to deliver better viewing to users seated or standing. This finding was not expected and disproved the initial assessment that this layout would not deliver comfortable viewing to standing users. Therefore, the second system layout (Figure 4-2) was irrelevant to improve user viewing on the MR System. The removal of this layout would reduce the waste of system resources since both viewing instances were possible with one layout. The purpose of allowing two possible viewing methods was to give users the freedom to personalise their viewing experience. While this layout was unnecessary, it gave users the freedom to adjust the system to their liking. The possible removal of this layout should be considered pending reviewal from further user testing.

The ASKA3D Plate and LCD screen's height control was found to be accurate and repeatable in its actuation. Allowing these components to adjust to their heights enabled the system to accommodate users with a minimum height of 1500 mm and a maximum height of 1800 mm when standing and a minimum height of 947 mm, and a maximum height of 1247 mm when seated (Section 4.4.3). User viewing was allowed within specified height ranges established in Section 7.7.1. This actuation created vibrations that affected the stability of the lead screw due to the unstable lead screw covers. Ensuring the lead screw covers were fixed in place reduced this stability issue.

The designed MR System did not require processing power to project mid-air images but did require software to perform interactions and specific operations on the system. Standard interaction on the MR System was given through inputs on the laptop with an option for gesture control using the CaptoGlove™. This was due to the poor-quality interactions currently available when using gesture control through a web camera. Gesture control was the desired interaction method for the system and should be implemented once it has improved.

Dedicated system software was not required as the MR System could display mid-air images using the OS on a laptop. Additionally, since interaction through the laptop's web camera was not implemented, the interaction did not require system software unless the CaptoGlove™ was used to simulate gesture control. When investigating system operation, specific software was used for entertainment and engineering design evaluations. Educational evaluation of the system demonstrated the lack of dedicated software. This investigation also proved that the MR System would support visual learning over entertainment and engineering design. This was due to the quality of the mid-air images displayed and the system's ability to draw user interest. The mid-air images displayed left a lasting impact on viewers, which benefited visual learning.

The total cost to manufacture the MR System was lower than currently available VR and AR systems. The total expenditure for the system was presented in Appendix A, Table A-1, as R18 556,98. The complete HTC VIVE™ Pro Starter Kit was found to cost €1099 (R19 202,37) on the VIVE™ website [52], and the HoloLens 2™ was found to cost $3500 (R52 102,40) on the Microsoft website [53]. This showed that the designed MR System delivered a virtual system at a lower cost due to its design choices for system operation and component manufacture.

The hypothesis statement in Section 1.5 was proven to be true. The system was able to deliver multiple user viewing through automated system adjustment. This was made possible by the Layout Control and Height Control sub-systems. Finally, the system proved its capability to facilitate entertainment, education and engineering design. Education was found to be more successful regarding system usage.

8.4 Limitations of research

Limited user testing was performed on the MR System. This was due to lockdown protocols initiated with the Covid-19 pandemic. Testing the system with multiple users would deliver diverse feedback, which was not subject to bias. This would optimise the results obtained from the author's testing of the MR System. The evaluation method used for user testing allowed single-user testing that gave accurate feedback. Therefore, the results presented were justified but could be improved with diverse user testing.

The desired interaction of web camera gesture control was not implemented on the MR System due to current disadvantages with its method. Although the interaction was successful, the method encountered various errors that would reduce the quality of interaction. Therefore, MR System allowed interaction through the laptops keyboard and mouse pad or the CaptoGlove™ was used to simulate the desired gesture control.

Three areas of use were investigated to assess the MR System's operation as a virtual system. A single software or method was used for each area to evaluate the system. An MR game was developed to assess the system's ability for entertainment. Images, videos, charts and diagrams were displayed in mid-air to evaluate the system for educational purposes. SolidWorks™ was used to evaluate the system's ability to perform engineering design. All three areas were limited to a single operation method that was used to assess the whole system. Exploring multiple operations could lead to different findings and give an in-depth review of the system's functionality.

8.5 Recommendations

MR is a technology in its research phase, and the system presented in this dissertation is a possible implementation. There is still room for developing similar MR systems that aim to deliver virtual scenes without robust technology or system software.

User interaction through a laptop allowed MR interaction but should not be considered in future designs. Interaction should be delivered through gestures or direct hand interaction with mid-air images. This would deliver an immersive system as interaction through a laptop was found to leave users unsatisfied. Hand or gesture interaction adds to the mid-air image's realism as it created a natural interaction environment.

The alternative to view-dependant rendering was successful and could be improved with additional actuation methods that influenced the system hardware. This method of system adjustment should be implemented in future work to investigate its potential over the software alternative of view-dependant rendering. Additionally, this system adjustment method allowed multiple users within specified height rangers to view and interact with mid-air image.

Further analysis should be implemented to assess the entertainment and design capabilities of MR Systems. These operations could be further successful on the MR System with the development of dedicated system software. This dissertation presented visual learning as the better operation for the current system.

8.6 Future work

Develop an accurate method of gesture recognition that could be implemented through a laptop's web camera. Building on the current method identified by Yeo [34], it will be possible to achieve this interaction. This interaction should be evaluated on its response time, hand tracking accuracy and its operational area. Implementing this method of interaction will complete the MR System developed in this dissertation.

This dissertation investigated MR system properties and operations. These findings should be used to develop an optimised MR System. The new system should be designed for educational purposes as a medium for visual learning. This should be a stand-alone system that does not require users to bring their technology for system operation. Viewing should be allowed on a single layout with a height adjustment of components to allow multiple user viewing. An effort should be made to improve the viewing angle of the system so that the viewing area increases, allowing more users to view the mid-air images. The ASKA3D Plate and LCD screen would require

further investigation to identify the appropriate size. Since these were primary components for mid-air image projection, most of the system cost can be allocated to these components. Interaction should be allowed through gesture control with a possible implementation of voice control. Gesture control should be allowed using a common web camera to reduce system cost. Voice control would require further research but can increase the immersive experience when viewing mid-air images. This theorised system can be implemented to advertise information in a way that grabs user attention. This will improve the learning environment at schools, improve the way information is advertised, create new self-service stations, and create an improved viewing and interacting method with virtual information.

8.7 Chapter summary

This chapter concluded on the research of the dissertation. The aim, objectives and research question were briefly discussed to highlight how these measures were met, and the findings obtained when achieving them. Key insights on the MR System were discussed to demonstrate the knowledge obtained throughout the dissertation. Limitations and recommendations were presented to identify and suggest improvements for the MR System and MR technology. The chapter concluded with suggestions concerning future work based on the information presented in this dissertation.

REFERENCES

[1] B. Marr, “These 25 Technology Trends Will Define The Next Decade,” Forbes, 20 April 2020. [Online]. Available: https://www.forbes.com/sites/bernardmarr/2020/04/20/these-25-technology-trends-will-define-the-next-decade/#699839429e3b. [Accessed 5 May 2020].

[2] J. Kellinger, “What is Mixed Reality?,” Researchgate, 10 May 2017. [Online]. Available: https://www.researchgate.net/post/What_is_Mixed_Reality. [Accessed 11 May 2020].

[3] R. Parés, “What is Mixed Reality?,” Researchgate, 11 May 2017. [Online]. Available: https://www.researchgate.net/post/What_is_Mixed_Reality. [Accessed 11 May 2020].

[4] J. Zhuo, “The Future of Design in Technology,” Medium, 12 May 2015. [Online]. Available: https://medium.com/the-year-of-the-looking-glass/the-future-of-design-in-technology-fe1697e5826. [Accessed 22 July 2019].

[5] G. Finn, “Why Augmented Reality and Virtual Reality Will be Important for Your Business,” 12 September 2017. [Online]. Available: https://www.entrepreneur.com/article/300071. [Accessed 24 January 2019].

[6] B. Marr, “5 Important Augmented And Virtual Reality Trends For 2019 Everyone Should Read,” 14 January 2019. [Online]. Available: https://www.forbes.com/sites/bernardmarr/2019/01/14/5-important-augmented-and-virtual-reality-trends-for-2019-everyone-should-read/#432aefcc22e7. [Accessed 24 January 2019].

[7] G. Dini and M. D. Mura, “Application of Augmented Reality Techniques in Through-life Engineering Services,” in *The Fourth International Conference on Through-life Engineering Services,* 2015.

[8] Y. Chong, D. K. Sethi, C. . Y. Loh and F. Lateef, “Going Forward with Pokemon Go,” *Journal of Emergencies Trauma and Shock ,* vol. 11, no. 10, p. 243, 2018.

[9] J. Tropp and A. Baetzgen, “Users’ Definition of Snapchat Usage. Implications for Marketing on Snapchat,” *The International Journal on Media Management,* vol. 21, no. 1, pp. 1-27, 2019.

[10] I. S. Madania and F. Fadillah, “Mixed Reality: The Future Media of Advertising,” in *International Moving Image Cultures Conference,* 2019.

[11] J. Heimgartner, “Augmented Reality for Architects and Civil Engineers,” 27 May 2016. [Online]. Available: https://www.engineering.com/BIM/ArticleID/12233/Augmented-Reality-for-Architects-and-Civil-Engineers.aspx. [Accessed 24 January 2019].

[12] A. Strange, “Onshape Partners with Magic Leap to Bring Its Collaborative Industrial 3D Design Tool to AR,” Next Reality, 10 October 2018. [Online]. Available: https://magic-leap.reality.news/news/onshape-partners-with-magic-leap-bring-its-collaborative-industrial-3d-design-tool-ar-0188407/. [Accessed 24 June 2020].

[13] Statista, “XR/AR/VR/MR technology and content investment focus worldwide from 2016 to 2019,” Statista, March 2019. [Online]. Available: https://www.statista.com/statistics/829729/investments-focus-vr-augmented-reality-worldwide/. [Accessed 16 March 2021].

[14] Accenture, “Waking Up To A New Reality,” Accenture, 2019.

[15] Statista, “Global market spend on extended reality (XR) technologies 2018-2023, by industry,” Statista, May 2019. [Online]. Available: https://www.statista.com/statistics/1096765/global-market-spend-on-xr-technologies-by-industry/. [Accessed 16 March 2021].

[16] S. Ho, P. Liu, D. J. Palombo, T. C. Handy and C. Krebs, “The role of spatial ability in mixed reality learning with the HoloLens,” *Anatomical Sciences Education,* 2021.

[17] M. Speicher, B. D. Hall and M. Nebeling, “What is Mixed Reality?,” in *ACM CHI Conference on Human Factors in Computing Systems*, Glasgow, 2019.

[18] H. Kim, I. Takahashi, H. Yamamoto, S. Maekawa and T. Naemura, “MARIO: Mid-air Augmented Reality Interaction with Objects,” *Entertainment Computing 5,* vol. I, no. 1, pp. 223-241, 2014.

[19] IGI Global, “What is Spatial Augmented Reality (SAR),” IGI Global, [Online]. Available: https://www.igi-global.com/dictionary/spatial-augmented-reality-sar/56556. [Accessed 13 May 2019].

[20] O. Hilliges, D. Kim, S. Izadi, M. Weiss and A. D. Wilson, “HoloDesk: Direct 3D Interactions with a Situated See-Through Display,” in *Morphing & Tracking & Stacking: 3D Interaction*, Austin, Texas, 2012.

[21] A. Aspect and M. Brune, Directors, *Quantum Optics - Beam splitter in quantum optics.* [Film]. Georgia: Intrigano, 2017.

[22] N. Zhang, T. Huang, X. Zhang and H. Liao, “A novel in-situ interactive 3D floating autostereoscopic display system with aerial imaging plate,” *International Conference on Display Technology (ICDT 2020),* vol. 52, no. S1, pp. 244-247, 2021.

[23] ASKA3D, “ASKA3D,” [Online]. Available: https://aska3d.com/en/. [Accessed 11 02 2020].

[24] R. Radkowski and J. Oliver, “Enhanced Natural Visual Perception for Augmented Reality-Workstations by Simulation of Perspective,” *Journal of Display Technology ,* vol. 10, no. 5, pp. 333-344, 2014.

[25] M. F. Deering, “Explorations of Display Interfaces for Virtual Reality,” IEEE, California, 1993.

[26] J. S. Roo and M. Hachet, “Interacting with Spatial Augmented Reality,” 7 March 2016. [Online]. Available: https://hal.archives-ouvertes.fr/hal-01284005/document. [Accessed 17 July 2019].

[27] R. Bickmann, C. Tran, N. Ruesch and K. Wolf, “Haptic Illusion Glove: A Glove for Illusionary Touch Feedback when Grasping Virtual Objects,” in *Proceedings of Mensch und Computer 2019*, 2019.

[28] HaptX, “HaptX,” HaptX Inc, [Online]. Available: https://haptx.com/. [Accessed 10 June 2020].

[29] Plexus, “Plexus,” Plexus, [Online]. Available: http://52.14.145.186/. [Accessed 10 June 2020].

[30] CaptoGlove, “CaptoGlove: Take Control of Your Technology,” CaptoGlove, [Online]. Available: https://www.captoglove.com/. [Accessed 11 02 2020].

[31] M. Shigapov, E. Zykov and V. Kugurakova, “Design of digital gloves with feedback for VR,” IEEE, Moscow, 2018.

[32] M. Hilman, D. K. Basuki and S. Sukaridhoto, “Virtual Hand: VR Hand Controller Using IMU and Flex Sensor,” in *2018 Internatinal Electronics Symposium on Knowledge Creation and Intelligent Computing (IES-KCIC)*, Surabaya, 2018.

[33] N. Lalithamani, “Gesture Control Using Single Camera For PC,” in *Procedia Computer Science*, Coimbatore, 2016.

[34] Z. X. J. Yeo, “Hand Recognition and Gesture Control Using a Laptop Web-camera,” SemanticScholar, California.

[35] S. Ong, Beginning Windows Mixed Reality Programming, Tukwila: Apress, Berkeley, CA, 2017.

[36] R. G. Thomas, N. W. John and I. S. Lim, “Mixed Reality Anatomy Teaching Tool,” in *Theory and Practice of Computer Graphics*, 2006.

[37] T. Baltrusaitis, “OpenFace,” 17 July 2019. [Online]. Available: http://www.github.com/TadasBaltrusaitis/OpenFace. [Accessed 10 October 2019].

[38] M. Roser, C. Appel and H. Ritchie, “Human Height,” Our World in Data, May 2019. [Online]. Available: https://ourworldindata.org/human-height. [Accessed 13 July 2020].

[39] J. Raiyn, “The Role of Visual Learning in Improving Students’ High-Order,” *Journal of Education and Practice*, vol. 7, no. 24, pp. 115-121, 2016.

[40] I. Clarke, T. B. Flaherty and M. Yankey, “Teaching the Visual Learner: The Use of Visual,” *Journal of Marketing Education*, vol. 28, no. 218, pp. 218-226, 2006.

[41] C.-C. Yen, C.-Y. Lee, J.-H. Wang and S.-H. Yang, “A Digital Reality Learning Environment with Instant Assessment on Learning with,” *2020 IEEE 20th International Conference on Advanced Learning Technologies (ICALT)*, pp. 77-78, 2020.

[42] L. Kent, C. Snider, J. Gopsill and B. Hicks, “Mixed reality in design prototyping: A systematic review,” *Design Studies,* vol. 77, pp. 1-35, 2021.

[43] L. Zhang, H. Dong and A. E. Saddik, “Towards a QoE Model to Evaluate Holographic Augmented Reality Devices: A HoloLens Case Study,” ResearchGate, Ottawa, 2018.

[44] D. Alexandrovsky, S. Putze, V. Schwind, E. D. Mekler, J. D. Smeddinck, D. Kahl, A. Krüger and R. Malaka, “Evaluating User Experiences in Mixed Reality,” in *Conference on Human Factors in Computing Systems*, 2021.

[45] B. Kelechava, “ISO 5725-2:2019 – Accuracy Method For Repeatability,” ANSI American National Standards Institute , 26 December 2019. [Online]. Available: https://blog.ansi.org/2019/12/iso-5725-2-2019-accuracy-method-repeatability/. [Accessed 19 January 2021].

[46] K. Beck, “How to Calculate the Accuracy of Measurements,” Sciencing , 3 November 2020. [Online]. Available: https://sciencing.com/calculate-accuracy-measurements-6391160.html. [Accessed 29 January 2021].

[47] C. Deziel, “How Do I Calculate Repeatability?,” Sciencing , 3 November 2020. [Online]. Available: https://sciencing.com/do-calculate-repeatability-7446224.html. [Accessed 29 January 2020].

[48] J. Kaufmann, “What do you consider a good standard deviation?,” Researchgate, 26 September 2014. [Online]. Available: https://www.researchgate.net/post/What-do-you-consider-a-good-standard-deviation#:~:text=For%20an%20approximate%20answer%2C%20please,1%20can%20be%20considered%20low.&text=A%20%22good%22%20SD%20depends%20if,spread%20out%20around%20the%20mean.. [Accessed 2 February 2021].

[49] A. Toet, T. Mioch, S. Gunkel, O. Niamut and J. B. F. Van Erp, “Assessment of Presence in Augmented and Mixed Reality Presence in Augmented and Mixed Reality,” in *Workshop Evaluating User Experiences in Mixed Reality,* Virtual, Online, 2021.

[50] D. Naidoo, G. Bright and J. Collins, “ Mid-air Imaging for a Collaborative,” in *In Proceedings of the 17th International Conference on Informatics in Control, Automation and Robotics*, Paris , 2020.

[51] K. Noonan, “The 9 Biggest Virtual Reality Stocks,” The Motley Fool, 26 January 2020. [Online]. Available: https://www.fool.com/investing/2020/01/26/the-9-biggest-virtual-reality-stocks.aspx. [Accessed 20 March 2021].

[52] VIVE, “VIVE PRO Starter Kit,” VIVE, [Online]. Available: https://www.vive.com/eu/product/vive-pro-starter-kit/. [Accessed 20 March 2021].

[53] Microsoft, “HoloLens 2,” Microsoft, [Online]. Available: https://www.microsoft.com/en-us/p/holoLens-2/91pnzzznzwcp/?activetab=pivot%3aoverviewtab. [Accessed 20 March 2021].

[54] R. Budynas and K. Nisbett, Shigley's Mechanical Engineering Design (Mcgraw-hill Series in Mechanical Engineering) 9th Edition, Mcgraw-Hill Series in Mechanical Engineering, 2010.

[55] J. Brouchoud, “Virtual reality tool offers real-world solutions,” Wisconsin State Journel, 24 September 2017. [Online]. Available: https://madison.com/wsj/business/technology/virtual-reality-tool-offers-real-world-solutions/article_66e6bb40-bbdc-515f-bca0-235fee5b168b.html. [Accessed 22 June 2020].

APPENDICES

APPENDIX A. PROJECT EXPENDITURE

Table A-1 lists the cost of components used to manufacture and test the dissertation's designed MR System.

Table A-1: Project expenditure

Component	Price /unit	Quantity	Cost
Mechanical			
RS Pro Lead screw	R161,61	1	R161,61
RS Pro Round Nut for Lead screw	R119,53	4	R478,12
Stepper Motor Mounting Bracket- NEMA 17	R34,95	2	R69,90
Radial Ball Bearing 5 mm diameter	R17	2	R34,00
Radial Ball Bearing 8 mm diameter	R14	4	R56,00
M4 Grub Screw	R0,95	4	R3,80
Assorted Nuts, Bolts & Screws	R 200	1	R200,00
Electronics			
Stepper Motor, 1 Nm, NEMA 23	R489	2	R978
Stepper Motor 0.28 Nm NEMA 17	R185	2	R370
LRS Compact 24 V 6.5 A 156 W PSU	R294	2	R588
TB6560 Stepper Motor Driver	R189,95	4	R760
Terminal block strip	R50	1	R50
Jumper wires (Male to female & Male to Male)	R22	1	R22
Breadboard 170TP	R13	1	R13
Switch	R12	1	R12
9 V Battery	R60	1	R60
SUNON 12 V 4010 Silent Axial Fan	R100	1	R100
Arduino UNO	R160	1	R160
Additive Manufacturing			
RS PRO 2.85 mm Black PLA 3D Printer Filament, 1 kg	R584,51	1	R584,51
RS PRO 1.75 mm Black PLA 3D Printer Filament, 1 kg	R583,62	1	R583,62
Miscellaneous			
ASKA3D Plate	R6 836,39	1	R6 836,39
CaptoGlove™	R4 439,49	1	R4 439,49
AOC USB 3.0 Monitor 15.6 1366X768	R1 646,74	1	R1 646,74
Wooden boards and blocks	R350	1	R350,00
Total Cost	**R18 556,98**		

APPENDIX B. PRODUCT DATASHEETS

B.1 ASKA3D Plate delivery specification

Delivery Specifications

Product Name: ASKA3D-200NT

Product No.: NT200_200Z1U1-3016

Contents

Date issued: Nov. 15, 2018

Asukanet Co., Ltd.

1. Applicable Scope

This Specification Sheet stipulates items related to quality for the "ASKA3D-200NT (Product No.: NT200_200Z1U1-3016)" holographic display delivered by Asukanet Co., Ltd. to the customer.

2. Specifications

2-1. Design Specifications

Item	Specification	Notes
External dimensions of finished product	200 +/- 1.0 x 200 +/- 1.0 [mm]	Refer to 2-2. External Drawings.
Finished product thickness	t = 6.3 +/- 0.5 [mm]	Refer to 2-2. External Drawings.
Weight	256 +/- 10 [g]	-

2-2. External Drawings

Drawing: NT200_200Z1U1-3016

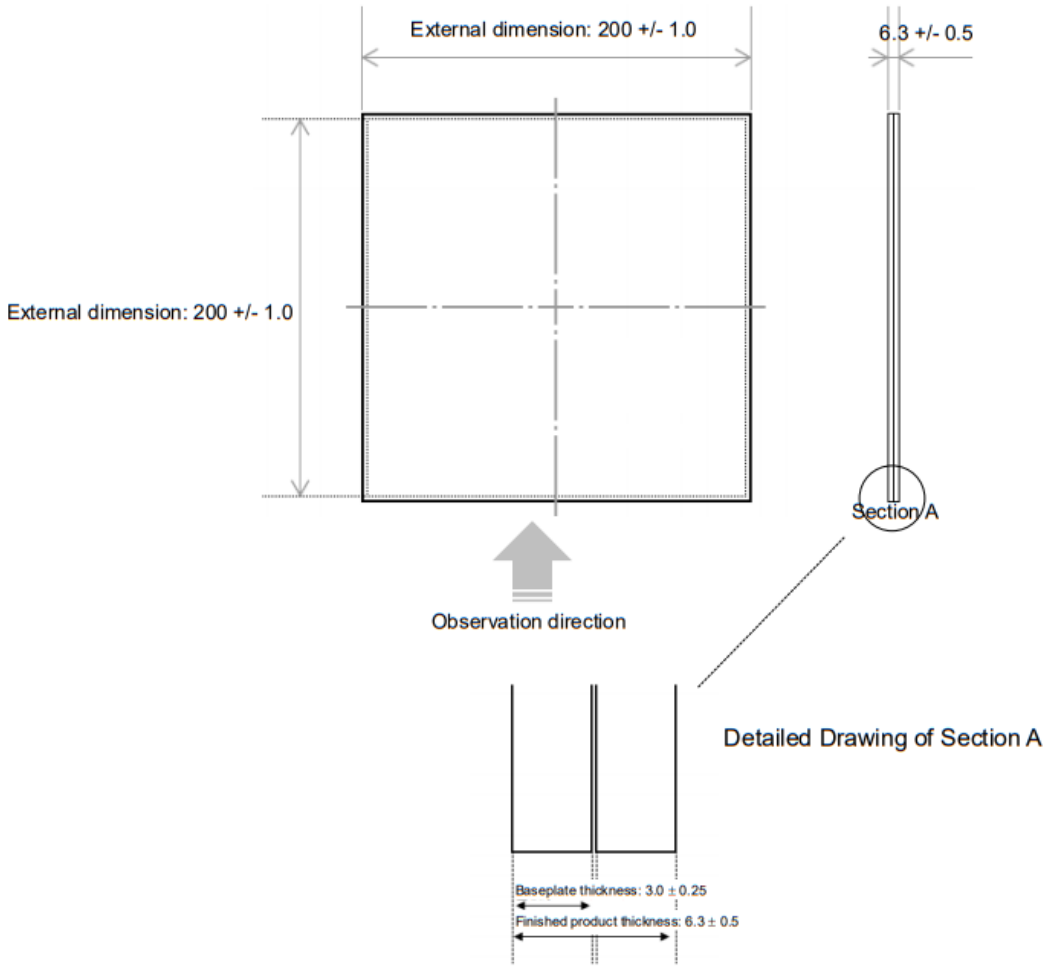

3. Testing Device

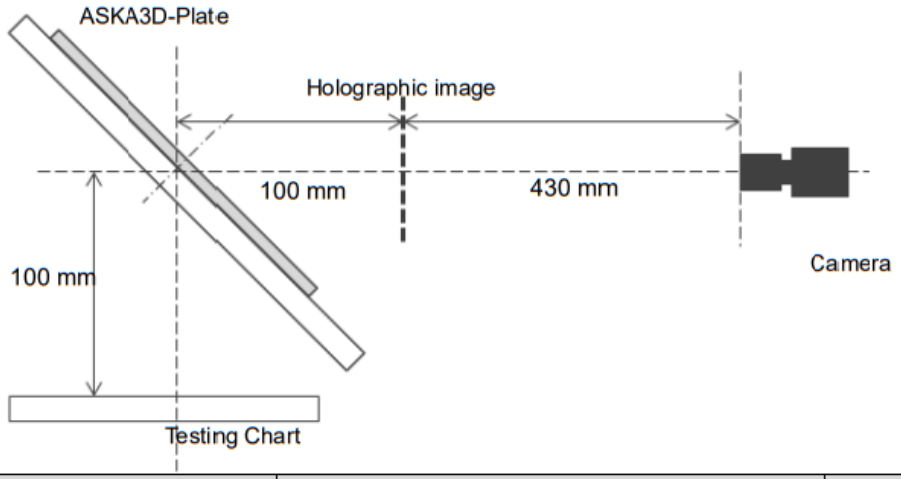

Item	Model No. / Specification	Notes
Camera / Lens	5 Megapixels / f = 12 mm	-
Monitor	7 inch, 1920 x 1200 [pix]	-

4. Optical Performance Standards

4-1. Optical Performance

Item	Performance	Notes
Distortion	Surface area difference in comparison with the master image must be 10% or less.	Image evaluation using the testing device
Definition	The maximum value of the difference in brightness when measured must be equal to or more than the standard value.	Image evaluation using the testing device

4-2. Image Evaluation

Evaluation Method

Testing Chart

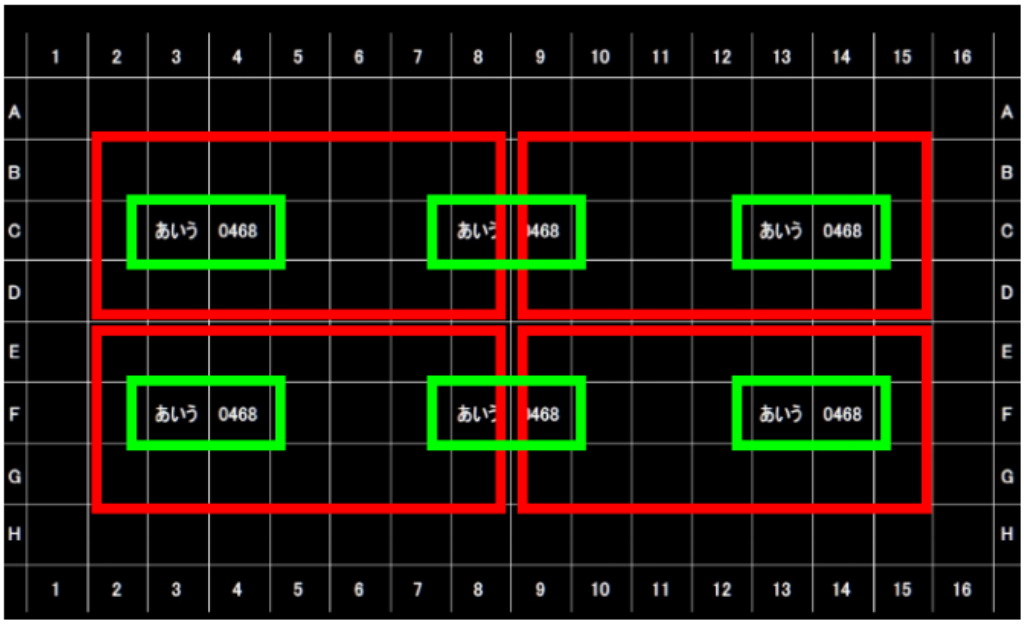

Capture a holographic image of the chart shown above and perform the following procedures to evaluate the image by using image processing.

<Red frame = Distortion measurement area>

- The image processing is considered acceptable if the surface area difference in comparison with the master image is 10% or less for all four measurement areas.

<Green frame = Definition measurement area>

- The image processing is considered acceptable if equal to or more than the standard value for all six measurement areas.

5. Exterior Testing Standards

5-1. Definition of Exterior Testing Scope

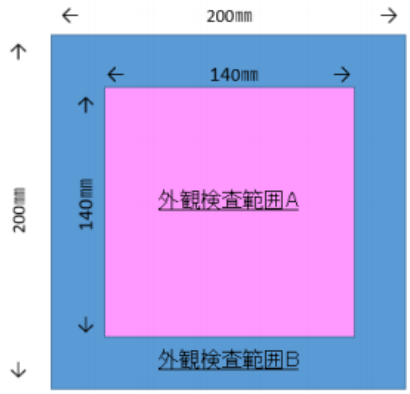

Definitions

<Exterior testing scope A: Red area>

- Area size: 140 mm x 140 mm
- Area location: Location at 20 mm from the top and bottom edges, and 20 mm from the right and left edges

<Exterior testing scope B: Blue area>

- Area other than exterior testing scope A

5-2. Exterior Testing Standards

Item	Area	Width	Length	Allowable Amount	Notes
Linear defects (Surface damage)	Exterior testing scope A	1) Less than 0.1 mm	Disregard	Disregard	• Visual inspection and inspection by testing device as necessary • Exterior testing scope A: Distance between defects of 3) must be 3.0 mm or more. • No specifications for distance between defects other than the above
		2) 0.1 mm to less than 0.3 mm	30 mm or less	Disregard	
		3) Same as above	30 mm or more	3 defects or less	
		4) 0.3 mm or more	30 mm or more	0 defects	
	Exterior testing scope B	1) Less than 0.1 mm	Disregard	Disregard	
		2) 0.1 mm to less than 0.3 mm	30 mm or less		
		3) Same as above	30 mm or more		
		4) 0.3 mm or more	30 mm or more		
Linear defects (Internal damage / Foreign material)	Exterior testing scope A	1) Less than 1 mm	Disregard	Disregard	• Striation patterns due to molds must be considered as defects. • Visual inspection and inspection by testing device as necessary • Exterior testing scope A: Distance between defects of 2) must be 3.0 mm or more. • No specifications for distance between defects other than the above
		2) 1 mm to 1.5 mm	30 mm or less	3 defects or less	
		3) Same as above	30 mm or more	0 defects	
	Exterior testing scope B	1) Less than 1 mm	Disregard	Disregard	
		2) 1 mm to 1.5 mm	30 mm or less	Disregard	
		3) Same as above	30 mm or more	3 defects or less	

Item	Area	Width	Length	Allowable Amount	Notes
Point-like defects (Foreign material / Black spots)	Exterior testing scope A	1) Less than φ0.5 mm	-	Disregard	• Visual inspection and inspection by testing device as necessary • If there are elliptical shapes, use the average value of the minimum and maximum diameters. • Exterior testing scope A: Distance between defects of 2) and 3) must be 5.0 mm or more. • No specifications for distance between defects other than the above
		2) φ0.5 mm to less than φ1.0 mm	-	4 defects or less	
		3) φ1.0 mm to less than φ2.0 mm	-	2 defects or less	
		4) φ2.0 mm or more	-	0 defects	
	Exterior testing scope B	1) Less than φ0.5 mm	-	Disregard	
		2) φ0.5 mm to less than φ1.0 mm	-		
		3) φ1.0 mm to less than φ2.0 mm	-		
		4) φ2.0 mm or more	-	2 defects or less	
Air bubbles	Exterior testing scope A	1) Less than φ0.6 mm	-	Disregard	• Visual inspection and inspection by testing device as necessary • If there are elliptical shapes, use the average value of the minimum and maximum diameters. • The same applies for air parts near foreign material. • Exterior testing scope A: Distance between defects of 2) and 3) must be 5.0 mm or more. • No specifications for distance between defects other than the above
		2) φ0.6 mm to less than φ1.0 mm	-	3 defects or less	
		3) φ1.0 mm to less than φ2.0 mm	-	1 defect or less	
		4) φ2.0 mm or more	-	0 defects	
	Exterior testing scope B	1) Less than φ2.0 mm	-	Disregard	
		2) φ2.0 mm to less than φ3.0 mm	-	1 defect or less	
		3) φ3.0 mm or more	-	0 defects	
Cracks	-	1) Less than 2 mm inward from the outermost edge	-	Disregard	• Visual inspection and inspection by testing device as necessary
		2) 2 mm or more inward from the outermost edge	-	2 defects or less	

6. Return Policy

We do not accept returns or offer exchanges due to the circumstances of the customer or agency.
We also do not accept returns or offer exchanges if we determine that we are not able to do so.

We do accept returns or offer exchanges in cases that correspond to the following "Return Conditions."

<Return Conditions>

1. The product does not meet the specifications in this Delivery Specification Sheet.
2. The shipping company damaged the product during transportation.
3. The wrong product was delivered through negligence of our company.
4. For items 1 to 3 above, you must contact us within 7 days after receiving the product.

Asukanet Co., Ltd.
3-28-14 Gion, Asaminami-ku, Hiroshima-shi, Hiroshima 731-0138 Japan

Tel. +81 82-225-6603
Mail. info@aska3d.com
Web. https://aska3d.com

B.2 ASKA3D Plate viewing angles

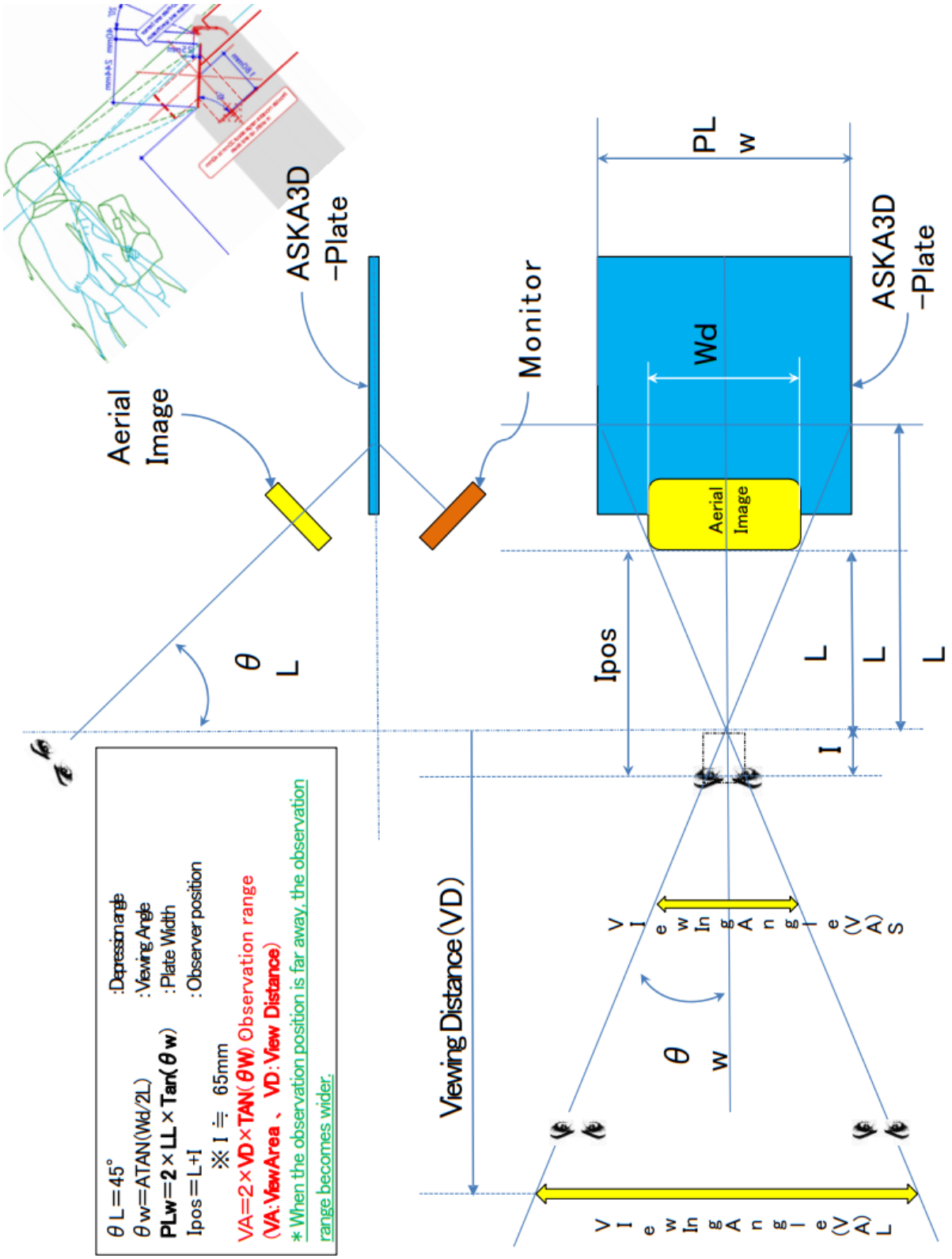

B.3 ASKA3D Plate layout specifications

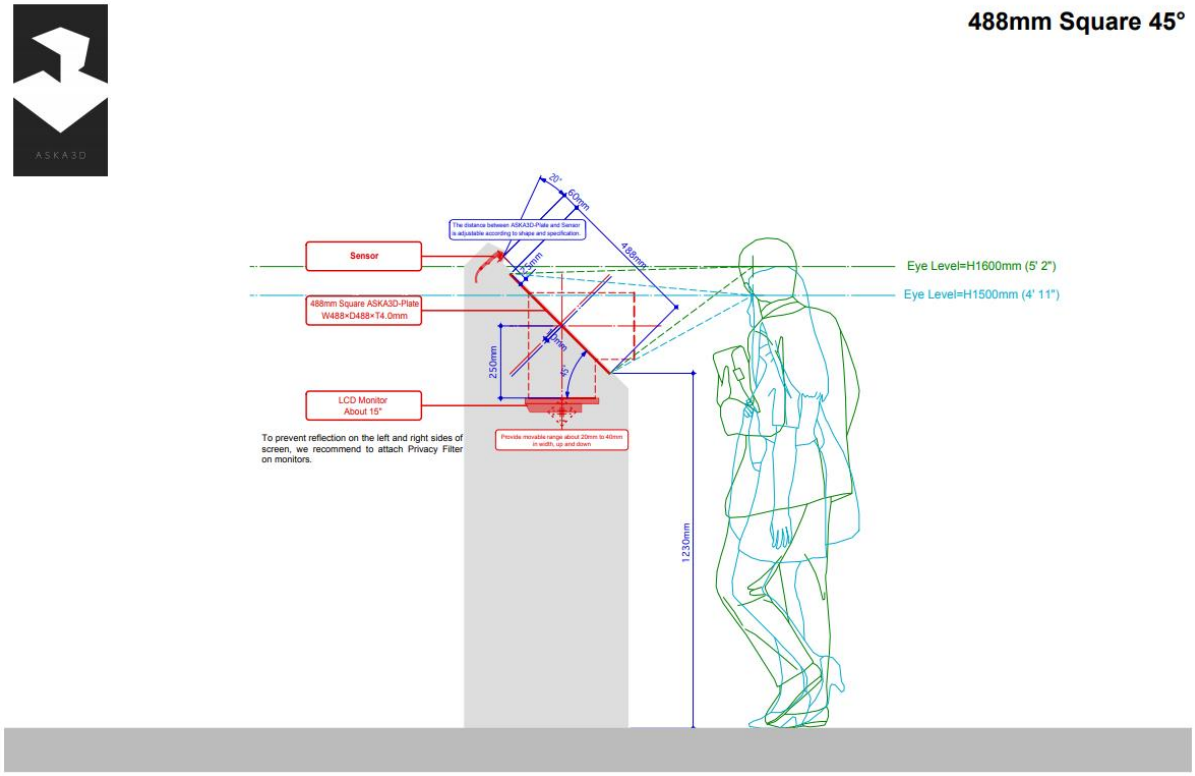

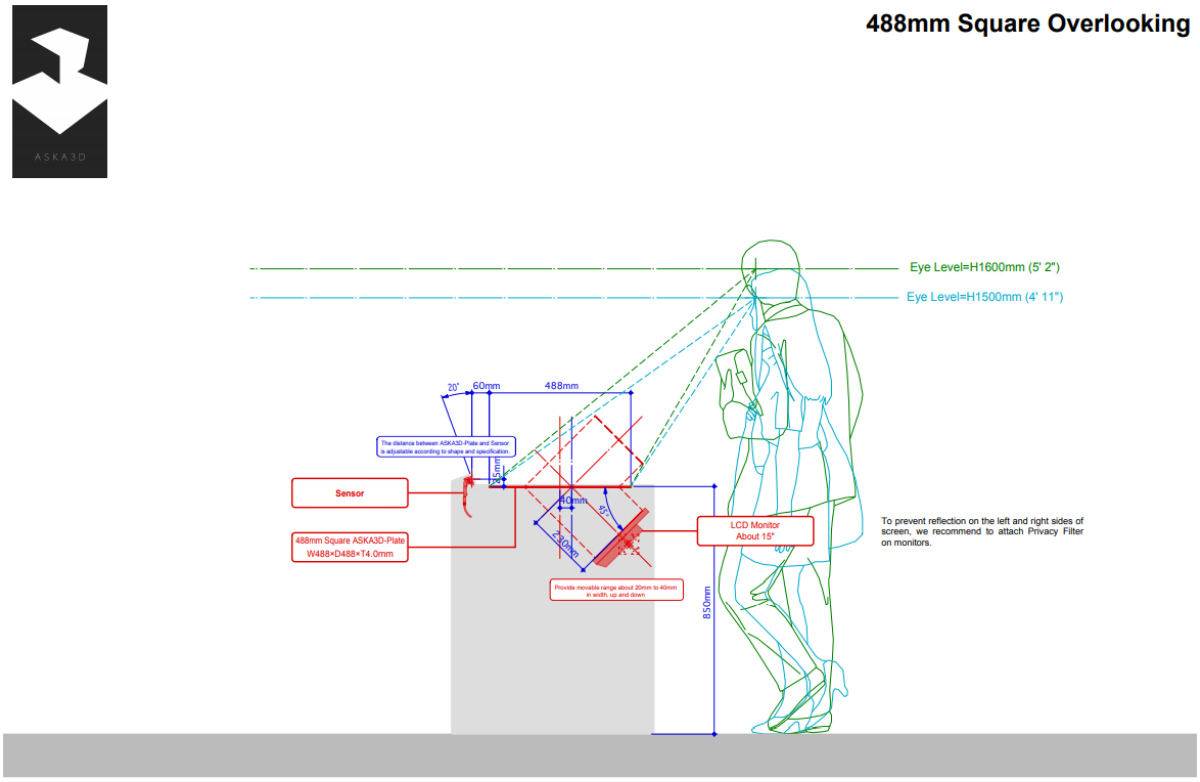

Scale=1/10

B.4 LCD screen datasheet

AOC E1659FWU 15.6" HD (1366 x 768) Desktop Monitor

Ultra portable on-the-go viewing

Get the ultimate convenience and portability with this USB-powered monitor that connects to your laptop or PC with a single cable. Easily rotate from portrait to landscape with the foldable stand.

USB monitor

Discover the freedom and flexibility of AOC's myConnect USB monitors. A single USB cable connects your laptop to the directly to the display, completely eliminating the need for extra media cables and a power supply. The USB cable transfers data to the screen, plus acts as an energy-efficient power source. For work or play, these monitors offer optimal portability. Besides ultra-easy connectivity, the innovative stand offers you a variety of viewing options.

SPECIFICATIONS:

Resolution	1366x768
Refresh rate	60Hz
Response time	5

Panel	TN
Backlight	WLED
Aspect Ratio	16:9
Brightness (typical)	200
Contrast (dynamic)	20M:1
Contrast (static)	500:1
Pixel Pitch (H) (V)	252
Diagonal (inch)	15.6
Active Screen Area (HxW)	344.23 x 193.54 mm
Viewing Angle (CR10)	90/50
Display Colours	16.7 Million
OSD languages	EN, FR , ES, PT, DE, IT, NL, SE, FI, PL ,CZ, RU, KR, CN (T), CN (S), JP
RoHS	Yes
Swivel	0 °
Powersupply	External
Power Consumption On	<7 watt
Power Consumption Off	0 watt
Power Consumption Standy	0.03 watt
Product dimensions incl base mm x mm x mm	369.8 x 219.14 x 22.2 mm
Carton dimensions mm x mm x mm	442x85x295 mm
Net weight excl package kg	1.2
Gross weight incl package kg	1.7
MTBF	50.000 hours
UPC Code	685417062485
TUV Bauart	Yes
Gost	Yes
PVC brf free	Yes
Rohs compliant	Yes
EUP compliant	Yes
FCC	Yes

B.5 Lead screw datasheet

ENGLISH

Datasheet

RS Trapezoidal Steel and Stainless Steel Lead Screw

General choice criteria

The choice between different types of screws and nuts available is generally carried out in light of the following considerations:

Choice of the screw

Working environment

For work environments where there are no particular corrosive or oxidizing agents C45 screws can be used. Where these conditions are not met, we recommend using stainless steel screws A2 or A4 which are particularly suitable in the following cases:

- With relative humidity of 70/80% and above.
- Immersed in water, even in sea water.
- In presence of particular corrosive agents such as chlorides. In case of highly corrosive agents please contact our Technical Department.
- Where, due to special construction requirements, components must not oxidise, for example in the food industry, where they are coupled with nuts HDA.
- Where screws can not be reached for lubrication. In particular, for lubricating "maintenance free" fittings they are coupled with plastic nuts.
- Where working temperature is relatively high because the stainless steel A2 and A4 feature a relatively high slag temperature due to the austenitic structure of the material.

ENGLISH

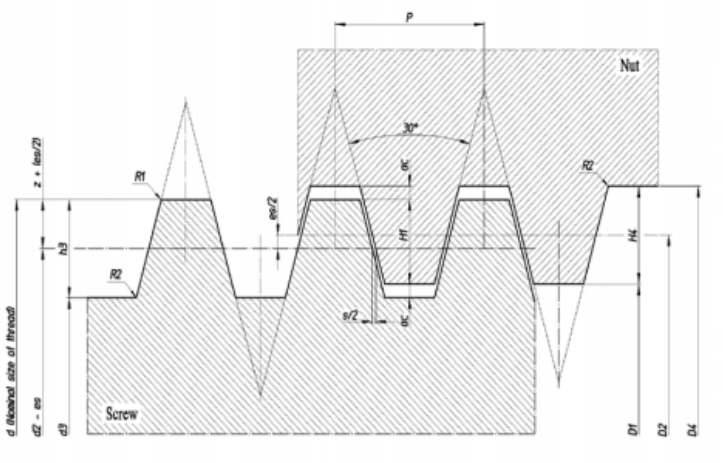

$H_1 = 0{,}5\ P$
$h_3 = H_4 = H_1 + a_c = 0.5\ P + ac$
$z = 0{,}25\ P = H_1/2$
$d_3 = d - 2\ h_3$
$d_2 = D_2 = d - 2\ z = d - 0.5\ P$
$D_2 = d + 2\ a_c$
a_c = bottom play
es = top deviation for screw
$s = 0{,}26795\ es$
R_1 max. $= 0.5\ a_c$
R_2 max. $= a_c$

RS Number	Screw Type	Material	Screw	Diameter x lead	Length	Thread starts	Laed accuracy µm /300 mm	Straightnes s mm / mm	Weight kg/mt	Surface Hardness after rolling
8625272	Trapezoidal	Carbon Steel C45 1.0503	Right	Tr10x2	1000 mm	1	100	0.5 / 300	0.48	App. 250 HB
8625281	Trapezoidal	Carbon Steel C45 1.0503	Right	Tr 12x3	1000 mm	1	100	0.5 / 300	0.65	App. 250 HB
8625284	Trapezoidal	Carbon Steel C45 1.0503	Right	Tr 14x3	1000 mm	1	100	0.5 / 300	0.93	App. 250 HB
8625288	Trapezoidal	Carbon Steel C45 1.0503	Right	Tr 16x4	1000 mm	1	100	0.5 / 300	1.17	App. 250 HB
8625297	Trapezoidal	Carbon Steel C45 1.0503	Right	Tr 18x4	1000 mm	1	100	0.5 / 300	1.53	App. 250 HB
8625290	Trapezoidal	Carbon Steel C45 1.0503	Right	Tr 20x4	1000 mm	1	100	0.5 / 300	1.94	App. 250 HB
8625294	Trapezoidal	Carbon Steel C45 1.0503	Right	Tr 22x5	1000 mm	1	100	0.2 / 300	2.29	App. 250 HB
8625304	Trapezoidal	Carbon Steel C45 1.0503	Right	Tr 24x5	1000 mm	1	100	0.2 / 300	2.78	App. 250 HB

RS Number	Screw Type	Material	Screw	Diameter x lead	Length	Thread starts	Laed accuracy µm /300 mm	Straightnes s mm / mm	Weight kg/mt	Surface Hardness after rolling
8625307	Trapezoidal	A4 Stainless Steel - AISI 316 1.4403	Right	Tr 10x2	1000 mm	1	200	1.5 / 300	0.48	App. 280 HB
8625301	Trapezoidal	A4 Stainless Steel - AISI 316 1.4403	Right	Tr 12x3	1000 mm	1	200	1.5 / 300	0.65	App. 280 HB
8625310	Trapezoidal	A4 Stainless Steel - AISI 316 1.4403	Right	Tr 14x3	1000 mm	1	200	1.5 / 300	0.93	App. 280 HB
8625313	Trapezoidal	A4 Stainless Steel - AISI 316 1.4403	Right	Tr 16x4	1000 mm	1	200	1.5 / 300	1.17	App. 280 HB
8625317	Trapezoidal	A4 Stainless Steel - AISI 316 1.4403	Right	Tr 20x4	1000 mm	1	200	1.5 / 300	1.94	App. 280 HB

B.6 Nut datasheet

ENGLISH

Datasheet

RS Trapezoidal Nut Type MZP – Cylindrical Steel

Material EN 10277-3 11 S Mn Pb 37 – 1.0737

Nut for fastening or manual movement with small load; steel-to-steel coupling tends to seize. Can be MIG welded only. Electrode welding is not recommended because of the lead.

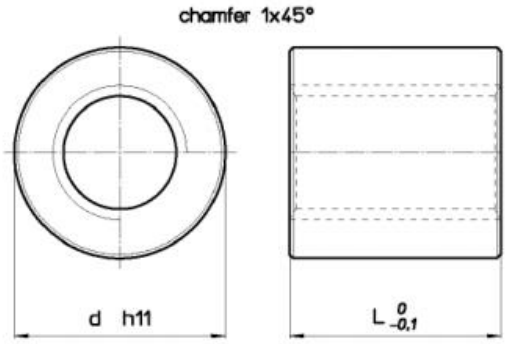

RS Number	Screw Type	Material	Screw	Diameter x lead	Thread starts	d mm	L mm	Wt. kg/each	At mm² (1)
8625379	Trapezoidal	Steel EN 10277-3 11 S Mn Pb 37 - 1.0737	Right	Tr 10x2	1	22	15	0.038	150
8625373	Trapezoidal	Steel EN 10277-3 11 S Mn Pb 37 - 1.0737	Right	Tr 12x3	1	26	18	0.061	296
8625382	Trapezoidal	Steel EN 10277-3 11 S Mn Pb 37 - 1.0737	Right	Tr 14x3	1	30	21	0.095	395
8625385	Trapezoidal	Steel EN 10277-3 11 S Mn Pb 37 - 1.0737	Right	Tr 16x4	1	36	24	0.158	528
8625389	Trapezoidal	Steel EN 10277-3 11 S Mn Pb 37 - 1.0737	Right	Tr 18x4	1	40	27	0.218	553
8625398	Trapezoidal	Steel EN 10277-3 11 S Mn Pb 37 - 1.0737	Right	Tr 20x4	1	45	30	0.308	847
8625391	Trapezoidal	Steel EN 10277-3 11 S Mn Pb 37 - 1.0737	Right	Tr 22x5	1	45	33	0.324	1010
8625395	Trapezoidal	Steel EN 10277-3 11 S Mn Pb 37 - 1.0737	Right	Tr 24x5	1	50	36	0.440	1215

(1) Total bearing surface between screw and nut teeth on plane perpendicular to axis.

B.7 NEMA 23 datasheet

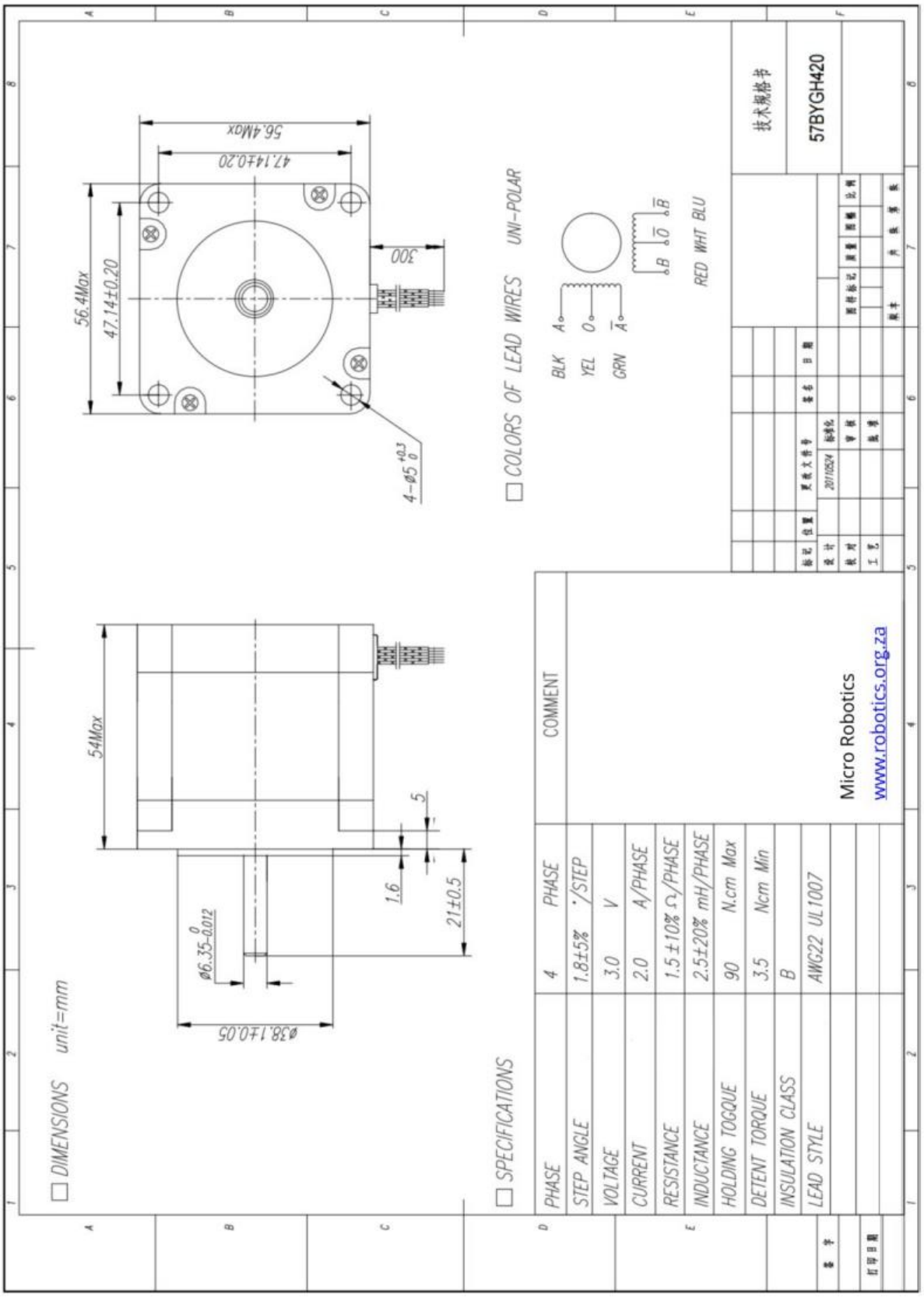

B.8 NEMA 17 datasheet

Open Impulse

http://www.openimpulse.com

42BYGHW208 Stepper Motor Datasheet

Wiring diagram (接线图):

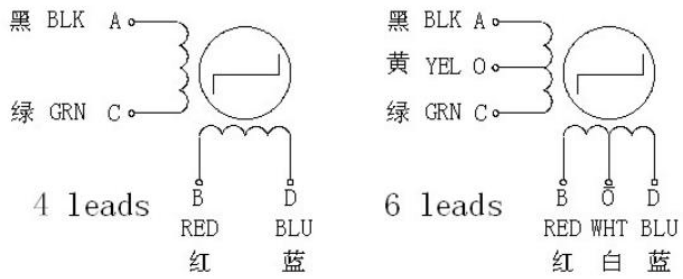

Model	Step Angle (°)	Motor Length L(mm)	Rate Voltage (V)	Rate Current (A)	Phase Resistance (Ω)	Phase Inductance (mH)	Holding Torque (g.cm)	Lead Wire (NO.)	Rotor Inertia (g. cm2)	Detent Torque (g.cm)	Motor Weight (kg)
42BYGHW208	1.8	34	12	0.4	30	37	2800	4	34	200	0.2

Mechanical Dimensions(外型图)

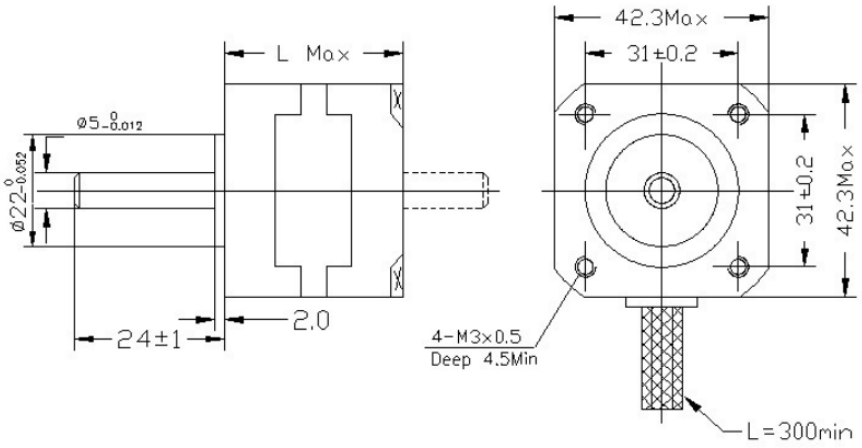

B.9 Stepper motor driver datasheet

DIY ELECTRONICS

Mechanics / CNC > Motors / Controllers > Motor Drivers > Stepper Motor Drivers > TB6560 Stepper Motor Driver

TB6560 STEPPER MOTOR DRIVER

Reference HWPMTB6560 Condition: New

The TB6560 Stepper Motor Driver is an affordable hobbyist stepper motor driver with 4 variable excitation modes – For 2/4-phase, 4/6-wire stepper motors.

The TB6560 stepper motor driver is a very basic driver designed to be used with 42,57,86 steppers within 3A and 5V. It can be utilized with 2 or 4-phase motors with 4 or 6 wires, and offers the new Toshiba TB6560AHQ chip with a 6N137 high-speed OptoCoupler – designed to provide high speed without step out.

Although this driver doesn't necessarily produce a lot of heat, it comes fully equipped with overheating protection, a large heat sink, as well as both over-current and low-voltage protection. These features ensure that this driver will maintain optimal performance, with built-in defences against a variety of typical stepper motor driver problems.

This driver also comes at a very affordable price as the low voltages and current don't require intense heat dispersion or other cost-adding features. Instead, this driver is basic and provides the precise amount of power necessary for a variety of hobbyist and home-project applications. If you are looking for more powerful Stepper Motor Drivers, consider the DQ860MA, DQ542MA or TB6600, although if you don't require any more power than the TB6560, then this is the ideal choice thanks to its value/performance rating.

TECHNICAL SPECIFICATIONS:

- **Operating Voltage** – 10V to 35V (Recommended Switch Power Supply DC24V)
- **Rated Output** – ± 3A ; Peak 3.5A
- **Microchip** – Original Toshiba TB6560AHQ
- **Selectable Excitation Modes** – 1/1 ; 1/2 ; 1/8 ; 1/16 Step
- **Overheating Protection** – Passive Heat Sink
- **Short Circuit Protection** – Over-current Protection with Low-voltage Shutdown
- **Dimensions** – 50 x 75 x 35 mm
- **Additional Features** – Automatic Half-Decay

  – Adjustable Decay Settings (0%/25%/50%/100%)

  – 6N137 High-Speed Optical Coupling

CONNECTOR PIN ASSIGNMENTS AND DESCRIPTIONS:

Pin Function	Details
+24V / GND	The Power positive and negative connections
A+ / A-	Motor Phase A positive and negative connections
B+ / B-	Motor Phase B positive and negative connections
CLK+ / CLK-	Pulse Input positive and negative connections
CW+ / CW-	Motor Direction Input – Motor rotates clockwise when CW is set low Motor rotates counterclockwise when CW is set high
EN+ / EN-	Enable Input positive and negative connections

EXCITATION MODE SETTINGS:

The TB6560 is far simpler than stepper motor drivers like the DQ862MA or DQ542Ma, and only dedicates two DIP switches (S3 and S4) to excitation mode settings. As such, the following table shows how these switches need to be set in order to achieve the desired excitation mode:

Excitation Mode	1/1	1/2	1/8	1/16
S3	**OFF**	**ON**	**ON**	**OFF**
S4	**OFF**	**OFF**	**ON**	**ON**

OUTPUT CURRENT SETTINGS:

The TB6560 stepper motor driver utilises the SPST switches SW1, 2 and 3, as well as the DIP switch S1 to set the output current. When setting these, refer to the following table to set the running current as close to your motor's required input current.

Running Current	SW1	SW2	SW3	S1
0.3A	**OFF**	**OFF**	**ON**	**ON**
0.5A	**OFF**	**OFF**	**ON**	**OFF**
0.8A	**OFF**	**ON**	**OFF**	**ON**
1.0A	**OFF**	**ON**	**OFF**	**OFF**
1.1A	**OFF**	**ON**	**ON**	**ON**

1.2A	OFF	OFF	OFF	ON
1.4A	OFF	ON	ON	OFF
1.5A	ON	OFF	ON	ON
1.6A	ON	OFF	OFF	OFF
1.9A	ON	ON	OFF	ON
2.0A	ON	OFF	ON	OFF
2.2A	ON	ON	ON	ON
2.6A	ON	ON	OFF	OFF
3.0A	ON	ON	ON	OFF

STOP CURRENT AND DECAY SETTINGS

The final three DIP switches (S2, S5 and S6) are dedicated to the stop current and decay settings. The S2 switch defines the stop current, and either sets it to 20% or 50%, where ON is 20% and OFF is 50%. The S5 and S6 switches are for setting the decay, and the following chart shows how the switches need to be set in order to achieve variable decay settings:

Decay	0%	25%	50%	100%
S5	OFF	ON	OFF	ON
S6	OFF	OFF	ON	ON

B.10 Power supply datasheet

LRS Compact 24V 6.5A 150W PSU

The new LRS standard is a new compact form factor and is very efficient and extremely low no load power consumption. The metallic mesh design ensure optimum cooling. The LRS-150 series delivers extremely low no load power consumption.

Quick Spec

- Output Voltage: 24V
- Output Current: 6.5A
- Power: 156W
- Input Voltage: 170 - 264VAC
- Protection: Short circuit / overload / over voltage/ over temperature
- Efficiency: 89%

Dimensions

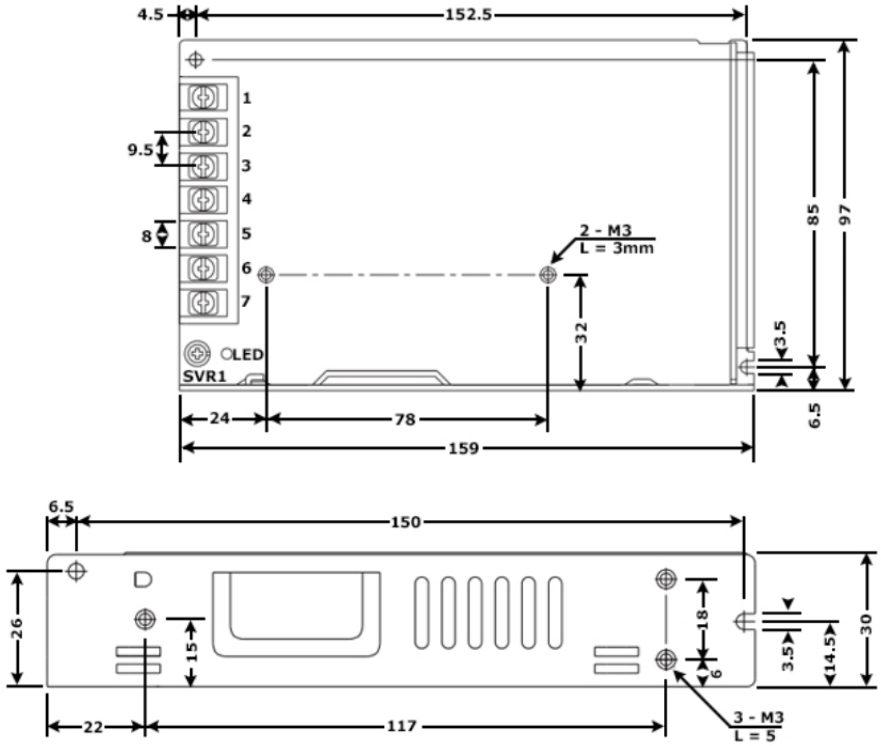

B.11 NEMA 17 mounting bracket datasheet

This motor bracket is the perfect mounting solution to secure your NEMA 17 Stepper Motor to your CNC project. Made from mild steel, featuring welded triangular gussets to increase structural rigidity, this is a solid bracket which fits all NEMA 17's with 31mm hole spacing. The mount can easily be attached to your project using two 30mm slots, and is powder coated black for rust protection and aesthetic appeal.

NEMA 17 STEPPER MOTOR MOUNTING BRACKET - TECHNICAL SPECIFICATIONS:

- **Material Composition** – Mild Steel
- **Finish** – Black Powder Coated
- **Dimensions** – 50 x 50 x 50mm
- **Motor Compatibility** – NEMA 17

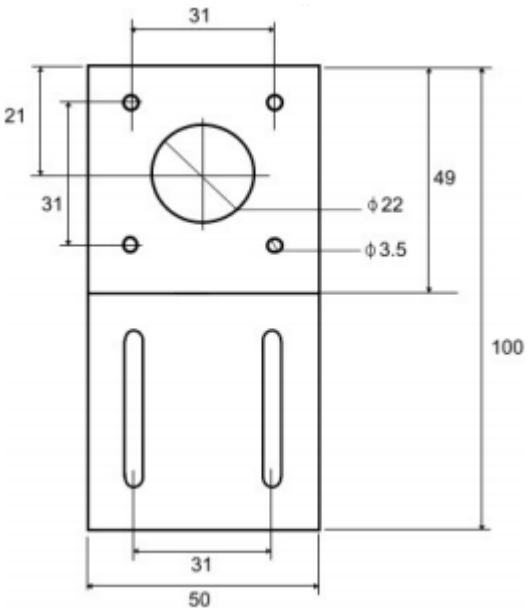

B.12 Flexible aluminium coupling datasheet

DIY ELECTRONICS

Mechanics / CNC > Linear Motion Components > Couplers / Supports > Flexible Aluminium Coupling (6.35mm/8mm)

FLEXIBLE ALUMINIUM COUPLING (6.35MM/8MM)

These couplers are made of machined aluminum and have a spiral cut that makes them slightly flexible so they can be fit to two shafts even if they are not perfectly co-linear and will help reduce binding effects and well as any wobbling that may occur. There profile is such that they're a little springy in the X Y & Z linear axis but not in the rotational axis. That means you can enjoy flexibility without increased backlash making them suitable for precision CNC work.

This coupler will connect a 6.35mm diameter shaft to an 8mm diameter shaft. A perfect add on for our stepper motors. Comes with two sets of double set-screws (two per side) for secure attachment. You'll need an allen wrench to tighten/loosen the set-screws.

8MM/6.35MM FLEXIBLE ALUMINIUM COUPLER - TECHNICAL SPECIFICATIONS:

• **Material**	– Aluminium
• **Length**	– 25mm
• **Outer Diameter**	– 19mm
• **Inner Diameter (Wide Side)**	– 8mm
• **Inner Diameter (Small Side)**	– 6.35mm

B.13 M5 ball bearing datasheet

DIY ELECTRONICS

Mechanics / CNC > Linear Motion Components > Bearings > Radial Bearings > Radial Ball Bearing - 625ZZ - 5x16x5mm

RADIAL BALL BEARING - 625ZZ - 5X16X5MM

When it comes to radial motion, as well as linear motion involving leadscrews and motors, there are few tools that can compare to Radial Bearings like these 625ZZ Radial Ball Bearings. Designed with small metal balls that roll between the outer and inner plates, Ball Bearings are built to offer incredibly smooth radial motion with an extremely low friction co-efficient, which results in consistent radial accuracy and a very low rate of wear and tear.

625ZZ RADIAL BALL BEARING - TECHNICAL SPECIFICATIONS:

- **Model** – 625ZZ
- **Inner Diameter** – 5mm

• **Outer Diameter**	– 16mm
• **Thickness**	– 5mm

TYPICAL APPLICATIONS FOR 625ZZ RADIAL BALL BEARINGS:

These 625ZZ Radial Ball Bearings offer an inner diameter (bore) of 5mm, with an outer diameter of 16mm and a thickness of 5mm, and these are really the only limitations to the plethora of use cases that these can be utilised in. One of the most recent popular applications for bearings like these include 3D Printers, in which these kinds of bearings are often used to act as inexpensive idler pulleys. However, the choice of how to use them is ultimately up to you, and you could certainly use these for your 3D printer just as easily as you could use it for slow-capture photography or any other application that can benefit from smooth radial motion.

B.14 M8 ball bearing datasheet

Mechanics / CNC > Linear Motion Components > Bearings > Radial Bearings > Radial Ball Bearing - 608ZZ - 8x22x7mm

RADIAL BALL BEARING - 608ZZ - 8X22X7MM

Within linear motion applications, friction can be a "drag", and can lead to serious problems relating to wear and tear, as well as consistent accuracy over an extended period of time. Fortunately, we humans are quite smart, and have developed specialised tools like these 608ZZ Radial Ball Bearings, which are designed to utilise rolling balls within enclosed chambers to drastically reduce the friction of moving parts.

These Radial Ball Bearings are built with an 8mm inner diameter, a 22mm outer diameter and a 7mm thickness, and are stocked specifically to cater to the classic Greg's Wade Extruder that utilises three of them. However, because of the relatively simple design, they can be used for almost any radial motion applications that suit the ID, OD and thickness of these bearings.

608ZZ RADIAL BALL BEARING - TECHNICAL SPECIFICATIONS:

• **Inner Diameter**	– 8mm
• **Outer Diameter**	– 22mm
• **Thickness**	– 7mm

TYPICAL APPLICATIONS FOR THESE 608ZZ RADIAL BALL BEARINGS:

While these were originally stocked for the Greg's Wade Extruder, 3D Printing has since moved on to much better, and more affordable, extruders like the E3D and MK variations. However, we still stock these to accommodate 3D Makers who may need them, but also for general Makers who can find a use for them. And thanks to the general sizing of these Bearings, they can actually be used for all sorts of radial motion applications, such as attaching Leadscrews to mounts or even attaching wheels to skateboards if that's what you're keen to do.

B.15 SUNON axial fan datasheet

DIY ELECTRONICS

3D Printing > Components > Electronic Components > Fans > Sunon 12V 4010 Silent Axial Fan - 15.7dBA Vapo-Bearing

SUNON 12V 4010 SILENT AXIAL FAN - 15.7DBA VAPO-BEARING

Reference HWFANHA40101V4 Condition: New

These Sunon 12V 4010 Axial Fans are even quieter than rustling leaves, offering very effective & extremely quiet operations for 3D Printing.

When looking at a whole 3D Printer in action, it's easy to be awestruck by the many little moving parts, all of which work together to produce results that none of the individual parts could achieve alone. And what always amazes us is how each and every single part plays a vital role in the success of the whole machine, and this even so for the fans that help to move heat and keep sensitive parts within safe operating temperatures.

With that being said, it's unfortunate that fans, despite being critical to the mechanical health and safety of 3D Printers, are often some of the loudest components on the machines. Additionally (in a similar way to humans) these fans tend to get louder with age, and it's never nice to have a fan moaning and complaining all day – especially when you're trying to sleep while your machine is bringing your creations to life.

This is why we've been on a mission lately to get quieter fans like these beautiful Sunon Original 12V 4010 Silent Axial Fans, which have an ultra-low noise rating of just 15.7dBA due to the clever MagLev Vapo-Bearing that Sunon is so well-known for. In fact, to give you some perspective on just how quiet these Cooling fans are compared to typical fans, the 15.7dBA noise rating means that this fan is REALLY quiet, with the loudness falling somewhere between the loudness of a pin dropping, and the loudness of leaves rustling from the wind.

Finally, we've really enjoyed equipping all of our 3D Printers at home with these beautifully quiet fans, and complementing them with Silent Stepper Drivers too. It has made a world of a difference in the overall loudness of the machine, and as long as we are willing to slow down the mechanical motions of the machine during prints, we all now enjoy near-absolute silence, even while bringing our obscure and wonderful creations to life.

SUNON 12V 4010 SILENT AXIAL FAN - TECHNICAL SPECIFICATIONS:

• **Manufacturer**	– Sunon
• **Model Number**	– HA40101V4-1000U-A99
• **Fan Type**	– Brushless Axial Fan
• **Bearing Type**	– MagLev: Vapo-Bearing
• **Operating Voltage**	– 12V DC (4.5V Startup | 13.8V Max)
• **Rated Current**	– 31mA (38mA Max)
• **Rated Speed (RPM)**	– 5000 ±15% (@ 12V DC)
• **Rated Air Flow**	– 5.4 CFM (0.151m^3/min)
• **Rated Static Pressure**	– 0.090 in H2O (22.4 Pa)
• **Rated Noise**	– 15.7dB(A)
• **3D Printer Compatibility**	– Creality CR-10S / CR-10 S4 / CR-10 S5
• **Cooling Application**	– Rear Control Box / Hotend Assembly
• **Weight**	– 15.4g
• **Dimensions**	– 40 x 40 x 10mm

HELPFUL NOTES FOR INSTALLING YOUR NEW SUNON 4010 SILENT AXIAL FAN:

Whilst many experienced Makers would consider the installation process of a cooling fan to be relatively simple, installing fans on Hobbyist 3D Printers is unfortunately not as simple as it should be. Fortunately, however, we've prepared these handy notes on this process, which should help you get your fan installed perfectly, and without any unexpected damage or hassles. They are as follows:

- **Check Your Polarities** – Because many of the hobbyist fans and 3D Printers available to Makers are typically supplied by different manufacturers from all over the world, the first step that you should take is to check the polarity of the fan with a simple multimeter. This simple and relatively quick polarity check will ensure that you don't break your new fan (or potentially worse) the moment you turn on the power.
- **Wiring Colours May Not Always Match** – Don't simply rely on colours that many of these fans are provided with, because they may not always have the same wiring colours as other fans with the exact same or similar specifications. Additionally, we've found that some 3D Printers may also have different wiring, which can sometimes even depend on the batch within the same series. As such, double-check the polarity and markings on the related boards as well, so that you don't end up running your fan backwards or causing unexpected damage before you even get a chance to use the fan.
- **Matching Your Mounting Points** – Given the fact that so many new models of 3D Printers come out each year, some machines might have slightly different mounting points. Fortunately though, this is one of the easiest problems to fix, and in addition to simply printing yourself a mounting unit to perfectly fit your fan, we have also provided a guide below that explains how you may be able to solve this problem with a simple pocket knife and a few minutes of time.

ADDITIONAL RESOURCES:

- Finally, if you find that the spare fan you purchase is just not quite the right size on your Creality machine, this Creality Fan Fitting Guide from the highly reputable TH3D brand offers some great insights into how you can remedy this with minimal effort and a simple pocket knife.

APPENDIX C. CONCEPT DESIGN SKETCHES

C.1 Robust design

Robust design

Specs.

1. Fixed system
2. Operated while seated for user comfort
3. A stand alone system that requires no additional hardware.
4. Can host multiple users on this single system
5. Provides direct hand interaction, mid-air imaging in front of optics and view dependant rendering.

Top View

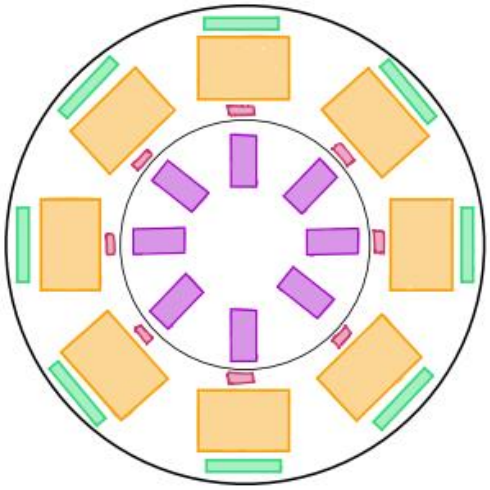

- RGB camera
- Microsoft kinect
- ASKA 3D Plate
- Computer tower
- LCD Screen
- Position of hologram
- Mounting for LCD Screens

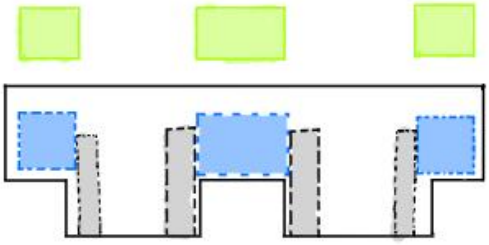

Front View

* Users can interact with their own MR scene and can share their own MR Scene to other users on the system.

C.2 Compact design

Compact design

Specs:

1. Portable system
2. Small scale desktop system
3. Used through laptop system
4. Can use both layouts available for the ASKA 3D plate
5. Single user system
6. Interaction is obtained through gesture control
7. View dependant rendering of mid-air images

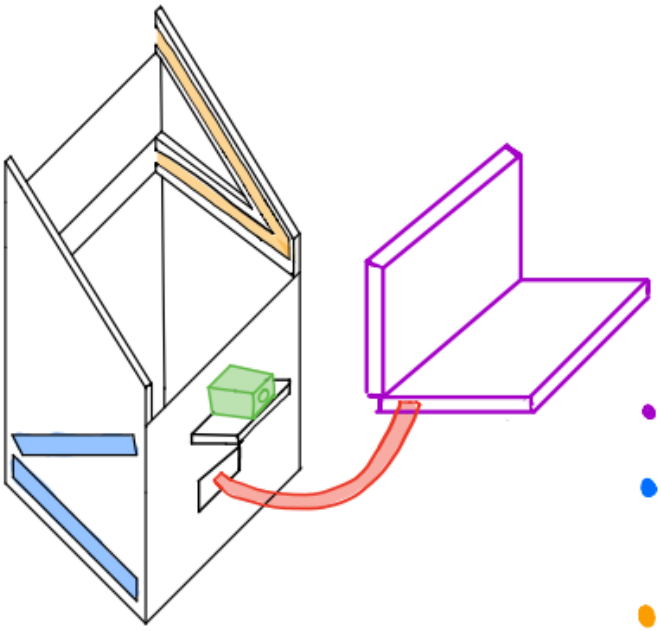

- Laptop
- LCD screen mounting Locations
- ASKA 3D mounting Locations
- Cable connection to Laptop
- Adjustable camera

C.3 Flexible design

Flexible System Concept

Key themes:

1. Plate rotates from horizontal position by 45°
2. Screen rotates from horizontal position by 45°
3. Plate moves up and down in line with the screen

Extra theme:

4. Entire system can rotate 360° to follow the user

Design

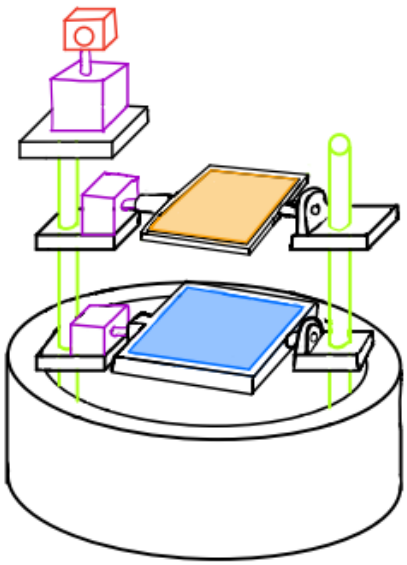

- Monitor Screen
- Motor
- Power screw
- ASKA 3D Plate
- Structural components

Another motor located at the base that can rotate the screen and plate 360°

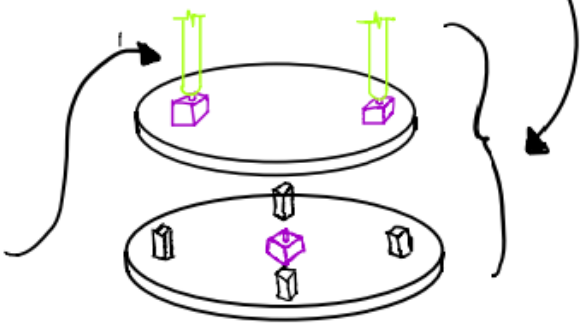

Each power screw will be coupled with a motor

APPENDIX D. CALCULATIONS

D.1 Viewing specification calculations

The viewing specifications were calculated using the datasheets provided by ASKA3D™. These can be found in Appendix B.1, B.2 and B.3. It was possible to calculate the following viewing measures for the MR System: depression angle, observer position, viewing angle, viewing distance and the observation range. The primary diagram used for these calculations can be seen in Figure D-1. This was obtained from Appendix B.2.

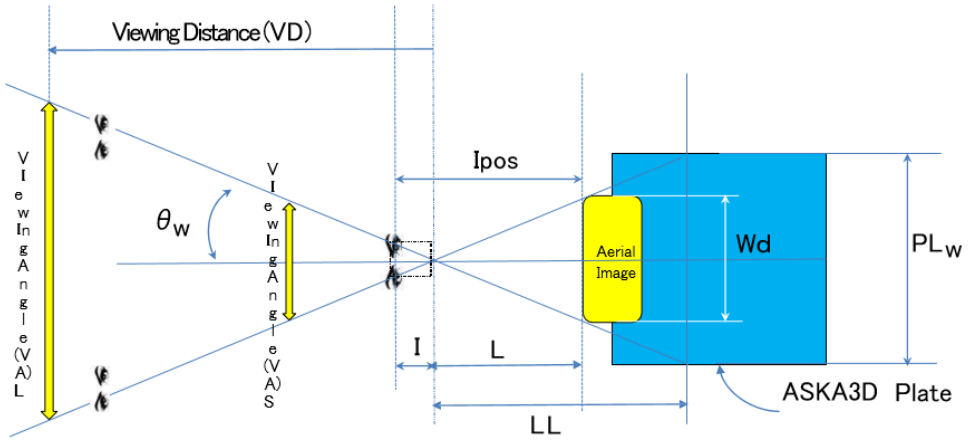

Figure D-1: User viewing diagram 1 for viewing calculations (Appendix B.2)

Depression angle:

The depression angle was given in the ASKA3D Plate datasheet (Appendix B.2) as a constant value that applies to the system when used in the standing and seated system layouts (Figures 4-1 and 4-2).

$$\text{Depression angle} = \theta_L$$

$$\therefore \theta_L = 45°$$

Observer position:

The observer position defined the minimum distance the user could be positioned to view the mid-air images. The distance between the mid-air image and the point at which the image can be viewed was given as 430 mm, in Figure D-2. This was true given that the distance between the plate and screen was 100 mm. This value was used to calculate the observer position.

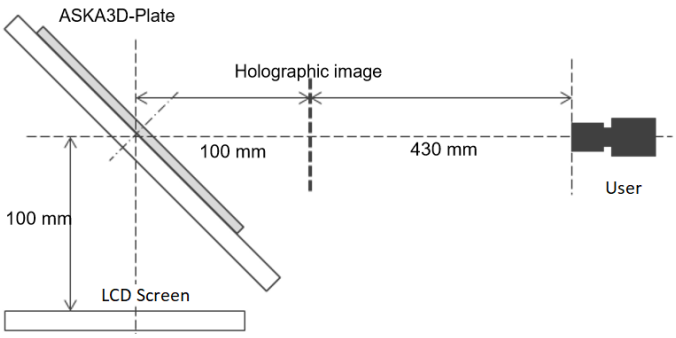

Figure D-2: User viewing diagram 2 for viewing calculations (Appendix B.1)

Equation:

$\text{Observer position} = I_{pos}$

$I_{pos} = L + I$ (Given in Appendix B.2)

Variables:

I = 65 mm (Given in Appendix B.2)

L = 430 mm (Given by Figure D-1 and Figure D-2)

Solution:

$\therefore\ I_{pos} = 430 + 65$

$\therefore I_{pos} = 495\ \text{mm}$

Viewing angle:

This angle was calculated using the equations given in the ASKA3D Plate datasheet (Appendix B.2). This value was calculated using the mid-air image's width and the distance between the mid-air image and the point at which the image could be viewed. In this sub-system, the mid-air image's width was defined by the width of the ASKA3D Plate since the plate was smaller than the LCD screen used in the system. If the plate was larger than the LCD screen, the mid-air image's width would be the same as the width of the LCD screen. The calculation for the MR System's viewing angle was presented, and the corresponding diagram used for this calculation was Figure D-1.

Equations:

Viewing angle $= \theta_w$ (Given in Appendix B.2)

$\theta_w = \tan^{-1}\left(\frac{W_d}{2L}\right)$ (Given in Appendix B.2)

Variables:

Mid-air image width = $W_d = 200$ mm (Given by plate specifications in Appendix B.1)

L = 430 mm (Given by Figure D-1 and Figure D-2)

Solution:

$\therefore\ \theta_w = \tan^{-1}\left(\frac{200}{2 \times 430}\right)$

$\therefore \theta_w = 13.09189306°$

$\therefore \theta_w \approx 13°$

Viewing distance:

The viewing distance was the maximum distance users could be positioned to view mid-air images. This was a user-defined value and should be identified as a restriction and not a calculated value. Figure D-1 indicated what the viewing distance of the system represented. The viewing distance was defined as "VD".

VD = Viewing distance

VD = 2500 mm

Observation range:

The observation range indicated the range that users could occupy to view the mid-air image in its best possible detail. The equation for the observation range was given in the ASKA3D Plate datasheet (Appendix B.2). It was possible to calculate the observation range using this equation and Figure D-1.

Equation:

$$\text{Observation range/View area} = \text{VA}$$

$\text{VA} = 2 \times \text{VD} \times \tan \theta_w$ (Given in Appendix B.2)

Variables:

VD = 2500 mm (specified value)

$\theta_w = 13°$

Solution:

$\therefore\ \text{VA} = 2 \times 2500\ \text{mm} \times \tan 13°$

$\therefore \text{VA} = 1154.340956\ \text{mm}$

$\therefore \text{VA} \approx 1154\ \text{mm}$

D.2 Layout Control sub-system weight calculations

The Layout Control sub-system was separated into two parts, one half regarding the ASKA3D Plate rotation and the second regarding the LCD screen rotation. For each half, the total weight on each motor shaft and support bearing was calculated. This was needed to make an accurate selection for the motors and bearings used in this sub-system. Drawing the components for this sub-system on SolidWorks™ made it possible to calculate the components' expected mass. These mass values were calculated for each component using the material specified with its density value. Cura was used in slicing the 3D printed components and specify the infill amount used when creating the components. Afterwards, Cura delivered the accurate mass value for the 3D printed components. The mass values calculated were used to create a force balance diagram to obtain the expected downward force on the motor shafts and bearings for both the ASKA3D Plate and the LCD screen.

D.2.1 Weight of ASKA3D Plate and mounting components:

There were four components used to mount the ASKA3D Plate. These components were presented in the physical design and material selection sections of this sub-system. SolidWorks™ and Cura were used to find the mass values of the components to be manufactured. Table D-1 listed these components with their corresponding density, quantity and calculated mass.

Table D-1: Mass values for the beam splitter components

Component	Quantity	Density	Infill	Mass (per component)
ASKA3D-200NT Plate	1	NA	NA	256 g ± 10 g (Given)
Beam splitter housing	1	1.24 g/cm³	20%	254 g
Motor/Bearing shaft connector	2	1.24 g/cm³	30%	31 g
Bearing shaft	1	7.85 g/cm³	NA	30.83 g

$$\therefore \text{Total Mass}_{\text{ASKA3D Plate \& Mountings}} = 266\ \text{g} + 254\ \text{g} + (2 \times 31\ \text{g}) + 30.83\ \text{g}$$

$$\therefore \text{Total Mass}_{\text{ASKA3D Plate \& Mountings}} = 612.83\ \text{g}$$

$$\therefore \text{Total Mass}_{\text{ASKA3D Plate \& Mountings}} = 0.61283\ \text{kg}$$

This was an approximate mass value that could vary to the actual mass that was present. A force balance diagram in Figure D-3 showed the expected forces and reaction forces present on the motor shaft and bearing.

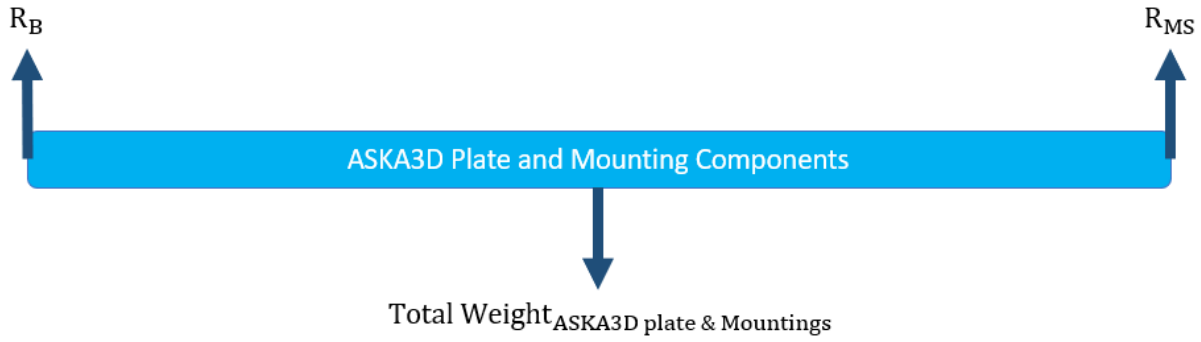

Figure D-3: Force balance diagram for ASKA3D Plate

Variables:

R_B = Reaction force at the bearing support

R_{MS} = Reaction force at the motor shaft

$R_B = R_{MS}$ (Fundamental weight distribution when fixed at two ends)

$g = 9.81\ \text{m/s}^2$

Solution:

$$\text{Total Weight}_{\text{ASKA3D Plate \& Mountings}} = \text{Total Mass}_{\text{ASKA3D Plate \& Mountings}} \times g$$

$$\text{Total Weight}_{\text{ASKA3D Plate \& Mountings}} = 0.61283 \times 9.81$$

$$\text{Total Weight}_{\text{ASKA3D Plate \& Mountings}} \approx 6.01 \text{ N}$$

$$\therefore R_{FM} + R_{MS} = \text{Total Weight}_{\text{ASKA3D Plate \& Mountings}}$$

$$\therefore 2 \times R_{MS} = \text{Total Weight}_{\text{ASKA3D Plate \& Mountings}}$$

$$\therefore 2 \times R_{MS} = 6.01 \text{ N}$$

$$\therefore R_{MS} \approx 3.01 \text{ N}$$

$$\therefore R_{B} \approx 3.01 \text{ N}$$

D.2.2 Weight of the LCD screen and mounting components:

There were five components used to mount the LCD screen. These components were presented in the physical design and material selection sections of this sub-system. SolidWorks™ and Cura were used to find the mass values of the components to be manufactured. Table D-2 listed these components with their corresponding density, quantity and calculated mass.

Table D-2: Mass values for the LCD screen components

Component	Quantity	Density	Infill	Mass (per component)
LCD screen, motherboard and USB hub	1	NA	NA	500 g (Approximate)
LCD screen front cover	1	1.24 g/cm³	20%	72 g
LCD screen back cover	1	1.24 g/cm³	20%	241 g
Motor/Bearing shaft connector	2	1.24 g/cm³	30%	31 g
Bearing shaft	1	7.85 g/cm³	NA	30.83 g

$$\therefore \text{Total Mass}_{\text{LCD Screen \& Mountings}} = 500 \text{ g} + 72 \text{ g} + 241 \text{ g} + (2 \times 31 \text{ g}) + 30.83 \text{ g}$$

$$\therefore \text{Total Mass}_{\text{LCD Screen \& Mountings}} = 905.83 \text{ g}$$

$$\therefore \text{Total Mass}_{\text{LCD Screen \& Mountings}} = 0.90583 \text{ kg}$$

This was an approximate mass value that could vary to the actual mass that was present. A force balance diagram in Figure D-4 showed the expected forces and reaction forces present on the motor shaft and bearing.

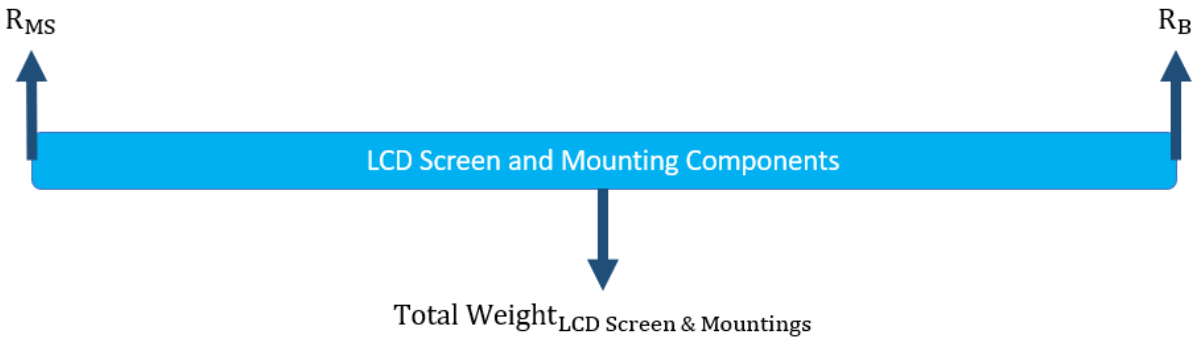

Figure D-4: Force balance diagram for LCD screen

Variables:

R_B = Reaction force at the bearing support

R_{MS} = Reaction force at the motor shaft

$R_B = R_{MS}$ (Fundamental weight distribution when fixed at two ends)

$g = 9.81\ m/s^2$

Solution:

$$\text{Total Weight}_{\text{LCD Screen \& Mountings}} = \text{Total Mass}_{\text{LCD Screen \& Mountings}} \times g$$

$$\text{Total Weight}_{\text{LCD Screen \& Mountings}} = 0.90583 \times 9.81$$

$$\text{Total Weight}_{\text{LCD Screen \& Mountings}} \approx 8.89\ N$$

$$\therefore R_{FM} + R_{MS} = \text{Total Weight}_{\text{LCD Screen \& Mountings}}$$

$$\therefore 2 \times R_{MS} = \text{Total Weight}_{\text{LCD Screen \& Mountings}}$$

$$\therefore 2 \times R_{MS} = 8.89\ N$$

$$\therefore R_{MS} \approx 4.44\ N$$

$$\therefore R_B \approx 4.44\ N$$

D.3 Height control sub-system calculations

Three calculations were presented in this section. The first, presented the methodology and calculations performed to view mid-air images while standing. The second, presented the methodology and calculations performed to view mid-air images while seated. The third, presented the methodology and calculations to determine the sub-system's axial force and torque values.

D.3.1 Viewing while standing calculation

The datasheet (Appendix B.3) provided by ASKA3D™ gave a base measurement for the system. It was now possible to calculate the changing height of the ASKA3D Plate for users with different heights. Figure 2-4 displayed the base measurement. A user height between $1500\,mm \leq h \leq 1600\,mm$ required the ASKA3D Plate positioned at 850 mm from the ground. The next height range specified was $1600\,mm \leq h \leq 1700\,mm$, the range increased by 100 mm. Therefore, the height of the ASKA3D Plate would need to increase by 100 mm since there was a direct relationship between the user's height and the height of the ASKA3D Plate.

$$\text{New ASKA 3D height Position} = \text{Old height Position} + \text{Change in user height range}$$

$$\text{New ASKA 3D height Position} = 850\text{ mm} + 100\text{ mm}$$

$$\text{New ASKA 3D height Position} = 950\text{ mm}$$

For a user height range of $1600\,mm \leq h \leq 1700\,mm$ the ASKA3D Plate would need to be positioned at the height of 950 mm from the ground. The same methodology and equation were used to calculate the plate height for the final user height range.

$$\text{New ASKA 3D height Position} = \text{Old height Position} + \text{Change in user height range}$$

$$\text{New ASKA 3D height Position} = 950\text{ mm} + 100\text{ mm}$$

$$\text{New ASKA 3D height Position} = 1050\text{ mm}$$

For a user height range of $1700\,mm \leq h \leq 1800\,mm$ the ASKA3D Plate would need to be positioned at the height of 1050 mm from the ground. The results of these calculations were presented in Table 4-11.

D.3.2 Viewing while seated calculation

Calculating the user height ranges while seated required a relationship between the height position of the ASKA3D Plate and the user height when using the system in the seated layout (Figure 4-1). It was possible to obtain the vertical distance between the center of the plate and the minimum user viewing height using the ASKA3D Plate datasheet in Appendix B.3. This measurement was used to calculate the minimum user height for the ASKA3D Plate at a specified height position configured to the layout seen in Figure 4-1. Therefore, by specifying the ASKA3D Plate height position and using the calculated distance from the plate's center to the minimum user height, it was possible to find the minimum user height to view the image. The maximum user height was defined as a 100 mm increase from the minimum height value. The calculation below displayed how the height ranges for seated users on the system were obtained using predefined ASKA3D Plate heights obtained from Appendix D.3.1.

The following diagram was obtained by using the ASKA3D Plate datasheet in Appendix B.3. It was possible to calculate the variables y_1, y_2 and y_3 using the diagram in Figure D-5.

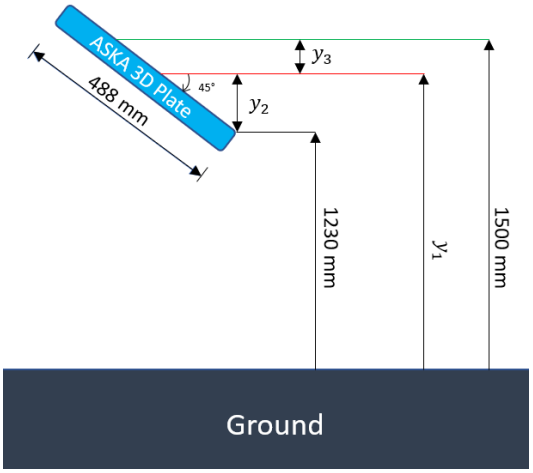

Figure D-5: Diagram for seated viewing calculations

Definition of variables:

y_1 = height measurement from the ground to the centre of the ASKA3D Plate

y_2 = distance between the centre of the plate and plate position height

y_3 = distance between the centre of the plate and the minimum user height

The plate position height = 1230 mm (Appendix B.3)

Minimum user height = 1500 mm (Appendix B.3)

ASKA3D Plate length = 488 mm (Appendix B.3)

Calculating y_2:

The following triangle was made using Figure D-5 to calculate the value for y_2:

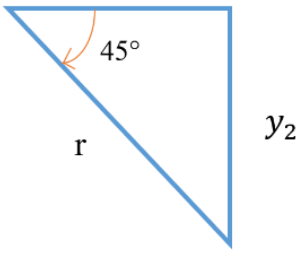

Figure D-6: Trigonometric diagram for seating viewing calculations

r = lenght of ASKA 3D plate $\div$ 2

r = 488 $\div$ 2

r = 244 mm

$\therefore \sin\theta = \frac{y_2}{r}$

$$\sin 45° = \frac{y_2}{244}$$

$$y_2 = 244 \times \sin 45°$$

$$y_2 = 172.5340546$$

$$\therefore\ y_2 \approx 173\ mm$$

Calculating y_1:

y_1 = height measurement from the ground to the centre of the ASKA 3D plate

y_1 = plate position height + y_2

$y_1 = 1230 + 173$

$\therefore y_1 = 1403$ mm

Calculating y_3:

y_3 = distance between the centre of the plate and the minimum user height

y_3 = minimum user height − y_1

$y_3 = 1500 - 1403$

$\therefore y_3 = 97$ mm

Calculating user height ranges while seated:

Using the calculated value of "y_3", it was possible to find the minimum user height at different ASKA3D Plate heights. Additionally, the maximum user height was given as an increment of 100 mm from the minimum plate height calculated.

For an ASKA3D Plate height = 850 mm (predefined value)

Minimum user height = 850 + 97 = 947 mm

Maximum user height = 974 + 100 =1047 mm

For an ASKA3D Plate height = 950 mm (predefined value)

Minimum user height = 950 + 97 = 1047 mm

Maximum user height = 1047 + 100 = 1147 mm

For an ASKA3D Plate height = 1050 mm (predefined value)

Minimum user height = 1050 + 97 = 1147 mm

Maximum user height = 1147 + 100 =1247 mm

The results of these calculations were presented in Table 4-12.

D.3.3 Axial force and torque calculations

The following calculations were used to obtain the expected axial forces on the motor shafts and the torque required to rotate the two lead screws in the Height Control sub-system. Once these two values were obtained, it was possible to select a stepper motor for this sub-system.

D.3.3.1 Axial force calculation

The Height Control sub-system was comprised of two lead screws on which the components were mounted. The weight of these components was calculated to obtain the total axial force on the lead screws. Additionally, the Layout Control sub-system components were also mounted on this sub-system and the weight of these components was taken into consideration. The two lead screws shared the total axial force equally when coupled to the two motor shafts due to the sub-system layout. Drawing the components for this sub-system on SolidWorks™ made it possible to calculate the components' expected mass. This mass value was calculated for each component using the material selected and its corresponding density. Cura delivered the accurate mass value for the 3D printed components. The calculated mass values were used to create a force balance diagram. This depicted the forces present on the motor shafts due to the components mounted on the lead screws.

There was a total of six components used in this sub-system. These components can be seen in the physical design section for this sub-system with each component's material selection. SolidWorks™ and Cura were used to find the mass values of the components to be manufactured. Table D-3 listed these components with their corresponding density, quantity and calculated mass.

Table D-3: Mass values for Height Control sub-system calculations

Component	Quantity	Density	Infill	Mass (per component)
TR8X8 Metric Lead Screw	2	8.05 g/cm³	NA	240 g
TR8X8 Metric Lead Screw Collar	4	8.05 g/cm³	NA	38 g
Mounting Platform	4	1.24 g/cm³	30%	31 g
NEMA 17 Stepper Motor Mounting Bracket	2	8.05 g/cm³	NA	96.68 g
Bearing Housing	2	1.24 g/cm³	30%	23 g
NEMA 17 Stepper Motor	2	NA	NA	200 g
Mass of ASKA3D Plate and Components	NA	NA	NA	612.83 g
Mass of LCD Screen and Components	NA	NA	NA	905.83g

A force balance diagram was shown in Figure D-7, displaying the forces present on the lead screws in this sub-system. The total axial force present on each motor shaft was calculated using Figure D-7 and Table D-3.

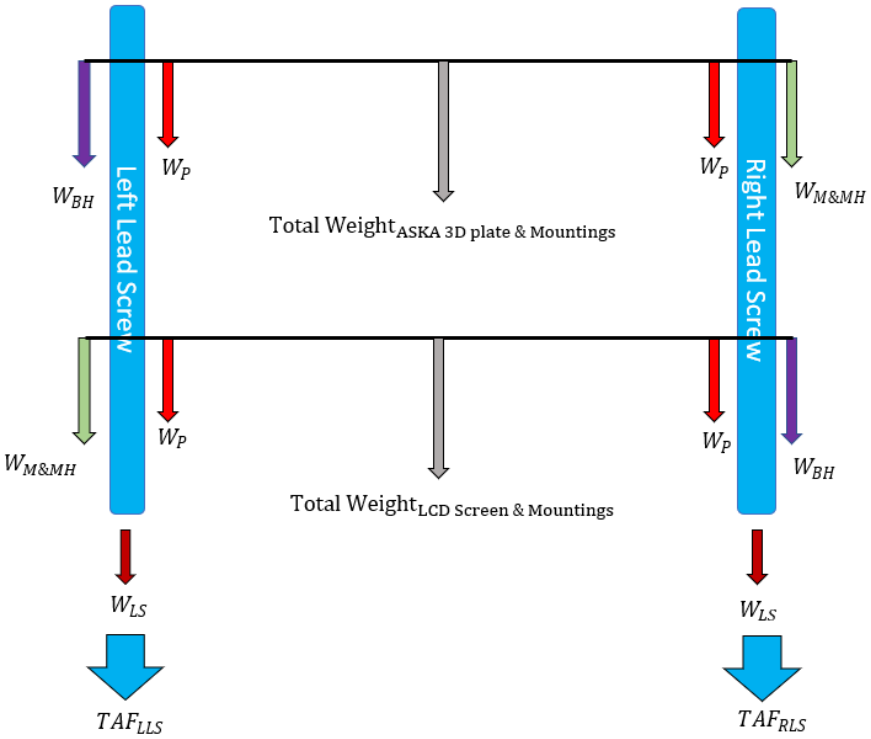

Figure D-7: Force balance diagram of the Height Control sub-system

Variables:

W_P = Weight of Mounting Platform and Collar

W_{BH} = Weight of Bearing Housing

$W_{M\&MH}$ = Weight of Motor & Motor Housing

W_{LS} = Weight of Lead Screw

TAF_{LLS} = Total Axial Force (Left Lead Screw)

TAF_{RLS} = Total Axial Force (Right Lead Screw)

Total Weight$_{\text{ASKA3D Plate \& Mountings}} \approx 6.01$ N (Appendix D.2.1)

Total Weight$_{\text{LCD Screen \& Mountings}} \approx 8.89$ N (Appendix D.2.2)

$g = 9.81\ m/s^2$

Solution:

$W_P = 9.81 \times (0.031 + 0.038)$

$W_P = 0.67689$ N

$W_{BH} = 9.81 \times 0.023$

$W_{BH} = 0.22563\ N$

$W_{M\&MH} = 9.81 \times (0.2 + 0.09668)$

$W_{M\&MH} = 2.9104308\ N$

$W_{LS} = 9.81 \times 0.24$

$W_{LS} = 2.3544\ N$

$TAF_{LLS} = W_P + W_{BH} + \frac{1}{2} \times \text{Total Weight}_{\text{ASKA3D Plate \& Mountings}} + W_P + W_{M\&MH} + \frac{1}{2} \times \text{Total Weight}_{\text{LCD Screen \& Mountings}} + W_{LS}$

$TAF_{LLS} = 0.67689 + 0.22563 + \frac{1}{2} \times 6.01 + 0.67689 + 2.9104308 + \frac{1}{2} \times 8.89 + 2.3544$

$TAF_{LLS} = 14.2942408\ N$

$TAF_{LLS} \approx 14.29\ N$

$TAF_{RLS} = W_P + W_{M\&MH} + \frac{1}{2} \times \text{Total Weight}_{\text{ASKA 3D plate \& Mountings}} + W_P + W_{BH} + \frac{1}{2} \times \text{Total Weight}_{\text{LCD Screen \& Mountings}} + W_{LS}$

$TAF_{RLS} = 0.67689 + 2.9104308 + \frac{1}{2} \times 6.01 + 0.67689 + 0.22563 + \frac{1}{2} \times 8.89 + 2.3544$

$TAF_{RLS} = 14.2942408\ N$

$TAF_{RLS} \approx 14.29\ N$

Due to the Motor Cover component withstanding this weight value, the stepper motors attached to the lead screws would not experience this axial force of 14.29 N. Therefore, the motor selection was dependent on the torque required to rotate the lead screws. The calculated axial force was used to obtain this torque value.

D.3.3.2 Torque calculation

A calculation was performed to determine the torque required to raise or lower the collars of this sub-system. This torque calculation assisted in the motor selection of the stepper motors directly coupled to the two lead screws in this sub-system. Additionally, a calculation was done to prove self-locking of the lead screws and collars in this sub-system. Specifications of the lead screw and collar purchased for this sub-system can be seen in Table D-4. This was used to perform the required torque calculation.

Table D-4: Lead screw and collar specifications for torque calculation

Component Name	**Quantity**	**Technical Specification**
RS PRO Lead Screw	2	Diameter: 10 mm Pitch: 2 mm Thread starts: 1 Screw type: Trapezoidal (30°) Material: Carbon Steel
RS PRO Round Collar for Lead Screw	4	Outside Diameter: 22 mm Shaft Diameter: 10 mm Pitch: 2 mm Screw type: Trapezoidal (30°) Material: Steel

The first calculation proved the collars in the sub-system were self-locking. Therefore, the collar would not spin without any external effort. If it did, it would be an over-hauling collar. This was proven by using the friction coefficient between the lead screw and collar material. This value was compared to the calculated value. If the friction coefficient was greater than or equal to the calculated value, it was considered a self-locking collar. The friction coefficient for the lead screw and collar was obtained from a materials textbook [54]. The friction coefficient was found to range from 0.15 to 0.25.

The second calculation determined the torque required to raise the load on one lead screw and the torque required to lower the load on one lead screw.

Variables:

$T_R = \text{Raising Torque}$

$T_L = \text{Lowering Torque}$

$W = \text{Applied Load}$

d_m = Mean Diameter

d_R = Root diameter

d_o = Outside diameter

$d_o = 10$ mm

f = screw/nut fricition coefficient

$f = 0.15 - 0.25$

L = Lead

P = Pitch

$P = 2$ mm

No. of starts $= 1$

α_n = Thread angle

$\alpha_n = 30°$

$\frac{W f_c d_c}{2} = 0$

Solution:

$L = P \times$ No. of starts

$L = 0.002 \times 1$

$L = 0.002$ m

$d_R = d_o - P$

$d_R = 0.010 - 0.002$

$d_R = 0.008$ m

$d_m = \frac{1}{2} \times (d_o + d_r)$

$d_m = \frac{1}{2} \times (0.010 + 0.008)$

$d_m = 0.009$ m

$$W = \text{Total Axial Force} - \text{Weight of lead screw}$$

$$W = 14.29 - 2.3544$$

$$W = 11.9356\ \text{N}$$

Self-Locking Calculation

For the system to be self-locking,

$$f \geq \frac{L \times \cos \alpha_n}{\pi \times d_m}$$

$$\therefore \frac{0.002 \times \cos 30°}{\pi \times 0.009} = 0.061$$

Therefore, the lead screw and collar selected were self-locking since the actual coefficient of friction was between 0.15 and 0.25, which was greater than the calculated value.

Torque Calculation

$$T_r = \frac{W d_m}{2}\left(\frac{f \times \pi \times d_m + L \times \cos 30°}{\pi \times d_m \times \cos 30° - f \times L}\right) + \frac{W f_c d_c}{2}$$

$$T_r = \frac{(11.9356)(0.009)}{2}\left(\frac{0.25 \times \pi \times 0.009 + 0.002 \times \cos 30°}{\pi \times 0.009 \times \cos 30° - 0.25 \times 0.002}\right) + 0$$

$$T_r = 0.01970641559\ \text{Nm}$$

$$T_L = \frac{W d_m}{2}\left(\frac{f \times \pi \times d_m - L \times \cos 30°}{\pi \times d_m \times \cos 30° + f \times L}\right) + \frac{W f_c d_c}{2}$$

$$T_L = \frac{(11.9356)(0.009)}{2}\left(\frac{0.25 \times \pi \times 0.009 - 0.002 \times \cos 30°}{\pi \times 0.009 \times \cos 30° + 0.25 \times 0.002}\right) + 0$$

$$T_L = 0.0114713397\ \text{Nm}$$

Therefore, the stepper motors used to rotate the two lead screws must generate 0.020 Nm of torque to raise the applied load and 0.011 Nm to lower the applied load.

D.4 Excel calculation tables

The calculations performed to evaluate the test data from Appendix G.1, and G.2 were completed using Microsoft Excel. This program was used to simplify the raw data sets' computation for accuracy and repeatability evaluations presented in Section 6.2. The computations were performed using tables to present the data in a readable format. These tables were used to hold reference data for the calculation functions that were written in Excel. This appendix presented screenshots of these tables when printed off Microsoft Excel.

D.4.1 Accuracy tables

The following screenshot displayed the computation tables used to measure the Layout Control and Height Control sub-systems' actuation accuracy.

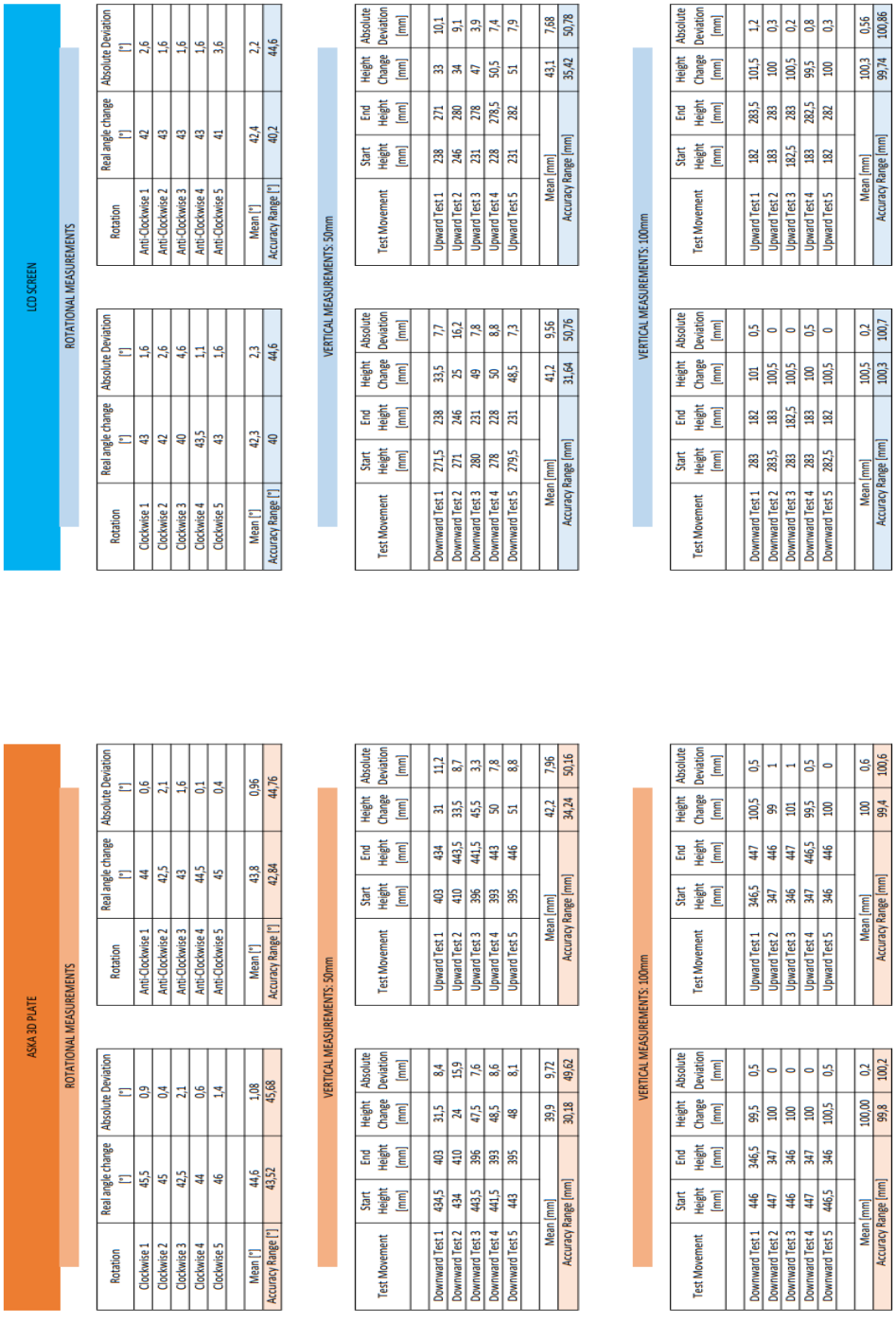

D.4.2 Repeatability tables

The following screenshot displayed the computation tables used to measure the Layout Control and Height Control sub-systems' repeatability.

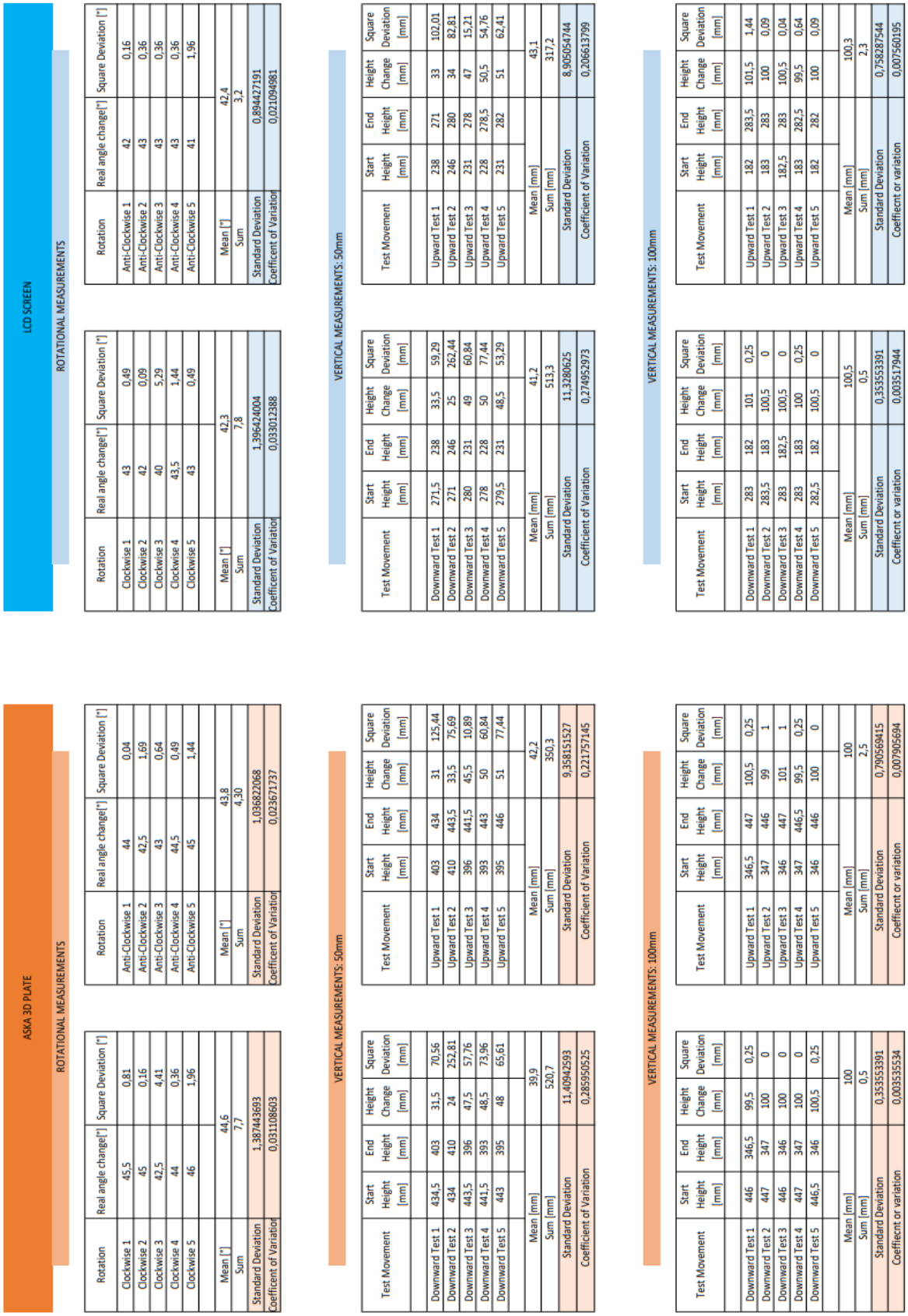

ASKA 3D PLATE

ROTATIONAL MEASUREMENTS

Rotation	Real angle change[°]	Square Deviation [°]
Clockwise 1	45,5	0,81
Clockwise 2	45	0,16
Clockwise 3	42,5	4,41
Clockwise 4	44	0,36
Clockwise 5	46	1,96
Mean [°]	44,6	
Sum	7,7	
Standard Deviation	1,387443693	
Coefficent of Variation	0,031108603	

Rotation	Real angle change[°]	Square Deviation [°]
Anti-Clockwise 1	44	0,04
Anti-Clockwise 2	42,5	1,69
Anti-Clockwise 3	43	0,64
Anti-Clockwise 4	44,5	0,49
Anti-Clockwise 5	45	1,44
Mean [°]	43,8	
Sum	4,30	
Standard Deviation	1,036822068	
Coefficent of Variation	0,023671737	

VERTICAL MEASUREMENTS: 50mm

Test Movement	Start Height [mm]	End Height [mm]	Height Change [mm]	Square Deviation [mm]
Downward Test 1	434,5	403	31,5	70,56
Downward Test 2	434	410	24	252,81
Downward Test 3	443,5	396	47,5	57,76
Downward Test 4	441,5	393	48,5	73,96
Downward Test 5	443	395	48	65,61
Mean [mm]			39,9	
Sum [mm]			520,7	
Standard Deviation			11,40942593	
Coefficient of Variation			0,285950525	

Test Movement	Start Height [mm]	End Height [mm]	Height Change [mm]	Square Deviation [mm]
Upward Test 1	403	434	31	125,44
Upward Test 2	410	443,5	33,5	75,69
Upward Test 3	396	441,5	45,5	10,89
Upward Test 4	393	443	50	60,84
Upward Test 5	395	446	51	77,44
Mean [mm]			42,2	
Sum [mm]			350,3	
Standard Deviation			9,358151527	
Coefficient of Variation			0,221757145	

VERTICAL MEASUREMENTS: 100mm

Test Movement	Start Height [mm]	End Height [mm]	Height Change [mm]	Square Deviation [mm]
Downward Test 1	446	346,5	99,5	0,25
Downward Test 2	447	347	100	0
Downward Test 3	446	346	100	0
Downward Test 4	447	347	100	0
Downward Test 5	446,5	346	100,5	0,25
Mean [mm]			100	
Sum [mm]			0,5	
Standard Deviation			0,353553391	
Coefficent or variation			0,003535534	

Test Movement	Start Height [mm]	End Height [mm]	Height Change [mm]	Square Deviation [mm]
Upward Test 1	346,5	447	100,5	0,25
Upward Test 2	347	446	99	1
Upward Test 3	346	447	101	1
Upward Test 4	347	446,5	99,5	0,25
Upward Test 5	346	446	100	0
Mean [mm]			100	
Sum [mm]			2,5	
Standard Deviation			0,790569415	
Coefficent or variation			0,007905694	

LCD SCREEN

ROTATIONAL MEASUREMENTS

Rotation	Real angle change[°]	Square Deviation [°]
Clockwise 1	43	0,49
Clockwise 2	42	0,09
Clockwise 3	40	5,29
Clockwise 4	43,5	1,44
Clockwise 5	43	0,49
Mean [°]	42,3	
Sum	7,8	
Standard Deviation	1,396424004	
Coefficent of Variation	0,033012388	

Rotation	Real angle change[°]	Square Deviation [°]
Anti-Clockwise 1	42	0,16
Anti-Clockwise 2	43	0,36
Anti-Clockwise 3	43	0,36
Anti-Clockwise 4	43	0,36
Anti-Clockwise 5	41	1,96
Mean [°]	42,4	
Sum	3,2	
Standard Deviation	0,894427191	
Coefficent of Variation	0,021094981	

VERTICAL MEASUREMENTS: 50mm

Test Movement	Start Height [mm]	End Height [mm]	Height Change [mm]	Square Deviation [mm]
Downward Test 1	271,5	238	33,5	59,29
Downward Test 2	271	246	25	262,44
Downward Test 3	280	231	49	60,84
Downward Test 4	278	228	50	77,44
Downward Test 5	279,5	231	48,5	53,29
Mean [mm]			41,2	
Sum [mm]			513,3	
Standard Deviation			11,32806625	
Coefficent of Variation			0,274952973	

Test Movement	Start Height [mm]	End Height [mm]	Height Change [mm]	Square Deviation [mm]
Upward Test 1	238	271	33	102,01
Upward Test 2	246	280	34	82,81
Upward Test 3	231	278	47	15,21
Upward Test 4	228	278,5	50,5	54,76
Upward Test 5	231	282	51	62,41
Mean [mm]			43,1	
Sum [mm]			317,2	
Standard Deviation			8,905054744	
Coefficent of Variation			0,206613799	

VERTICAL MEASUREMENTS: 100mm

Test Movement	Start Height [mm]	End Height [mm]	Height Change [mm]	Square Deviation [mm]
Downward Test 1	283	182	101	0,25
Downward Test 2	283,5	183	100,5	0
Downward Test 3	283	182,5	100,5	0
Downward Test 4	283	183	100	0,25
Downward Test 5	282,5	182	100,5	0
Mean [mm]			100,5	
Sum [mm]			0,5	
Standard Deviation			0,353553391	
Coefficent or variation			0,003517944	

Test Movement	Start Height [mm]	End Height [mm]	Height Change [mm]	Square Deviation [mm]
Upward Test 1	182	283,5	101,5	1,44
Upward Test 2	183	283	100	0,09
Upward Test 3	182,5	283	100,5	0,04
Upward Test 4	183	282,5	99,5	0,64
Upward Test 5	182	282	100	0,09
Mean [mm]			100,3	
Sum [mm]			2,3	
Standard Deviation			0,758287544	
Coefficent or variation			0,007560195	

D.4.3 Additional tables

The following screenshot displayed the additional computation tables used to measure the accuracy and repeatability of the Height Control sub-system. The original tables were presented for comparison.

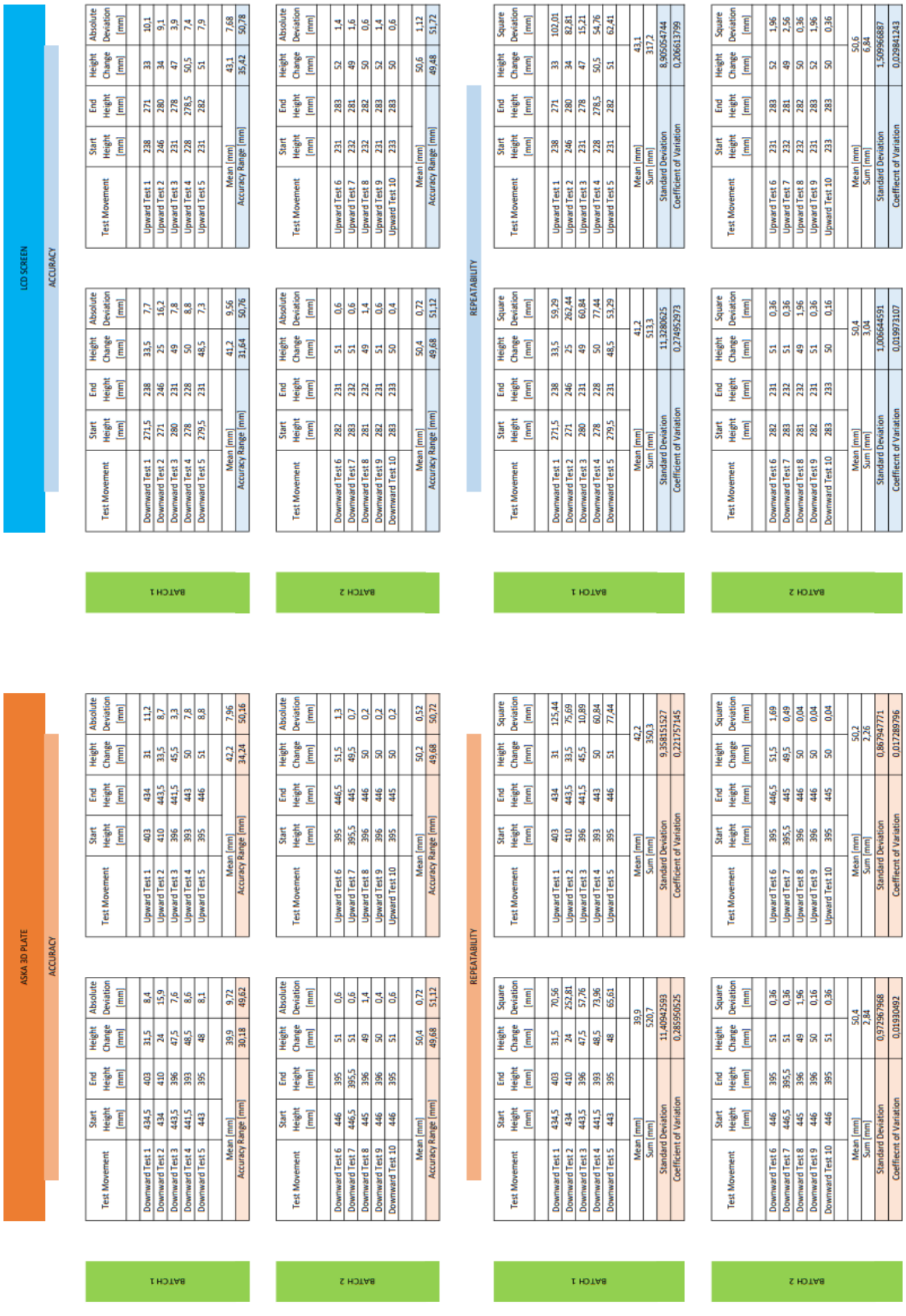

APPENDIX E. ELECTRONIC CONTROL CODE

The following scripts were written in Arduino Programming Language, a coding langue unique to the Arduino IDE. Three main control scripts were developed to control the stepper motors in the system. The first script (Layout Control Script) controlled a pair of NEMA 17 motors and had them rotate to a precise angle depending on the system layout required. This rotation was not simultaneous and occurred successively. The second script (Height Control Script) controlled a pair of NEMA 23 stepper motors and rotated them simultaneously by a select number of revolutions defined by the users.

The final script generated combined the Layout Control and Height Control scripts on a single script. This created a single script on which all the mechatronic components in the MR System could be controlled.

Note, sentences that start with two forward slashes (//) were comments in the script and text enclosed by an asterisk with a forward slash (/*….*/) should also be taken as a comment in the script.

E.1 MR layout control script

```
#include <Stepper.h>

#include <AccelStepper.h>

#include <MultiStepper.h>

//Control Scrip for NEMA 17 motors

//Bi-polar stepper motors

//Voltage = 12 V, Current = 0.4 A

//4-wire

//1.8 degree per step (200 steps per rev)


//Constants

const int stepsPerRevolution = 200;

const int platelayout1 = 25;

const int screenlayout1 = 25;

const int platelayout2 = 0;

const int screenlayout2 = 25;


// initialize stepper library

Stepper platemotor(stepsPerRevolution, 2, 3);
```

```
Stepper screenmotor(stepsPerRevolution, 4, 5);

void setup() {

// set the speed at in rpm:

  platemotor.setSpeed(30);

  screenmotor.setSpeed(30);


// initialize the serial port:

  Serial.begin(9600);

 platemotor.step(platelayout1);

screenmotor.step(screenlayout1);

//The motors to rotate by the number of steps then stop


//Layout1 reset constants: platemotor = -25 steps , screenmotor = 0 steps

//Layout2 reset constants: platemotor = 0 steps , screenmotor = -25 steps

}
```

E.2 MR System height control script

```
#include <AccelStepper.h>

#include <MultiStepper.h>


//Control Script for NEMA 23 Motors

//Uni-polar stepper motors

//Voltage = 3 V, Current = 2 A

//4 Phase

//1.8 degrees per step (200 steps per rev)

//1 rotation = 2 mm vertical movement


//Constatnts

const int stepsPerRevolution = 200;


// initialize stepper library

AccelStepper rightmotor(AccelStepper::DRIVER, 6, 7);

AccelStepper leftmotor(AccelStepper::DRIVER, 8, 9);

//Defining steps for motor rotation

int pos1 = 200;

int pos2 = 200;


void setup() {

  // Setting acceleration and speed of motor rotation

 rightmotor.setMaxSpeed(2000);

 rightmotor.setAcceleration(800);

 leftmotor.setMaxSpeed(2000);

 leftmotor.setAcceleration(800);

}
```

```
void loop() {
  // Rotation of the motor shafts:
if (rightmotor.distanceToGo() == 0)
  { rightmotor.moveTo(pos1);}
  if (leftmotor.distanceToGo() == 0)
  { leftmotor.moveTo(pos2);}
  rightmotor.run();
  leftmotor.run();
}
```

E.3 Final MR System control script

//This is a four-stepper motor control script. One pair of motors was rotated separately to a predefined angle. The other pair were rotated simultaneously at the same speed and by the same number of steps.

/*Motor Details:

Two NEMA 17 motors (1st pair)

Bi-polar stepper motors

Voltage = 12 V, Current = 0.4 A

4-wire

1.8 degree per step (200 steps per rev)

Two NEMA 23 Motors (2nd pair)

Uni-polar stepper motors

Voltage = 3 V , Current = 2 A

4 Phase

1.8 degrees per step (200 steps per rev)

1 rotation = 2 mm vertical movement

*/

//Libraries used

#include <AccelStepper.h>

#include <MultiStepper.h>

#include <Stepper.h>

int stepsPerRevolution = 200;

//Constants for NEAM 17 motors, this is where the number of steps can be changed for the two motors.

const int platelayout1 = 25;

const int screenlayout1 = 0;

```
const int platelayout2 = 0;
const int screenlayout2 = 25;

//Constants for NEMA 23 motors. This is where the number of steps can be changed for the two motors.
int pos1 = 200;
int pos2 = 200;

//Initialize stepper library for NEMA 17 stepper motors.
Stepper platemotor(stepsPerRevolution, 2, 3);
Stepper screenmotor(stepsPerRevolution, 4, 5);

//Initialize stepper library for NEMA 23 stepper motors
AccelStepper rightmotor(AccelStepper::DRIVER, 6, 7);
AccelStepper leftmotor(AccelStepper::DRIVER, 8, 9);


void setup() {
  //Initialize the serial port:
  Serial.begin(9600);

  //Set the speed of NEMA 17 motors in rpm:
  platemotor.setSpeed(30);
  screenmotor.setSpeed(30);

  //Set the speed of the NEMA 23 motors:
  rightmotor.setMaxSpeed(2000);
  rightmotor.setAcceleration(800);
  leftmotor.setMaxSpeed(2000);
```

```
  leftmotor.setAcceleration(800);


  //Rotation of NEMA 17 motors by the specified steps under constants
  platemotor.step(platelayout1);
  screenmotor.step(screenlayout1);


  //Layout1 reset: Plate = -25 steps, screen = 0 steps
  //Layout2 reset: Plate = 0 steps, screen = -25 steps
}
void loop() {
//Rotation of NEMA 23 motors by the specified steps under constants
if (rightmotor.distanceToGo() == 0)
  {  rightmotor.moveTo(pos1);  }
  if (leftmotor.distanceToGo() == 0)
  { leftmotor.moveTo(pos2);  }
  rightmotor.run();
  leftmotor.run();
}
```

APPENDIX F. SCRIPTS FOR SOFTWARE DEVELOPMENT

What followed was a list of scripts that were created in Microsoft Visual Studio and imported into the Unity3D™ application to control specific elements in the entertainment program created.

F.1 Constant velocity script

```
using System.Collections;

using System.Collections.Generic;

using UnityEngine;


public class AddConstantVelocity : MonoBehaviour

{

    [SerializeField]

    Vector3 v3Force;

    // Update is called once per frame

    void Update()

    {

        GetComponent<Rigidbody>().velocity += v3Force;

    }

}
```

F.2 Player controlled velocity

```
using System.Collections;

using System.Collections.Generic;

using UnityEngine;


public class AddPlayerControledVelocity : MonoBehaviour

{

    [SerializeField]

    Vector3 v3Force;


    [SerializeField]

    KeyCode keyPositive;

    [SerializeField]

    KeyCode keyNegative;

    // Update is called once per frame

    void Update()

    {

        if(Input.GetKey(keyPositive))

        GetComponent<Rigidbody>().velocity += v3Force;


        if(Input.GetKey(keyNegative))

        GetComponent<Rigidbody>().velocity -= v3Force;

    }

}
```

F.3 Restart button script

```
using System.Collections;

using System.Collections.Generic;

using UnityEngine;

using UnityEngine.SceneManagement;



public class RestartButton : MonoBehaviour

{

    [SerializeField]

    KeyCode keyRestart;



    // Update is called once per frame

    void Update()

    {

        if (Input.GetKey(keyRestart))

            SceneManager.LoadScene(SceneManager.GetActiveScene().name);

    }

}
```

APPENDIX G. TESTING RESOURCES

G.1 Raw layout control test data

Table G-1: Raw test data (Layout Control sub-system)

ASKA3D Plate		
Rotation	**Programmed angle change**	**Measured angle change**
Clockwise test 1	45°	45.5°
Clockwise test 2	45°	45°
Clockwise test 3	45°	42.5°
Clockwise test 4	45°	44°
Clockwise test 5	45°	46°
Mean	**45°**	**44.6°**
Rotation	**Programmed angle change**	**Measured angle change**
Anti-clockwise test 1	45°	44°
Anti-clockwise test 2	45°	42.5°
Anti-clockwise test 3	45°	43°
Anti-clockwise test 4	45°	44.5°
Anti-clockwise test 5	45°	45°
Mean	**45°**	**43.8°**
LCD Screen		
Rotation	**Programmed angle change**	**Measured angle change**
Clockwise test 1	45°	43°
Clockwise test 2	45°	42°
Clockwise test 3	45°	40°
Clockwise test 4	45°	43.5°
Clockwise test 5	45°	43°
Mean	**45°**	**42.3°**
Rotation	**Programmed angle change**	**Measured angle change**
Anti-clockwise test 1	45°	42°
Anti-clockwise test 2	45°	43°
Anti-clockwise test 3	45°	43°
Anti-clockwise test 4	45°	43°
Anti-clockwise test 5	45°	41°
Mean	**45°**	**42.4°**

G.2 Raw height control test data

Table G-2: ASKA3D Plate raw test data (Height Control sub-system)

ASKA3D Plate 50 mm Height Change			
Test movement	**Starting height (mm)**	**Ending height (mm)**	**Real-life height change (mm)**
Downward test 1	434.5	403	31.5
Downward test 2	434	410	24
Downward test 3	443.5	396	47.5
Downward test 4	441.5	393	48.5
Downward test 5	443	395	48
Mean	**439.3**	**399.4**	**39.5**
Test movement	**Starting height (mm)**	**Ending height (mm)**	**Real-life height change (mm)**
Upward test 1	403	434	31
Upward test 2	410	443.5	33.5
Upward test 3	396	441.5	45.5
Upward test 4	393	443	50
Upward test 5	395	446	51
Mean	**399.4**	**441.6**	**42.2**
ASKA3D Plate 100 mm Height Change			
Test movement	**Starting height (mm)**	**Ending height (mm)**	**Real-life height change (mm)**
Downward test 1	446	346.5	99.5
Downward test 2	447	347	100
Downward test 3	446	346	100
Downward test 4	447	347	100
Downward test 5	446.5	346	100.5
Mean	**446.5**	**346.5**	**100**
Test movement	**Starting height (mm)**	**Ending height (mm)**	**Real-life height change (mm)**
Upward test 1	346.5	447	100.5
Upward test 2	347	446	99
Upward test 3	346	447	101
Upward test 4	347	446.5	99.5
Upward test 5	346	446	100
Mean	**346.5**	**446.5**	**100**

Table G-3: LCD screen raw test data (Height Control sub-system)

LCD Screen 50 mm Height Change			
Test movement	**Starting height (mm)**	**Ending height (mm)**	**Real-life height change (mm)**
Downward test 1	271.5	238	33.5
Downward test 2	271	246	25
Downward test 3	280	231	49
Downward test 4	278	228	50
Downward test 5	279.5	231	48.5
Mean	**276**	**234.8**	**41.2**
Test movement	**Starting height (mm)**	**Ending height (mm)**	**Real-life height change (mm)**
Upward test 1	238	271	33
Upward test 2	246	280	34
Upward test 3	231	278	47
Upward test 4	228	278.5	50.5
Upward test 5	231	282	51
Mean	**234.8**	**277.9**	**43.1**
LCD Screen 100 mm Height Change			
Test movement	**Starting height (mm)**	**Ending height (mm)**	**Real-life height change (mm)**
Downward test 1	283	182	101
Downward test 2	283.5	183	100.5
Downward test 3	283	182.5	100.5
Downward test 4	283	183	100
Downward test 5	282.5	182	100.5
Mean	**283**	**182.5**	**100.5**
Test movement	**Starting height (mm)**	**Ending height (mm)**	**Real-life height change (mm)**
Upward test 1	182	283.5	101.5
Upward test 2	183	283	100
Upward test 3	182.5	283	100.5
Upward test 4	183	282.5	99.5
Upward test 5	182	282	100
Mean	**182.5**	**282.5**	**100.3**

G.3 Additional height control test data

Table G-4: Additional raw test data (Height Control sub-system)

ASKA3D Plate 50 mm Height Change			
Test movement	**Starting height (mm)**	**Ending height (mm)**	**Real-life height change (mm)**
Downward test 6	446	395	51
Downward test 7	446.5	395.5	51
Downward test 8	445	396	49
Downward test 9	446	396	50
Downward test 10	446	395	51
Mean	**445.9**	**395.5**	**50.4**
Test movement	**Starting height (mm)**	**Ending height (mm)**	**Real-life height change (mm)**
Upward test 6	395	446.5	51.5
Upward test 7	395.5	445	49.5
Upward test 8	396	446	50
Upward test 9	396	446	50
Upward test 10	395	445	50
Mean	**395.5**	**445.7**	**50.2**
LCD screen 50 mm Height Change			
Test movement	**Starting height (mm)**	**Ending height (mm)**	**Real-life height change (mm)**
Downward test 6	282	231	51
Downward test 7	283	232	51
Downward test 8	281	232	49
Downward test 9	282	231	51
Downward test 10	283	233	50
Mean	**282.2**	**231.8**	**50.4**
Test movement	**Starting height (mm)**	**Ending height (mm)**	**Real-life height change (mm)**
Upward test 6	231	283	52
Upward test 7	232	281	49
Upward test 8	232	282	50
Upward test 9	231	283	52
Upward test 10	233	283	50
Mean	**231.8**	**282.4**	**50.6**

G.4 Completed questionnaire from user testing

Questionnaire for MR System QoE Evaluation

Participant No: 1 Name: Dashlen Naidoo Gender: Male/Female

Age: 24

a) Do you have experience using a VR device? □Y □N

b) Do you have experience using an AR device? □Y □N

c) Do you have experience using an MR device? □Y □N

Content Quality:

1. To what extent did the system provide realistic visual information?

Not realistic Completely realistic

1 2 3 4 5

2. To what extent did the system provide accurate visual information?

Not accurate Highly Accurate

1 2 3 4 5

3. To what extent did the application require your focused attention?

Not at all Completely Focused

1 2 3 4 5

4. To what extent did the system deliver transparent/opaque images?

Completely transparent Not transparent

1 2 3 4 5

5. To what extent did the system deliver sharp image quality?

Blurry edges Defined edges

1 2 3 4 5

6. To what extent did the system affect your depth perception?

No effect Severely affected

1 2 3 4 5

7. Based on your ratings for Q1-6, give an overall rating for the content quality.

Very bad Very good

1 2 3 (4) 5

Hardware Quality:

8. To what extent could you freely move while using the system?

Not at all Completely Free

1 2 3 4 (5)

9. To what extent did you feel visual fatigue using this system (eye soreness)?

Very sore Not sore

1 2 3 (4) 5

10. Based on your ratings for Q8-9, give an overall rating for the hardware quality.

Very bad Very good

1 2 3 (4) 5

Environment Understanding:

11. To what extent did the mid-air images fit the real environment?

Not at all Completely Fit

1 2 (3) 4 5

12. To what extent did the image quality change due to your position changes?

Big change No change

1 2 3 (4) 5

13. To what extent did the mid-air images interact with foreign objects?

No interaction Interacts with foreign objects

(1) 2 3 4 5

14. To what extent did the MR System display mid-air images at a distance?

Not at all Full image displayed

1 2 3 (4) 5

15. To what extent did the MR System display the size of the mid-air images?

Very small Very big

1 2 (3) 4 5

16. Based on Q11-16, give an overall rating for the environment understanding.

Very bad Very good

1 2 (3) 4 5

User interaction:

17. To what extent did the system respond precisely to your interaction instructions?

Not at all Completely precise

1 2 3 4 (5)

18. To what extent did the system respond quickly to your interaction instructions?

Not at all Very quickly

1 2 3 4 (5)

19. Based on Q17-18, give an overall rating for the environment understanding.

Very bad Very good

1 2 3 4 (5)

Entertainment capability:

20. To what extent did you enjoy playing the MR game on the MR System?

Not enjoyable Very enjoyable

1 2 (3) 4 5

21. To what extent did the MR System immerse you in your gameplay?

No immersion High immersion

(1) 2 3 4 5

22. To what extent did you enjoy the controls for the MR game?

Not enjoyable Very enjoyable

1 2 3 4 (5)

23. To what extent did the game challenge you?

Not challenging Very challenging

1 2 (3) 4 5

24. To what extent was the content realistic when playing the game on the MR System?

Not realistic Very realistic

1 2 (3) 4 5

25. Based on Q20-24, give an overall rating for the entertainment experience given on the MR System.

Very bad Very good

1 2 (3) 4 5

Education capability:

26. To what extent did the MR System accurately display diagrams and images in mid-air?

Very bad Very good

1 2 3 4 (5)

27. To what extent did the MR System display videos and moving imagery in mid-air?

Very bad Very good

1 2 3 (4) 5

28. To what extent did the MR System deliver readable text in mid-air?

Not readable Very readable

1 2 3 4 (5)

29. To what extent did the MR System deliver depth of colour?

Poor sense of colour Complex sense of colour

1 2 3 (4) 5

30. To what extent could you identify similarities and differences between different mid-air images displayed?

Difficult to identify Easy to identify

1 2 3 4 (5)

31. To what extent did the images and videos displayed hold your attention?

Not at all Very captivating

1 2 3 4 (5)

32. To what extent could you identify solid edges and contours of the images displayed?

Difficult to identify Easy to identify

1 2 3 (4) 5

33. Based on Q26-32, give an overall rating for the educational capability for visual learning given on the MR System.

Very bad Very good

1 2 3 4 (5)

Engineering design capability:

34. To what extent were you able to accurately view SolidWorks™ models on the MR System?

Poor viewing Detailed viewing

1 2 3 4 (5)

35. To what extent were you able to perform 3D CAD design?

Limited capability Full capability

1 2 3 (4) 5

36. To what extent were you able to use the features available on the SolidWorks™ program through the MR System?

Limited usability Full usability

1 2 (3) 4 5

37. To what extent were you able to able to interact with the SolidWorks™ software on the MR System?

Poor interaction Good interaction

1 2 3 (4) 5

38. To what extent were you able to perform mechanical assembly on the MR System?

Limited capability Full capability

1 2 (3) 4 5

39. To what extent did the MR System improve current CAD design on a computer?

No improvement Significant improvement

(1) 2 3 4 5

40. Based on Q34-39, give an overall rating for the Engineering design capability of the MR System.

Very bad Very good

1 2 (3) 4 5

Finally, please give a grade for the overall quality of this MR experience: __80__/100.

If you have any comments, please let us know below:

_____

_____

_____

Thank you for your assistance in completing this survey.

APPENDIX H. MIXED REALITY SYSTEM DRAWINGS